AN AUTOPHAGY-RELATED SINGLE NUCLEOTIDE POLYMORPHISM IN ARTEMISININ-RESISTANT *PLASMODIUM FALCIPARUM*



Kimberly F. Breglio

Merton College

University of Oxford

A thesis submitted for the degree of

Doctor of Philosophy

Hilary 2018

“It’s the best possible time to be alive,

when almost everything you thought you knew is wrong.”

-Tom Stoppard, *Arcadia*

ABSTRACT

Artemisinin-resistant *Plasmodium falciparum* parasites have been reported in the Greater Mekong Subregion since 2007. Artemisinin combination therapy (ACT) is the mainstay of antimalarial treatment and is responsible for decreases in malaria-related morbidity and mortality over the past fifteen years. The slowed parasite clearance rates following ACT indicates resistance to artemisinin derivatives. This resistance places increasing selective pressure for variants or traits that confer resistance to the partner drug used in combination and has led to the rapid failure of several partner drugs. While a single nucleotide polymorphism (SNP) in *kelch13* has been shown to mediate some resistance phenotypes, the complete mechanism of artemisinin resistance is poorly understood. The known mechanisms of resistance hint at a connection to autophagy, an intracellular pathway that cells use to degrade waste molecules or organelles in response to stress and starvation, which is poorly characterized in *Plasmodium*. In this doctoral thesis project, I investigated the role of an autophagy-like mechanism in *P. falciparum* in the mechanism of artemisinin resistance. I found a SNP in *autophagy-related gene 18* (*atg18*) that was associated with clinical delayed parasite clearance half-life following ACT. This gene encodes PfAtg18, a protein that I characterized as being similar to mammalian/yeast homologues in terms of structure, binding abilities, and ability to form puncta in response to stress. In order to investigate the contribution of the mutation in this protein, I edited the *atg18* gene using CRISPR/Cas9 and screened the mutant and parent parasites against a drug library of over 6000 unique compounds. I discovered that while the SNP did not change the mutant parasite's susceptibility to any of the antimalarial compounds using a 72-hour drug pulse, it did alter the susceptibility to 227 other compounds. Further, I found that the SNP offers parasites a fitness advantage by allowing them to grow better in nutrient-limited settings. Finally, I determined that neither this *atg18* SNP nor several polymorphisms in *kelch13* modulate a dormancy phenotype that appears to be involved in the artemisinin-resistance mechanism.

DECLARATION OF WORK

This thesis is my own work and includes nothing which is the outcome of work done in collaboration except as declared in this section and as specified in the text. No part of this thesis has already been submitted, or is being concurrently submitted for any degree, diploma, or other qualification at the University of Oxford or any other university or similar institution. *Ex vivo* IC50 experiments were performed by Dr. Pharath Lim (National Institutes of Health). Mouse injections of VR2001 plasmids and bleeding was performed by Dr. Anderson Costa (National Institutes of Health). The production of polyclonal antibodies was performed by Dr. Louise Turner (Copenhagen University Hospital). Confocal imaging was performed in collaboration with Dr. Sundar Ganesan (National Institutes of Health). Electron microscopy fixation, processing, and imaging were performed by Dr. David Dorward (National Institutes of Health). The drug screens were performed with the help of Dr. Richard Eastman, and by the NCATS Automation Group: Carleen Klumpp-Thomas and Jamie Travers; and Compound Management: Paul Shinn, Danielle Bougie, Crystal McKnight, Misha Itkin and Zine Itkin (National Institutes of Health). Parasitemia flow cytometry for dormancy assays were performed on some days by Dr. Juliana Sa and Rifat Rahman (National Institutes of Health). Bioinformatics analyses were performed by Dr. Roberto Amato (University of Oxford/Wellcome Sanger Institute) and Dr. Rajarshi Guha (National Institutes of Health).

ACKNOWLEDGEMENTS

The debt I owe to others who helped me in the production of this doctoral work is vast. Thank you to those who helped with experiments as mentioned in the Declaration of Work section: I could not have completed this without you.

Thank you to those involved in the NIH's Cambodian clinical sites, especially Dr. Chanaki Amaratunga for her work overseeing and coordinating these sites. Thank you to the Pursat team: physician Dr. Mao Sivanna; microscopists Sokunthea Sreng, Sdoeung Saray, and Prum Phoeun; nurses Pech Eng Ly, Koeuth Savuth, Eam Tieng, and Tith Malis; and technician Lor Vanny. Thank you to the Ratanakiri team: physician Dr. Sam Baramey; microscopists Tieng Rada and Kong Sochea; nurses Sor Bunleng, Chan Marann, Phong Davi, Touch Buntheun, and Tor Hatlisa. Thank you to the Preah Vihear team: physician Dr. Sopha Chantha; microscopists Chun Tain Kea, Mork Neang, and Seng Sam Enn; nurses Say Sovann, Lem Vinh, Bet Phalla, and Meas Savat; and technician Phrom Neth. Thank you to the team at National Center for Parasitology, Entomology, and Malaria Control (CNM): site manager Dr. Suon Seila; laboratory manager Dr. Pharath Lim; data managers Ngor Pengby and Ou Vunsokserey; and technicians Try Vorleak and Dek Dalin.

Thank you for study participants in Cambodia, who are the backbone of this work.

Thank you to my mentors, both formal and informal. To Dr. Chanaki Amaratunga, thank you for keeping me afloat. To Dr. Katja Simon, thank you for your mentorship, reliability, and honesty. To Dr. David Roberts, thank you for the time you spent teaching and mentoring me. To Dr. Craig Thomas, thank you for taking a risk on me and for pushing me through to the end. To Dr. Thomas Wellems, thank you for your support through tumultuous times and for supporting my project and its offshoots. To Dr. Rick Fairhurst, thank you for supporting my independence in my project.

Thank you to family and friends and to lab mates across three continents. I owe special thanks for the comradery of Dr. Jessica Hostetler, Dr. Brandy St. Laurent, Megan Ansbro, and Erin Coonahan.

To my parents, Thomas and Sarah Faldetta, thank you for your unending stream of encouragement. I could never have gone this far without your love, kindness, example, support, and care.

Finally, my husband, Andrew Breglio, who has been there through triumphs and defeats, is owed the greatest thanks of all. Thank you for building this incredible life with me. My beautiful son, who performed experiments with me for nine months, has been my muse in writing this work. Thank you, Thomas Breglio, for making these last months some of the best. I am infinitely lucky to have both of you.

ABBREVIATIONS

Apicoplast ribosomal protein S10 (arps10)

Artemisinin (ART)

Artemisinin combination therapy (ACT)

Autophagy-related gene 8 (atg8)

Autophagy-related gene 18 (atg18)

Autophagy-related genes (*ATG*)

Autophagy-related protein 1 (Atg1)

Autophagy-related protein 2 (Atg2)

Autophagy-related protein 3 (Atg3)

Autophagy-related protein 4 (Atg4)

Autophagy-related protein 5 (Atg5)

Autophagy-related protein 6 (Atg6)

Autophagy-related protein 7 (Atg7)

Autophagy-related protein 8 (Atg8)

Autophagy-related protein 9 (Atg9)

Autophagy-related protein 10 (Atg10)

Autophagy-related protein 11 (Atg11)

Autophagy-related protein 12 (Atg12)

Autophagy-related protein 13 (Atg13)

Autophagy-related protein 14 (Atg14)

Autophagy-related protein 16 (Atg16)

Autophagy-related protein 17 (Atg17)

Autophagy-related protein 18 (Atg18)

Autophagy-related protein 29 (Atg29)

Autophagy-related protein 31 (Atg31)

Biological safety cabinet (BSC)

Blasticidin S deaminase (*bsd*)

Broad complex_Tramtrack_Bric-a-brac (BTB)

Chloroquine resistance transporter (crt)

Clustered Regularly Interspaced Short Palindromic Repeats (CRISPR)

Column volumes (CV)

Communist Party of Kampuchea (CPK)

CRISPR RNAs (crRNAs)

CRISPR associated protein 9 (Cas9)

Cytosine deaminase/uridyl phosphoribosyl transferase (*CDUP*)

Differential inference contrast (DIC)

Digestive vacuole (DV)

Dihydroartemisinin (DHA)

Dihydrofolate reductase-thymidylate synthase (DHFR-TS)

Ferrodoxin (fd)

Fluorouracil (5-FC)

FYVE-domain containing protein (FCP)

Genome wide association study (GWAS)

Half-maximal activity concentration (AC50)

Half-maximal inhibitory concentration (IC50)

Hematocrit (Hct)

Histidine-rich proteins (HRPs)

Homology directed repair (HDR)

Hours post invasion (HPI)

Human dihydrofolate-reductase-thymidylate synthase (*hDHFR*)

Isopentenyl pyrophosphate (IPP)

Isopropyl β-d-1-thiogalactopyranoside (IPTG)

Kelch13 (k13)

Kelch-like ECH-associated protein 1 (Keap1)

Laboratory of Malaria and Vector Research (LMVR)

Low-complexity regions (LRCs)

Mahidol Oxford Tropical Medicine Research Unit (MORU)

Malaria Parasite Metabolic Pathways (MPMP)

Maximum response (MaxR)

Mechanism Interrogation Plate (MIPE)

Methylerythritol phosphate (MEP)

Minimum inhibitory concentration (MIC)

Multi-drug resistance protein 2 (mdr2)

National Center for Advancing Translational Sciences (NCATS)

Neomycin phosphotransferase II (neo)

NF-E2-related factor 2 (Nrf2)

Non-communicable diseases (NCDs)

Open reading frame (ORF)

Plasmodial surface anion channel (PSAC)

Plasmodium reactive oxidative stress complex (PROSC)

Phosphatidylethanolamine (PE)

Phosphatidylinositol-3-kinase (PI3K)

Phosphatidylinositol 3-phosphate (PI3P)

Pox virus_zinc finger (POZ)

Pre-autophagosomal structure (PAS)

Protospacer adjacent motif (PAM)

Puromycin-N-acetyltransferase (*pac*)

Quantitative High-Throughput Screening (qHTS)

Reactive oxygen species (ROS)

Red blood cell (RBC)

Ring-stage survival assay (RSA)

Room temperature (RT)

Single guide RNA (sgRNA)

Single nucleotide polymorphism (SNP)

T-complex protein-1 (TCP-1)

TCP-1 ring complex (TRiC)

Thymidine kinase (*TK*)

Tissue plasminogen activator (TPA)

Tracking Resistance to Artemisinin Collaboration (TRAC)

Tracking Resistance to Artemisinin Collaboration-II (TRAC-II)

Trans-activating crRNA (tracrRNA)

Triple artemisinin combination therapies (TACT)

Unfolded protein response (UPR)

Whole genome sequencing (WGS)

Yeast dihydroorotate dehydrogenase (ydhodh)

Zinc-finger nuclease (ZFN)

TABLE OF CONTENTS

Abstract i

Declaration of Work ii

Acknowledgements iii

Abbreviations iv

1 Introduction 1

1.1 Malaria 1

1.1.1 The history of malaria infections 1

1.1.2 *Plasmodium falciparum* lifecycle 3

1.1.3 *Plasmodium falciparum* hemoglobin digestion 6

1.1.4 *Plasmodium falciparum* pathogenesis 7

1.1.5 Epidemiology of malaria 8

1.2 Antimalarial chemotherapeutics 13

1.2.1 Treatment of *Plasmodium falciparum* 13

1.3 Autophagy 26

1.3.1 The discovery of autophagy 26

1.3.2 Autophagy pathway 28

1.3.3 Autophagy function 33

1.3.4 Autophagy in *Apicomplexa* 37

1.4 Thesis aims 40

2 General methodology 42

2.1 *Plasmodium falciparum* parasite culture 42

2.1.1 Thawing parasites and general culture conditions 42

2.1.2 Parasite lines used 43

2.1.3 Sorbitol synchronization of ring stage parasites 45

2.1.4 Percoll gradient separation of late stage parasites 46

2.1.5 Parasite cloning by dilution 47

2.1.6 Saponin lysis 49
2.2 Statistical analysis 49
3 Single nucleotide polymorphisms in autophagy-related gene 18 (*atg18*) and artemisinin resistance 51
3.1 Introduction and aims 51
3.1.1 Introduction 51
3.1.2 Aims 55
3.2 Materials and methods 55
3.2.1 Bioinformatics of Autophagy related genes 55
3.2.2 CRISPR/Cas9 genome editing 57
3.3 Results 67
3.3.1 Bioinformatics 67
3.3.2 CRISPR/Cas9 Transfections 75
3.4 Discussion 78
4 Phenotypic changes and drug sensitivities associated with an atg18 polymorphism in *Plasmodium falciparum* 88
4.1 Introduction and aims 88
4.1.1 Introduction 88
4.1.2 Aims 90
4.2 Materials and methods 90
4.2.1 Atg18 alignment with homologues 90
4.2.2 VR2001 Anti-Atg18 antibody production 91
4.2.3 Polyclonal antibody production 94
4.2.4 Production of GFP-tagged Atg18 lines 95
4.2.5 Confocal Microscope Imaging 97
4.2.6 PIP binding assay 101
4.2.7 PI3P measurements 102
4.2.8 Electron microscopy 102

4.2.9 Drug screen Dd2$^{R539T/T38I}$ 103
4.2.10 Nutrient deprivation assays 107
4.3 Results 109
4.3.1 *P. falciparum* Atg18 protein characterization 109
4.3.2 Phenotypic changes in parasites with T38I Atg18 SNP 117
4.4 Discussion 126
4.4.1 Understanding PfAtg18 126
4.4.2 Phenotypic changes associated with the T38I polymorphism in *atg18* 132
5 *Plasmodium falciparum* dormancy in response to artemisinin as a mechanism of resistance 142
5.1 Introduction and aims 142
5.1.1 Introduction 142
5.1.2 Aims 148
5.2 Materials and methods 148
5.2.1 Sorbitol lysis assay 148
5.2.2 Dormancy induction 149
5.2.3 Parasitemia by FACS 150
5.3 Results 152
5.3.1 Dormancy recrudescence assays 152
5.4 Discussion 160
6 Summary of findings 170
7 References 172
Appendix A: Differential compounds 242
Appendix B: Reagents & Equipment Used 247

1 INTRODUCTION

1.1 MALARIA

1.1.1 The history of malaria infections

Plasmodium, a protozoa in the phylum *Apicomplexa*, causes human malaria infections. The term "malaria" comes from Italian for "bad air," as the infection was originally associated with the foul smells emanating from swamps surrounding Rome. The *Plasmodium* parasite has been a scourge of humankind for thousands of years, with Hippocrates himself describing the cyclical fevers and splenomegaly that are often attributed to malaria infections between the 5th and 4th centuries BC (Cunha and Cunha, 2008). The oldest known malaria DNA was found in a Roman cemetery and dates back to the 5th century AD (Abbott, 2001), although it is believed that these parasites originated in Africa, possibly infecting amphibians, reptiles, and birds before moving on to primates and eventually, the earliest humans (Bruce-Chwatt, 1965, Schlagenhauf, 2004).

Although the disease of malaria was well-known throughout history, the *Plasmodium* parasite was first discovered by Charles Louis Alphonse Laveran on November 6, 1880 (Bruce-Chuvatt, 1981) (Figure 1). He received the Nobel Prize in Physiology or Medicine in 1907 for his discoveries. In the 1890s, Giovanni Battista Grassi distinguished the different *Plasmodium* species and outlined the *P. falciparum* lifecycle. Adding to the original work by Grassi, we now know of six major species that afflict humans: *P. falciparum, P. vivax,* two species of *P. ovale, P. malariae,* and *P. knowlesi*.

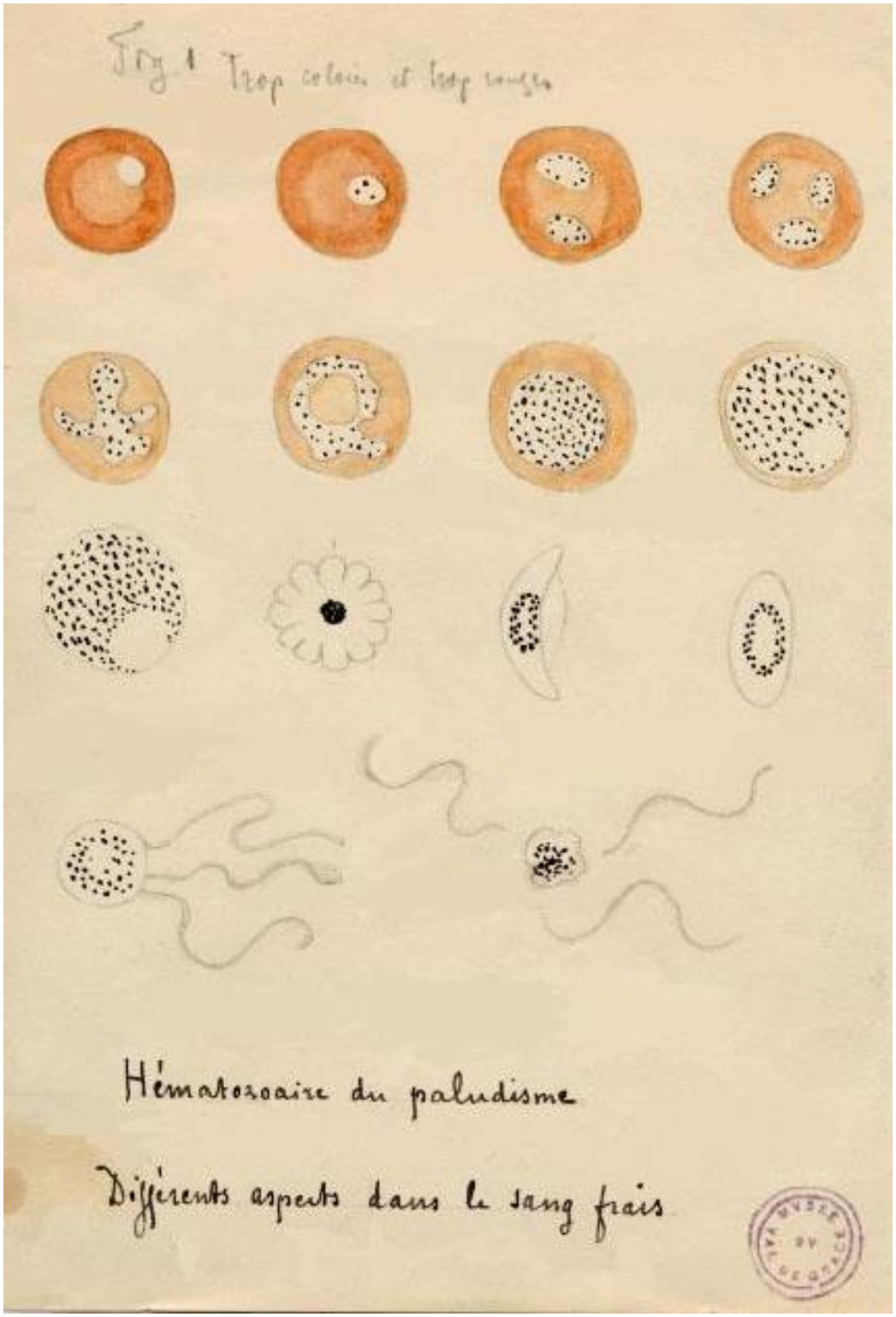


Figure 1: Drawings of malaria by Charles Louis Alphonse Laveran

Drawings of developing malaria parasite made from fresh blood. Top two rows depict intraerythrocytic development in the asexual cycle. Bottom two rows depict gametocyte maturation and exflagellation in the sexual cycle. This figure is in the public domain.

Plasmodium parasites in humans are transmitted by the *Anopheles* mosquito. The theory that mosquitoes transmitted malaria was first postulated by Sir Patrick Manson in 1894 (Manson, 1894). Sir Ronald Ross, under the guidance of Manson, confirmed the theory by discovering avian malaria parasites in the salivary glands of a mosquito in India in 1897. Ross was awarded the Nobel Prize for Physiology or Medicine in 1902 for his discovery.

1.1.2 *Plasmodium falciparum* lifecycle

The *P. falciparum* parasite lifecycle exists in two distinct life phases: the sexual cycle, which occurs mainly within the mosquito vector, and the asexual or intraerythrocytic cycle, which occurs inside the human host (Figure 2). To begin the sexual cycle, haploid gametocytes (both male and female) are taken up by a female mosquito during a blood meal. The male and female gametocytes meet in the midgut of the mosquito, and within seconds of exposure to the conditions of the midgut, undergo gametocytogenesis to form gametes (Billker et al., 1998). Males undergo replication (Janse et al., 1988) followed by the formation of flagella known as exflagellation to form mature male gametes. The male and females join, forming a diploid zygote which then develops into an ookinete, during which process genetic recombination occurs (Sinden, 1983). The ookinete invades the wall of the midgut and forms an oocyst, which ruptures to release sporozoites (Sinden, 1999). The sporozoites migrate to the mosquito salivary glands where they are ready for inoculation into humans during the mosquito's next blood meal (Pimenta et al., 1994).

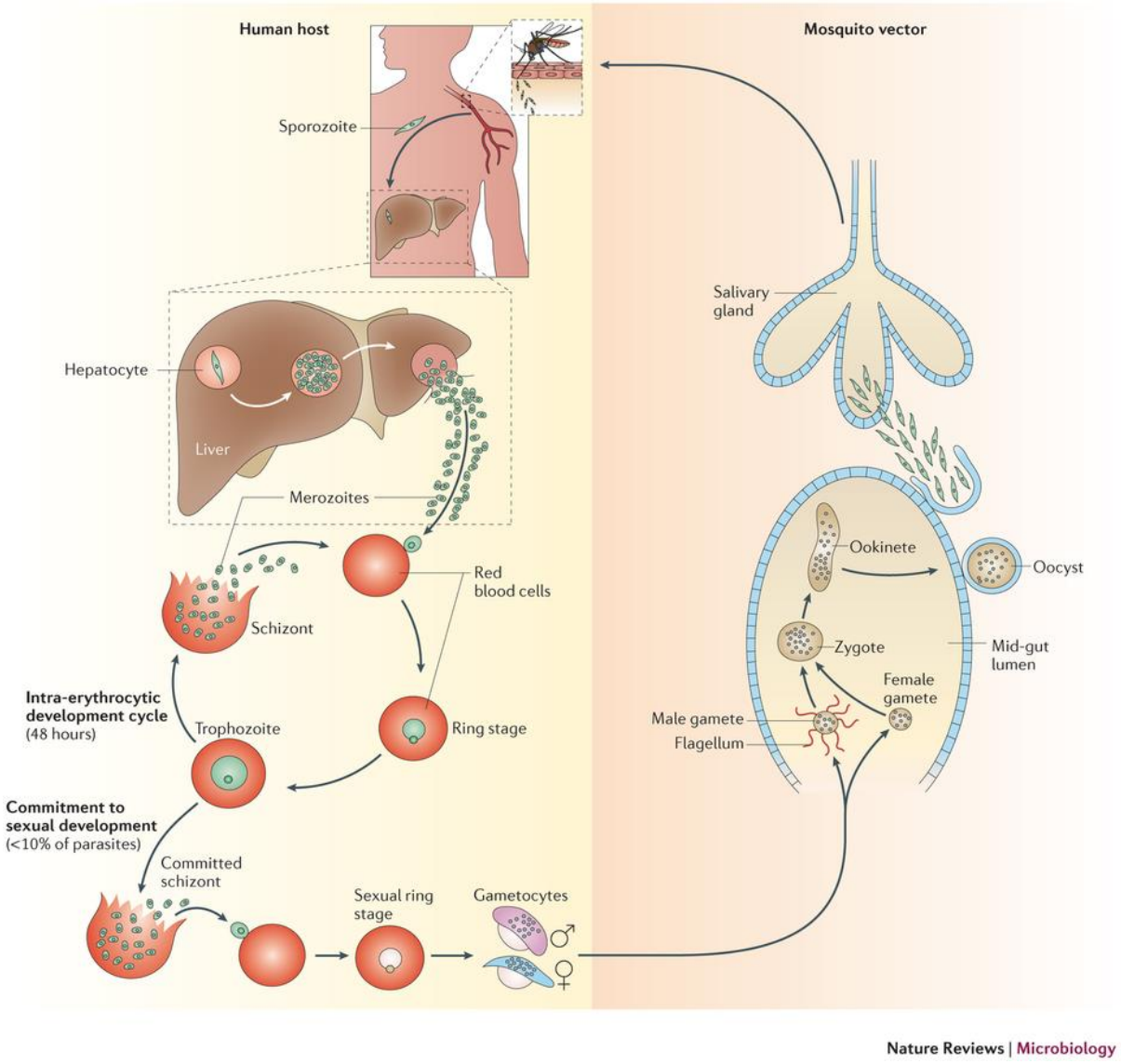


Figure 2: Plasmodium falciparum lifecycle

The lifecycle is propagated with an infected mosquito biting a human and injecting parasite sporozoites into the human blood. The sporozoites travel to the liver via the blood where they infect hepatocytes, develop into merozoites, and eventually burst the hepatocyte to be released back into the blood. The merozoite invades a red blood cell, develops into a ring, then trophozoite, and either a schizont to become a merozoite and repeat the asexual cycle anew or it commits to sexual development. Sexually committed parasites develop into gametocytes (male and female) which are then taken up by a mosquito and reproduce in the mosquito midgut. They form a zygote then ookinete, then an oocyst, which releases its sporozoites into the mosquito salivary gland, ready to be injected into the next host. This figure has been reproduced with permissions from (Josling and Llinás, 2015).

A female mosquito carrying these parasites in its salivary glands bites a human and transmits *Plasmodium* sporozoites into the skin (Ross, 2002). These sporozoites migrate through the vasculature and travel via the blood to the liver where they infect a liver cell known as a hepatocyte. The sporozoites differentiate and replicate within the hepatocyte to form schizonts with thousands of merozoites in merosomes. The hepatocyte detaches and ruptures to release merozoites into the blood. Merozoites quickly locate an erythrocyte and invade, beginning the intraerythrocytic cycle.

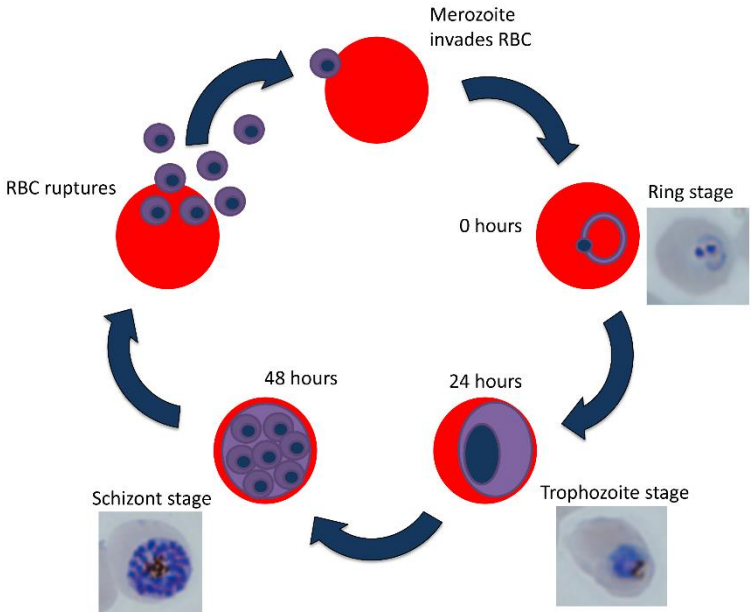


Figure 3: Example smears of developing P. falciparum parasites

Giemsa thin smears demonstrate the development of P. falciparum parasites over time. Parasites at 0 hours post invasion (HPI) demonstrate ring-stage morphology, then transform into early trophozoites at 24 HPI. They appear as segmented schizonts at 48 HPI, and have reinvaded new red blood cells to appear as rings and repeat the cycle.

Plasmodium parasites grow within the erythrocyte from a ring stage parasite to a trophozoite and finally a schizont. The schizont ruptures the erythrocyte and releases merozoites, which then reinvade new erythrocytes and begin the cycle anew.

This project focuses on the asexual, erythrocyte stages: ring, trophozoite, and schizont. After the invasion of an erythrocyte by a merozoite, the parasite becomes a discoid early trophozoite that is termed a ring, as it morphologically resembles a ring on Giemsa smear as viewed by light microscopy (Figure 3) (Langreth et al., 1978). The ring is an immature stage and lacks some of the more specialized organelles present in the later stages. The

parasite does, however, contain its nucleus, mitochondrion, apicoplast, and endoplasmic reticulum (Bannister et al., 2000b, Bannister et al., 2000a). The ring contains a cytostome ("cell mouth", Latin) that gobbles up hemoglobin present from the erythrocyte and sends it to a number of small vacuoles for digestion.

After approximately 24 hours post invasion (HPI), the ring grows into a mature trophozoite, with filled-in cytoplasm on Giemsa smear (Figure 3). The organelles present in the immature trophozoite increase in size, especially the ER and Golgi apparatus, signaling an increase in protein synthesis during this stage. The smaller vacuoles fuse to form a single large digestive vacuole (DV) (Bannister et al., 2000a). Hemozoin crystals, the byproducts of hemoglobin digestion, can be seen in the digestive vacuole at this time, appearing as dark purple dots. Maurer's clefts are structures that develop along the parasitophorous vacuole membrane, which may be involved in protein trafficking (Aikawa et al., 1986).

The trophozoite eventually begins dividing and the schizont stage begins. The final schizont typically has approximately 16 nuclei, although this number can vary considerably within and between species (Atkinson and Aikawa, 1990). Each of these nuclei will become an individual merozoite upon schizont rupture; therefore, proteins for invasion are synthesized during the schizont stage. Apical proteins, including the rhoptries, micronemes, and dense granules, are used for merozoite invasion (Counihan et al., 2013). The mitochondrion and apicoplast multiply, each providing one organelle for each daughter merozoite. When the merozoites are fully developed, the erythrocyte membrane ruptures and the merozoites are released into the blood to find new erythrocytes and begin the cycle again. The asexual cycle typically takes 48 hours, but can be shorter or longer depending on the species (Bannister and Mitchell, 2003).

1.1.3 *Plasmodium falciparum* hemoglobin digestion

Plasmodium digestion of hemoglobin is a vital part of its metabolism. This digestion not only gives parasites a source of amino acids for metabolism, it also is part of the remodeling that occurs when a parasite invades an erythrocyte, giving the parasite more space within the host cell to grow (Klonis et al., 2013a). Human hemoglobin contains four heme groups each connected to a globular protein subunit. An individual heme group is made of a porphyrin bound to an iron ion (giving heme the alternate name of ferroprotoporphyrin), which can bind to oxygen to transport it from the lungs to the heart

to the body. Of note, although hemoglobin A, which consists of two alpha globular subunits and two beta subunits, is the most common form worldwide, there are other polymorphisms in the human population. Hemoglobin S, which contains two alpha subunits and two mutated beta subunits, is responsible for sickle cell disease. Hemoglobin E, which has two alpha subunits and two beta subunits with a different mutation, is very common in people of Southeast Asian descent, especially those in Cambodia (Steinberg et al., 2009).

Hemoglobin digestion begins in the mid-ring stage (Abu Bakar et al., 2010) and is believed to occur through vesicle-dependent (Elliott et al., 2008) and vesicle-independent (Lazarus et al., 2008) pathways. However the hemoglobin is procured, it is eventually delivered to the acidic DV for digestion. The DV contains three cysteine proteases, known as the falcipains, and four aspartic proteases known as the plasmepsins. These proteases appear to be redundant (Liu et al., 2006), although there is renewed interest in their functions due to an apparent association between plasmepsin copy number and piperaquine resistance (Witkowski et al., 2017, Amato et al., 2017). During digestion, a heme polymerase has been suggested to link one hematin (ferriprotophorphyrin IX [FP]) to another by creating an iron-carboxylate link between the ferric irons of each hematin molecule (Slater et al., 1991). This crystalline polymer is known as hemozoin and is relatively non-toxic to the parasite, as opposed to the high toxicity of ferriprotophorphyrin IX (Fitch et al., 1982). The hemozoin stays within the DV for the life of the parasite, then is released into the blood with schizont rupture.

1.1.4 *Plasmodium falciparum* pathogenesis

Upon infection with *Plasmodium*, the most common symptom is fever. A person may also develop headaches, myalgia, fatigue, rigors, nausea, or vomiting (Genton and D'Acremont, 2001). On exam, splenomegaly, hepatomegaly, jaundice, conjunctival icterus, tachycardia, and orthostatic hypertension are often found. Anemia, thrombocytopenia, hyperbilirubinemia, and elevated aminotransferase levels are commonly noted on laboratory work (D'Acremont et al., 2002).

Severe malaria is defined as end organ dysfunction in the presence of an acute malaria infection in the absence of other causes of organ dysfunction (WHO, 1990, WHO, 2015a) and is almost exclusively caused by *P. falciparum*. It typically develops within 3-7 days following the onset of fever (Trampuz et al., 2003). In cases of severe malaria,

complications can include cerebral malaria, severe anemia, pulmonary edema, acute respiratory distress syndrome, disseminated intravascular coagulation, and acute renal failure. Cerebral malaria is a diagnosis of exclusion for a patient with a Glasgow Coma Scale score less than 9. The patient must be unarousable for at least 30 minutes if loss of consciousness followed a generalized seizure (WHO, 1990). The mortality rate for severe malaria surpasses 20% in returning travels managed in intensive care units (Kain et al., 1998) and therefore represents a deadly sequelae of malaria infection.

Following clinical suspicion of malaria, the diagnosis is confirmed with light microscopy of a thin and thick smear of patient blood. Smears are fixed in methanol and stained with Giemsa, which stains the phosphate groups of DNA and will therefore stain the *Plasmodium* parasite but not the erythrocyte. Differential staining was originally pioneered by Dimitri Leonidovitch Romanowsky in 1891 with his discovery of methylene blue-eosin stain (Fleischer, 2004), which became the basis for Giemsa stain, developed by Gustav Giemsa in 1904 (Giemsa, 1904). The thick smear is often used for diagnosis, while the thin smear is used for parasitemia calculation and species identification. A microscopist typically examines at least 500 white blood cells (WBC) in a thick smear before ruling out *Plasmodium* infection (Amaratunga et al., 2012). Although this is the gold standard for malaria diagnosis, a variety of rapid diagnostic tests exist, the most popular of which detects histidine-rich protein 2 (HRP-2), a malaria antigen, in human blood (Rock et al., 1987, Beadle et al., 1994).

1.1.5 Epidemiology of malaria

Malaria is a globally important pathogen which caused 212 million cases and 429,000 deaths in 2015 (WHO, 2016b). Over 2.7 billion people, or 49.6% of the world's population, are at risk from malaria infection. Although malaria is endemic in 91 countries across five continents, the vast majority of these cases (90%) and deaths (92%) occur in Africa. The overwhelming majority of worldwide cases (96%) were due to *P. falciparum*; however, outside of Africa, 41% of cases were due to *P. vivax*. Of the worldwide deaths, 99% have been attributed to *P. falciparum*. (WHO, 2016b). The majority of deaths are in children under five years of age, although disease burden varies, especially in lower transmission zones where adults are unexposed as children and therefore are more susceptible as adults.

Despite the high number of cases and deaths, there has been progress towards decreasing the burden of malarial disease. In the past five years, global malaria incidence has decreased by 21% and the mortality rate has decreased by 29% (WHO, 2016b). Although this is far short of the Millennium Development Goal of 40% reduction in these two metrics by 2020, these numbers represent a trend in the right direction towards malaria control, elimination, and eradication.

1.1.5.1 Spotlight on malaria in Cambodia

The focus of this thesis is on clinical research sites in the country of Cambodia, which is located in Southeast Asia in the Greater Mekong Subregion and shares its borders with Thailand, Laos, and Vietnam. The climate of Cambodia is tropical, with average temperatures ranging from 25^{o}C to 27^{o}C and the rainy season lasting from May to October (Annear et al., 2015).

In 802 AD, Jayavarman II proclaimed himself king of the world and officially established the Angkor Empire. This Hindu, and later Buddhist, empire lasted until the mid-15th century and left behind grand temples, including Angkor Wat. The Dark Ages of Cambodia followed, during which time Cambodia slowly lost land to the west to Siam (Thailand) and land to the east and south to Vietnam. Cambodia was then colonized by the French in 1863 and subsequently by the Japanese in 1953. In 1970, a coup d'etat overthrew the government and a civil war ensued between the Khmer Rouge, also called the Communist Party of Kampuchea (CPK), allied with the North Vietnamese and Chinese against the Khmer Republic allied with the South Vietnamese and United States. The Khmer Rouge won and its leader, Pol Pot, came into power in 1975, establishing Cambodia as a communist society. The Khmer Rouge carried out a genocide against former government officials, professionals, and ethnic minorities. It is estimated that up to 3 million people were killed during the reign of the Khmer Rouge. In 1979, the Vietnamese army and Kampuchean United Front for National Salvation overthrew the Khmer Rouge, spurring on another civil war which ended in 1991. Cambodia held elections in 1993 and a new constitution was established.

From 1994-2015, Cambodia has experienced rapid economic development and growth, with an average growth rate of 7.6%, mainly due to tourism (World Bank, 2017), and is now a lower-middle income country. Poverty is declining and in 2014 the poverty rate was at 13.5%, down 34.3% since 2007 (World Bank, 2017). The vast majority of poverty occurs in rural areas, with approximately 25% of the rural population living below the

poverty line in 2009 (Annear et al., 2015). Approximately 78% of Cambodians are literate (Annear et al., 2015). Life expectancy at birth has been climbing and stood at approximately 69 years in 2015 (World Bank, 2017). Coupling the increase in life expectancy with a decreased birthrate (2.9 births per woman), it is predicted that the

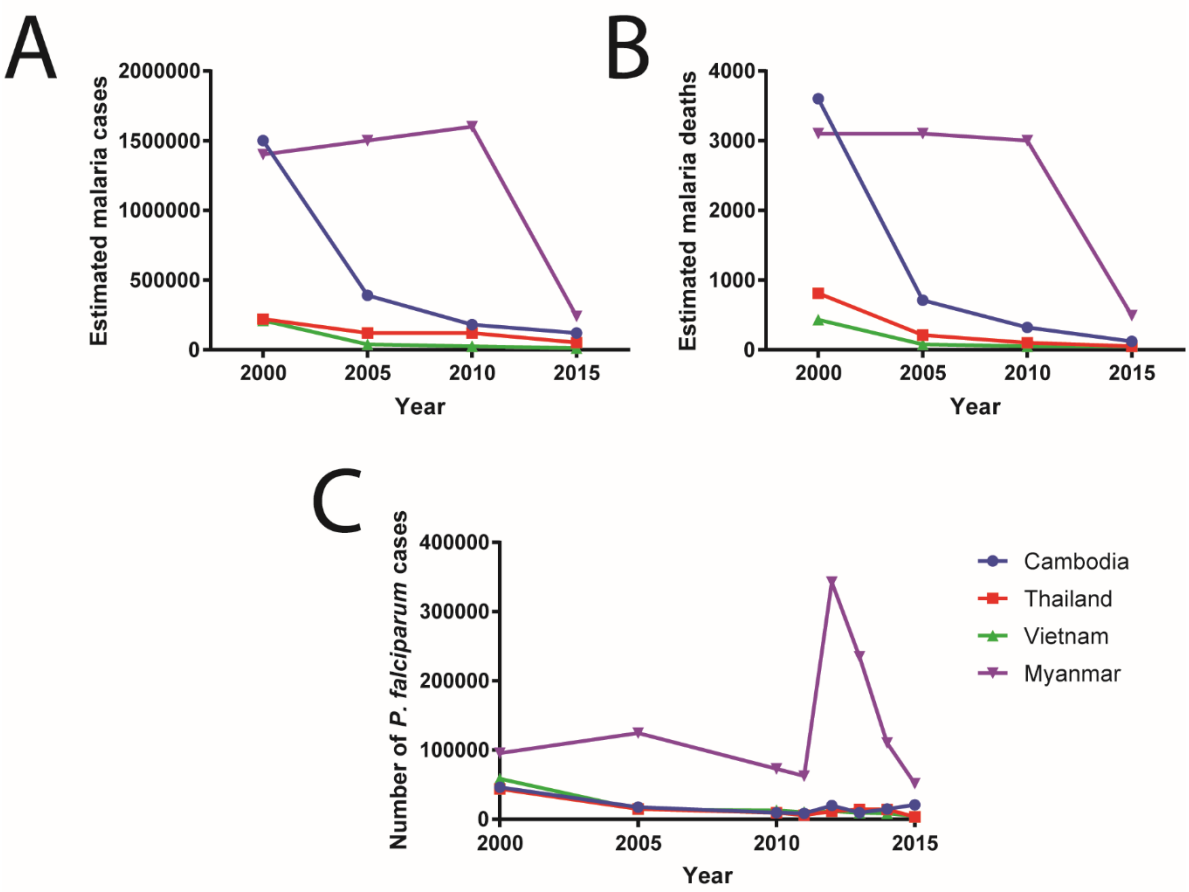


Figure 4: Malaria cases and deaths in select countries in Southeast Asia

(A) The estimated number of cases of malaria in select countries in Southeast Asia. (B) The estimated number of deaths attributed to malaria. (C) The number of confirmed cases of P. falciparum. Data from Cambodia is shown in blue, Thailand in red, Vietnam in green, and Myanmar in purple. These figures were created using data from (WHO, 2016b).

Cambodian population structure will age over the next 50 years (Annear et al., 2015). Although Cambodia has a public healthcare system through the Ministry of Health, there is also a large number of private providers that account for a significant percentage of healthcare (Annear et al., 2015), though the country has only 0.71 hospital beds per 1000 people (Annear et al., 2015). As has been seen in many countries, there has been a transition from communicable to non-communicable diseases (NCDs) as the major cause of death. In 2008, NCDs represented the cause of death in 47% of cases, up from 34% in 2002 (WHO, 2006, WHO, 2011). Even given this overall shift, infectious diseases continue to plague children under 5 years old. In 2010, pneumonia caused 16% of deaths

in children under 5, diarrhea caused 5%, neonatal sepsis caused 6%, malaria caused 2%, and HIV/AIDS caused 1% (Annear et al., 2015). Cambodia is in some ways a country in transition, having emerged recently from a difficult civil war and now establishing itself with a rapidly growing economy and flourishing tourism industry.

Table 1: Population estimates of four select countries in Southeast Asia in 2015

Country	UN estimated population, 2015
Thailand	67,959,359
Myanmar	53,897,154
Cambodia	15,577,899
Vietnam	93,447,601

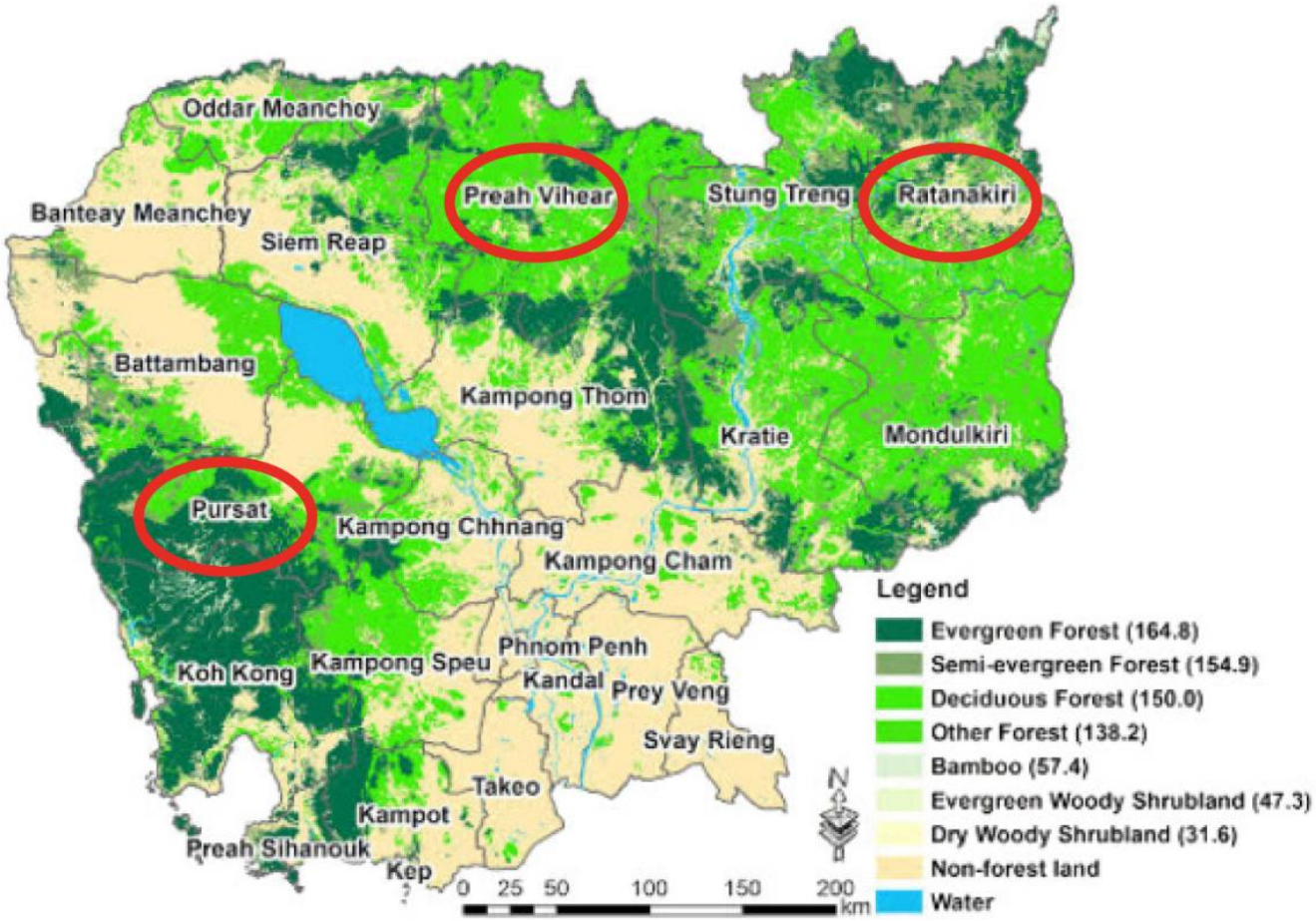
Data from (WHO, 2016b).

In Southeast Asia, the majority of malaria cases are due to *P. vivax*; however, *P. falciparum* cases do occur and carry a high risk of mortality. From 2013-2015 in Cambodia, just under 60% of cases were due to *P. falciparum*; in Thailand, over 50% in Myanmar, over 60%; and in Vietnam, approximately 50% of cases (WHO, 2016b). Coinciding with the deployment of highly effective antimalarial medications and renewed efforts in malaria eradication in Southeast Asia, cases and deaths attributed to malaria have been falling over the past fifteen years (Figure 4). Although Cambodia has by far the smallest population of the countries examined (Table 1), it maintains a higher number of malaria cases and deaths than some of its neighbors. Malaria was the 10th leading cause of death in 2005, but has fallen to the 16th in 2015 (GBD, 2015). Similarly, malaria was the 8th leading cause of premature death in 2005, and has again fallen to 14th in 2015 (GBD, 2015). Over 3 million Cambodians are thought to be at risk for malaria (Annear et al., 2015).

The geographic regions of Cambodia have differing landscapes and many areas of the country are remote, causing malaria control efforts to face challenges due to low levels of infrastructure. The three clinical sites in this thesis project are located in three distinct Cambodian provinces. The first clinical site is located in Pursat province in western Cambodia, bordering Thailand. Approximately 70.2% of Pursat province was covered by forest in 2005 (Figure 5) (Sasaki et al., 2016). The population was 397,107 people as of the last Cambodian census in 2008 (Planning, 2008). This site is historically the harbinger of drug resistance. It was the first of the three clinical sites to identify artemisinin delayed

clearance as well as piperaquine failure. The next clinical site is situated in Preah Vihear, located in the north of the country, bordering Thailand and Laos. Preah Vihear has 95.1% forest cover (Sasaki et al., 2016) and a population of 170,852 people (Planning, 2008). This clinical site generally acquires resistance slightly later than Pursat province. The final province is Ratanikiri in the east, covered by 89.8% forest (Sasaki et al., 2016) with a population of 149,997 people (Planning, 2008). Ratanakiri has generally been the last clinical site to acquire resistance.

Figure 5: Map of Cambodian provinces and forest cover, 2005



The country of Cambodia has several types of forest cover. Of particular interest are the landscapes of the three clinical sites used for this thesis project (circled in red): Pursat, Preah Vihear, and Ratanakiri. In western Cambodia, Pursat is covered with evergreen forest (dark green). In the northern part of Cambodia, Preah Vihear has mainly deciduous forest (bright green). In eastern Cambodia, Ratanakiri has a mix of evergreen and deciduous forests with some dry woody shrubland. This figure was modified from (Sasaki et al., 2016) under a creative commons license.

1.2 ANTIMALARIAL CHEMOTHERAPEUTICS

1.2.1 Treatment of *Plasmodium falciparum*

The current first-line treatment for uncomplicated *P. falciparum* malaria is artemisinin-based combination therapy (ACT), which pairs a short-acting artemisinin derivative with a long acting partner drug. The exception to this is in treating women in their first trimester of pregnancy, at which time the preferred regime is clindamycin plus quinine for 7 days (WHO, 2015a).

The earliest commercially available antimalarial drug was quinine, which had been used for over 350 years. Resistance developed to quinine and was reported in 1844 (Cowman and Foote, 1990, Payne, 1987).

Prior to the development of artemisinin, chloroquine was the drug of choice for *P. falciparum*. Chloroquine was cheap and effective, and its widespread use led to malaria eradication in a number of countries. Chloroquine works by diffusing into and accumulating within the DV: almost 85% of chloroquine can be found in the DV (Bray et al., 2006). Within the DV, chloroquine prevents the formation of hemozoin, the non-toxic byproduct of hemoglobin digestion. Instead, heme accumulates as well as ferriprotophorphyrin IX (also called hematin), which is toxic to the cell (Roepe, 2009). However, significant resistance to chloroquine developed in the 1950s along the border of Cambodia and Thailand, rendering it ineffective (Payne, 1987). Resistance arose independently in South America, but spread from Southeast Asia to Africa in the 1970s, causing devastating morbidity and mortality (Payne, 1987).

The mechanism of resistance was elucidated by the discovery of a SNP in *chloroquine resistance transporter* (*pfcrt)* via the HB3xDd2 genetic cross, discussed further in Chapter 5 (Fidock et al., 2000). Analyses of *pfcrt* identified a 48 kb chromosomal segment that associated with the resistance phenotype (Wellems et al., 1991, Su et al., 1997), and allelic exchange experiments proved that the polymorphisms in *pfcrt* were responsible for chloroquine resistance (Sidhu et al., 2002). From a number of *pfcrt* polymorphisms in clinical isolates, the K76T polymorphism was identified and allelic exchange experiments have determined that this polymorphism is important in chloroquine resistance *in vitro* (Lakshmanan et al., 2005). However, the impact of *pfcrt* mutations is dependent on the genetic background of the isolate, as evidenced by the muted chloroquine resistance phenotype when K76T was introduced into sensitive lines 3D7 and D10 (Valderramos et

al., 2010). It is believed that polymorphisms in *pfmdr1* are also important in chloroquine resistance, as the HB3xDd2 cross secondarily mapped to a region on chromosome 5 containing *pfmdr1* that accounted for chloroquine resistance variability within the progeny (Patel et al., 2010). The 7G8xGB4 genetic cross also found that *pfmdr1* mutations could impact the chloroquine resistance phenotype (Sa et al., 2009, Sanchez et al., 2011). Thus, while initial studies may point to a single gene, or SNP, as the determinant of resistance, these studies showed it is also important to investigate the genetic background as it relates to resistance phenotypes.

The *pfcrt* gene encodes the PfCRT protein, which is a drug/metabolite transporter (Martin and Kirk, 2004) that localizes to the membrane of the DV (Fidock et al., 2000, Cooper et al., 2002). Chloroquine can be transported by mutant PfCRT out of the DV (Naude et al., 2005, Martin et al., 2009). Not surprisingly, chloroquine resistant isolates accumulate chloroquine at lower concentrations in their DVs than chloroquine sensitive isolates (Chinappi et al., 2010). However, there is also some evidence that chloroquine accumulation in the DV does not influence the resistance phenotype (Cabrera et al., 2009, Gligorijevic et al., 2008). The resistance-associated mutations in *pfcrf* cause PfCRT to transport protonated chloroquine, thus causing a leak of chloroquine and H^+ from the DV (Lehane et al., 2008, Lehane and Kirk, 2008).

The *pfmdr1* gene encodes PfMDR1, also called P-glycoprotein homologue 1 (PfPgH-1), an ABC transporter that shares homology with the human MDR1 transporter. This transporter is located on the membrane of the DV. Although it was originally believed to modulate chloroquine resistance, *pfmdr1* increased copy number has been more definitively associated with increased resistance to mefloquine (Wilson et al., 1993). There are also some reports linking *pfmdr1* increased copy number to decreasing susceptibility to piperaquine (Veiga et al., 2012, Chaorattanakawee et al., 2015), although it does not appear that these duplications are the major modulators of the piperaquine resistance phenotype.

Following the development of chloroquine resistance, dihydrofolate reductase inhibitors, including pyrimethamine, were used to treat *P. falciparum*, but resistance also developed in the 1980s (Schapira, 1984, Watkins et al., 1984). Mefloquine was used in the 1980s, but within 6 years, resistance had developed along the Thailand-Myanmar (then Burma) border (Nosten et al., 1991).

1.2.1.1 Artemisinin drug development

The discovery of artemisinin has been credited to Youyou Tu for her work in its development. During the Vietnam War, the Chinese-supported North Vietnamese army was experiencing high morbidity and mortality due to malaria. The North Vietnamese requested help from the Chinese government in combating malaria, spurring Chairman Mao to initiate Project 523, a secret project designed to develop novel antimalarial medications, in 1967. Almost immediately, several antimalarial combinations were sent to the North Vietnamese army to be tested. To increase the number of antimalarials in the pipeline long term, the pharmacopoeia of traditional Chinese medicine was screened, naming two plants with potential antimalarial activities: yingzhao and qinghao (Cui and Su, 2009). Concurrently, the Americans, also scourged by malaria in Vietnam, began a project that culminated in the discovery of another antimalarial: mefloquine (Trenholme et al., 1975).

Qinghao (*Artemisia annua*), also called sweet wormwood, had been used in traditional Chinese medicine for thousands of years and people in rural China often ate fresh qinghao to treat a malaria infection at the time of its reformulation by Project 523. Ancient texts, including those by fourth century physician Ge Hong specifically cited qinghao as a treatment for fever (presumably, a malarial fever) (Tu, 2011).

The plant origin of an effective antimalarial should have been no surprise, considering the original commercially available antimalarial, quinine, was isolated from the bark of the Peruvian cinchona tree in 1820. Similarly, it had long been used by the Quechua people of Peru for shivering. The cinchona tree was imported to Europe and used as an antipyretic in the 17th century and beyond (Cui and Su, 2009).

In order to find a stable and efficacious form of qinghao, scientists in Project 523 tried numerous formulations, but the ultimate recipe was devised by Youyou Tu using Ge Hong's original methods as a guide (Tu, 2011). In 1972, she presented her findings and proceeded with a small clinical trial of 30 patients (*P. falciparum* and *P. vivax*), noting that parasite clearance was achieved within 36 hours for *P. falciparum* following treatment. Active compounds, later named qinghaosu or artemisinin, were isolated and sent to Guangzhou University of Traditional Chinese Medicine where they provided promising results in clinical trials. The structure was solved by anomalous diffraction x-ray crystal analysis in 1976, spurring on the development of several artemisinin derivatives that are still in use today: artemether (1987), artesunate (1987), and

dihydroartemisinin (DHA) (1992). Youyou Tu was awarded the 2015 Nobel Prize in Medicine for her role in the discovery of artemisinin (Cui and Su, 2009).

Artemisinins are metabolized to the active metabolite, DHA, by the cytochrome P450 system, although the speed of conversion varies by derivative. DHA is quickly glucuronidated and eliminated, with a half-life of between 1-2 hours (Li et al., 1998). Artemisinins can kill parasites in the asexual and sexual cycles, meaning that they not only treat an infected patient, but block transmission by killing gametocytes (Skinner et al., 1996). Parasites are more than 100 times less sensitive to artemisinin derivatives in the ring stage than in the trophozoite stage (Klonis et al., 2013b), but they are nevertheless still killed by artemisinins. Artemisinins are inactive against the liver stage (Meister et al., 2011) and mature (stage V) gametocytes (Adjalley et al., 2011). Even so, the artemisinins are the most potent and fastest acting of the known antimalarials (Skinner et al., 1996).

Even with these new highly potent and fast-acting artemisinin derivatives, patients still experienced recrudescences where blood stage infection becomes patent after an initial phase of reduction of blood stage parasitemia. To combat this problem, the Institute of Microbiology and Epidemiology, and Chinese Academy of Military Medical Sciences focused on pharmaceuticals to pair with artemisinin derivatives to create novel combinations. They developed artemether-lumefantrine, artemisinin-piperaquine, and DHA-piperaquine phosphate (Cui and Su, 2009).

1.2.1.2 Mechanism of artemisinin action

Artemisinin and its derivatives are sesquiterpene lactones, meaning they have three isoprene units with a lactone ring. Sesquiterpene lactones are often found in plants, including artichokes, ginkgo biloba, and spinach. The mechanism of action of artemisinin remains controversial. Artemisinin must first be activated, beginning with the reaction of the 1,2,4-trioxane structure containing an endoperoxide bridge, with either erythrocytic heme (Wang et al., 2015b) or ferrous iron (Fe^{2+}) (Meshnick et al., 1993) or a product of hemoglobin digestion (Klonis et al., 2011). Given that parasites do not digest hemoglobin until mid-ring stage, it is believed that two falcipains are involved in artemisinin activation in the absence of hemoglobin in the early ring stage (Xie et al., 2016). In any case, this opening of the endoperoxide bridge creates an alkoxy radical, followed by a C-centered primary radical, which then alkylates heme to make a covalent heme-artemisinin adduct (Meunier and Robert, 2010, Kannan et al., 2002, Li and Zhou, 2010). These

adducts accumulate and the parasite dies at least partially from the toxic effects of heme, which damages through reactive oxygen species (ROS). ROS are formed by the one-electron reduction of oxygen, leading to the production of a highly reactive free radical. ROS are also often produced by the mitochondrial electron transport chain, which create O_2^- during aerobic respiration. This O_2^- is then converted by superoxide dismutase (SOD) to make H_2O_2. The Fenton reaction proceeds as follows: $Fe^{2+} + H_2O_2 \rightarrow Fe^{3+} + [H_1O_2^-] \rightarrow OH + OH^-$ (Winterbourn, 1995). This hydroxyl radical is highly reactive and toxic.

Other theories of artemisinin action include more traditional models of drug action, in which artemisinins bind to one or more target and exert their effects. Some evidence suggests that artemisinins may bind to and inhibit a calcium ATPase, PfATP6, which may function as a sarcoplasmic endoplasmic reticulum calcium ATPase (SERCA) (Krishna et al., 2010, Eckstein-Ludwig et al., 2003). This mechanism is close to the mechanism of thapsigargin, another sesquiterpene lactone that inhibits the SERCA and also inhibits the fusion of autophagosomes and lysosomes in the autophagic pathway in mammalian cells (discussed later) (Ganley et al., 2011). Recently, an alkyne-tagged artemisinin derivative with a biotin tag identified 124 proteins covalently bound to the derivative, the PfATP6 among them (Wang et al., 2015b). This experiment suggested that artemisinins may bind many proteins and therefore have many modes of action targeting different parasite processes. Although this result may suggest that artemisinins will react with anything and everything, previous work using radiolabeling suggested that artemisinins bound to specific proteins rather than the most abundant proteins (Asawamahasakda et al., 1994). Another hypothesis suggests that artemisinins bind to and inhibit phosphatidylinositol-3-kinase (PfPI3K) (Mbengue et al., 2015), the protein that produces the lipid phosphatidylinositol 3-phosphate (PI3P) and has been implicated in hemoglobin trafficking (Vaid et al., 2010). In addition to damaging the parasite with ROS from heme, there is also evidence to suggest that artemisinin plays a role in mitochondria and plasma membrane depolarization; these effects were dampened by iron chelators and free radical scavengers (Antoine et al., 2014).

1.2.1.3 Development of artemisinin resistance

Artemisinin monotherapy does not cure and recrudescence following treatment (R1 failures as defined by the WHO) have been a hallmark of artemisinin monotherapy since its development (Li et al., 1984). Hence, the recommendation for treatment with artemisinin has been to use ACT, which allows the bulk of the parasitic biomass to be

killed by the artemisinin derivative and keeps a long-acting partner drug in the patient's system for weeks to prevent recrudescence with parasites that may have survived the initial doses of artemisinin. Artemisinin efficacy is measured by the parasite clearance curve, which measures the decrease in parasite density that accompanies antimalarial treatment (White, 2011). Even sensitive parasites will still recrudesce following artemisinin treatment and, therefore, there needed to be a method to measure effectiveness apart from a lack of clinical recrudescences. The parasite clearance half-life, or the time at which a patient's parasitemia has decreased by half, is a clinical marker of artemisinin derivative efficacy, as the artemisinin derivative has a rapid onset, efficiently kills parasites, and then is rapidly excreted. The parasite clearance half-life became the metric to judge clinical effectiveness of artemisinin.

Delayed parasite clearance half-life was first reported as a clinical artemisinin resistance phenotype by the Mahidol Oxford Tropical Medicine Research Unit (MORU) out of their study site in Pailin, Cambodia near the border with Thailand, from 2007-2008 (Dondorp et al., 2009). Parasite clearance half-life of greater than 5 hours following artesunate monotherapy or ACT treatment is considered artemisinin-resistance (WHO, 2015b). Delayed parasite clearance half-life has now been reported throughout Southeast Asia (Thriemer et al., 2014, Phyo et al., 2012, Kyaw et al., 2013, Huang et al., 2015, Hien et al., 2012, Amaratunga et al., 2012, Ashley et al., 2014).

Parasite clearance times are logistically difficult to determine. They require patients to remain at the hospital or study site following diagnosis and treatment for the measurement of parasitemia over the course of several hours. Clearance times necessitate multiple blood draws or finger pricks from a given patient, which cause discomfort to the patient and require clinical personnel for collection and assessment. Therefore, the measurement of parasite clearance times are not always feasible, especially in low resource settings.

Due to the difficulties in collecting parasite clearance times, parasitemia on day 3 (approximately 72 hours) following treatment by microscopy can be a surrogate for clinical artemisinin resistance assessment. If more than 10% of a given population is positive by microscopy at day 3 following ACT, it is likely that clinical artemisinin-resistance is present in that population (White et al., 2015). This is an imperfect measure, especially since it depends heavily on initial parasitemia as well as the skill of a microscopist and precision of the measurement of parasitemia (Fairhurst and Dondorp,

2016); however, given the logistical difficulties in obtaining parasite clearance times, day 3 positivity represents another test for resistance.

These clinical assessments of artemisinin resistance do not tend to correlate with artemisinin-derivative half-maximal inhibitory concentration (IC50) values. As previously discussed, ring parasites are more than 100 times less sensitive to artemisinin derivatives in the ring stage than in the trophozoite stage (Klonis et al., 2013b). However, rings that are 2-4 hours post invasion (HPI) are uniquely sensitive to artemisinins (Klonis et al., 2013b). Oddly, other reports have indicated that the most artemisinin-resistant stage is 0-3 HPI rings (Witkowski et al., 2013a, Witkowski et al., 2013c). This increased resistance in early ring stages became the basis for the ring-stage survival assay (RSA), an *in vitro* measure of artemisinin resistance. In the RSA, a culture is pulsed with 700nM DHA in DMSO for 6 hours, the drug is washed away, and the culture is grown for 66 hours without drug. The surviving parasites are compared to those that survive DMSO alone. Less than 1% of artemisinin-sensitive parasites survive the assay, while *in vitro* artemisinin resistance is defined by $\geq$1% survival (Witkowski et al., 2013a). Thus, the RSA has become a standard assay for laboratory detection of parasite artemisinin sensitivity.

The threat of delayed parasite clearance remains somewhat controversial. On the one hand, patients with delayed clearance generally eventually clear their infections, largely due to the contribution of the partner drug in ACT. However, the increased survival of parasites past the initial exposures to an artemisinin derivative places increasing pressure on the partner drug with a larger burden of parasites to kill (Dondorp et al., 2011). Partner drug failures, in the form of recrudescence, have been reported as well (Amaratunga et al., 2016, Wongsrichanalai and Meshnick, 2008, Duru et al., 2015), prompting WHO guidelines in Cambodia to change from DHA-piperaquine to artesunate-mefloquine (WHO, 2016a). Since mefloquine resistance was previously ubiquitous in Southeast Asia, it is likely that artesunate-mefloquine will remain efficacious for a short time before a new ACT partner drug must be employed (Amaratunga et al., 2016).

If it is allowed to persist unchecked, this delayed parasite clearance half-life or partial resistance could lead to complete resistance to artemisinin derivatives. The deployment of ACT has led to recent declines in morbidity and mortality (White et al., 2014a, Carrara et al., 2006, Barnes et al., 2009, Landier et al., 2016, Adjuik et al., 2004) and therefore

losing this important tool could be devastating to malaria elimination efforts (White et al., 2014a).

Furthermore, the slow clearance rates decrease the utility of artemisinin derivatives as a treatment for severe malaria. Artemisinin derivatives have been a mainstay in the treatment of severe malaria and show improved clinical outcomes including reduction in the rates of coma, convulsions, and mortality as compared to quinine (Dondorp et al., 2005, Dondorp et al., 2010). Given the high rates of mortality of severe malaria and the large burden of malarial disease in Africa (Dondorp et al., 2008, Taylor et al., 2004, Newton et al., 1998, Seydel et al., 2015), the loss of artemisinin's efficaciousness could result in a jump in morbidity and mortality from severe malaria alone (White, 2008).

1.2.1.3.1 Proposed mechanisms of artemisinin-resistance

Initial studies investigating the genetic determinants of artemisinin resistance implicated polymorphisms on chromosome 13 (Cheeseman et al., 2012, Takala-Harrison et al., 2013). A subsequent study pressuring a Tanzanian line, F32, *in vitro* with a 125-cycle regimen of artemisinin over several years identified a single nucleotide polymorphism (SNP) in the *PF3D7_1343700 kelch13* (*k13*) gene that increased survival in the RSA (Ariey et al., 2014). Follow-up studies have determined that a number of polymorphisms in *k13* associate with delayed parasite clearance half-life (Ashley et al., 2014, Menard et al., 2016, Talundzic et al., 2015, Huang et al., 2015) and that genetic editing of a number of these loci modulates the *in vitro* resistance phenotype (Ghorbal et al., 2014, Straimer et al., 2015). Interestingly, editing different *k13* polymorphisms into the same genetic background resulted in differing levels of *in vitro* resistance (Straimer et al., 2015), suggesting that other factors may also influence resistance. Of the 124 non-synonymous *k13* polymorphisms that have been reported, only 20 have been associated with artemisinin resistance, and only 4 have been validated through genetic editing (Fairhurst and Dondorp, 2016).

In addition to the presence of these *k13* polymorphisms, the *P. falciparum* genetic population in Southeast Asia has an unusual structure. Genetically distinct clonal subpopulations known as founder populations have emerged in Southeast Asia, possibly indicating a bottleneck followed by expansion (Miotto et al., 2013, Amaratunga et al., 2014). Several of these founder populations carry different *k13* polymorphisms, suggesting the independent development of *k13* mutations. The *k13* mutations tend to

occur on a similar genetic background which includes SNPs in *apicoplast ribosomal protein s10* (*arps10*), *chloroquine resistance transporter* (*crt*), *ferredoxin* (*fd*), and *multidrug resistance 2 transporter* (*mdr2*) along with others (Miotto et al., 2015). The function of these background mutations is unknown, although it is hypothesized that they may contribute to parasite fitness, transmissibility, or partner drug susceptibility.

The kelch protein K13 is made of three domains: (1) a Broad complex_Tramtrack_Bric-a-brac (BTB)/Pox virus_zinc finger (POZ) domain (2) a *Plasmodium*-specific N-terminal domain and (3) a C-terminal domain with six kelch motifs that each form a six-bladed β-propeller (Tilley et al., 2016, Adams et al., 2000). This protein is homologous to the mammalian protein Kelch-like ECH-associated protein 1 (Keap1), an E3 ubiquitin ligase substrate that is important in modulating cellular stresses by targeting NF-E2-related factor 2 (Nrf2) (Itoh et al., 1999, Itoh et al., 2003, Kobayashi et al., 2004). Keap1 acts by constitutively ubiquitinating Nrf2 and therefore targeting it for degradation via the proteasome. However, upon the sensing of environmental stress, Keap1 does not ubiquitinate Nrf2, Nrf2 accumulates and then translocates to the nucleus where it acts as a transcription factor for anti-inflammatory and pro-survival gene pathways (Suzuki and Yamamoto, 2017, Cullinan et al., 2003). Unfortunately, no Nrf2 homologue appears to exist in *Plasmodium* (Gacesa et al., 2015) and, therefore, alternative mechanisms of action for K13 must be explored.

Based on the association of artemisinin resistance with *k13* polymorphisms, several possible resistance mechanisms have been posited wherein the resistant isolate is able to withstand the deleterious effects of artemisinin based on an ability to withstand oxidative stress. Resistant isolates appear to have lower levels of ubiquitin following artemisinin treatment *in vitro*, indicating more efficient responses to cellular stressors (Dogovski et al., 2015). An *ex vivo* transcriptomics study revealed the upregulation of proteins involved in the unfolded protein response (UPR), specifically the *Plasmodium* reactive oxidative stress complex (PROSC) and T-complex protein-1 (TCP-1) ring complex (TRiC) (Mok et al., 2015). Given the connection of the UPR to the ubiquitin-proteasome pathways, it is unsurprising that proteasome inhibitors appear to act synergistically with artemisinin, perhaps by mitigating the parasite's ability to endure damage by artemisinin (Dogovski et al., 2015, Li et al., 2016).

The upregulation of a stress response pathway in artemisinin-resistant isolates appears to divert energy from progression through the lifecycle in favor of the preservation and

repair of the parasite in earlier stages. Multiple groups have reported cell cycle arrest following artemisinin treatments (Mok et al., 2015, Witkowski et al., 2010) and others have reported prolongation of the ring stage beyond the typical 24 hour period in resistant isolates (Mok et al., 2015, Hott et al., 2015a). This growth deceleration occurs in other organisms in response to oxidative stress events that activate repair pathways while downregulating most metabolic pathways (Ron and Walter, 2007, Gosline et al., 2011, Amm et al., 2014).

Parasite dormancy, also called quiescence, has been demonstrated by *P. falciparum* following certain drug treatments, most notably artemisinin treatment. Lower doses of artemisinin have been shown to slow growth *in vitro* (Klonis et al., 2011). Artemisinin-resistant lines produced from *in vitro* drug pressure remain in a quiescent ring stage following treatment with artesunate (Witkowski et al., 2010). Artemisinin-sensitive lines with different genetic backgrounds have demonstrated the ability to remain in the dormant state for consistent but varying lengths of time following treatment with DHA (Teuscher et al., 2010). Early recovery from dormancy after artemisinin treatment may be an advantage to surviving drug treatment, possibly due to a transient arrest at the ring stage of development following drug exposure (Witkowski et al., 2013c, Tucker et al., 2012, Teuscher et al., 2012). Witkowski et al. (Witkowski et al., 2013c) demonstrated that a higher proportion of parasites from patients with prolonged parasite clearance half-life were able to enter dormancy during a 24-hour pulse of DHA, thus accounting for a culture's shorter recrudescence time. Amino acid starvation has also been shown to arrest growth *in vitro*, in particular, restriction of isoleucine, which is the only amino acid that is not present in human hemoglobin (Liu et al., 2006, Istvan et al., 2011). There may be some relationship between the ability of a parasite to enter a dormant state and its ability to survive artemisinin.

An understanding of the function of the K13 protein is important to elucidate the mechanism of artemisinin resistance. One function of K13 in *P. falciparum* is to bind and target PI3K for degradation (Mbengue et al., 2015). This binding has been shown to be disrupted by the C580Y *k13* polymorphism, which is associated with artemisinin resistance, increasing the levels of PI3K and its product, PI3P, in resistant isolates (Mbengue et al., 2015). However, the changes reported in PI3K and PI3P were relatively slight, with the isogenic kelch mutant line having only 1.5x the amount of PI3P as the

wild-type; further, these findings have not been repeated in an independent laboratory (Tilley et al., 2016).

1.2.1.3.2 Future directions to curb artemisinin resistance

Novel antimalarials are in development, but will require more time before they are widely available. Such drugs include spiroindolones (White et al., 2014b), endoperoxides (Phyo et al., 2016), and imidazolopiperazines (Leong et al., 2014). The endoperoxide, OZ439, has a longer half-life than the artemisinins and is therefore expected to be more effective than artemisinin (Phyo et al., 2016, Moehrle et al., 2013). Repurposing already developed drugs as antimalarials may represent a quicker path to effective treatment. Proteasome inhibitors including Carfilzomib and Bortezomib show promise against *P. falciparum* and display synergy with artemisinins (Dogovski et al., 2015). PI3K inhibitors also show activity against *P. falciparum*, although it is unknown if they are efficacious against artemisinin-resistant isolates (Mott et al., 2015). An understanding of the current mechanism of artemisinin resistance may reveal novel targets for future drug development. The K13 protein represents a possible drug target, especially in the current age of antibody-based therapies (Copple, 2012).

Perhaps the fastest way forward involves rotating the current arsenal of antimalarials. This has been deployed in Cambodia with the changing first-line regimen from DHA-piperaquine to artesunate-mefloquine based on the recent emergence of piperaquine resistance (WHO, 2016a). While this currently remains temporarily effective, it seems it is only a matter of time before parasites develop resistance to all the currently available antimalarials, as they have been subject to their selective pressure for years already. Further, it is logistically difficult to deploy these co-formulated combination therapies on a rotating basis, especially in a low resource setting. Co-formulated drugs must be manufactured and deployed to all areas, while drugs with the previous co-formulation must be destroyed since they are no longer efficacious. While it would be possible to circumvent this problem by producing artemisinin-derivative monotherapy and supplementing it with a partner drug, rather than co-formulating them in a single pill, this presents its own challenges. This may introduce artemisinin monotherapy, which is not curative even with sensitive parasites, into circulation. Clinicians may be more likely to erroneously prescribe monotherapy and patients may be more likely to take only one rather than both drugs, even if combination therapy is provided to them. With an oscillating regimen, clinicians must be educated about the new formulations and must

keep up with the ever-changing recommendations. The idea of cycling drugs is reactive rather than proactive and so this method of drug deployment will constantly lag emerging parasite drug-resistance profiles.

Another option is triple artemisinin-based combination therapies (TACTs) which are currently being studied by the Tracking Resistance to Artemisinin Collaboration-II (TRAC-II) to determine safety and efficacy of DHA-piperaquine plus mefloquine and artemether-lumefantrine plus piperaquine in 17 countries in Asia and Africa (WWARN, 2017). The usage of these antimalarial regimens may buy enough time to bridge the gap while waiting for novel antimalarial development. While this may be temporarily effective, combination therapies again represent a stopgap. Lessons should be learned from other diseases with a history of drug resistance, such as *Mycobacterium tuberculosis*. Tuberculosis, the disease caused by *M. tuberculosis*, is treated with a four drug regimen; here resistance has appeared, evolved, and spread against this treatment. Multidrug-resistant and extensively drug-resistant tuberculosis, are treatable, but have worse outcomes than drug-susceptible stains (Dheda et al., 2014). Additionally, these multi-drug regimens have not stopped the evolution of resistance, as extremely drug-resistant and totally drug-resistant tuberculosis have since appeared (Velayati et al., 2009, Johnston et al., 2009). Therefore, it is important to understand that simply adding more drugs will not be a final solution to the issue of drug-resistant *P. falciparum*.

Malaria elimination should be a priority in Southeast Asia before all available antimalarials become obsolete. Malaria elimination has been successful in a number of areas following the widespread use of insecticides and other mosquito control measures such as the draining of swamplands. From 1955-1969, the WHO drove forth a campaign against malaria known as the "Global Malaria Eradication Programme" (GMEP), mainly utilizing chloroquine, insecticides, and active case detection towards the goal of eradicating malaria worldwide. Although there were gains in a number of countries, the program was ultimately abandoned as elimination did not seem within reach in a number of countries (Nájera et al., 2011). Following the GMEP, some countries experienced resurgences of malaria even after the interruption of transmission brought on by the GMEP efforts. Some of these setbacks can be attributed to resistance in chloroquine, as well as resistance, both biological and societal, to the use of insecticides. The GMEP, along with the idea of eradication, was ultimately abandoned in favor of control measures.

However, since 2000, global eradication efforts have been revamped. This revitalization is due to an increase in funding from a variety of sources, in particular a commitment of $2.5 billion by the Bill and Melinda Gates Foundation. This outpouring of funding along with the development and deployment of artemisinins, have led to a drop in prevalence and mortality, and a renewed hope of the idea of malaria eradication. The WHO has recently updated their strategies in the region, calling for the urgent elimination of malaria in the Greater Mekong Subregion of Southeast Asia (WHO, 2015c). Their proposal calls for active case detection and management, disease prevention via vector control, and malaria/entomological surveillance (Kazadi Mulombo, 2015). The new goals include malaria elimination in Cambodia by 2020 and elimination in all Greater Mekong Subregion countries by 2030. These are ambitious goals and time will tell if they are achievable in the region.

These goals are threatened by the prospect of drug resistance, both from artemisinin and from partner drugs. Without a viable vaccine, malaria will not be eradicated without an arsenal of highly efficacious antimalarial drugs. If artemisinin resistance is allowed to evolve and spread, the gains of the past fifteen years may quickly be erased in favor of renewed transmission and epidemics in previously eliminated areas.

1.3 AUTOPHAGY

Macro-autophagy, hereafter referred to as autophagy, is an intracellular recycling pathway by which cells target damaged organelles or bulk cytoplasmic material to the lysosome, where it is broken down. The degraded materials are ultimately recycled for cellular functions. A general schematic of the autophagy pathway can be seen in Figure 6.

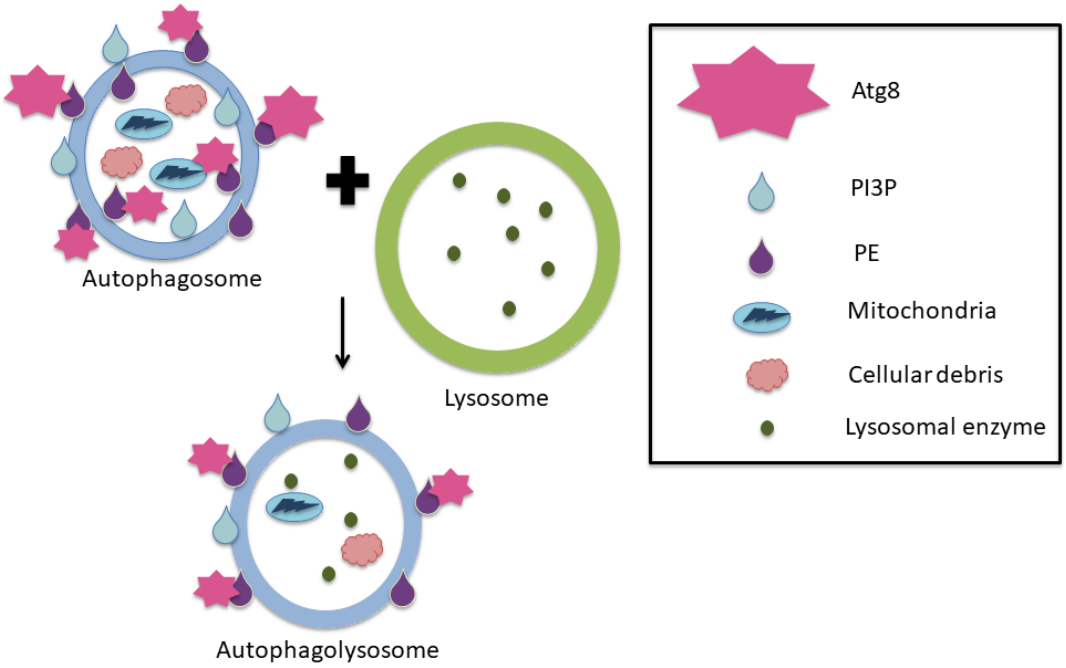


Figure 6: Autophagy schematic

The autophagy pathway consists of a double-membraned autophagosome decorated with lipid (PI3P represented by blue teardrops and PE represented by purple teardrops) and protein (Atg8 represented by pink stars) markers containing cytoplasmic material and organelles. This autophagosome fuses with the lysosome to form an autophagolysosome. The autophagolysosome is single-membraned, as the inner membrane of the autophagosome is degraded by the acidic lysosome. The cytoplasmic contents (mitochondria represented by blue ovals with zigzags and cellular debris represented by peach clouds) of the autophagosome are degraded in the autophagolysosome as well and the breakdown products are used again by the cell.

1.3.1 The discovery of autophagy

The history of the discovery of autophagy begins at the end of the pathway. The lysosome was discovered by Christian de Duve in 1955 by a cellular fractionation study of a rat liver using consecutive centrifugation leading to the detection of an organelle with a number of hydrolytic enzymes, a low pH, and an acid phosphatase (De Duve et al., 1955). This work eventually garnered him the 1974 Nobel Prize in Physiology or Medicine.

Electron microscopy was then used to visualize lysosomes *in situ* again in rat liver cells (Novikoff et al., 1956). Studies of the lysosome led to an understanding of endocytosis, a process by which a cell engulfs foreign extracellular material, packaging it into a phagosome. The phagosome traverses the cell and fuses with the lysosome for degradation.

Although they were not named such at the time, the first autophagosomes were visualized in murine kidney tubule cells by electron microscopy (Clark, 1957). These murine autophagosomes were found to have rare organelles, including mitochondria. Later, the autophagosome was found to be a double-membraned compartment containing cytoplasmic material, including organelles, but lacking in hydrolytic enzymes characteristic of the lysosome (Arstila and Trump, 1968). This structure was differentiated from an autophagolysosome, which had a single membrane and contained enzymes specific to the lysosome, thus representing the fusion product of the autophagosome and the lysosome (Arstila and Trump, 1968). In 1963, Christian de Duve coined the term "autophagy" to mean the pathway of targeting cytoplasmic contents to lysosomes (Figure 6) (Ohsumi, 2014).

Autophagic bodies filled with cytoplasm and organelles were visualized in the yeast vacuole by light microscopy following nitrogen starvation (Baba et al., 1994). In the cytoplasm, these vesicles were double-membraned and determined to be autophagosomes (Baba et al., 1995). Therefore, autophagy could be measured by following autophagic bodies using light microscopy. This was the first rudimentary autophagy monitoring assay. A more reliable system was soon created, using a pro-form of a vacuolar alkaline phosphatase, Pho8Delta60, which was engineered to remain in the cytosol (Noda and Klionsky, 2008). This enzyme is delivered to the vacuole only by autophagy. Once in the vacuole, the enzyme is cleaved and activated. The enzymatic activity, therefore, is a surrogate marker for the level of autophagy. Following the creation of these assays, numerous other autophagy measuring assays have been developed (Klionsky et al., 2016).

The majority of autophagy-related genes were discovered by a yeast screen to identify mutants that did not survive nitrogen starvation (Tsukada and Ohsumi, 1993). Further studies also identified a number of autophagy-related genes in yeast, creating a list of the core machinery that forms the basis for the autophagy pathway (Thumm et al., 1994, Harding et al., 1995). These genes were later unified under the nomenclature of *ATG* (autophagy-related genes). For his efforts in characterizing the genetic basis for

autophagy in yeast, Yoshinori Ohsumi was awarded the 2016 Nobel Prize in Physiology or Medicine.

1.3.2 Autophagy pathway

Autophagy takes three major forms: (1) macroautophagy, (2) microautophagy, and (3) chaperone-mediated autophagy (CMA). Neither CMA nor microautophagy use an autophagosome. Microautophagy instead targets cytoplasmic contents directly into the lysosome through the invagination of the lysosomal membrane. CMA, which only occurs in mammalian cells, uses a chaperone which binds to and unfolds a targeted protein and then transports the protein to the lysosome.

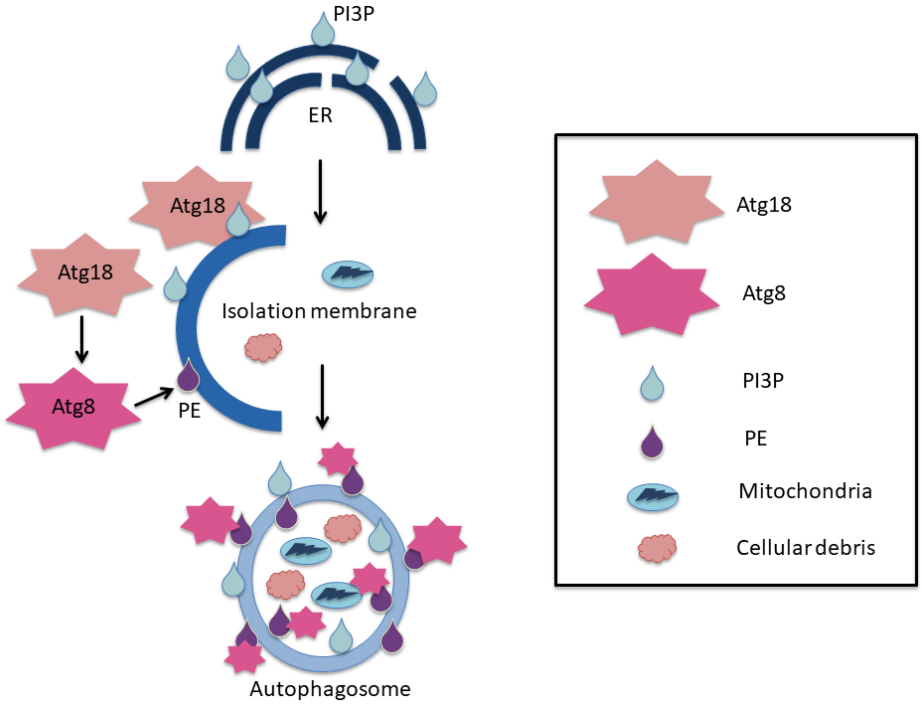


Figure 7: Autophagy initiation pathway

After receiving signals from mTOR and other upstream proteins, autophagy is initiated by the production of an isolation membrane from the endoplasmic reticulum (ER). PI3P (represented by blue teardrops) decorates the isolation membrane and Atg18 (represented by peach stars) binds to the lipid. Atg18 is then involved in the recruitment of Atg8 (represented by pink stars) and the lipidation of Atg8 with phosphatidylethanolamine (PE) (represented by purple teardrops). There are a number of other steps involving other autophagy-related proteins that are involved in the lipidation of Atg8, which are detailed in the text. The isolation membrane then pinches off to form a double-membraned autophagosome decorated with PI3P and Atg8-PE with cytoplasmic contents inside.

The autophagy pathway is highly conserved from yeast up to humans. The autophagy pathway begins with the formation of a membrane, called the phagophore or isolation

membrane (Figure 7). This membrane elongates and forms a crescent, which eventually pinches off and seals to form the autophagosome, a double-membraned vesicle full of cytoplasmic contents. The autophagosome then fuses with the lysosome, and the lytic enzymes of the lysosomal compartment degrade the inner autophagosomal membrane, leaving the structure single-membraned. This structure then becomes a residual body and the degradation products are recycled back to the cell for cellular maintenance.

The autophagy pathway is tightly controlled by a variety of autophagy-related proteins called Atgs. Autophagy is in part controlled by TORC1. When nutrients are plentiful, Autophagy-related protein 13 (Atg13) is phosphorylated by TORC1 and is dephosphorylated in starvation conditions (Kamada et al., 2000). Atg13 binds to Autophagy-related protein 1 (Atg1) with higher affinity when it is dephosphorylated, forming Atg1-Atg13, which in turn binds to the Autophagy-related protein (Atg17)-Autophagy-related protein 29 (Atg29)-Autophagy-related protein 31 (Atg31) complex under starvation conditions (Ragusa et al., 2012, Kabeya et al., 2009). These complexes form at the pre-autophagosomal structure (PAS), which is akin to a cellular meeting spot for autophagy-related proteins to gather at the start of autophagy. Autophagy-related protein 9 (Atg9) vesicles also gather at the PAS to bind to Atg17 and then recruit Phosphatidylinositol-3-kinase (PI3-K). Atg9 is thought to act as a courier, delivering lipids needed for the growing membranes—initially the isolation membrane and then the autophagosomal membrane. PI3-K is also required to begin autophagy. PI3-K complex I is made of Vps34, Vps15, Vps30, and Autophagy-related protein (Atg14) and it is essential for autophagy (Kihara et al., 2001). PI3P, the product of PI3-K, is important for the formation of the isolation membrane and in autophagosome membrane formation (Obara et al., 2008). Atg18 binds to PI3P at the beginning of autophagy. It has also been shown to bind PI3,5P, although this is not involved in the autophagy pathway, but rather in the regulation of the vacuole (Stromhaug et al., 2004). The binding of PI3P to Atg18 at the PAS allows for the recruitment of the Atg12-Autophagy-related protein 5 (Atg5)-Autophagy-related protein 16 (Atg16) complex. An essential step in the autophagy pathway is Atg8 lipidation. The C-terminal arginine on the end of Atg8 is processed by the cysteine protease Autophagy-related protein 4 (Atg4), then Atg8 is activated by the E1 protein Autophagy-related protein 7 (Atg7) and transferred to E2 enzyme Autophagy-related protein 3 (Atg3) (Ichimura et al., 2000). Atg3 is activated by the Atg12-Atg5 complex, which facilitates Atg8 lipidation by phosphatidylethanolamine (PE) to form

Atg8-PE (Ichimura et al., 2000). Atg12 is an ubiquitin-like protein that is similarly activated by E1 protein Atg7 and transferred to Autophagy-related protein 10 (Atg10), an E2 enzyme. The C-terminal glycine of Atg12 is then conjugated to a lysine residue of Atg5 to form the Atg12-Atg5 complex used for the lipidation of Atg8 (Mizushima et al., 1998, Sakoh-Nakatogawa et al., 2013, Hanada et al., 2007). Atg8-PE is the active form, which is involved in elongation of the isolation membrane and the delivery of cellular contents to the autophagosome (Xie et al., 2008).

Although much of the autophagy pathway was originally elucidated in yeast, this pathway is highly conserved among species. Because of the importance of autophagy in higher eukaryotic cells, Atg proteins tend to have paralogues that perform similar functions, though it is possible that the additional functions of these proteins are yet to be identified. In addition to these duplications, there are differences in function. As stated, the CMA occurs only in mammalian cells. There are also differences in nomenclature. Atg8 is dubbed LC3 and upon processing and lipidation is known as LC3-I and LC3-II, respectively (Kabeya et al., 2000). Similar to Atg8-PE, the amount of LC3-II has been used to monitor autophagosome formation (Kabeya et al., 2000).

Atg18 is a PROPPIN also called WD repeat domain phosphoinositide-interacting protein (WIPI) in mammalian systems. There are four WIPI proteins: WIPI1-4 (Proikas-Cezanne et al., 2004), which all fold into seven-bladed β-propeller structures (Baskaran et al., 2012, Proikas-Cezanne et al., 2004, Watanabe et al., 2012). WIPI1 and WIPI2 are closely related to Atg18 and have well-known functions in autophagy, while WIPI3 and WIPI4 are distinct (Behrends et al., 2010, Polson et al., 2010a, Proikas-Cezanne et al., 2004). WIPI2 has several splice variants, with WIPI2B and WIPI2D functioning similarly to WIPI1. WIPI1 and WIPI2 are important in the binding of PI3P at the beginning of autophagy, much like Atg18 in other organisms. Both WIPI1 and WIPI2 decorate the inner and outer membranes of autophagosomes upon the induction of autophagy (Proikas-Cezanne and Robenek, 2011, Proikas-Cezanne et al., 2007), although in yeast Atg18 only decorates the luminal membrane (Cheng et al., 2014). Both WIPIs bind to PI3P and are regulated by the production of PI3P (Codogno et al., 2011). WIPI1 is necessary for the lipidation of LC3 (Mauthe et al., 2011), as has also been shown with WIPI2B. When WIPI2B is disturbed with siRNA, LC3 lipidation and puncta formation are both inhibited (Polson et al., 2010a). WIPI2 is also important in the movement of Atg9, much like Atg18 (Reggiori et al., 2004). It was determined by mass spectrometry that WIPI2B binds to the

ATG12-ATG5-ATG16L1 complex and that its binding to ATG16L1 by two arginines on WIPI2B is essential for autophagy (Dooley et al., 2014, Dooley et al., 2015). WIPI2B is important to localize the ATG16L1 complex to the isolation membrane, as seen when the addition of a KRAS CAAX motif directed WIPI2B and subsequently the ATG16L1 complex to the plasma membrane, independent of PI3P binding (Dooley et al., 2014).

Less is understood about WIPI3 and WIPI4. The function of WIPI3 is unknown (Proikas-Cezanne et al., 2015). WIPI4 is essential for autophagy, much like WIPI1 and WIPI2. WIPI4 localizes to the autophagosome upon starvation, and a siRNA disrupted WIPI4 caused impairment of autophagosome membrane formation (Lu et al., 2011). WIPI4 may be involved in binding Autophagy-related protein 2 (Atg2) and the recruitment of the Atg2-Atg5-Atg16L1 complex to the autophagosome membrane. However, WIPI4 appears to act downstream of LC3-II in the formation of the autophagosome, unlike WIPI1 and WIPI2, which function before LC3-II (Proikas-Cezanne et al., 2015). A recent study has also implicated both WIPI3 and WIPI4 in modulating the size of autophagosomes (Bakula et al., 2017). Further, unlike WIPI1 or WIPI2, WIPI3 and WIPI4 appear to be involved in glucose-starvation induced autophagy (Bakula et al., 2017).

The common thread among these WIPI proteins is their ability to bind phosphoinositides. Phosphoinositides are phospholipids that exist in cellular membranes that make up less than 15% of the total phospholipids in eukaryotic cells (Di Paolo and De Camilli, 2006). They are composed of two fatty acid chains and a phosphate esterified to a glycerol backbone. A cyclic polyol myoinositol forms the polar head group with hydroxyl groups at each carbon position, other than the carbon attaching to the phosphate (Falkenburger et al., 2010). This lipid is referred to as a phosphatidylinositol and is synthesized in the ER then distributed about the cell by proteins or vesicles. Phosphoinositides are embedded in membranes, forming a signaling network and a type of cellular barcode specific to each membrane type. Each of the seven phosphoinositides are created from phosphorylation of the phosphatidylinositol at the 3, 4, and/or 5 position. Each of these lipids is primarily localized to a specific type of membrane in the cell: PI4,5P2, PI3,4,5P3, PI4P, and PI3,4P2 at the plasma membrane, PI4P in the Golgi apparatus, PI3P on early endosomes and autophagosomes, PI3,5P on late endosomal vesicles, and PI5P is not well understood (Di Paolo and De Camilli, 2006). These lipids can bind proteins from their positions in membranes and therefore form important signaling and localization

components of membranes. The phosphoinositides that are located at the plasma membrane are important in signal transduction. The specific phosphoinositides membrane composition can form a code that helps the cell identify membrane type and organelle identity.

PI3P is of particular interest to this thesis work. It is in relatively low abundance in cells, but it is nonetheless very important for the endosomal and autophagy pathways. PI3P binds to several protein domains to facilitate its function as a signaling lipid. It can bind to FYVE domains, which are cysteine-rich motifs approximately 70 residues long (Burd and Emr, 1998, Birkeland and Stenmark, 2004). The sequence that binds PI3P is a (R/K)(R/K)HHCR sequence that forms a basic binding pocket and a hydrophobic projection that can enter the membrane to facilitate binding (Misra and Hurley, 1999). PI3P can similarly bind PX domains, which are approximately 120 residues long and can be found in $p40^{phox}$ and $p47^{phox}$ subunits (Ponting, 1996, Birkeland and Stenmark, 2004, Balla, 2005). PI3P is important in a variety of functions in endosomes: membrane tethering, fusion, cytoskeleton interactions, and signaling (Di Paolo and De Camilli, 2006). PI3P can be phosphorylated to form PI3,5P2, which is thought to initiate endosomal buds (Michell et al., 2006).

In *P. falciparum,* PI3P has been found in relatively large quantities in the infected erythrocyte (Tawk et al., 2010). Although this PI3P could be involved in parasitic autophagy, it may also facilitate hemoglobin digestion. The plasmodial PI3K is exported into the erythrocyte, most likely by a secretory pathway given its sensitivity to treatment with brefeldin A and its lack of PEXEL motif (Vaid et al., 2010, Marti et al., 2004). It is possible that this *P. falciparum* generated PI3P is used to hijack erythrocytic endosomal pathways in order to target hemoglobin to the parasite for hemoglobin digestion (Payrastre et al., 2012).

As mentioned earlier, PI3P is synthesized by PI3K class III, also called Vps34 or PIK3C3 in mammals (Schu et al., 1993). PI3K also exists as class I, which are important in cancer development and inflammation, and class II, which has an unknown role (Vanhaesebroeck et al., 2010). *Plasmodium* parasites only have class III PI3K as do *S. cerevisiae* (Herman and Emr, 1990). Generally, PI3K enzymes are kinases that phosphorylate the hydroxyl group at the 3 position of phosphoinositides and are important in regulating cell growth, cell cycle, survival, vesicle trafficking, and migration. PI3K class III has three complexes in yeast: complex I is involved in autophagy, complex II in

vacuole protein sorting, and complex III in a pheromone response (Vanhaesebroeck et al., 2010). Complex I is made up of Vps15, Vps30 (also called Beclin1 in mammalian systems), Vps34, and autophagy-related protein 14 (Atg14). Vps34 is essential for autophagy in yeast, as it is the source of PI3P needed for autophagosome formation and Atg18 binding (Kihara et al., 2001). It also is important in mammalian systems for the initiation of the omegasome, which goes on to form the autophagosome at the beginning of autophagy (Axe et al., 2008). Although it is important in autophagy, Vps34 is also vital for endosomal trafficking. The endosomal pathway involves early endosomes, multivesicular bodies, and late endosomes, which, just like autophagosomes, ultimately fuse with the lysosome (Tooze et al., 2014).

1.3.3 Autophagy function

One of the principle functions of autophagy is as a metabolic pathway, which recycles cellular contents, especially during times of stress. Autophagy is upregulated by fasting and downregulated during a fed state. This was first demonstrated by increases in the number of autophagosomes following glucagon treatment and decreases using insulin (Pfeifer and Warmuth-Metz, 1983, Deter et al., 1967). Similarly, protein degradation experiments showed that protein degradation increased as amino acid content decreased in the media (Mortimore and Ward, 1976). Specifically in yeast, the presence of tyrosine, phenylalanine, glutamine, proline, histidine, tryptophan, methionine and, most starkly, leucine (Seglen et al., 1980) inhibits autophagy (Mortimore et al., 1983).

Control of the autophagy pathway is by the mammalian target of rapamycin complex 1 (mTORC1). For example, blockage of the solute carrier family 1 member 5 (SLC1A5) transporter, which blocks the uptake of L-glutamine, leads to mTORC1 inhibition and the activation of autophagy (Nicklin et al., 2009). Conversely, when nutrients abound, mTORC1 represses autophagy (Sheen et al., 2011). ULK1/2 complexes with mTORC1 during nutrient-rich conditions, but the complex dissociates during nutrient deprivation. ULK1/2 is dephosphorylated and autophosphorylates its active sites, allowing it to activate autophagy through the phosphorylation of other Atgs (Chan, 2009, Jung et al., 2009). Thus, autophagy is intricately involved in nutrient balance and acquisition.

Autophagy is important in cellular homeostasis and provides the cell with a mechanism to renew cellular components. Because of this, autophagy is linked with other cellular degradation pathways including the proteasome and ubiquitination pathways. Cells

naturally accumulate damaged organelles and other cellular debris, such as misfolded or aggregated proteins, that needs to be removed periodically. When Atg5 was knocked out in neuronal cells, this cellular garbage, in the form of ubiquitinated proteins, accumulated and were associated with neurodegeneration (Hara et al., 2006). Defects in mitophagy lead to Parkinson's disease, due to mutations in *PARK2* and *PINK1* (Kitada et al., 1998). *PARK2* encodes parkin, an E3 ubiquitin ligase, which is defective in familial forms of Parkinson's disease (Youle and Narendra, 2010). In skeletal muscle, knocking out Atg5 leads to the accumulation of ubiquitinated proteins and defective mitochondria (Masiero et al., 2009). Similarly, autophagy knockouts in hepatocytes lead to hepatic failure; when autophagy is knocked out in cardiomyocytes there is hypertrophy and dysfunction (Mizushima and Levine, 2010).

Autophagy is always active at a basal level, although it can be upregulated during times of stress. During starvation, as well as other stressors, mitochondria create ROS including H_2O_2 as discussed earlier. H_2O_2 oxidizes Atg4, inactivating it and thus allows Atg8 to remain lipidated and activated (Scherz-Shouval and Elazar, 2007). ROS also upregulate the expression of a subset of autophagy related genes in yeast, demonstrating that ROS can trigger autophagy (Thorpe et al., 2004). Once ROS induce autophagy, autophagy functions to reduce both the production and the effects of ROS. By inducing mitophagy, which is autophagy specifically targeted to mitochondria, autophagy can often remove the source of the ROS (Jin and White, 2007). ROS damage a number of organelles and proteins, which can be removed via autophagy. ROS can cause proteins to unfold and aggregate (Fink, 1998), which can be removed by autophagy. Thus, ROS can activate autophagy, which acts as a pro-survival mechanism to repair cellular functioning during stress. Autophagy is also induced by hypoxia through hypoxia-inducible factor 1α (HIF1α) and through AMPK in the presence of severe hypoxia (Bellot et al., 2009, Papandreou et al., 2008). Increased cytoplasmic calcium levels inhibit mTORC1, causing upregulated autophagy in an AMPK-independent manner (Hoyer-Hansen et al., 2007, Grotemeier et al., 2010). Thus, autophagy can be induced through a variety of mechanisms.

Autophagy has a number of different functions. The following paragraphs provide an overview of the field but are by no means exhaustive. Further, as autophagy is a relatively recently discovered pathway, there are many unknowns within each of these fields.

Autophagy has diverse functions in cancer, with conflicting evidence regarding whether it promotes or suppresses tumors. There is strong evidence that autophagy can be important in the suppression of cancer, depending on the context. *Beclin 1* is a homolog of Autophagy-related protein 6 (Atg6) that was shown to be deleted in a large proportion of breast and ovarian cancers (Aita et al., 1999). The autophagy functions of Beclin 1 inhibit proliferation, clonigenicity, and tumorigenesis of MCF7 breast cancer cells *in vitro* (Liang et al., 1999). Tumor suppressor genes such as *PTEN*, *TSC1*, *TSC2*, and *p53* can inhibit TOR, thus inducing autophagy (Levine and Kroemer, 2008). Upon the deletion of p62 in mice, hepatic tumor sizes were reduced (Takamura et al., 2011). Autophagy degrades p62, which causes KEAP to bind to and degrade NRF2. Given that NRF2 promotes tumor survival through the expression of proinflammatory and prosurvival genes, the degradation of NRF2 is decidedly anticancer (Komatsu et al., 2010, Duran et al., 2008). More direct evidence of the role of autophagy in cancer is the finding that tumor proliferation was accelerated in *Atg7* deleted murine lung cancer (Strohecker et al., 2013). Autophagy can protect against the development of cancer by removing dysfunctional, leaky mitochondria and thus preventing the accumulation of DNA damage by ROS (Goldsmith et al., 2014). These findings demonstrate that autophagy can function to protect against cancer.

Although autophagy can suppress cancer initially, it can also be utilized by cancer cells for nutrient acquisition and survival under stress (Rabinowitz and White, 2010). Fibroblasts with constitutively high levels of autophagy also had high levels of tumor growth (Salem et al., 2012). Pancreatic ductal adenocarcinomas demonstrated high levels of basal autophagy (Yang et al., 2011). When autophagy was blocked pharmacologically, growth of the tumor cells decreased. Similarly, when CMA is blocked in lung cancer cells, the rate of tumor growth slows (Kon et al., 2011). Tumor cells often favor glycolysis over oxidative phosphorylation for metabolism. Therefore, mitophagy can be helpful in the removal of mitochondria and a shift towards the uptake of glucose and glycolysis pathway (Ermak et al., 2012). The near exclusive use of the glycolysis pathway can create an acidic cellular microenvironment, which further requires cellular autophagy for increased survival under acidic stress (Wojtkowiak et al., 2012). Therefore, the relationship between autophagy and cancer is complex: autophagy can be tumor-suppressive, but it also is needed by tumor cells for rapid growth.

Autophagy has diverse roles in development and differentiation. A number of *ATG* knockouts prove to be embryonically lethal in mice, suggesting that autophagy is necessary at even the earliest stages of mammalian development (Mizushima and Levine, 2010). Cellular development requires autophagy in a number of cell lineages, particularly hematopoietic cells. Autophagy, specifically mitophagy, is required to remove mitochondria during development of erythroid cells from reticulocytes to mature erythrocytes. When autophagy is blocked, mitochondria accumulate in mature erythrocytes (Mortensen et al., 2010). Memory T cells and regulatory T cells also appear to need autophagy to maintain their metabolic function as long-lived cells (Puleston et al., 2014, Xu et al., 2014a). B1 B cells are dependent on autophagy, as the deletion of *Atg7* led to the loss of this B cell subset (Clarke et al., 2018). Neutrophils need autophagy for differentiation, especially for their provision of free fatty acids (Riffelmacher et al., 2017).

Autophagy is important in the immune system, not only for the development of immune cells, but also in defense mechanisms against bacteria and viruses. For example, Group A Streptococcus can be engulfed by an autophagosome and targeted to the lysosome for destruction (Nakagawa et al., 2004). This activity was blocked in an autophagy knockout system, which allowed bacteria to propagate. Conversely, autophagy machinery can be hijacked by intracellular bacteria, including *Brucella abortus*, *Porphyromonas gingivalis*, and *Legionella pneumophila*, which can use the autophagosomal vesicles to hide from the immune system (Swanson and Isberg, 1995, Pizarro-Cerda et al., 2000, Dorn et al., 2001).

Autophagy has important roles in aging. The activation of autophagy has been shown to be important in lifespan extension in a number of organisms including *Caenorhabditis elegans* and *Drosophila*. Calorie restriction, which is associated with an increased lifespan, activates autophagy in *C. elegans* (Jia and Levine, 2007). Similarly, amino acid restriction increases the lifespan of yeast (Alvers et al., 2009). The deletion of two autophagy related genes, *ATG1* and *ATG7*, resulted in a shortened yeast lifespan in this study. Senescence is a largely irreversible arrest of the cell cycle (Kuilman et al., 2010). Consistent with a role for autophagy in preventing aging, autophagy is downregulated in senescent cells (Rubinsztein et al., 2011, Chang et al., 2017). Primary senescent $CD8^+$ T cells have decreased levels of autophagy (Phadwal et al., 2012). Older cells have dysfunctional mitochondria that often produce ROS, which can damage the cell (Sohal and Sohal, 1991).

As opposed to senescence, quiescence is a reversible cell cycle arrest (Yao, 2014). Blocking mTOR demonstrated a shift from senescence to quiescence (Serrano, 2010), thus, implicating autophagy in the maintenance of quiescent cells. Quiescent cells have decreased metabolic activity, but continue to utilize autophagy as governed by mTOR for metabolic function and cellular repair against damage from ROS (Chen et al., 2008). The relationship between quiescence and autophagy is discussed in greater detail in Chapter 5.

1.3.4 Autophagy in *Apicomplexa*

Autophagy is a highly conserved pathway among eukaryotes from yeast up to humans. Although autophagy tends to be highly conserved, a number of the autophagy-related genes are not found in the genomes of *Plasmodium* nor *Toxoplasma* (Gardner et al., 2002, Besteiro, 2017). Given the relative ease of working with *Toxoplasma* as compared to *Plasmodium*, more information is known regarding autophagy in *Toxoplasma*. Although these two parasites are closely related, the understanding of autophagy in one system merely hints at its presence and function in the other.

Putative autophagosomes have been observed in Apicompexa. In *Toxoplasma* tachyzoites, multi-membranous vesicles containing partially degraded cytoplasmic content have been visualized by electron microscopy (Ghosh et al., 2012, Besteiro et al., 2011). These autophagosomes have been induced by a variety of stressors including ER stress and starvation. Using a GFP-tagged *Toxoplasma* Atg8, pharmacologically-induced ER stress caused accumulation of autophagic vesicles tagged with Atg8 (Nguyen et al., 2017). Autophagosomes have also been observed in the bradyzoite, a quiescent form of *Toxoplasma* important in transmission (Di Cristina et al., 2017).

Toxoplasma parasites do not have a lysosome; however, they do contain a vacuolar compartment (VAC) that contains proteases and functions as the degradation vacuole (Miranda et al., 2010, Parussini et al., 2010). When the VAC proteases were inhibited, putative autophagosomes accumulated in the cytoplasm, thus demonstrating the function of the VAC as the end organelle of autophagy in *Toxoplasma* (Di Cristina et al., 2017).

Although the presence of autophagosomes and a degradation vacuole may suggest that autophagy is occurring in *Toxoplasma*, there are some reasons to doubt that it occurs in the traditional sense. Atg8 co-localizes with the apicoplast (Kong-Hap et al., 2013, Leveque et al., 2015). Depletion of Atg8 in a conditional knockout caused aberrant

segregation of apicoplasts to daughter cells, thus implicating the autophagy machinery to apicoplast inheritance (Leveque et al., 2015). Given that the apicoplast has no apparent autophagic function, the localization of autophagy-related proteins to the apicoplast suggests that these proteins may have evolved a different function in Apicomplexa.

1.3.4.1 Autophagy in Plasmodium falciparum

In the intraerythrocytic *Plasmodium* parasite, putative autophagosomes have been visualized (Tomlins et al., 2013); however, given the preponderance of multi-membraned organelles, it is difficult to ascertain whether or not these structures were indeed autophagosomes.

The DV is the functional lysosome, or acidic compartment, of the parasite (Goldberg et al., 1990). Trophozoites have been shown to have additional DV-like compartments, which, in some images, appear to be fusing with the DV (Abu Bakar et al., 2010). Additionally, some early endocytic compartments appear weakly acidified and contain hemoglobin (Abu Bakar et al., 2010). Therefore, the DV is likely the end organelle for degradation of cargo in an autophagosome. Although the DV has been well-characterized in the intraerythrocytic lifecycle, there is no evidence of a DV in liver-stage parasites. Without an acidic vacuole, it is unclear whether or not liver-stage parasites could undergo autophagy. There is some evidence that autophagosomes may fuse with multivesicular bodies and form amphisomes that then release their contents from the cell through fusion with the plasma membrane (Voss et al., 2016). This would not be considered autophagy in the traditional sense, but would represent an adaptation likely specific to *Plasmodium*.

There are a number of putative functions for autophagy in *Plasmodium* (Figure 8). One possible function of autophagy in the ring stage is in facilitating quiescence. This hypothesis is detailed in Chapter 5. As the parasite progresses through its lifecycle, it gains additional organelles. These organelles could become damaged for a number of reasons, including oxidative stress or drug treatment, and autophagy would be useful in the clearance of these organelles. Another possible function of autophagy in *Plasmodium* is for the clearance of intact organelles as part of the parasite's normal progression through the lifecycle. Ultrastructural analysis of liver-stage parasites has demonstrated the expulsion of unnecessary organelles, such as micronemes, in a stage-specific manner (Jayabalasingham et al., 2010). Furthermore, autophagy has been implicated in the sexual stages in the formation of gametocytes (Cervantes et al., 2014).

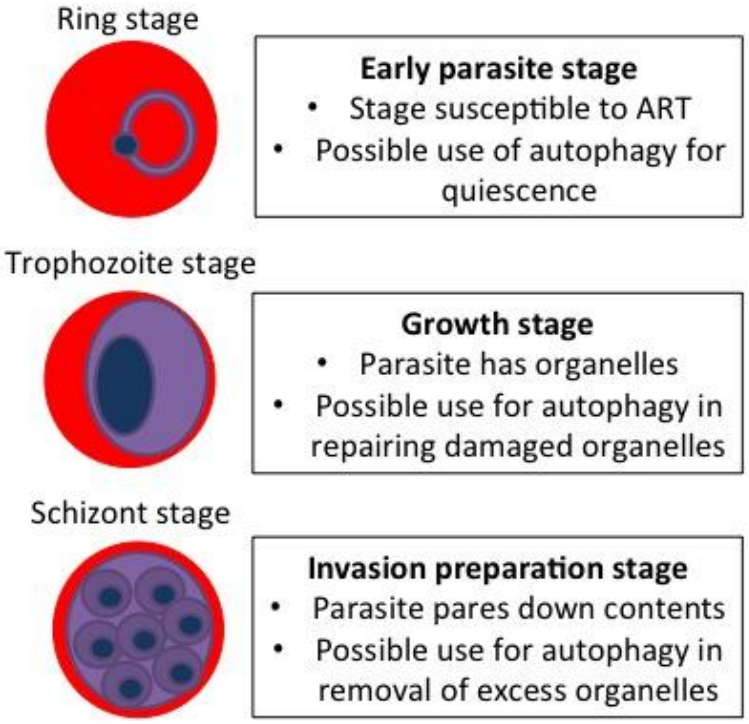


Figure 8: Possible functions for autophagy in P. falciparum parasites

Autophagy has a number of possible roles in plasmodial parasites that can be roughly broken down by parasite stage. In the ring stage, parasites may use autophagy for a dormancy or quiescence phenotype. In the trophozoite stage, parasites may use autophagy to remove and repair damaged organelles or to clear cytoplasmic material. In the schizont stage, parasites may use autophagy to remove excess organelles prior to invasion.

Much like in *Toxoplasma*, autophagy proteins and the apicoplast are also linked in *Plasmodium*. Multiple studies have demonstrated co-localization of Atg8 with the apicoplast (Tomlins et al., 2013, Kitamura et al., 2012). Another autophagy related protein, Atg18, has also been shown to co-localize with the apicoplast (Bansal et al., 2017). Further, both Atg8 and Atg18 have been implicated in the biogenesis and inheritance of the apicoplast (Bansal et al., 2017, Walczak et al., 2018). In the liver-stage, overexpression of Atg8 leads to the production of non-functional merozoites due to defective apicoplast formation (Voss et al., 2016). Whether the functions of autophagy related proteins as they relate to the apicoplast concern autophagy or another mechanism all together is yet to be seen.

Chloroquine has been used in mammalian cells as an inhibitor of autophagy. It is believed to prevent the acidification of lysosomes and thereby blocking the final fusion step of the autophagy pathway. As previously discussed, chloroquine is an antimalarial drug that was widely used until resistance developed in the second half of the 20th century. Interestingly,

one of the proposed mechanisms of action of chloroquine in *Plasmodium* is that it accumulates in the DV and other acidic compartments to prevent hemozoin formation, thus leaving the parasite inundated with toxic metabolites (Geary et al., 1990, Hawley et al., 1996). It is possible that one of the antimalarial actions of chloroquine is to block autophagy in the parasite.

While there is some evidence that autophagy exists in *Plasmodium*, it is far from conclusive. The majority of this evidence is detailed in Chapter 4. The presence of a set of putative autophagy-related genes does not prove the existence of autophagy in the parasite. More detailed studies, including the creation of a series of knockout parasites, are needed to map the autophagy pathway. While this thesis project centers around one protein, Atg18, it by no means proves that autophagy exists in the parasite.

1.4 THESIS AIMS

The purpose of this thesis is to investigate the role of an autophagy-like pathway in artemisinin-resistant *Plasmodium falciparum*. Although the function and mechanism of autophagy is poorly understood in *P. falciparum*, this project sought to connect the function of a single autophagy-related protein, Atg18, to drug resistance.

My first aim was to determine if any mutations in autophagy-related genes are associated with the artemisinin resistance phenotypes as is discussed in Chapter 3. This work necessitated sub-analysis of the TRAC WGS database to associate SNPs in *atg*s with clinical artemisinin resistance as defined by delayed parasite clearance half-life. *Ex vivo* IC50 data would then be examined to determine broadly if any autophagy-related SNP appeared to have any importance in artemisinin or partner drug resistance. To determine the contribution of any found SNP to drug resistance, the SNP would be edited using CRISPR-Cas9 targeted genome editing.

After identifying the *atg18* SNP and editing it via CRISPR-Cas9, my second aim was to characterize the contribution of the SNP to parasite functioning and drug sensitivity, as discussed in Chapter 4. I briefly characterized the *Plasmodium* Atg18 protein, leaning on its known functions in other systems. The newly created CRISPR-edited lines were compared to parent lines using *in vitro* drug resistance assays including IC50s. Further, the contribution of the SNP towards fitness and nutrient acquisition was assessed.

Finally, I adapted an existing dormancy assay to act as a drug resistance assay to determine if my SNP of interest changed the dormancy phenotype, as detailed in Chapter 5. I observed the dormancy phenotype in several isogenic Cambodian clinical lines with and without SNPs in *k13* to determine if these mutations modulated the phenotype. Next, I observed the dormancy phenotype in the parents (803 and GB4) and progeny of a genetic cross to determine if the dormancy phenotype segregated with clinical artemisinin resistance.

2 GENERAL METHODOLOGY

2.1 *PLASMODIUM FALCIPARUM* PARASITE CULTURE

2.1.1 Thawing parasites and general culture conditions

Culturing was performed in a biologic safety cabinet (BSC) using precautions outlined by each institution. Culture procedures were based on laboratory methods developed by Trager & Jenson (Trager and Jensen, 1976, Trager and Jenson, 1978) with some adaptations.

P. falciparum isolates were thawed from laboratory stocks kept in at -80^{o}C or in liquid nitrogen by first thawing for 2-3 minutes in a 37^{o}C bead bath. The volume of the thawed isolate was assessed and 0.1*volume of 12% NaCl was added dropwise. All culture solutions were pre-warmed to 37^{o}C. The isolate was allowed to stand for 5 minutes at room temperature. Then 10*volume of 1.6% NaCl was added dropwise. Where available, 10*volume of 0.9% NaCl was added dropwise as well. The isolate was then centrifuged in an Eppendorf Centrifuge 5810 at 340xg for 5 minutes. The supernatant was aspirated and the culture was re-suspended in 10mL serum/albumax free media (Table 2). The culture was then centrifuged again at 340xg for 5 minutes. The culture was re-suspended in complete media and fresh red blood cells (RBCs).

Table 2: Recipe for complete media

Reagent	Amount	Final concentration
RPMI 1640	500mL	
HEPES	18.75mL	37.5mM
Glucose solution (45%)	2mL	0.2%
Sodium hydroxide (1M)	3mL	1.5mM
Gentamicin sulphate solution	1.25mL	25µg/mL
Hypoxanthine solution (100x)	5mL	1x
Pooled human serum or albumax	Serum: 100mL Albumax: 2.5g	

Parasites were cultured in leukocyte-depleted RBCs. Cultures were kept at 5% hematocrit in complete media (Table 2) and between 0.1-15% parasitemia in an incubator at 37^{o}C. Cultures were gassed with 5% oxygen, 5% carbon-dioxide, and balance nitrogen.

2.1.2 Parasite lines used

Several parasite lines were used for the purpose of this thesis and are summarized in Table 3: Summary of parasite lines used. The 967^{R539T} line is a contemporary clinical isolate from Cambodia that has been culture adapted. As detailed in Straimer et al., an endogenous *k13* mutation (R539T) occurs in 967, which is denoted 967^{R539T} (Straimer et al., 2015). The line was then edited using zinc finger endonuclease editing and reverted back to wild-type *k13* (without any mutation), forming 967 wild-type reverted (967^{WTrev}). Similarly, 967^{C580Y} is an isogenic line from 967^{R539T}, with a C580Y *k13* mutation rather than R539T. The original 967^{R539T} line is resistant to both chloroquine and artemisinin, though it is sensitive to piperaquine. This line is from the NIH Cambodian clinical research site in Pursat province, while the isogenic lines were obtained from the laboratory of Dr. David Fidock (Columbia University).

Dd2, a laboratory line adapted from Indochina was edited to include an R539T *k13* mutation, forming the $Dd2^{R539T}$ line. Dd2 (WT) is known to be chloroquine resistant,

although it is artemisinin and piperaquine sensitive. The isogenic Dd2 lines were also obtained from the laboratory of Dr. David Fidock (Columbia University).

As detailed in subsequent chapters, Dd2, Dd2^{R539T}, 967^{WTrev}, and 967^{R539T} were transfected with GFP-Atg18 to form lines that expressed GFP-tagged Atg18. Additionally, Dd2^{R539T} was successfully edited by CRISPR/Cas9 editing to include a T38I mutation in *atg18*, creating Dd2$^{R539T/T38I}$.

Parasite line KH002-009 is a contemporary Cambodian clinical isolate from the NIH Cambodian clinical research site in Preah Vihear province. It is wild-type for *k13* and *atg18*, and is sensitive to artemisinin. The original clinical isolate was cloned by serial dilution prior to experiments.

Parasite lines from the cross originated from parents 803 and GB4. The line 803 is a contemporary clinical isolate from Cambodia with an endogenous C580Y *k13* mutation. The parasite GB4 is a clone of Ghana III which was adapted to infect *Aotus* monkeys (Sullivan et al., 2004, Hayton et al., 2008). The progeny of this cross contain genes from either of the parents, namely either a C580Y *k13* mutation or the wild-type C580.

Table 3: Summary of parasite lines used

Name	Date collected	Region of origin	*k13* genotype	*atg18* genotype
967^{R539T}	2010	Pursat, Cambodia	MT (*R539T*)	MT (*T38I*)
967^{WTrev}	Isogenic editing of 967^{R539T}	Pursat, Cambodia	WT	MT (*T38I*)
967^{C580Y}	Isogenic editing of 967^{R539T}	Pursat, Cambodia	MT (*C580Y*)	MT (*T38I*)
Dd2	1980	Indochina	WT	WT
$Dd2^{R539T}$	Isogenic editing of Dd2	Indochina	MT (R539T)	WT
915	2010	Pursat, Cambodia	WT	WT
915^{C580Y}	Isogenic editing of 915	Pursat, Cambodia	MT (C580Y)	WT
4912^{I534T}	2011	Mondulkiri, Cambodia	MT (I534T)	Unknown
4912^{WT}	Isogenic editing of 4912^{I534T}	Mondulkiri, Cambodia	WT	Unknown

The following lines have been published under alternative names in (Straimer et al., 2015): 967^{R539T} as $Cam3.II^{R539T}$, 967^{WTrev} as $Cam3.II^{rev}$, 967^{C580Y} as $Cam3.II^{C580Y}$; 915 as CamWT, 915^{C580Y} as $CamWT^{C580Y}$; 4912^{I534T} as $Cam5^{I534T}$, 4912^{WT} as $Cam5^{rev}$.

2.1.3 Sorbitol synchronization of ring stage parasites

Parasites were synchronized at the ring stage via sorbitol lysis (Lambros and Vanderberg, 1979). Cultures were centrifuged in a Eppendorf Centrifuge 5810 at 1578xg for 5 minutes and supernatant was aspirated. Cells were re-suspended in 10*volume of 5% sorbitol solution. Cultures were returned to the incubator and allowed to stand at 37ºC for 30

minutes. Cultures were centrifuged at 1578xg for 5 minutes, sorbitol was aspirated, and the cells were re-suspended in 10*volume of media. Cultures were centrifuged at 1578xg for 5 minutes, media was aspirated, and the cells were re-suspended in the appropriate volume of complete media.

2.1.4 Percoll gradient separation of late stage parasites

Percoll gradients were used to isolate mature parasites. RPMI1640 (14mL) and 10µL heparin were pre-warmed to 37ºC while 65% Percoll (in heparinized RPMI1640) and 35% Percoll (in heparinized RPMI1640) were made. The culture was transferred to a 15mL conical tube and centrifuged in an Eppendorf Centrifuge 5810 at 1578xg. The supernatant was aspirated and 3mL of heparinized RPMI was added per 300µL pellet. This was incubated at 37ºC for 15 minutes.

The Percoll gradient was prepared by slowly layering 3mL of 35% Percoll on top of 65% in at 15mL conical tube via Pasteur pipette, and then 3mL of the culture was layered on top. This was centrifuged at 1500xg for 15 minutes with no brake applied. The tube had distinct layers after centrifugation (Figure 9). The top layer was aspirated and the intermediate layer (schizonts and trophozoites) was collected and transferred to a 15mL conical tube. Pre-warmed RPMI was added to make a final volume of 14mL and then it was centrifuged at 800xg for 5 minutes. The supernatant was aspirated and a smear (using only 0.5-1µL) was made to ensure that only mature stages were present.

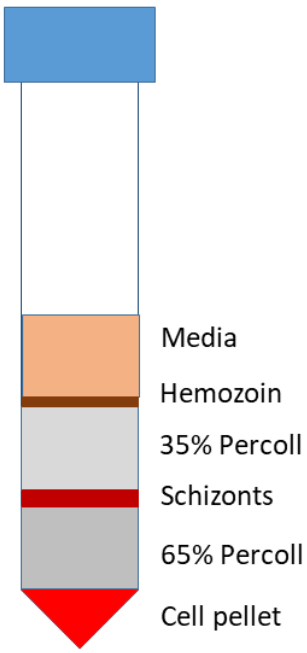


Figure 9: Percoll separation of late-stage parasites

Following layering of the 65% Percoll, the 35% Percoll, and the culture mixture, the tube comes out of the centrifuge with distinct layers. The bottom layer is the cell pellet, which includes uninfected erythrocytes and early-stage parasites (rings and trophozoites). Above that, is a layer of 65% Percoll. Just above that is a thin layer of schizonts. Above that is a layer of 35% Percoll. Above that is a very thin layer of hemozoin and debris, including extracellular parasites. Finally, the top layer is media.

2.1.5 Parasite cloning by dilution

The purpose of cloning by limiting dilution is to obtain less than one parasite per well in a 96-well plate, allow the culture to propagate, and therefore obtain homogenous, clonal parasite populations, derived from a single parasite. In this case, I wanted to obtain 60 parasites/plate. The parasitemia of the culture was recorded via smear using a 40x objective and 10x eye piece (400x magnification). The assumption was made that 1mL of packed RBCs has approximately 10E10 RBCs. The culture was spun down and 20µL packed culture was mixed with 1mL of media. A 1:100 dilution was made of this culture, followed by a second 1:100 dilution. The amount of diluted culture to add to a final tube with 22.5mL media and RBCs at 2% Hct was calculated as follows:

- Parasites per mL = (Number of RBCs in 1mL packed RBCs) * (parasitemia) * (volume packed culture added to 1mL media) / (dilution factor) / (second dilution factor)
    - Parasites per mL = 10E10 * (parasitemia) * (20/1000) / (100) / (100)
- Amount of culture to add to 22.5mL media (in μL) = ((Number of desired parasites per plate) / (parasites per mL)) * (μL per mL)
    - Amount of culture to add to 22.5mL media (in μL) = (60 / parasites per mL) * 1000

The final culture mixture was plated in 96-well plates at 200μL per well. This was incubated at 37°C in with tri-gas.

Weekly, media was changed and fresh RBCs (0.5% Hct) were added. On day 21, plates were assessed using Malstat reagent. Briefly, 50μL culture supernatant per well was plated onto a fresh 96-well plate and 90μL Malstat (Table 4) was added and incubated overnight in the dark. Color changes were detected by eye or using a plate reader at 650nm (Figure 10). Positive clones were grown up first in 3mL of media and then transferred to 10mL of media when they were growing well.

Table 4: Malstat reagent recipe per 96-well plate

Reagent	**Amount**
3-acetyl pyridine adenine dinucleotide (APAD) solution (50mg/mL in H_2O)	116μL
Nitro blue tetrazolium (NBT) (50mg/mL in 70% dimethylformamide)	17μL
Diaphorase solution (8mg/mL in H_2O)	35μL
Malstat solution (recipe below)	8.8mL
ddH_2O	212.5mL
Lithium L-lactate	5g
Triton X-100	500μL
ddH_2O	QS to 250mL

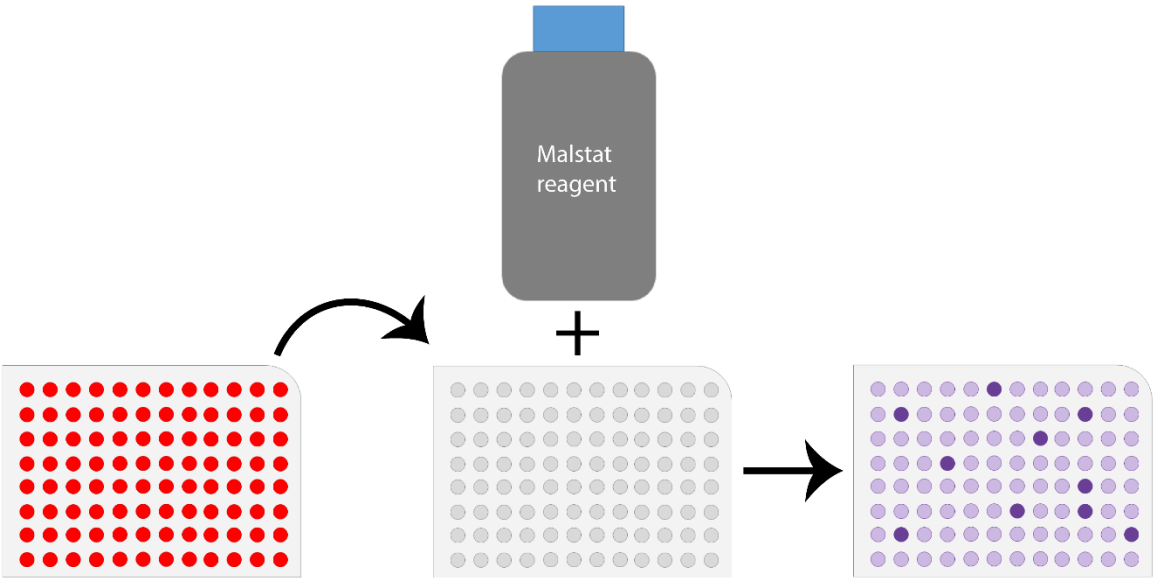


Figure 10: Schematic of Malstat reagent protocol

For dilution cloning, Malstat reagent was used to detect parasite growth in wells. 96-well cloning plates with culture were removed from the incubator and 50µL media per well was pipetted into a new 96-well plate. Then 90µL Malstat reagent was added and the plate was incubated in the dark overnight. Positive wells developed dark purple in color as compared to negative wells which were pink or light purple.

2.1.6 Saponin lysis

Saponin was used to lyse RBCs and release parasite proteins and DNA. Stock saponin solutions were made at 1% saponin in PBS and stored in 1mL aliquots at -20^{o}C. An aliquot was thawed and 0.01% saponin in PBS was made on the day of experiment. At room temperature, 1mL 0.01% saponin was added per 200µL RBCs in each sample and mixed. Samples were spun in a microcentrifuge tube in an Eppendorf Centrifuge 5415D at 15,682xg for 5 minutes. The supernatant was aspirated, while being careful not to disturb the fluffy white "ghost" layer, and saponin solution was again added and the samples spun at 15,682xg for 5 minutes. This procedure was repeated until the supernatant and pellet no longer appeared red. Samples were then washed once in PBS.

2.2 STATISTICAL ANALYSIS

Significance was set at $p \leq 0.05$ for the majority of experiments with notable exception. In several instances, a correction for multiple comparisons was employed to make the criteria for significance more stringent to reduce the chance of obtaining a statistically

significant result based on chance (type I error). Given the number of statistical tests performed during a genome-wide association study (GWAS), the potential for false discovery is high. Therefore, a correction was made to increase the threshold of significance by lowering the p value to less than 5E-6 using a Bonferroni correction based on the 17,395 SNPs tested. Ex vivo IC50 data was analyzed using unpaired t-test. The transcriptomics pathway enrichment analysis was performed using the hypergeometric test. PI3P measurements by HPLC were analyzed using unpaired t-tests with the Holm-Sidak method of correction. Drug screen statistical analyses were performed using an ANOVA to determine if MaxR were different among a variety of parasite lines, followed by a Tukey post-hoc test. Class enrichment was assessed by a Fishers test with Benjamini-Hochberg correction for multiple comparisons. Time to recrudescence following dormancy induction and untreated time to growth was analyzed using one-way ANOVA with Tukey's multiple comparisons test. Growth rates during nutrient deprivation studies were compared using 2-way ANOVA with Tukey's multiple comparisons test.

3 SINGLE NUCLEOTIDE POLYMORPHISMS IN AUTOPHAGY-RELATED GENE 18 (*ATG18*) AND ARTEMISININ RESISTANCE

3.1 INTRODUCTION AND AIMS

3.1.1 Introduction

Sentinel cases of delayed parasite clearance half-life, the clinical artemisinin-resistance phenotype, were first reported at the Thai-Cambodian border in 2006 and 2007. In 2011, in response to these cases, the University of Oxford at the Mahidol Oxford Tropical Medicine Research Unit (MORU) in collaboration with the National Institutes of Health (NIH) and several other research institutes worldwide set up a study called Tracking Resistance to Artemisinin Collaboration (TRAC). The study included 15 sites in 10 countries, with three of Cambodia's four sites being run by the NIH. Other Asian countries included in the TRAC study were Thailand, Laos, Myanmar, Vietnam, Bangladesh, and India. Three African countries were also included: Kenya, Nigeria, and the Democratic Republic of the Congo, to determine whether or not artemisinin resistance had made the crucial leap from Asia to Africa. The results of this study determined that artemisinin resistance (parasite clearance half-life over 5 hours) had spread throughout much of Southeast Asia, particularly western Cambodia and eastern Thailand but had neither yet traveled to the TRAC's India site of Jalpaiguri nor the three sites in Africa. Although some cases of delayed parasite clearance half-life were detected in Africa, none of these had an associated *k13* mutation (Ashley et al., 2014).

The TRAC study not only followed parasite clearance times, it also allowed researchers to collect blood samples and extract parasite genomic DNA for whole genome sequencing (WGS) by the Wellcome Trust Sanger Institute. A genome wide association study (GWAS) was performed to find SNPs associated with delayed parasite clearance half-life (Miotto et al., 2015). This study determined that more than 20 mutations in *k13* were associated with delayed parasite clearance half-life. Furthermore, these *k13* mutations tended to arise on a conserved genetic background, including mutations in genes *fd, arps10, mdr2,* and *crt* among others. The importance of these background mutations remains unknown, but it is hypothesized that these SNPs provide changes in parasite

fitness to compensate for possible losses in fitness due to drug-resistance causing mutations.

Autophagy was investigated as a possible mechanism related to artemisinin resistance due to a number of connections between an autophagy-like pathway in *P. falciparum* and known mechanisms of artemisinin action and resistance (Figure 11). As mentioned in the introduction, artemisinin can damage cells by ROS; ROS are potent activators of autophagy. This would indicate that artemisinins, even in the absence of resistance, induce an autophagy-like pathway. The resistance mechanism also hints at a connection to autophagy through the increased levels of PI3P and upregulation of UPR associated

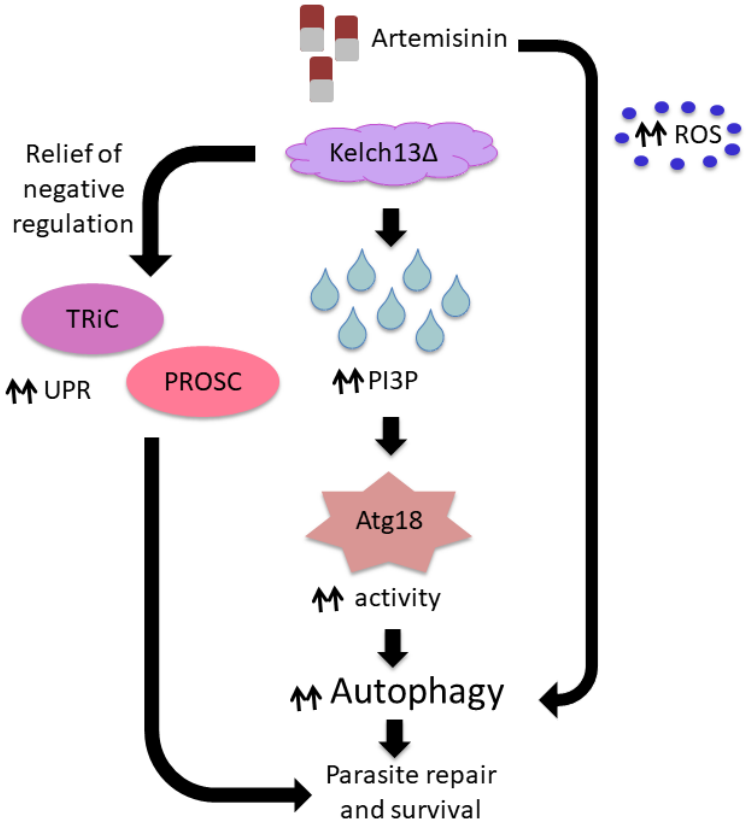


Figure 11: Model for contribution of Atg18 to mechanism of artemisinin resistance

Artemisinin damages cells by producing reactive oxygen species, which are potent inducers of autophagy. Kelch mutant lines have higher levels of PI3P which, through binding to Atg18 and combined with a possible increase in Atg18 activity due to the T38I SNP, may lead to increases in autophagy. Kelch mutations may be involved in the upregulation of the unfolded protein response, possibly by relieving negative regulation on the TRiC and PROSC. These two proteins were shown to be upregulated in ex vivo transcriptomics studies of resistant vs. sensitive isolates. Combined, these pathways could lead to the upregulation of autophagy, allowing for parasite repair and survival in the face of artemisinin treatment.

with resistance. Therefore, I sought to elucidate the ostensible connection between an autophagy-like pathway and artemisinin resistance in *P. falciparum*.

The investigation of the impact of specific SNPs has been assisted by the advent of Clustered Regularly Interspaced Short Palindromic Repeats (CRISPR)/Cas9 editing. CRISPR sequences are a natural immunity system used by bacteria and archaea to defend against viruses or bacteriophage (Barrangou et al., 2007) that has been harnessed as a powerful genome editing tool. Upon invasion of a bacteria by foreign genetic material, the bacteria inserts some of the foreign DNA, known as a protospacer, into its genome in the CRISPR locus (Mojica et al., 2009) using genes *cas1* and *cas2* (Yosef et al., 2012, Datsenko et al., 2012). In the viral genome, the protospacer contains a protospacer adjacent motif (PAM) (Deveau et al., 2008). The protospacer is known as a spacer when it is in the bacterial genome and does not contain a PAM sequence (Jinek et al., 2012). The bacteria then uses CRISPR RNAs (crRNAs), which contain complementary protospacer sequences, to search for foreign DNA within a cell. Upon detecting a complementary sequence, this single guide RNA (sgRNA) sequence binds to the foreign DNA and targets a CRISPR associated (Cas) endonuclease to degrade the sequence at the PAM site in a process known as interference.

CRISPR systems are diverse, but the focus of CRISPR editing has been in the use of Type II systems, and that will be the focus of this thesis. Type II is the least common of the three major CRISPR-Cas types, present in approximately 5% of bacterial genomes and absent in archaea (Chylinski et al., 2014). Type II acquisition also requires the presence of a trans-activating crRNA (tracrRNA) which complexes with the endonuclease and pre-crRNA (Heler et al., 2015) and allows for RNase III cleavage of pre-crRNA to create crRNA with a resulting 20 nucleotides of complementarity (Chylinski et al., 2014, Deltcheva et al., 2011). In type II systems, Cas9 endonuclease is used for this crRNA processing as well as for PAM sequence targeting and cleavage (Jinek et al., 2012). The Cas9 has two lobes: a nuclease lobe and an α-helical or recognition lobe (Nishimasu et al., 2015, Nishimasu et al., 2014). The nuclease lobe has two nuclease domains: a HNH nuclease which is responsible for cleavage of the target strand and a RuvC-like nuclease domain which cleaves the non-target strand (Anders et al., 2014, Nishimasu et al., 2015, Nishimasu et al., 2014). The α-helical lobe interacts with the sgRNA and is involved in targeting the complex to the foreign DNA (Jinek et al., 2014, Chylinski et al., 2014).

This understanding of basic bacterial immunity has been utilized as a biotechnology to allow for efficient editing of specific target sequences in almost any genome. Editing using CRISPR/Cas9 technology involves the creation of a plasmid encoding a sgRNA region that targets the Cas9 endonuclease to a specific sequence of a genome followed by a PAM site (Figure 12). The Cas9 protein is targeted to the region of the genome that is complementary to the sgRNA sequence and produces a double strand break at the PAM site, much as it would if it were functioning in a bacterial immune system. This double strand break triggers host DNA repair mechanisms. An additional plasmid, or additional sequence within the original plasmid, provides a homology region containing homologous sequences to the region surrounding the double strand break as well as any desired sequence editing. The cell's own homology directed repair (HDR) mechanisms use the homology region as a guide to repair the double strand break, thus inserting in the desired edited sequence. *Plasmodium* lacks the cellular machinery to preform non-homologous end-joining, which is the alternative pathway to HDR in most other systems, meaning that double strand breaks are typically repaired using HDR.

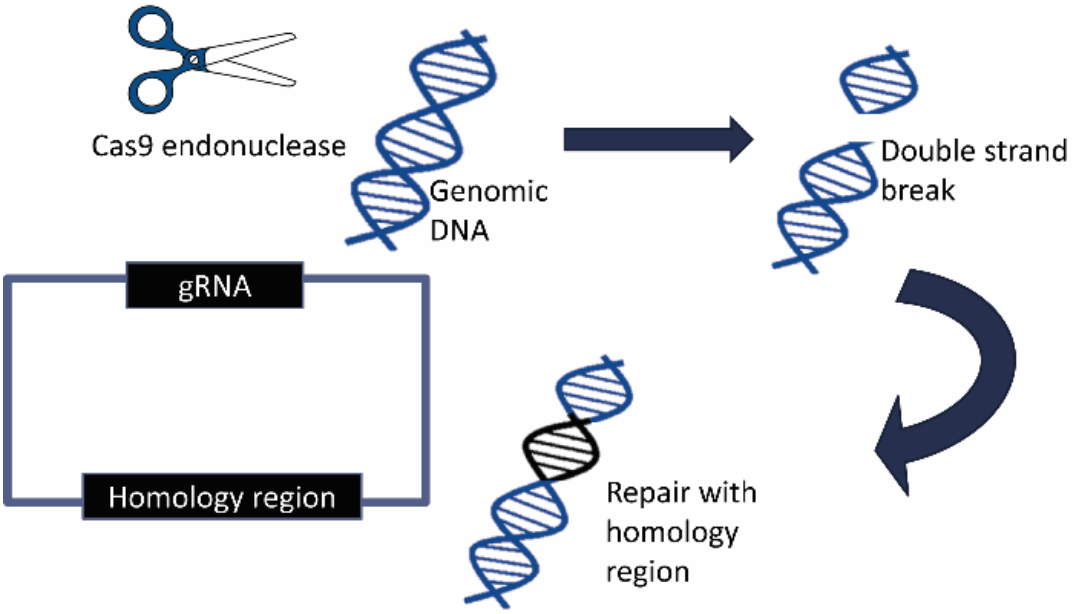


Figure 12: CRISPR/Cas9 editing schematic

Cas9 endonuclease is targeted to the genome by a guide sequence and then cuts at a designated site, causing a double strand break. The genome is then repaired using homology directed repair with the provided homology region as a template. This inserts the desired edit into the genome.

The first successful CRISPR/Cas9 editing of the *P. falciparum* genome was published in 2014 (Ghorbal et al., 2014) and demonstrated the use of CRISPR in editing the *k13* gene

to modulate artemisinin resistance. Prior to the advent of CRISPR for *Plasmodium*, zinc-finger nucleases (ZFN) were used to introduce double strand breaks to specific DNA-binding sites (Straimer et al., 2012). However, ZFN production is costly and the design of these nucleases often time consuming. In contrast, CRISPR/Cas9 plasmids can be generated for minimal costs in any laboratory equipped for molecular biology.

3.1.2 Aims

(1) The first aim is to determine if any SNPs in putative autophagy-related genes are associated with clinical drug resistance.

(2) The second aim is to determine if any SNPs from Aim 1 are important in *ex vivo* drug susceptibility in three clinical sites in Cambodia.

(3) The final aim is to use CRISPR/Cas9 targeted genome editing to edit any SNPs from Aim 1 to create isogenic parasite lines.

3.2 MATERIALS AND METHODS

3.2.1 Bioinformatics of Autophagy related genes

3.2.1.1 Whole Genome Sequencing Analysis

Putative autophagy-related genes in the *P. falciparum* genome were found through the conversion of a previously published list of human autophagy-related genes from Behrends et al. 2010 (Behrends et al., 2010). Using Ensembl.org, Entrez gene IDs and protein IDs were determined for all listed genes. OrthoMCL version 5 was used to find ortholog groups from Entrez protein IDs and then converted into *P. falciparum* genes. To supplement this incomplete list, PlasmoDB was searched for the key word “autophagy.” Finally, the Malaria Parasite Metabolic Pathways (MPMP) website was reviewed for the autophagy pathway.

A sub-analysis of a previously performed GWAS on 782 isolates from Southeast Asia was performed to determine if any SNPs on genes involved in autophagy were associated with delayed artemisinin resistance or partner drug resistance (IC50s). The resistance phenotype was a quantitative trait in a linear mixed model. A Bonferroni correction was applied, placing statistical significance at p-values less than 5E-6. Dr. Roberto Amato performed the statistics for this analysis.

IC50 experiments for chloroquine, piperaquine, quinine, artesunate, and DHA were performed by Dr. Pharath Lim *ex vivo* in Cambodia as previously described (Lim et al., 2013). Briefly, IC50s were performed using venous blood samples from patients in Cambodia. Blood was washed three times with media and smears were made to determine starting parasitemia. Parasitemias were either diluted to 0.5-1% if too high, allowed to reinvade for another cycle if too low, or the assay was begun if the parasitemia was between 0.5-1%. A SYBR green I fluorescence assay was used as described (Bacon et al., 2007). Briefly, drug plates were made in 96-well, flat-bottomed plates, with serial dilutions of artemisinin derivatives and partner drugs at 50µL/well in duplicate. These plates were dried in a BSC and stored for no more than one month at 4ºC. To perform the assay, 200µL RBCs diluted in media at 1% Hct were added to the drug plate and incubated at 37ºC for 72 hours in a gassed incubator. Plates were then frozen at -20ºC for cell lysis, thawed for 2 hours at room temperature, and shaken for 10 minutes. Then, 100µL/well cell suspension was removed and 100µL SYBR green I solution was added (Table 5) then incubated at room temperature for 30 minutes. Fluorescence was assessed using a FLUOstar OPTIMA. IC50 calculations were performed using ICEstimator, version 1.2 software's inhibitory sigmoid maximum-effect (E_{max}) model.

Table 5: SYBR green I lysis solution recipe

Ingredient	**Concentration**
Tris	20mM, pH 7.5
EDTA	5mM
Saponin	0.008% weight/volume
Triton-X 100	0.08% volume/volume
SYBR green I	0.02% volume/volume

This data was pooled and matched with sequencing data from WGS. Samples were excluded from the IC50 analyses if data was missing for either *atg18* (n = 265) or *k13* (n = 311) or both (n = 196) or if the final sequence was heterogeneous for that locus (*atg18*: n = 22; *k13*: n = 37). In total, 334 isolates were excluded, making the final cohort of 448 samples (Table 6). Data was analyzed using GraphPad Prism 6, unpaired t-test.

Table 6: Number of clinical isolates with polymorphisms in atg18 and/or k13

	k13 mutant (any)	*k13* wild-type
atg18 mutant	170	85
atg18 wild-type	15	178

3.2.1.2 Transcriptomics Analysis

A transcriptomics study was performed on 1043 isolates from Southeast Asia collected as part of the TRAC study as previously described (3.2.1) to determine gene regulation in ART-sensitive vs. ART-resistant parasites. Clinical blood samples were collected and passed through a CF11 column to remove white blood cells. Samples were stored at 4^{o}C, then frozen at -80^{o}C and shipped to Nanyang Technological University, Singapore where RNA isolation using TRIzol and transcriptomics analyses were performed by Dr. Sachel Mok as described in (Mok et al., 2011). Reverse transcription synthesized cDNA from 500ng RNA per sample and then 19 cycles of PCR amplification were performed to create aminoallyl-coupled cDNA for hybridization. From this material, 4µg of DNA was labeled with Cy5 dye and mixed with Cy3-labeled reference pool made up of 3D7 asexual stages. This material was hybridized on a custom microarray chip for 20 hours at 65^{o}C in a rotating hybridization oven at 10RPM. A PowerScanner was used for microarray scanning at 10µM as described in (Mok et al., 2015).

The data was processed to remove noise as described in (Mok et al., 2015) to improve quality control. The average of the ratios for all probes that map to the open reading frame (ORF) of a gene were used to calculate the gene expression ratio. A linear regression was applied to obtain a correlation coefficient for the expression of each gene in association with parasite clearance half-life following ACT. Correction was performed with Benjamani and Hochberg false discovery rate. A sub-analysis of this data set was performed to determine the expression of genes specific to autophagy using gene set enrichment techniques. Analysis of enrichment was performed using the hypergeometric probability using GeneProf.

3.2.2 CRISPR/Cas9 genome editing

The gene for *atg18* (*PF3D7_1012900*) was selected for CRISPR/Cas9 genome editing. Guide primers were designed to recognize 19 unique bases followed by NGG (PAM site)

by BLASTing potential guide primers against the 3D7 genome on PlasmoDB.org. Two sequences were chosen per gene based on low off-target sequence identity (to prevent off target effects), location of potential off-target sequences mainly in 5' residues, and proximity to region of interest.

The homology region sequences were designed to include the desired phenotype, either a reversion from *atg18* SNP to wild-type or vice versa. The *atg18* SNP construct was designed with a SNP changing the 38th amino acid from a threonine to an isoleucine (T38I). The PAM guide sequence was edited to include multiple synonymous SNPs to prevent cutting of the new sequence via the PAM-directed Cas9. PciI sites flank the sequences for later infusion reactions.

3.2.2.1 Eastman plasmid system

The initial attempts at CRISPR/Cas9 editing used a plasmid backbone created by Dr. Richard Eastman. Guide primers were designed with T7pro 15 base pair overhang for infusion reaction followed by guide annealing sequence (Table 7).

Table 7: Chosen PAM sequence primer sites

Gene	Guide RNA	Off target	Final Eastman guide primers	Final Lopez-Rubio guide primers
atg18	tgtgtatggctaatgagaaagg	13/19	CGACTCACTATAGGGgtgtgtatggctaatgagaaGTTTTAGAGCTAGAAATA	TAAGTATATAATATTATATCATTTAACCAGGATTAGTTTTAGAGCTAGAA
	tatcatttaaccaggattatgg	13/19	CGACTCACTATAGGGgTatcatttaaccaggattaGTTTTAGAGCTAGAAATA	TAAGTATATAATATTTTGTGTATGGCTAATGAGAAGTTTTAGAGCTAGAA

Guide RNA sequences include the PAM sites. Off target scores indicate the number of shared base pairs between the guide RNA sequence and the next most similar sequence. The final Eastman guide primers include uppercase letters to indicate regions of homology to the plasmid backbone(s) and lowercase letters to indicate guide RNA sequence(s), excluding the PAM sequence.

PCR amplification was performed to generate a chimeric target amplicon using pMTE pf14_0244 plasmid (obtained from Dr. Richard Eastman, NIH, Table 8) as the template. The following mixture was used for PCR: 25µL SapphireAmp Fast PCR Master Mix, 25µL PCR quality water, 0.1µL 18S Infusion BmtI Rev primer (Table 8), 0.1µL guide T7 terminal template, and 0.1µL specific guide primer (Table 7). All primers are at 100µM unless otherwise specified. The thermocycler conditions for these reactions were as follows: 92ºC for 2 minutes, followed by 40 cycles of 92ºC for 20 seconds, 60ºC for 20 seconds, and 68ºC for 30 seconds. Finally, the reaction went to 68ºC for 45 seconds and then held at 4ºC. The product was then run at 120V for 30 minutes in a gel and gel purified with a Qiagen QIAquick Gel Extraction kit (standard gel extraction unless otherwise specified). A pMTE Neo T7RNAP T7exp vector (Figure 13) was digested overnight at 37ºC with Bmtl and BamHI then gel purified. An infusion reaction was performed to combine 10.2ng of the chimeric target amplicon with 200ng of pMTE Neo T7RNAP T7exp vector in 2uL 5X Infusion Mix at 10µL total reaction at 50ºC for 15 minutes then at held 4ºC. The product (1.5µL) was immediately transformed into β-10 *E. coli* for 30 minutes on ice then 30 seconds at 42ºC then the cells were grown up in SOC broth at 37ºC for one hour. The contents were plated onto LB agarose plates with 100µg/mL ampicillin (standard concentration unless otherwise specified) and grown overnight at 37ºC. Colonies were screened with pMTE S1/guide AS4 primers (Table 8) and run on E-gels with SYBR safe. Positive clones were isolated by miniprep using QIAprep Spin Miniprep Kit and the targets and guide sequences were sequence verified with sequencing by Genewiz.

Table 8: Generation of chimeric target amplicon for Eastman plasmid system

Name	Sequence
pMTE pf14_0244 plasmid	GTTTTAGAGCTAGAAATAGCAAGTTAAAATAAGGCTAGTCCGTTATCAACTTGAAAAAGTGGCACCGAGTCGGTGCTTTTCATCTGTTTTATCTGTTATCTGTTAGAAGTCGTAACAAGGTTTCCGTAGGTGAACCTGCGGAAGGATCATTAATATATGC
Infusion BmtI Rev primer	ACCGAGCTCGGATCGGCATATATTAATGATCCTTCC
Guide AS4 primer	ATATATTAATGATCCTTC
pMTE S1 primer	CTAGTGGATCGAAGTATATGAG
Guide T7 terminal template	TAATACGACTCACTATAGGGNNNNNNNNNNNNNNNNNNNGTTTTAGAGCTAGAAATAGCAAGTTAAAATAAGGCTAGTCCGTTATCAACTTGAAAAAGTGGCACCGAGTCGGTGCTTTTCATCTGTTTTATCTGTTATCTGTTAGAAGTCGTAACAAGGTTTCCGTAGGTGAACCTGCGGAAGGATCATTAATATATGC

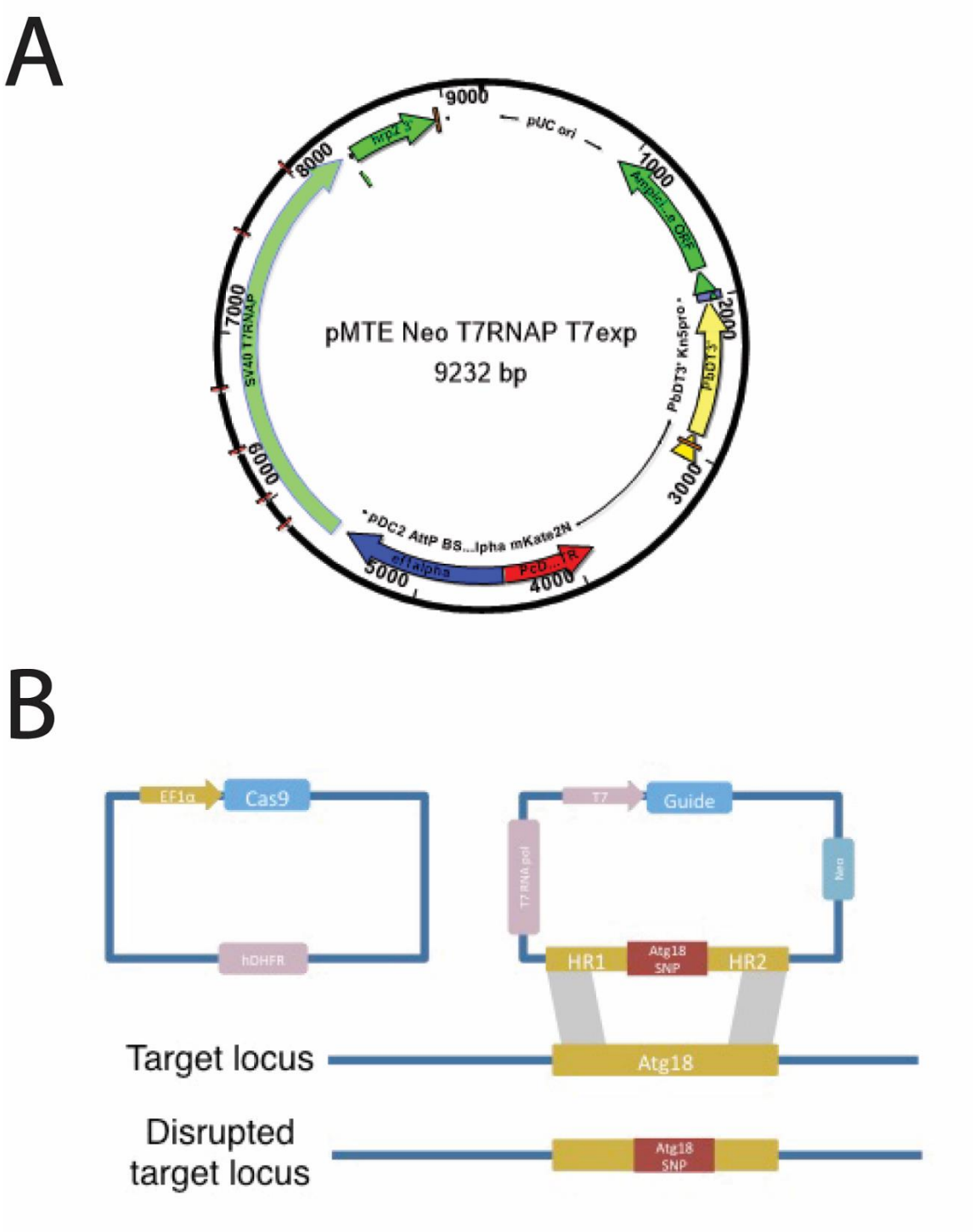


Figure 13: CRISPR vector backbone design for Eastman guide/repair plasmid

(A) The plasmid backbone was designed and provided by Richard Eastman. Appropriate sequences were cloned into the provided backbone using steps detailed in the methods. (B) Plasmid schematic showing two plasmid design for CRISPR/Cas9 editing using the Eastman plasmid system.

Upon confirmation of successful integration of the sgRNA sequence, plasmids were digested with PciI at 37°C overnight in NEB 3.1 buffer. Genestrings were synthesized by Genewiz and were cloned into the digested plasmid backbone via infusion. Digested vector (200ng), insert, infusion mix (5x) were mixed and incubated at 50°C for 15 minutes as described above. The infusion mix was transformed into bacteria as previously described, plated on pre-warmed LB agar plates containing ampicillin, and incubated overnight at 37°C. Colonies were screened for the insert via PCR then confirmed with sequencing. Confirmed sequences were grown up in 500mL LB/ampicillin and plasmids were isolated via maxiprep using a QIAGEN Plasmid Maxi kit according to the manufacturer's instructions. Plasmids were transfected as described below.

3.2.2.2 Lopez-Rubio plasmid system

Later, following unsuccessful attempts at editing using the Eastman plasmids, the Lopez-Rubio plasmid system was employed (Figure 14). sgRNA sequence design was determined as described above. Plasmid pUF1-Cas9 for Cas9 nuclease expression and pL6-GFP were obtained from Dr. David Ito. sgRNA primers were designed according to a protocol by Lopez-Rubio (Table 7). The pL6-GFP plasmid (3µg) was digested with

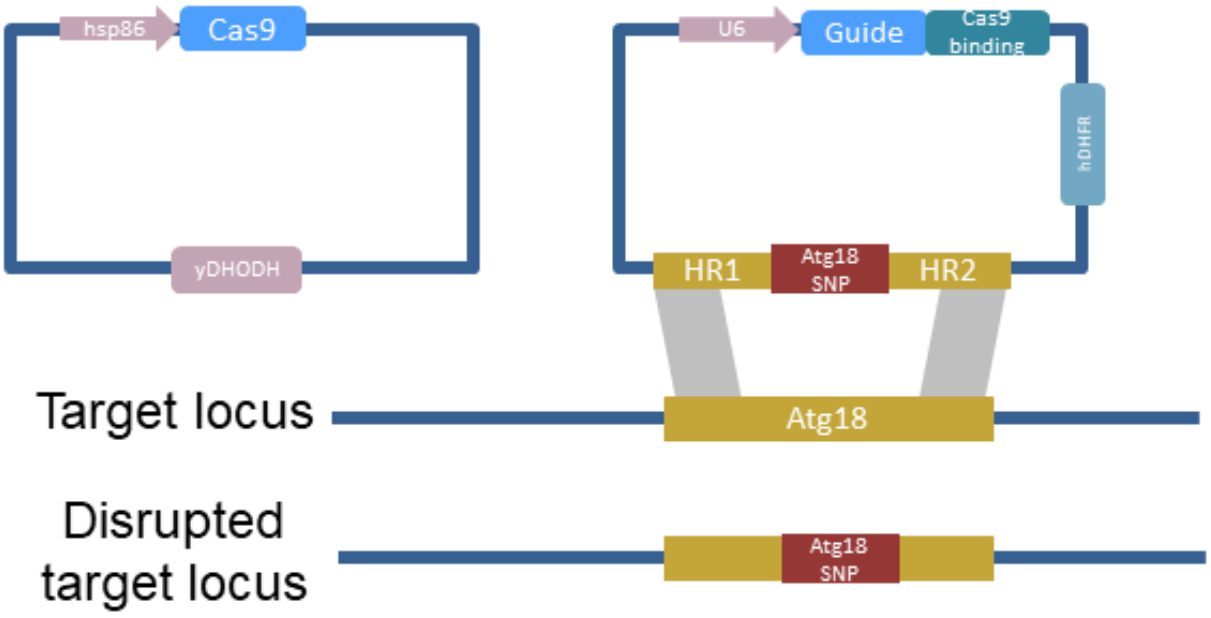


Figure 14: CRISPR vector backbone design for Lopez-Rubio guide/repair plasmid

Plasmid schematic showing two plasmid design for CRISPR/Cas9 editing using the Lopez-Rubio plasmid system. The guide sequence is driven by a U6 promoter.

BtgZI (1 unit/µg) in Cutsmart buffer for 3 hours at 60ºC and inactivated at 80ºC for 20 minutes. Digested plasmid was purified with NucleoSpin Gel and PCR Clean-up kit per the manufacturer's instructions.

sgRNA primers were annealed at 45µM each in NEB Cutsmart buffer in a reaction size of 22.2µL, using the below thermocycler program (Table 9). The product was diluted to 0.5µM in cold H_2O (1µL annealed oligonucleotides into 89µL H_2O). Diluted annealed oligonucleotides (1µL) were incubated with 100ng digested pL6-GFP and 1µL infusion HD mix (5x) in a 5µL reaction at 50ºC for 15 minutes. This infusion reaction (1µL) was transformed into Clontech Stellar competent cells as previously described with other bacteria. Cells were plated on pre-warmed LB agar plates containing ampicillin and incubated at 37ºC overnight.

Table 9: Thermocycler program for annealing guide primers

95ºC x 10 minutes
95ºC x 1 second with a reduction of 0.6ºC (0.6ºC/sec) for 16 cycles
85ºC x 1 second with a reduction of 0.6ºC (0.6ºC/sec) for 16 cycles
75ºC x 1 second with a reduction of 0.6ºC (0.6ºC/sec) for 16 cycles
65ºC x 1 second with a reduction of 0.6ºC (0.6ºC/sec) for 16 cycles
55ºC x 1 second with a reduction of 0.6ºC (0.6ºC/sec) for 16 cycles
45ºC x 1 second with a reduction of 0.6ºC (0.6ºC/sec) for 16 cycles
35ºC x 1 second with a reduction of 0.6ºC (0.6ºC/sec) for 16 cycles
25ºC x 1 minute
4ºC forever

Colonies were screened by PCR using Paq5000 mix at thermocycler conditions of 95ºC for 1 minute, 95ºC for 30 seconds, 54ºC for 30 seconds, 60ºC for 15 seconds (repeat 2-4, 25 times) followed by 60ºC for 1 minute and hold at 4ºC. The products were run on a 1% agarose gel with ethidium bromide. Positive clones were isolated by miniprep using QIAprep Spin Miniprep Kit and the targets and guide sequences were sequence verified with sequencing by Genewiz.

Plasmids (pL6, 3000ng) with the correct guide sequences were digested with 0.15µL EcoRI and 0.1µL NcoI in 5µL CutSmart QS to 50µL with water overnight at 37ºC. The enzymes were inactivated at 80ºC for 20 minutes. The plasmid containing Genestrings of the homology regions (pUC57, 1000ng) were digested using 1µL XmnI and 1µL PciI in

5µL CutSmart and 33µL water at 37ºC for 1 hour, then the enzymes were inactivated at 80ºC for 20 minutes. The band corresponding to 2215bp included the homology region and was gel extracted. The resulting fragment was used as a template for PCR to amplify the homology region using Atg18_HR_JJ_F1 and Atg18_HR_JJ_R1 (Table 10) as primers and CloneAmp Hifi PCR master mix using the thermocycler conditions as above for colony screening with Paq5000. The resulting amplicons were PCR purified.

The resulting digested pL6 plasmid backbone (100ng) was incubated with the corresponding homology region (30ng) with 2µL Infusion mix for 15 minutes at 50ºC then held at 4ºC. Immediately, 1µL of the product was used to transform 50µL Stellate Cells as previously described for other bacteria. Cells were plated on pre-warmed LB agar plates containing ampicillin and incubated at 37ºC overnight.

Colonies were screened by PCR using Atg18_F1 and U6 Upstream R primers in 5µL Sapphire as previously described. Positive clones were isolated by miniprep using QIAprep Spin Miniprep Kit and the targets and guide sequences were sequence verified with sequencing by Genewiz.

Confirmed sequences were grown up in 500mL LB/ampicillin and plasmids were isolated via maxiprep using a Qiagen kit according to the manufacturer's instructions. Plasmids were transfected as described below.

Table 10: Primers used for Lopez-Rubio plasmids

Name	**Sequence**
Atg18_HR_JJ_F1	ATTAAATCTAGAATTTGAATATATATATAT
Atg18_HR_JJ_R1	TTTTACCGTTCCATGTTAATACATCCAATA
Atg18_F1	ATGGTATCATTAAGATTAGATAATA
U6 Upstream R	CTTTCTTGAAACGGTTGTCCCTTTG

3.2.2.3 Transfection of erythrocytes

Erythrocytes were transfected in the presence of the plasmids and then late stage parasites (schizonts) were allowed to invade (Wu et al., 1995, Deitsch et al., 2001). In order to transfect parasites with plasmids, 350µL RBCs (50% Hct) were spun down, washed twice with 5mL cold Cytomix (Table 11), and re-suspended in Cytomix containing approximately 60µg of each plasmid DNA (for later described GFP transfections, 100µg

of plasmid). These RBCs were transferred to a cuvette (0.2cm) and electroporated with a voltage of 0.31kV and capacitance of 975µFD on a Bio-Rad Gene Pulser Xcell (Fidock and Wellems, 1997). Electroporated RBCs were immediately placed on ice, then removed from cuvettes using 5mL of cold culture media, transferred to a centrifuge tube, and rested for approximately one hour on ice.

Table 11: Cytomix composition

Reagent	Amount
KCl	8.95g
$CaCl_2$	0.017g
EGTA	0.76g
$MgCl_2$	1.02g
K_2HPO_4	0.871g
KH_2PO_4	0.68g
HEPES	7.08g

During this one-hour rest, late stage parasites were isolated via the Percoll protocol as previously described in the General Methodology section. Approximately 5µL late-stage parasites per flask was added to culture flasks. The electroporated RBCs were spun down, washed with media, and then added to culture flasks. Cultures were gassed and kept at 37ºC with complete media under normal culture conditions for the first two days. Parasitemias were checked on day 2 post-transfection and culture media with drug for selection was added if parasitemia exceeded 2%. Parasites edited using the Lopez-Rubio CRISPR/Cas9 plasmids were selected with complete media with 1.5µM DSM1 and 2nM WR99210. Parasites transfected with mCherry or GFP episomal plasmids were selected with complete media with 4µM blasticidin (BSD).

Drug selection media was changed every day for one week until all parasites appeared dead by microscopy. Media was then changed three times a week and blood was added once weekly. Smears were checked three times a week for parasites until day 60 post-transfection.

3.2.2.4 Screening for editing

Parasites that grew under drug selection were screened using the corresponding forward primer and JJ_HR_R reverse primer (Table 12). A 50µL aliquot of culture was boiled in a microcentrifuge tube at 98ºC for 10 minutes. The culture was then spun down for 10 minutes in an Eppendorf Centrifuge 5415D at 15,682xg. One microliter of supernatant was used as the template for the PCR reaction and added to 8µL Paq5000 pre-mix with 0.5µL of the forward and reverse primers at 10µM. Edited parasites showed a band in the reaction using JJ_PAM1_HR2 while unedited parasites showed a band using the JJ_PAM1_Genomic_F_screen primer. Controls were parasites that had not been transfected spiked with the corresponding plasmid of interest. Thermocycling conditions were as follows: 95ºC for 2 minutes, followed by 30 cycles of 95ºC for 30 seconds, 65ºC for 30 seconds, then 65ºC for 1 minute. The reaction was then held at 65ºC for 5 minutes and then held indefinitely at 4ºC.

Table 12: Primers used for screening following CRISPR/Cas9 editing with Lopez-Rubio plasmids

Name	Sequence
JJ_PAM1_HR2	GTATGGCTAACGAAAAG
JJ_PAM1_Genomic_F_screen	ATATCATTTAACCAGGATTATGG
JJ_HR_R	GTAACAAGTAATTTACCATCATTACTTAAA

Parasites that screened positive by PCR were cloned by dilution as previously described in General Methodology. Positive wells were grown up and clonal cultures were screened by PCR as above. Cultures with positive PCR results were sequenced using Atg18_F1 (Table 10) and JJ_HR_R (Table 12) primers using the thermocycling conditions used for PCR screening of edited parasites. PCR products were purified using PCR purification kit from Qiagen and 20ng of product was sent to GeneWiz for sequencing using JJ_PAM1_HR and Atg18_F1 for separate sequencing reactions.

3.3 RESULTS

3.3.1 Bioinformatics

3.3.1.1 Whole Genome Sequencing Sub-analysis

The GWAS comparing 782 isolates from Southeast Asia revealed that a nonsynonymous SNP in *PF3D7_1012900* (encoding a T38I substitution) was significantly associated with slow parasite clearance rate in patients treated with an ART derivative (p=5.89E-7) and non-significantly associated with chloroquine resistance (p=0.0002) (Table 13). This gene putatively encodes autophagy-related protein 18 (Atg18). Not surprisingly, clinical isolates with any *k13*-propeller mutation and the *atg18* T38I mutation had higher half inhibitory concentration (IC50) values than parasites with wild-type *k13*-propeller and *atg18* alleles for chloroquine (t-test, p<0.0001), piperaquine (p<0.0001), quinine (p<0.0001), artesunate (p<0.0001), and DHA (p<0.0001) (Figure 15, Table 14). Interestingly, parasites with wild-type *k13*-propeller sequences and the *atg18* T38I mutation had higher IC50 values than parasites with wild-type *k13*-propeller and *atg18* sequences for chloroquine (p<0.0001), piperaquine (p<0.01), quinine (p<0.001), artesunate (p<0.001), and DHA (p<0.01) (Figure 15, Table 14). The IC50 values of parasites with mutant *k13*-propeller and wild-type *atg18* sequences were not significantly higher than parasites with wild-type *k13*-propeller and *atg18* sequences, although the sample size for the former group of parasites was relatively low.

Table 13: Single-nucleotide polymorphisms (SNPs) in autophagy-related genes

Gene	Annotation	Putative protein	Position	Amino acid change	Mutation type	P value	Phenotype
PF3D7_1343700	Kelch protein K13	Kelch 13	1725259	X	N	4E-26	Parasite clearance half-life
PF3D7_1012900	Autophagy-related protein 18 (Atg18), putative	Atg18	497461	T38I	N	5.89E-07	Parasite clearance half-life
PF3D7_1239800	Conserved *Plasmodium* protein, unknown function	Atg11	1669294	D2948E	N	3.92E-05	Parasite clearance half-life
PF3D7_1012900	Autophagy-related protein 18 (Atg18), putative	Atg18	497461	T38I	N	0.0002	Chloroquine IC50
PF3D7_1239800	Conserved *Plasmodium* protein, unknown function	Atg11	1670910	N3487S	N	0.0002	Parasite clearance half-life
PF3D7_0709400	Cg7 protein	Atg14	426753	V161E	N	0.0007	Chloroquine IC50
PF3D7_1239800	Conserved *Plasmodium*	Atg11	1674565	N4705K	N	0.0007	Piperaquine IC50

	protein, unknown function						
PF3D7_1126100	ThiF family protein, putative	Atg7	1018965	1177C	S	0.0044	Chloroquine IC50
PF3D7_1126100	ThiF family protein, putative	Atg7	1018965	1177C	S	0.0129	Quinine IC50

The annotations were derived from PlasmoDB. Putative proteins are as annotated by PlasmoDB or through BLAST searches when the protein was unknown on PlasmoDB. The amino acid change for Kelch13 is denoted as "X" to represent a number of different SNPs that have been found within that gene. Mutation type "N" stands for non-synonymous mutation, whereas "S" stands for synonymous mutation. The P values shown are unadjusted.

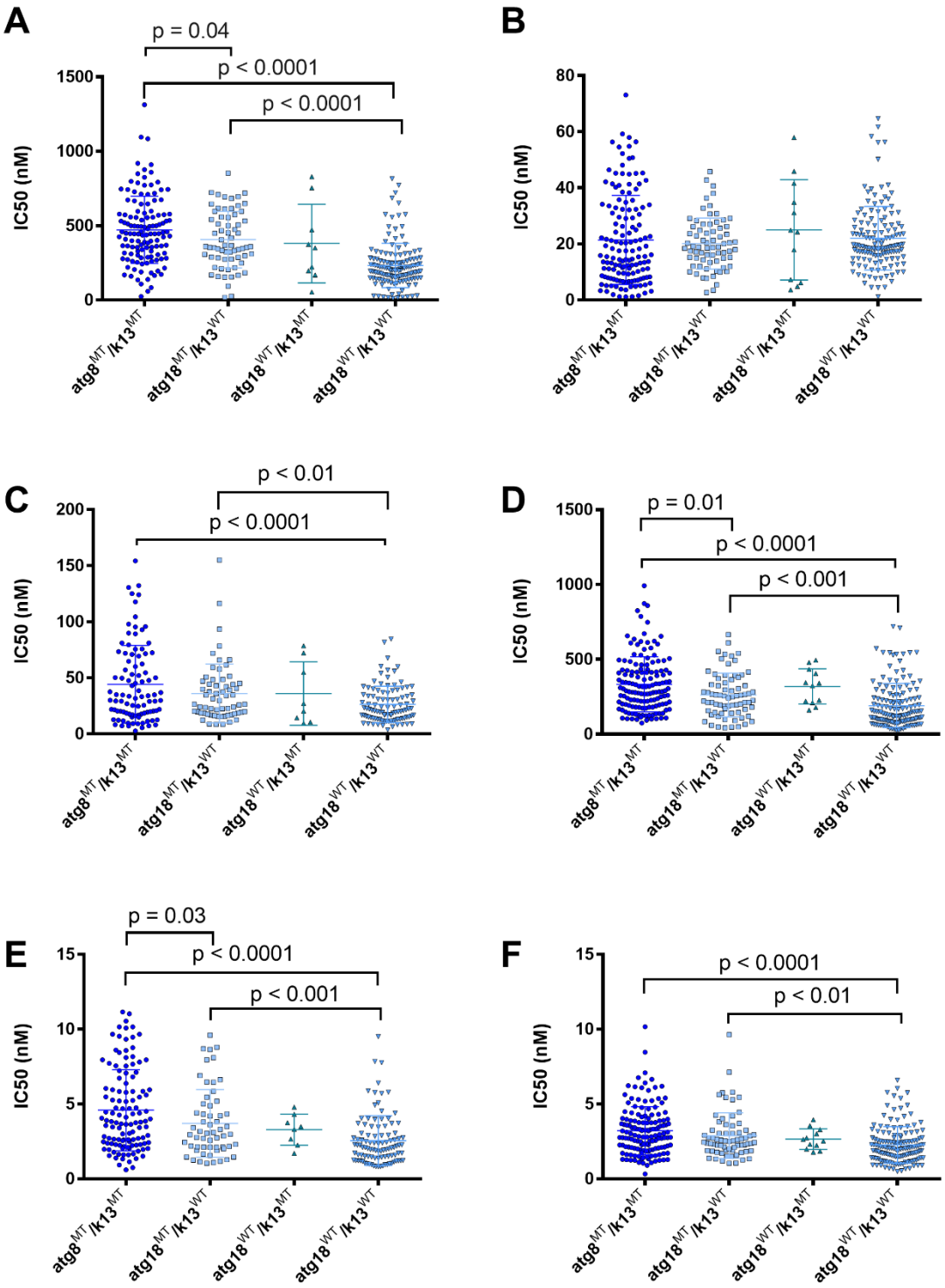


Figure 15: IC50 values for T38I parasites with or without K13-propeller mutations

IC50 values for six antimalarial drugs according to the presence of any K13-propeller mutation and the atg18 T38I mutation in Cambodian parasite isolates. Chloroquine (A), mefloquine (B), and piperaquine (C) are drugs that are currently or have been previously used as monotherapy or as partner drugs in artemisinin combination therapies. Quinine (D) is not routinely used in Cambodia. Artesunate (E) and DHA (F) are synthetic artemisinin derivatives. DHA is the active metabolite of artemisinin and artesunate.

Table 14: Interquartile range for antimalarial IC50 values

Genotypes	Chloroquine	Mefloquine	Piperaquine	Quinine	Artesunate	DHA
atg18^{+}/*k13*$^{+}$	310.2-578.1 (n=127)	8.3-32.7 (n=141)	17.8-69.4 (n=95)	190.2-427.0 (n=145)	2.4-6.4 (n=119)	2.0-4.0 (n=146)
atg18^{+}/*k13*^{WT}	282.1-562.1 (n=66)	13.9-26.1 (n=71)	18.5-45.1 (n=63)	151.5-353.4 (n=73)	2.1-4.9 (n=58)	1.9-3.3 (n=69)
atg18^{WT}/*k13*^{WT}	150.0-275.3 (n=141)	15.6-26.6 (n=141)	14.0-35.7 (n=101)	89.9-250.8 (n=145)	1.4-3.1 (n=100)	1.4-2.7 (n=145)

Values in nM

When parasites were stratified based on the polymorphism that corresponded to the partner drug of interest, the pattern changed drastically. Although it had appeared that the T38I *atg18* SNP had an impact on chloroquine, mefloquine, and piperaquine IC50s, this structure disappeared for each partner drug when the samples were grouped based on mutations pertinent to that specific partner drug (Figure 16). Chloroquine resistance has been linked to *crt* mutations, mefloquine to *mdr* increased copy number, and piperaquine to increased *plasmepsin* copy number. This evidence suggests that T38I *atg18* is only associated with an increase in resistance for artemisinin-derivatives, rather than for all antimalarial drugs.

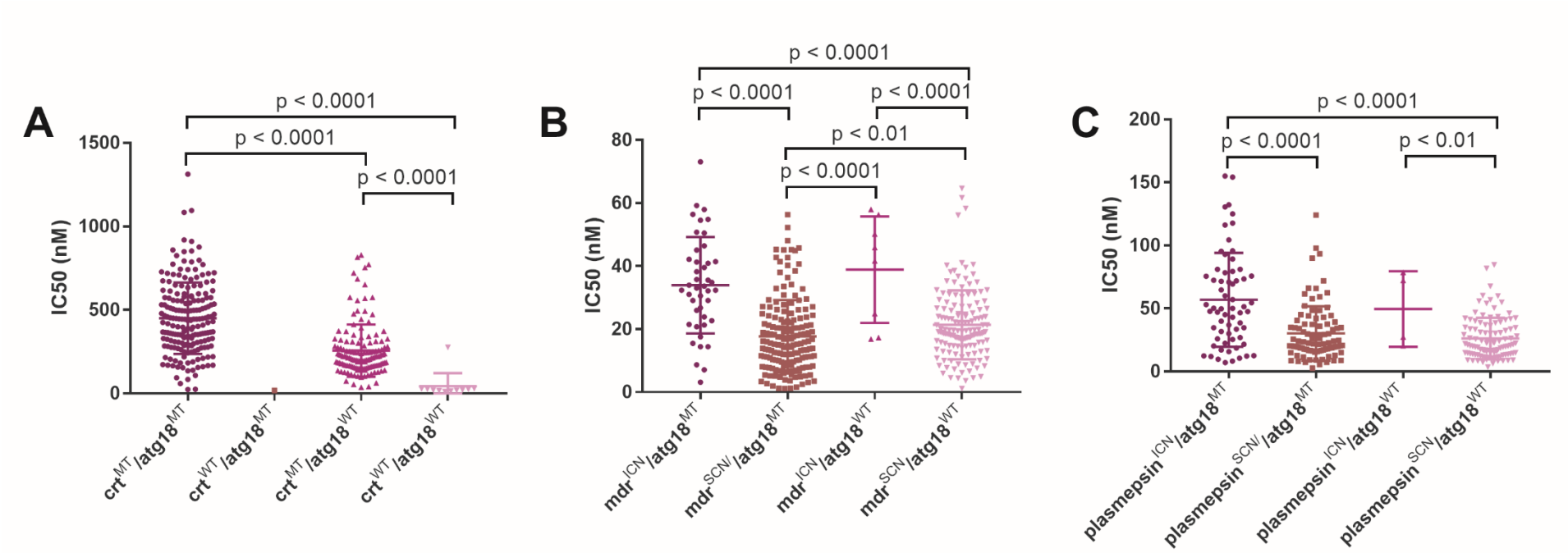


Figure 16: IC50 values for T38I parasites with or without mutations associated with partner drug resistance

Chloroquine in the presence or absence of crt mutations. Given the single value in $crt^{WT}/atg18^{MT}$, it was not possible to statistically test for differences between this and the other groups. (B) Mefloquine in the presence or absence of mdr copy number variations. (C) Piperaquine in the presence or absence of plasmepsin copy number variations. SCN denotes single copy number; ICN denotes increased copy number.

3.3.1.2 Transcriptomics

The transcriptomics sub-analysis demonstrated that many putative autophagy-related genes are modified in ART-resistant parasites as compared to ART-sensitive parasites (Table 15). There is significant enrichment of these genes compared to all samples (hypergeometric test, p=0.01). Although transcriptional changes are not recommended as a technique to determine autophagy levels (Klionsky et al., 2016), the vast number of autophagy-related genes that are modified in ART-resistant parasites suggests that this is an important pathway that is impacted by ART exposure.

Table 15: Transcriptome of autophagy-related genes in ART-resistant vs. ART-sensitive parasites ex vivo

Gene	**Annotation**	**Putative protein**	**P value**	**Correlation coefficient**	**Direction with resistance**
PF3D7_0822800	U5 snrnp-specific protein, putative	Atg16	0.0226	0.12	Up
PF3D7_0303000	N-ethylmaleimide-sensitive fusion protein (NSF)	NSF	0.0001	0.20	Up
PF3D7_0812400	karyopherin alpha	VAC8	0.0002	0.18	Up
PF3D7_1337800	calcium-dependent protein kinase 5	Atg1 kinase	0.0020	-0.16	Down
PF3D7_1417300	cysteine protease ATG4, putative	Atg4	1.23E-6	-0.24	Down
PF3D7_1430400	conserved *Plasmodium* protein, unknown function	Atg5	0.0001	-0.19	Down
PF3D7_1126100	autophagy-related protein 7 (Atg7), putative	Atg7	0.0436	-0.11	Down

PF3D7_1019900	autophagy-related protein 8 (Atg8)	Atg8	0.0021	-0.16	Down
PF3D7_0422200	erythrocyte membrane-associated antigen	Atg9	0.0322	-0.11	Down
PF3D7_1239800	conserved *Plasmodium* protein, unknown function	Atg11	0.0342	-0.11	Down
PF3D7_0709400	Cg7 protein	Atg14	0.0187	-0.12	Down
PF3D7_0203000	conserved *Plasmodium* protein, unknown function	Atg17	0.0590	-0.10	Down
PF3D7_0321700	microtubule and actin binding protein, putative	Atg23	0.0055	-0.14	Down
PF3D7_0823000	protein kinase, putative	VPS15	0.0002	-0.19	Down
PF3D7_1454300	serine/threonine protein kinase, putative	AMPK	0.7627	0.02	NS
PF3D7_0905700	autophagy-related protein 3, putative	Atg3	0.7536	0.02	NS
PF3D7_1335400	reticulocyte binding protein 2 homologue a	Atg6	0.1431	-0.08	NS
PF3D7_0216700	conserved *Plasmodium* protein, unknown function	Atg11	0.4420	-0.05	NS
PF3D7_1470000	autophagy-related protein 12 (Atg12), putative	Atg12		Not determined	NS
PF3D7_1201400	*Plasmodium* exported protein, unknown function	Atg13	0.9464	-0.01	NS
PF3D7_1012900	autophagy-related protein 18 (Atg18), putative	Atg18	0.5707	0.04	NS

PF3D7_1124100	neutral-sphingomyelinase activation factor protein (NSAF), putative	NSAF	0.0991	-0.09	NS
PF3D7_0515300	phosphatidylinositol 3-kinase (PI3K)	PI3K	0.3330	0.06	NS
PF3D7_0311300	phosphatidylinositol 3- and 4-kinase, putative (PI4K)	PI3K, PI4K	0.2656	0.06	NS
PF3D7_1431500	mitogen-activated protein kinase 1	TOR kinase	0.0734	0.10	NS
PF3D7_0203100	protein kinase, putative		0.9473	-0.01	NS

The annotations were derived from PlasmoDB. Putative proteins are as annotated by PlasmoDB or through BLAST searches when the protein was unknown on PlasmoDB. Correlation coefficient is based on the association of expression of a particular gene with parasite clearance half-life, with positive values indicating more expression in resistant isolates and negative values indicating less expression in resistant isolates. The direction of expression with resistance is noted in the final column for ease of reading and clarity.

3.3.2 CRISPR/Cas9 Transfections

Given the evidence of the involvement of the T38I *atg18* SNP in drug resistance, CRISPR/Cas9 editing was attempted in four different lines. Two systems were used and each was attempted a number of times. For a summary of transfection attempts, recrudescences, and cultures screened positive for editing by PCR, see Table 16. All successes came with the Lopez-Rubio plasmid system and the only cultures that screened PCR positive were in the $Dd2^{R539T}$ line.

Table 16: Summary of CRISPR/Cas9 outcomes in editing T38I ATG18 SNP

Parasite line	Eastman plasmid system			Lopez-Rubio plasmid system		
	Attempts	Recrudescence	Positive (PCR)	Attempts	Recrudescence	Positive (PCR)
967^{WTrev}	8	2	0	12	1	0
967^{R539T}	8	2	0	12	3	0
Dd2	8	2	0	12	1	0
$Dd2^{R539T}$	8	2	0	12	3	2

"Attempts" denotes the number of times a line was transfected with the given plasmid system. "Recrudescence" indicates that a culture had viable parasites following drug pressure. "Positive (PCR)" indicates that a culture screened positive by PCR for the edited sequence.

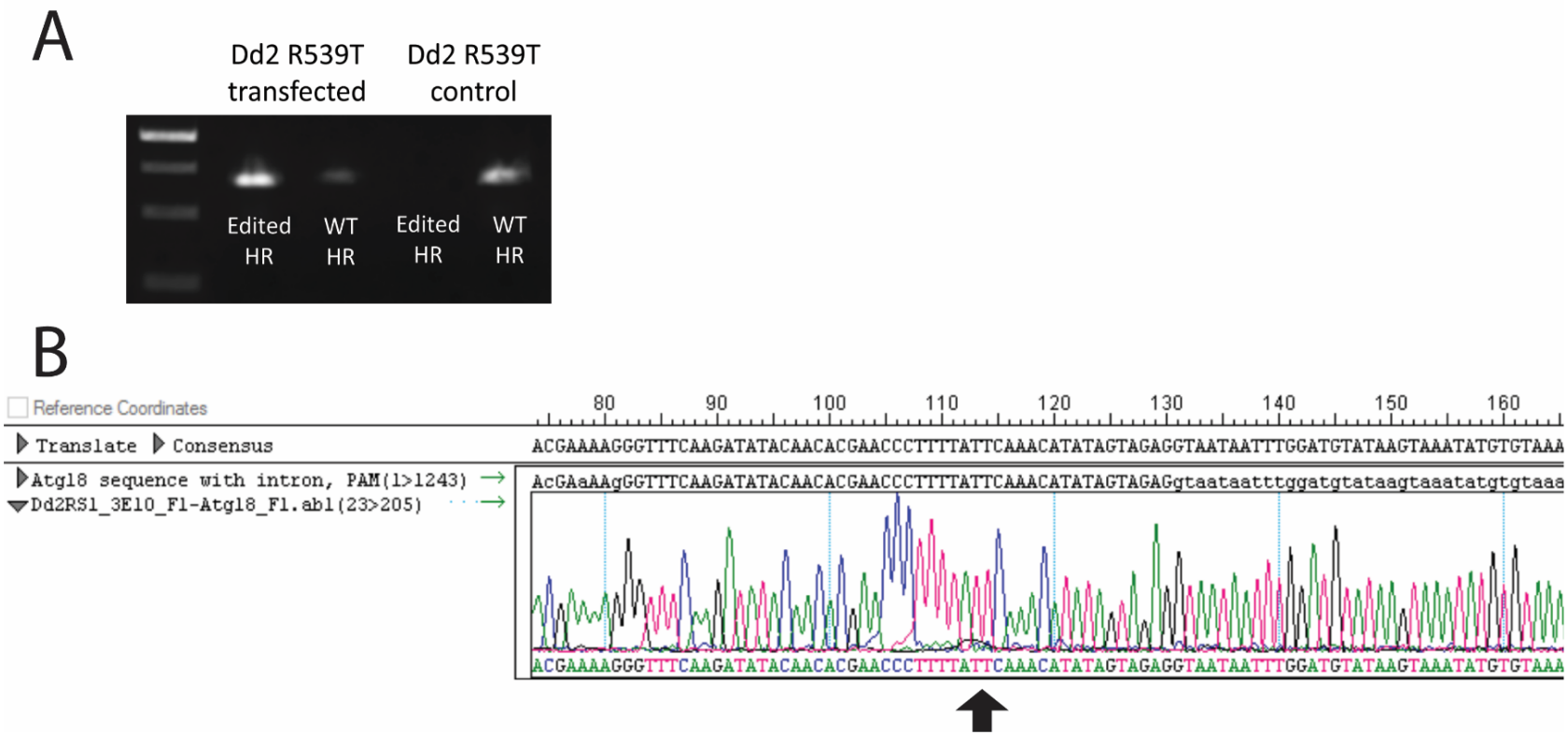


Figure 17: Screens for CRISPR/Cas9 editing

Cultures that grew following drug pressure were screened by PCR to determine if the culture had the edited homology region. The representative gel here shows a heterogeneous population of parasites with and without editing, as there are bands corresponding to reactions using primers specific for the edited (column 1) and non-edited (column 2) homology regions. The controls showed no editing (column 3). (B) Shown is a representative image of a chromatogram demonstrating editing of the locus of interest (T to I). The arrow denotes the changed base pair causing the sequence to encode isoleucine.

Cultures that recrudesced under drug selection were screened as per above methods by PCR to determine if editing had occurred (Figure 17A). Cultures that screened positive by PCR were cloned by limiting dilution and positive cultures were screened again via PCR then sent to Genewiz for sequencing (Figure 17B).

3.4 DISCUSSION

The emergence and spread of drug resistance is a constant scourge in the battle to eliminate malaria worldwide. As a new antimalarial drug enters clinics, it seems that it is only a matter of time before parasites mutate to evade the drug's mechanism of action. Because of the seeming inevitability of the emergence of drug resistance, it is important to understand the ways that parasites can change and survive drug exposure. The first step in understanding how resistance occurs is to understand where and when these resistant parasites arise. Parasite surveillance is vital to swift action against emerging antimalarial resistance. In some cases, this action has taken the form of the development of novel drugs while in others a simple change in the recommended drug regimen has bought more time. In either case, a surveillance program like TRAC has provided the malaria community with an invaluable resource toward helping understand the emergence and spread of drug resistance in Southeast Asia.

Whole genome sequencing data has been an instrumental part of the TRAC study. While clinical studies of efficacy allow us to see a moment in time, WGS data can be mapped to elucidate relationships between parasite populations and ultimately determine origin and timing. As the malaria community works towards pinpointing the origin of ART-resistant parasites, we have gained insight into the complex genetic background that appears important for selection especially within Cambodia and the surrounding countries.

Kelch13 mutations appear on a unique genetic background that seems to be important in selection within the region. Although some parasites have been found with *k13* mutations elsewhere in the world, including Africa, they are not always associated with delayed parasite clearance half-life in response to ACT treatment (Taylor et al., 2015, Mukherjee et al., 2017, Kheang et al., 2017, Ouattara et al., 2015, Muwanguzi et al., 2016, Cooper et al., 2015). The genetic background specific to some areas of Southeast Asia may be

responsible for some amount of the drug resistance phenotype. Alternatively, these mutations may be important in transmission or may confer a survival advantage over parasites without this array of SNPs. Another possibility is that the frequency of polyclonal infections and high rates of reinfection (therefore recombination) create an ultra-selective environment in Africa that does not allow for any decreased fitness costs that *k13* mutations may incur and thus may mask the mild clinical artemisinin resistance phenotype (Tilley et al., 2016).

Autophagy-related genes associated with ACT prolonged parasite clearance half-life and *in vitro* partner drug resistance were examined and several significant SNPs were discovered. Non-synonymous SNPs were found in PF3D7_1012900 (*atg18*), PF3D7_1239800 (*atg11*), and PF3D7_0709400 (*atg14*). Given time constraints of this DPhil program, only one SNP could be selected for further study.

The SNPs found in *atg11* were of interest as there were three separate SNPs that associated with different antimalarial resistance phenotypes (parasite clearance half-life and piperaquine IC50, Table 13). In other organisms, Autophagy-related protein 11 (Atg11) protein is involved in targeting another protein, Atg9, to the pre-autophagosomal structure (PAS) (He et al., 2006). Atg9 is important to build the PAS and therefore Atg11 is an important player in the initiation of autophagy (Yorimitsu and Klionsky, 2005), especially selective autophagy (Backues and Klionsky, 2012). Although there were multiple SNPs in *atg11*, none of them rose to the level of significance in the GWAS and, therefore, these SNPs were not selected to be a focus of this study. However, given the number of non-synonymous SNPs in *atg11* that associate with drug resistance phenotypes, this gene could be very important in parasite drug responses and warrants investigation.

There was only one SNP that associated with an antimalarial resistance phenotype in *atg14*. The SNP non-significantly associated with an increased chloroquine IC50, making it out of scope for this project which centers on the artemisinin resistance phenotype. It is important to note that in other organisms, the Atg14 protein forms part of the PI3K complex (class III), specifically in complex I of PI3K which is involved in the localization of PI3K to the PAS at the beginning of the autophagy pathway (Obara and Ohsumi, 2011, Obara et al., 2006). In *Plasmodium*, PI3K has been implicated in the mechanism of

artemisinin resistance (Mbengue et al., 2015) and therefore this SNP also merits further review.

The non-synonymous SNP found in *atg18* significantly associated with delayed parasite clearance half-life. Atg18 binds to PI3P on the pre-autophagosomal membrane to initiate autophagy in yeast. Given this SNP's association with the artemisinin resistance phenotype and owing to the fact that it was the only SNP in a putative autophagy-related gene whose association with drug resistance achieved statistical significance, this SNP was chosen for further investigation.

All three genes with associated drug resistance phenotypes (*atg11*, *atg14*, and *atg18*) encode proteins that are important in the initiation of autophagy. Further, two homologous genes (*atg18* and *atg14*) translate to form proteins that are involved in PI3K or PI3P. This bolsters recent theories that PI3K/PI3P are involved in the mechanism of ART resistance (Mbengue et al., 2015, Mott et al., 2015).

The decision to investigate the SNP in *atg18* was corroborated by the later discovery of a similar SNP in the same location on the genome, encoding for a different amino acid change in a different region of Southeast Asia. Wang et al. 2016 found the T38N SNP in *atg18* in parasites found in patients along the border between China and Myanmar (Wang et al., 2016). The geographic separation and different substitution mean that these SNPs arose independently and do not represent migration of the same SNP. This indicates that it is unlikely that the SNP represents a random mutation and rather it is being specifically selected for in the population.

For more evidence of the importance of the *atg18* SNP, *ex vivo* IC50 data collected from three Cambodian clinical research sites, Ratanakiri, Preah Vihear, and Pursat, was assessed. Parasites were sorted based on mutations in *atg18* and/or *k13* genes. As expected, IC50 values for artemisinin derivatives (Figure 15E-F) were higher for parasites with mutations in both *k13* and *atg18* than parasites with wild-type loci. Interestingly, parasites with an *atg18* mutation but without a *k13* mutation also had increased IC50 values above wild-type. This increased IC50 indicates that *atg18* may provide a boost in resistance that is independent of *k13* mutations.

Partner drug *ex vivo* IC50s showed a similar pattern for chloroquine, piperaquine, and quinine (Figure 15A, C, D), though not mefloquine (Figure 15B) based on *k13* and *atg18*

mutations. However, separate mutations have been identified that associate with partner drug resistance for chloroquine, mefloquine, and piperaquine. When parasites were separated based on the presence or absence of these mutations (*crt* for chloroquine (Fidock et al., 2000, Sidhu et al., 2002, Djimde et al., 2001), *mdr* increased copy number for mefloquine (Price et al., 2004, Nelson et al., 2005, Wilson et al., 1993, Basco et al., 1995), or *plasmepsin* increased copy number for piperaquine (Amato et al., 2017, Witkowski et al., 2017)) the pattern disappears. With chloroquine, the *crt/atg18* double mutant has a higher average IC50 value than that for *crt* mutant *atg18* wild-type parasites, which itself is higher than the double wild-type parasites. Since there are limited samples with the *crt* wild-type and *atg18* mutation, the contribution of the *atg18* mutation can only be assessed in the context of *crt* mutations. This pattern of data indicates that it is unlikely that the *atg18* SNP is important in mefloquine or piperaquine partner drug resistance, but it may still be important in chloroquine partner drug resistance.

The major limitation of these *ex vivo* IC50 data is that they are from clinical samples. Each parasite has many different SNPs in various other genes that are not accounted for in the simplistic analysis of separating based on the presence of a few mutations. It is entirely possible that the *atg18* SNP represents a marker of a genetic background rather than an important independent contributor to a resistance phenotype. Additionally, it is not clear from these studies whether the *atg18* SNP represents an advantage in surviving drug exposure or if the mutation confers a fitness advantage. Such a fitness advantage may help parasites be selected for in a population by improving transmission or growth but would not necessarily relate to drug resistance. Therefore, in order to determine the contribution of the *atg18* SNP alone, it was necessary to derive parasites with an isolated *atg18* SNP through genetic editing.

CRISPR/Cas9 editing technology was used to edit the genome. The advantages of CRISPR over previous editing technology in *Plasmodium* include cost-effectiveness, speed, and its relative ease. The CRISPR system that has been previously used successfully in *Plasmodium* is a type II system using a Cas from *Streptococcus pyogenes*. This particular Cas endonuclease, Cas9, necessitates a specific NGG PAM sequence for the double strand break (Jinek et al., 2012). Typically, there is an NGG site every 8-12 base pairs in the human genome (Hsu et al., 2013, Cong et al., 2013) and there were numerous NGG sites within the *Plasmodium atg18* gene; therefore, the necessity of selecting a nearby NGG site was not an issue in this case.

One limitation of CRISPR technology is the potential for off-target effects. To minimize off-target effects, care must be given to the design of the sgRNA and the selection of the appropriate PAM site. Given a list of possible sgRNA sequences, two sequences were chosen based on low off-target sequence identity. Mismatch tolerance was positional—preference was given to mismatches at the 3' end of the sequence as the Cas9 is less tolerant of those than 5' (Ran et al., 2013). Generally, Cas9 is intolerant of more than 3 mismatches in a guide sequence (Ran et al., 2013). As seen by Table 7, the sequences chosen had off-target sequences with no fewer than 6 mismatches. The Benchling program was consulted after sgRNA selection to confirm that sequences were optimal for editing. Editing efficiency decreases with increasing distance from the cut site and so the selected PAM site was nearby, only 29 base pairs away from, the SNP site of interest (McNamara et al., 2013).

The homology region for the repair template must also be carefully designed to facilitate editing. Homology arms were approximately 500bp in length (slightly shorter or longer depending on sequence and the ability to make primers for easy PCR) (Thomas et al., 1986, Hasty et al., 1991). In order to prevent Cas9 from cutting the homology region in a repaired genome, silent mutations were added to the homology region in the sequence leading up to the PAM sequence. These silent mutations prevent recognition by the sgRNA directed Cas9 and therefore prevent repeated double strand breaks directed at the newly edited genome. Although changing the PAM site (NGG) would have been preferable (Fu et al., 2013), this was unfortunately not possible in the case of either chosen sgRNA/PAM sequences as that would have changed the coding sequences. As previously stated, Cas9 is less tolerant of mismatches at the 3' end and, therefore, the silent mutations were added closer to the 3' end of the sgRNA sequences (Ran et al., 2013).

Although CRISPR/Cas9 technology represents a huge leap forward in genomic editing, difficulties persist in editing optimization, especially in *P. falciparum*. The first difficulty lies inherently in the *P. falciparum* genome. The genome itself is extremely AT-rich, with the 3D7 reference genome being comprised of 80.6% AT (Gardner et al., 2002, Nikbakht et al., 2014)—approximately 75% in coding sequences and 87% in non-coding sequences (McCutchan et al., 1984, Gardner et al., 2002). This can be compared to the *Homo sapiens* genome of 58.9% AT (Hamilton et al., 2017). Even another apicomplexan parasite, *Toxoplasma gondii*, is only comprised of 47.7% AT (Hamilton et al., 2017) and, perhaps more surprisingly, *P. vivax* is comprised of 59.4% AT (Hamilton et al., 2017). The AT-

rich genome is thought to contribute to the ability of *P. falciparum* parasites to mutate rapidly, as indel mutations have been shown to be associated with regions of high AT content (Hamilton et al., 2017).

In addition to the high AT content of the genome, the *P. falciparum* genome also contains large swaths of low-complexity regions (LRCs) (Pizzi and Frontali, 2001, Zilversmit et al., 2010), which represent sequences with low diversity of amino acids and typically include repeated amino acids either singularly or in motifs (Wootton and Federhen, 1993). In *P. falciparum*, these LCRs are often AT-rich and made of short tandem repeats which differ from homologous sequences found in other organisms (Xue and Forsdyke, 2003, DePristo et al., 2006). It is not clear why *P. falciparum* has adapted to include so many LRCs, but theories include that these regions function as introns (Xue and Forsdyke, 2003), are important for host immune evasion (Hughes, 2004) or serve no function (DePristo et al., 2006).

Taken together, the AT-rich genome full of LRCs makes *P. falciparum* a difficult subject for molecular biology. *E. coli*, the organism used to generate large quantities of plasmids by mini- or maxi-preps, does not like repetitive genomes and thus sequences are frequently recombined or deleted all together (Hommelsheim et al., 2014). PCR is also difficult in sequences of low complexity as polymerase slippage can occur, causing the insertion of additional base pairs or deletion of needed base pairs (Shinde et al., 2003, Kunkel and Bebenek, 2000). The LCRs make finding a suitable primer for PCR difficult as well—primers with high AT content have lower annealing temperatures, which can lead to non-specific binding of the primers with other areas of the genome and create non-specific products. Ideal primers contain 40-60% GC content as these nucleotides contain three bonds, rather than the two bonds of AT, and are therefore more thermodynamically stable (Chuang et al., 2013). Primers with high AT content can have low primer specificity, meaning that they are complementary to other regions of the genome as well as the desired region of amplification.

Once plasmids are produced, transfection is the next hurdle to overcome with *P. falciparum*. Transfection is the introduction of genetic material, typically a plasmid, into a eukaryotic cell. There are many methods for transfection into a eukaryotic cell (Loyter et al., 1982, McCutchan and Pagano, 1968, Potter et al., 1984, Tang et al., 1996, Felgner

et al., 1987, Cudd et al., 1984), but generally *P. falciparum* is transfected using electroporation (Wu et al., 1995) or polyamidoamine dendrimers (Mamoun et al., 1999b).

The first major difficulty in transfection lies in the parasite biology: DNA must traverse three membranes to enter the cell. The erythrocyte has a membrane, followed by the parasitophorous vacuolar membrane, followed by the parasite plasma membrane. In order for parasites to be genetically edited by CRISPR plasmids, the Cas9 protein and a plasmid containing the sgRNA must also enter the nucleus to access the genome, thus representing yet another membrane and hurdle for editing.

Several methods for electroporation-based transfection have been developed specifically for *P. falciparum*. Parasites themselves can be electroporated, either as rings (Wu et al., 1995), schizonts (Waters et al., 1997), or merozoites (Kaiser et al., 2017), or erythrocytes can be transfected and parasites incubated with the transfected erythrocytes (Deitsch et al., 2001). The success of transfection using pre-loaded erythrocytes is based on the parasite's ability to spontaneously take up plasmids from the erythrocyte cytoplasm (Deitsch et al., 2001). The electroporation of parasites themselves has been shown to cause 50-70% reduction in viable parasites as compared to pre-loaded erythrocytes (Deitsch et al., 2001). The success of pre-loading is attributed to its minimal impacts on parasite viability, as opposed to the trauma incurred by parasites upon electroporation (Skinner-Adams et al., 2003) (Hasenkamp et al., 2012). Further, additional erythrocytes loaded with plasmid can be added to culture to improve the odds of success (Deitsch et al., 2001).

The stage specificity necessary for these transfection protocols represents another barrier towards the production of an edited line. Synchronizing parasites can be a laborious process, especially when dealing with multiple lines and different life cycle lengths. Synchronization methods can be taxing on the parasites themselves, potentially causing stress and inducing gametocytes in an otherwise healthy culture.

Furthermore, efficiency of transfection is quite low. For *P. falciparum*, efficiency has been estimated between 10^{-6} to 10^{-9} as compared to other *Plasmodium* species, including *P. berghei*, which has a transfection efficiency between 10^{-2} to 10^{-3} (Janse et al., 2006). This low efficiency means that very few parasites in a culture will become transfected with a plasmid of interest and, therefore, the process of growing up transfectants under

drug selection can take several weeks to months. Historically, this has been a major drawback to using *P. falciparum* and has encouraged researchers to use the rodent model, *P. berghei*.

Another difficulty in molecular editing of *P. falciparum* is that there are only a few selectable markers to pressure a culture. One of the most popular markers is *human dihydrofolate-reductase-thymidylate synthase* (*hDHFR*) gene, which confers resistance to WR99210 (de Koning-Ward et al., 2000). Another marker that was used in this project was blasticidin S deaminase (*bsd*) (Mamoun et al., 1999a). The CRISPR/Cas9 plasmids used in Ghorbal et al. (Ghorbal et al., 2014) employed the selectable marker *yeast dihydroorotate dehydrogenase* (*ydhodh*) to confer resistance to DSM1 (Ganesan et al., 2011). *Neomycin phosphotransferase II* (*neo*) confers resistance to geneticin G418 (Mamoun et al., 1999a). *Puromycin-N-acetyltransferase* (*pac*) confers resistance to puromycin (de Koning-Ward et al., 2001). Negative selectable markers include *thymidine kinase* (*tk*), which allow parasites to be killed using ganciclovir (Duraisingh et al., 2002), and *cytosine deaminase/uridyl phosphoribosyl transferase* (*CDUP*), which are killed using fluorouracil (5-FC) (Maier et al., 2006). The paucity of selectable markers can impede editing, as parasites that have previously been edited using one selectable marker may continue to be resistant to that marker, unless a negative marker has been used to remove the plasmid.

Despite these difficulties, it was surprising when the Eastman plasmids did not ultimately produce any edited parasites. However, it has since been learned that no individual has had success using this plasmid system and, therefore, we may be able to assume that the major issue is with the plasmids themselves rather than a user error. It is possible that the plasmids themselves are toxic to the parasites, although parasites were still able to grow following transfections. There is the possibility that Cas9 was not expressed, although it was driven by the tried and true EF1α promoter that was used successfully in other aspects of this project. This could be tested using an anti-Cas9 antibody or qPCR to determine expression of the protein; however, investing too much time in troubleshooting this plasmid system seemed beyond the scope of this project.

The Lopez-Rubio plasmids ultimately worked, although the success was limited. Given the variability in successful CRISPR editing in *Plasmodium* using this system, it is likely that the limited success was due to user error rather than the plasmids themselves.

Investigators have observed wide variation in success, which seems to associate not to a particular method but to the lab member performing the transfection. Careful separation of late stage schizonts from uninfected erythrocytes was necessary for transfection using pre-loaded erythrocytes. It is possible that too many uninfected RBCs were included in the Percoll separation, which would allow schizonts to reinvade RBCs which were not transfected with the plasmids. Smears of the Percoll purified schizonts indicated that approximately 80% of RBCs were infected. The low efficiency of transfection means that a relatively small number of parasites take up a selectable plasmid, let alone both selectable plasmids in this case. Therefore, it is possible that these parasites did not survive the culturing process following transfection. Further, parasites 967^{WTrev} and $Dd2^{R539T}$ had already been edited in the past and, despite being maintained in the absence of drug selection, may still contain *hdhfr*-containing plasmids. This would render these parasites resistant to WR99210, which was one of the drugs used to pressure the cultures.

In addition to shortcomings of these plasmid sets in *Plasmodium*, CRISPR itself has its limitations. The major caveat is unknown off-target mutations, which could occur when Cas9 cuts a region other than that targeted by the sgRNA (Schaefer et al., 2017). The chance of this increases with the amount of Cas9 used and the similarity of the sgRNA sequence to other genomic sequences (Ran et al., 2013). Although care was taken to prevent sgRNA homology to another region of the genome, this could still have occurred. A second PAM sequence was selected and attempts were made to edit the sequence using the Eastman plasmid system; however, these were ultimately unsuccessful.

3.4.1.1 Autophagy transcriptomics

The same list of autophagy-related genes was used to perform a sub-analysis on *ex vivo* transcriptomics of ART-resistant and ART-sensitive isolates. There were several proteins that were upregulated, although many more were downregulated, in resistant samples as compared to sensitive samples. Of note is the upregulation of *atg16*. Given that Atg16 binds to Atg18 (Nair et al., 2010), its upregulation could reflect increasing activity of Atg18. Overall, there was enrichment of the autophagy pathway, suggesting that there may be general modulation (increase or decrease) of this pathway.

The upregulation of several autophagy-related genes correlates with increased levels of autophagy in other organisms. The particular genes include *atg7* (Bernard et al., 2015),

atg8 (Nara et al., 2002, Kirisako et al., 1999), *atg9* (Jin et al., 2014), *atg12* (Kouroku et al., 2007), and *atg14* (Xiong et al., 2012). WIPI1 transcription has also been associated with increased autophagosome formation (Tsuyuki et al., 2014); however, autophagosome formation is not necessarily an indication of increased autophagy, as it could represent a blockage of autophagosome/lysosome fusion. With the exception of *atg12* (which did not have data), all of these genes were downregulated in our sub-analysis.

This ostensibly suggests that the autophagy pathway is downregulated in resistant isolates; however, transcriptomics is not recommended as a mechanism for quantifying autophagy for several reasons (Klionsky et al., 2016). First, the majority of autophagy-related genes show no change in transcription even when autophagy is induced (Klionsky et al., 2016). It is generally preferable to monitor changes in protein level rather than mRNA itself. Second, changes in transcription represent a population of cells and, therefore, an average across a variety of cells. Especially in this case, with asynchronous, *ex vivo* cultures, the true signal of the autophagy transcriptome could be masked by the diverse nature of the population as a whole. It would have been preferable to perform single cell sequencing, which would be able to attribute subtle changes in mRNA to a specific cell rather than a population. Therefore, rather than inferring a specific directionality (increased or decreased) of autophagy, it is preferable to state that the autophagy-like pathway appears to be modified.

In summary, an *atg18* SNP was identified that associated with delayed parasite clearance half-life in response to artemisinin combination therapy. This SNP was also associated with increased *ex vivo* IC50 values in response to artemisinin-derivatives, even in the absence of *k13* mutations. The association of this SNP in a putative autophagy-related gene, suggests that there may indeed be a connection between artemisinin resistance mechanisms and an autophagy-like pathway in *P. falciparum*. Consequently, this SNP was edited using CRISPR/Cas9 editing to create a set of isogenic lines differing only in the *atg18* SNP so that the contribution of the SNP could be isolated and assessed in the following chapters.

4 PHENOTYPIC CHANGES AND DRUG SENSITIVITIES ASSOCIATED WITH AN ATG18 POLYMORPHISM IN *PLASMODIUM FALCIPARUM*

4.1 INTRODUCTION AND AIMS

4.1.1 Introduction

Autophagy, an intracellular process to degrade and recycle damaged organelles, has been well-characterized in many organismal systems, but it is not well-described in *P. falciparum*. A limited set of putative autophagy-related proteins is encoded by the genome of *P. falciparum,* but the function of the majority of these proteins is yet to be defined.

P. falciparum Atg8 (PfAtg8), whose homologs, Atg8 and LC3, are vital to autophagy in yeast and mammalian systems respectively, has been briefly studied. However, PfAtg8 has been shown to have a major role outside the canonical autophagy pathway. PfAtg8 co-localizes with the apicoplast (Navale et al., 2014, Tomlins et al., 2013, Walczak et al., 2018, Bansal et al., 2017, Cervantes et al., 2014, Kitamura et al., 2012), a plastid that has no known autophagic functions. Although the apicoplast also has a role in fatty acid biosynthesis (Ramakrishnan et al., 2012), heme biosynthesis (Sato et al., 2004), and iron-sulfur cluster assembly (Seeber, 2002, Ralph et al., 2004), the only function necessary for the intraerythrocytic lifecycle is the production of a metabolite called isopentenyl pyrophosphate (IPP) (Yeh and DeRisi, 2011). IPP is an isoprenoid precursor that is involved in the methylerythritol phosphate (MEP) pathway (Jomaa et al., 1999, Rohmer, 1999). While the functions of IPP are not well understood at this time, IPP is an essential metabolite and parasites are unable to survive without its production (Yeh and DeRisi, 2011). A PfAtg8 knockdown parasite exhibited a slow growth phenotype, which was rescued by the addition of IPP, demonstrating that the essential function of PfAtg8 is its involvement in apicoplast biogenesis (Walczak et al., 2018). This finding suggests that the primary role of PfAtg8 is independent of an autophagy pathway, although it does not

exclude the possibility that the apicoplast is involved in autophagy, perhaps in the provision of nutrients such as IPP.

There is, however, some evidence that PfAtg8 participates in an autophagy-like pathway. PfAtg8 has been shown to appear on vesicles (Cervantes et al., 2014) and to co-localize with the DV in response to starvation (Tomlins et al., 2013). These functions would be expected based on the homologous autophagic functions in other organisms, given that the DV is the acidic compartment of the parasite and can be likened to the lysosome of other cells (Goldberg et al., 1990). PfAtg8 function has been used as a measure of autophagy. Upon the application of stress to a parasite, PfAtg8 appears to form puncta by confocal microscopy (Gaviria et al., 2013, Mott et al., 2015). The formation of puncta by Atg8/LC3 has been a well-used assay in other organisms (Klionsky et al., 2016), thus the finding of stress-induced puncta formation may indicate a secondary role of PfAtg8 in an autophagy-like pathway.

Other plasmodial proteins in the autophagy cascade have also been studied. Plasmodial Atg7 appears to be essential for normal growth (Walker et al., 2013). Plasmodial Atg3 has been shown to bind PfAtg8, as in other organisms, where it is responsible for lipidation of Atg8 with PE (Hain et al., 2012). Inhibiting this interaction with various compounds has caused parasite death (Hain et al., 2014, Hain et al., 2016). Based on the PlasmoGem data set, which knocked out a number of autophagy related genes in *P. berghei*, homologs for Atg3, Atg4, Atg5, Atg8, Atg11, Atg18, Vps15, and Vps34 were all deemed essential to parasite growth (Bushell et al., 2017, Schwach et al., 2015).

At the time that this thesis project was initiated, there were no studies characterizing PfAtg18. The gene encoding PfAtg18, *PF3D7_1012900*, has since appeared in a second GWAS along the China-Myanmar border, where it also associated with artemisinin resistance, as discussed earlier (Wang et al., 2016). In another investigation to establish a connection between PfAtg18 and artemisinin, a study of the mechanism of action of artemisinin found PfAtg18 as one of 124 proteins covalently bonded to artemisinin (Wang et al., 2015b). An additional study has since demonstrated that PfAtg18 binds to PI3P and that it has a role in apicoplast biogenesis (Bansal et al., 2017). Increasing levels of PI3P correlate with increased artemisinin resistance in parasites from Southeast Asia (Mbengue et al., 2015). Thus, the ability of PfAtg18 to bind to PI3P could implicate it in the mechanism of artemisinin resistance. This limited body of literature suggests that

PfAtg18 has a role in apicoplast biogenesis and may be involved in artemisinin resistance. In other organisms, Atg18/WIPI puncta formation is a powerful assay to measure autophagy; however, the ability of PfAtg18 to form puncta has not previously been demonstrated. This chapter seeks to characterize PfAtg18 further.

There are a variety of reasons that the *atg18* SNP, or any SNP, could be selected for in a population of parasites. The first, and possibly most obvious, would be selection due to drug pressure. As is detailed in the introduction chapter, a variety of antimalarial drugs have been utilized in Southeast Asia and this drug pressure has continually forced parasites to adapt to survive. However, there are many other pressures, outside of drug pressure, that exist and that could facilitate the selection of an advantageous mutation. A mutation could cause a change in fitness, allowing the mutant parasite to outcompete its fellow parasites. A fitness advantage could make a parasite better at transmission, more efficient at growing in the conditions of its human host population, or able to modulate its metabolism to evade drug, to name but a few possibilities. This chapter investigates phenotypic contributions of the T38I SNP in *atg18*, including drug susceptibility and a growth phenotype.

4.1.2 Aims

(1) The first aim is to characterize the protein encoded by the plasmodial gene *PF3D7_1012900*, the putative P. *falciparum* Atg18 (PfAtg18) protein.

(2) The next aim is to determine whether the T38I SNP in *atg18* changes parasite susceptibility to antimalarial drugs or any other drug included in the NCATS drug libraries.

(3) The final aim is to determine whether the T38I SNP in *atg18* changes parasite growth rate.

4.2 MATERIALS AND METHODS

4.2.1 Atg18 alignment with homologues

Genes for proteins in the WIPI family were aligned using MegAlign version 12.2.0 using protein sequences from *Homo sapiens* WIPI1 (AAH39867.1), WIPI2a-d (NP_056425.1, NP_057087.2, NP_001028690.1, NP_00102891.1) and *P. falciparum* Atg18

(XP_001347411.1). Analysis was performed using the Clustal V method, although relevant findings did not differ when Clustal W or Jotun Hein methods were used.

Using the sequence from PlasmoDB and the currently available crystal structure of Hsv2, the homologue of Atg18 in *K. lactis*, a model of PfAtg18 was created with UCSF Chimera version 1.10.1. The sequence for PI3P binding, FRRG, was highlighted in addition to the SNP of interest, T38I, and Atg16 binding site.

4.2.2 VR2001 Anti-Atg18 antibody production

The VR2001 anti-Atg18 antibody was produced with a plasmid that encodes PfAtg18 for immunizations, allowing for cellular uptake of the plasmid, expression and secretion of PfAtg18, and consequently the production of anti-Atg18 polyclonal antibodies. The *PF3D7_1012900* (Atg18) sequence was taken from PlasmoDB, optimized for *Mus musculus,* and a DNA fragment was synthesized by GeneArt of Life Technologies (Table 17). Importantly, *PF3D7_1012900* does not have a secretory signal or a transmembrane domain, according to analysis using SignalP Server 4.1 and TMHMM Server 2.0 respectively. Forward and reverse primers were created for PCR amplification (Table 17). The fragment was amplified via PCR using 5µL Accuprime buffer II, 1µL Accuprime polymerase, 1µL Atg18 forward primer, and 1µL Atg18 reverse primer (Table 17), 37µL PCR water, and 5µL Atg18 gene string. The thermocycler conditions were as follows: 94^{o}C for 5 minutes, then 25 cycles of 94^{o}C for 30 seconds, 65^{o}C for 30 seconds, 72^{o}C for 1 minute, followed by 72^{o}C for 7 minutes, and held at 4^{o}C. The PCR product was run on a 1% agarose gel with ethidium bromide (1:100) at 120V for 30 minutes (standard gel conditions unless otherwise specified) to confirm the product size. A ligation reaction was performed immediately following with 4µL PCR product, 0.6µL VR2001-TOPO vector (Figure 18) (Oliveira et al., 2006) (from Jose Valenzuela, NIH), 1µL TOPO salt solution, and 0.4µL water for 10 minutes at room temperature followed by 2 minutes on ice. The VR2001-TOPO plasmid has a TOPO/TA cloning site for fragment insertion and a tissue plasminogen activator (TPA) signal peptide at the 5' end of the sequence insertion site to ensure protein secretion. The plasmid also has a kanamycin resistance gene and the cytomegalovirus promoter.

Table 17: Constructs for plasmid anti-Atg18 antibody production

Name	Sequence
Atg18 gene sequence	ATGGTGTCCCTGAGACTGGACAACAACCGGTACATCAGCTTCAACC AGGACTACGGCTGCCTGTGCATGGCCAACGAGAAGGGCTTCAAGAT CTACAACACCAACCCCTTCACCCAGACCTACAGCAGGGACCTGACC GACAGAAACAAGAACGGCCTGTACCTGGCCGAGATGCTGTACAGA TGCAACATCCTGGCCATCACCGGCAACAAGAATGACAAGAAAGGC AAGTGGGCCAAGAACGTGCTGATCATCTGGGACGACAGACAGATG AGAGAGATCGCCAAGCTGACCTTCAGCAGCAACATCATCGGCGTGC GGCTGCTGCGCGAGATCATCGTCGTGATCCTGGAGTACAAGCTGTG CATCTACCGGCTGAAGGACATCATCCTGCTGGAAACCCTGAACACC TCTAAGAACGTGTCCGGCCTGTGCTGCCTGAGCAACATCGACAAGA ACATCATCATTGCCTACCTGAGCCCCATCAAGGGCAGAGTGAACAT CCACATCTTCGAGATCAACAGCAGCGAGAATATCCACGAGGAACTG CCCTACATCAACTTTAAGACCAACCTGAGCATCTACGCCCACGACA ACAGCATCGGCTGCATCAACCTGTCCAACGACGGCAAGCTGCTCGT GACCAGCAGCACCAAGGGCACCATCATCAGACTGTTCAACACCTTC GACGGCACCCTGCTGAACGAGTTCAGAAGAGGCACCAAGAACGCC AAGATCCTGAGCCTGAACATCAGCGAGGATAACAACTGGCTGTGCC TGACCAGCTCCAGAAACACCGTGCATGTGTTCTCCATCTACAAGAA GAAGAGGCCCCTGAGGAAGGTGGACATTATCTGCAAGGGCAAGAA TGTGTCCCCCCCTGCTCTGCTGAACTACGAGAAAGAGTCCAAGAAC AAGAAAAGCAGCCTGAAGTGCCTGCTGCCCTGCCACCCCTACCTGA ACAGCGAGTGGTCCTTCGCCAGCTACAAGCTGCCCGGCAAGAAGAT CAGCAGCATCTGCGCCTTCGTGAACGACCAGAACTGCATCATCGTG ATCTGCAGCAACGGCATCATCTATAAGCTGCGGTTCAACGAGCACA TCGGCGGCGACATGTTCAAGATCAGCTCCCACAGCTTCGACTGA
Forward primer	ATGGTATCATTAAGATTAGAT
Reverse primer	TTAATCAAAACTGTGTGATGA
VRFb	ACAGGAGTCCAGGGCTGGAGAGAA
VRRb	AGTGGCACCTTCCAGGGTCAAGGA

One Shot TOP-10 cells were transformed with the plasmid by adding 2µL of the ligation reaction to 25µL of cells and incubating the mixture on ice for 15 minutes followed by 30 seconds at 42ºC then incubation on ice for 2 minutes. SOC medium (250µL) was added and the tube was incubated at 37ºC on a shaker at 250RPM for 30 minutes. The mixture was then grown overnight on LB plates with kanamycin at 50µL/mL (standard concentration unless otherwise specified). Colonies were selected and screened by PCR for sequence insertion using 0.5µL VRFb primer (10µM), 0.5µL VRRb primer (10µM),

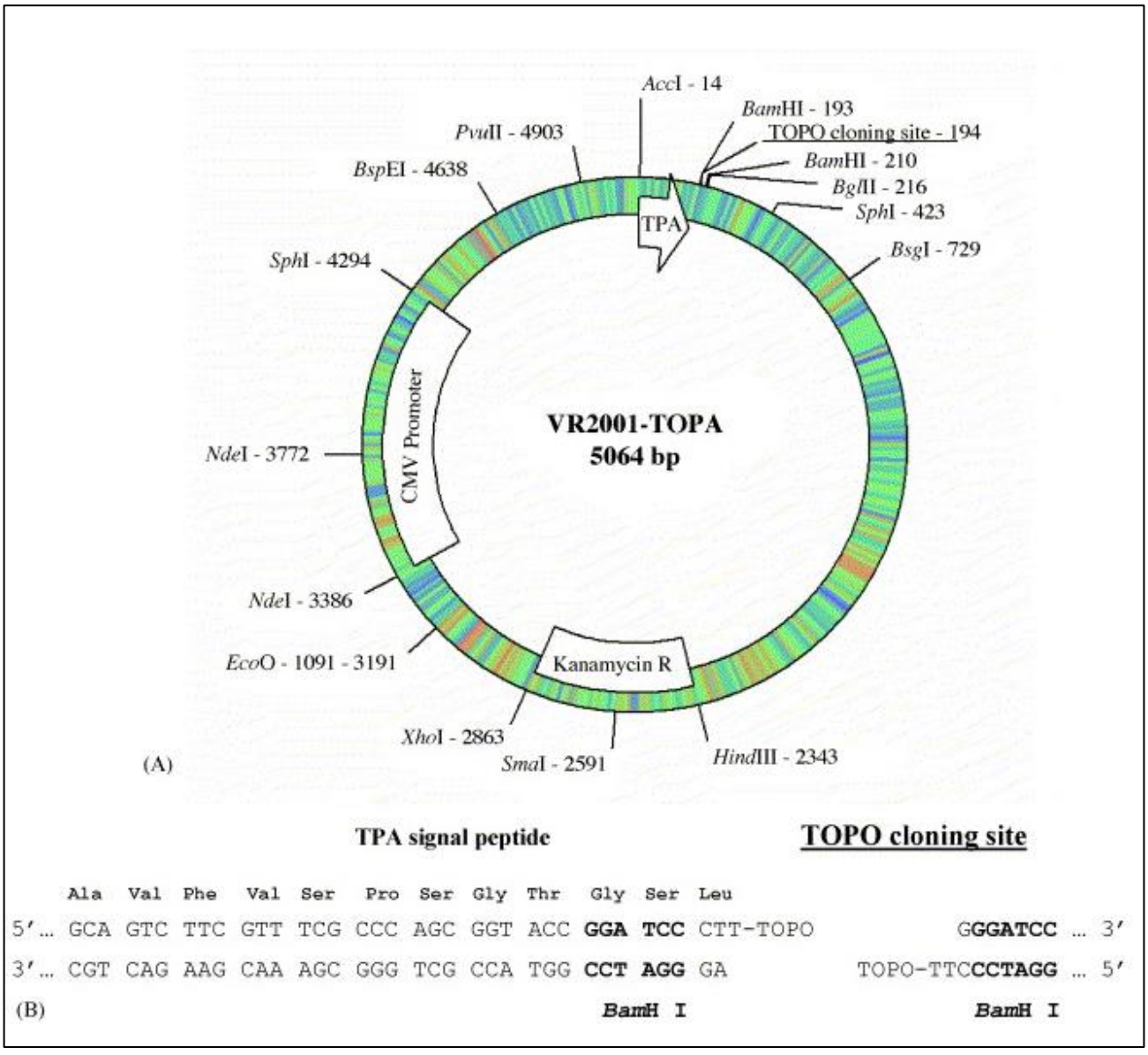


Figure 18: VR2001-TOPO vector backbone for anti-PfAtg18 antibody production.

Figure depicts VR2001 plasmid with TPA for protein secretion, CMV promoter, and kanamycin resistance gene for selection. This figure was reproduced with permissions from (Oliveira et al., 2006).

2µL diluted clone, and 10µL DreamTaq Green MM. The thermocycler conditions were 95ºC for 5 minutes followed by 30 cycles of 95ºC for 30 seconds, 50ºC for 30 seconds, 72ºC for 1 minute 20 seconds, followed by 72ºC for 10 minutes and held at 4ºC. The product was run on a gel and positive clones were grown overnight in 5mL LB with kanamycin. Plasmids were isolated using the Qiagen miniprep standard protocol. Plasmids were then sent to Operon for sequencing. Plasmids with the correct sequences were grown up in 750mL of LB with kanamycin overnight then isolated via NucleoBond PC EF plasmid DNA purification megaprep protocol.

Five female Swiss Webster mice were immunized with the plasmid intradermally in both ears (10µg/ear), every two weeks, three times. These experiments were carried out by Dr. Anderson Costa under the appropriate animal licenses. Mice were terminally bled and sera were analyzed by western blot. Parasite culture lysate and the insoluble fraction from a recombinant protein expression of Atg18 each were mixed with NuPAGE LDS Sample Buffer (4X) and NuPAGE Sample Reducing Agent (10X) and then were run in separate wells of a NuPAGE Novex 4-12% Bis-Tris Protein Gel (1mm, 10 well) at 200V for 50 minutes. Bands were transferred to a nitrocellulose membrane using a Thermo Fisher Scientific Pierce G2 Fast Blotter. The nitrocellulose membrane was blocked overnight in PBS-tween 5% milk (Blotting-grade Blocker non-fat dry milk, Bio-Rad) at 4ºC on a shaker. The membrane was cut and each piece of the membrane was incubated in an individual sera (1:50) in PBS-tween 5% milk overnight at 4ºC on a shaker. The membranes were then washed three times for 5 minutes each in PBS-tween on a shaker at room temperature followed by a single wash of PBS for 5 minutes on a shaker at room temperature. The membranes were dried then Pierce ECL Western Blotting Substrate solution was prepared according to the manufacturer's instructions and added for 1-5 minutes and the membranes were exposed to film for 30 seconds to 2 minutes in a dark room and developed on a Kodak X-OMAT 2000A processor.

4.2.3 Polyclonal antibody production

The production of Atg18 protein and subsequent polyclonal antibody production was performed by Dr. Louise Turner. The *atg18* gene was amplified from *P. falciparum* genomic DNA by PCR, using the forward and reverse primers (Table 18). *E. coli* expression vector pet15 was digested with NcoI and NotI, then the *atg18* PCR fragment was cloned in. The plasmid was transformed into the BL21 *E. coli* cells using the

transformation protocol as previously described. Bacterial cultures were grown at 37°C overnight in 50μg/mL ampicillin, then inoculated into 1L fresh 2xYT medium with ampicillin (50μg/mL) in a 1:50 ratio. Cultures were incubated at 37°C until an OD600 of 0.5–0.7 was detected, then gene expression was induced by the addition of 0.5mM isopropyl β-d-1-thiogalactopyranoside (IPTG) at 37ºC for 4 hours. Cultures were centrifuged at 4,000*g* for 10 minutes, then re-suspended in 50mM Tris·HCl, pH 7.5, 200mM NaCl (Buffer A) supplemented with EDTA-free protease inhibitors. A cell disruptor at pressure 30 kpsi lysed bacterial cells and the lysate was then centrifuged at 20,000*g* for 40 minutes. The soluble fraction of each construct was loaded into a gravity flow column containing nickel-nitrilotriacetic acid resin (Ni2+-NTA), which had been previously equilibrated with Buffer A. The Ni2+-NTA resin was washed with 10 column volumes (CV) of Buffer A plus 30mM imidazole, and the proteins were eluted in 3 CV of Buffer A plus 0.7M imidazole. Imidazole was then removed by buffer exchange in PBS with a PD-10 desalting column (GE Healthcare). Proteins were detected by western blot using an anti-pentahistidine HRP conjugated antibody.

Five BALB/c mice were immunized subcutaneously with 15μg of the above purified PfAtg18 protein in PBS every 3 weeks, three times. Freunds Incomplete adjuvant was used in all immunizations. Blood was collected 2 weeks following the last immunization.

Table 18: Polyclonal antibody production primers

Primer name	**Primer sequence**
Polyclonal Atg18 forward	TTTCCATGGGCTTAACTGATAGAAATAAGAATGG
Polyclonal Atg18 reverse	AAAGCGGCCGCTTAATCAAAACTGTGTGATGATATTTTAAAC

4.2.4 Production of GFP-tagged Atg18 lines

The plasmid backbone for pDC2 AttP BSD (Figure 19) was obtained from Dr. Richard Eastman at LMVR. The DNA sequence for *atg18* with an N-terminal GFP was synthesized by Integrated DNA Technologies. Promoter ef1α was used to increase expression of the construct. The plasmid (1μg) was digested with 2μL AvrII and 0.5μL

XhoI in 5µL Cutsmart buffer (QS to 50µL) overnight at 37ºC then heat inactivated at 65ºC for 20 minutes. The digested band (approximately 6360bp) was gel extracted and purified using the Monarch DNA gel extraction kit. The plasmid was then ligated using 110ng plasmid with 29.5ng insert (at 1:1 per NEB ligation calculator) and 1µL T4 ligase with 1µL 10X ligase buffer QS to 10µL at room temperature for 2 hours. The plasmid was then transformed into β10 cells, plated, and incubated overnight at 37ºC on LB agar plates with ampicillin. Colonies were screened by PCR using Atg18 repair primer F1 and p863 reverse primer in Sapphire master mix (10µL) and 10µL H_2O. Thermocycling conditions were 95ºC for 5 minutes, then 40 cycles of 95ºC for 30 seconds, 53ºC for 30 seconds, 68ºC for 1 minute, then a hold at 68ºC for 5 minutes followed by an infinite hold at 4ºC. Positive colonies were grown up overnight in 3mL LB broth with ampicillin, isolated using miniprep as per Qiagen, and sequenced by GeneWiz using Atg18 repair F1 primer and p863 reverse primer. Plasmids were then grown up in 500mL LB broth with ampicillin overnight at 37ºC and plasmid was isolated using maxi prep as per Qiagen Plasmid Maxi Kit standard protocol. Parasite lines Dd2, $Dd2^{R539T}$, 967^{WTrev}, and 967^{R539T} were transfected as previously described in Section 3.2.2.3.

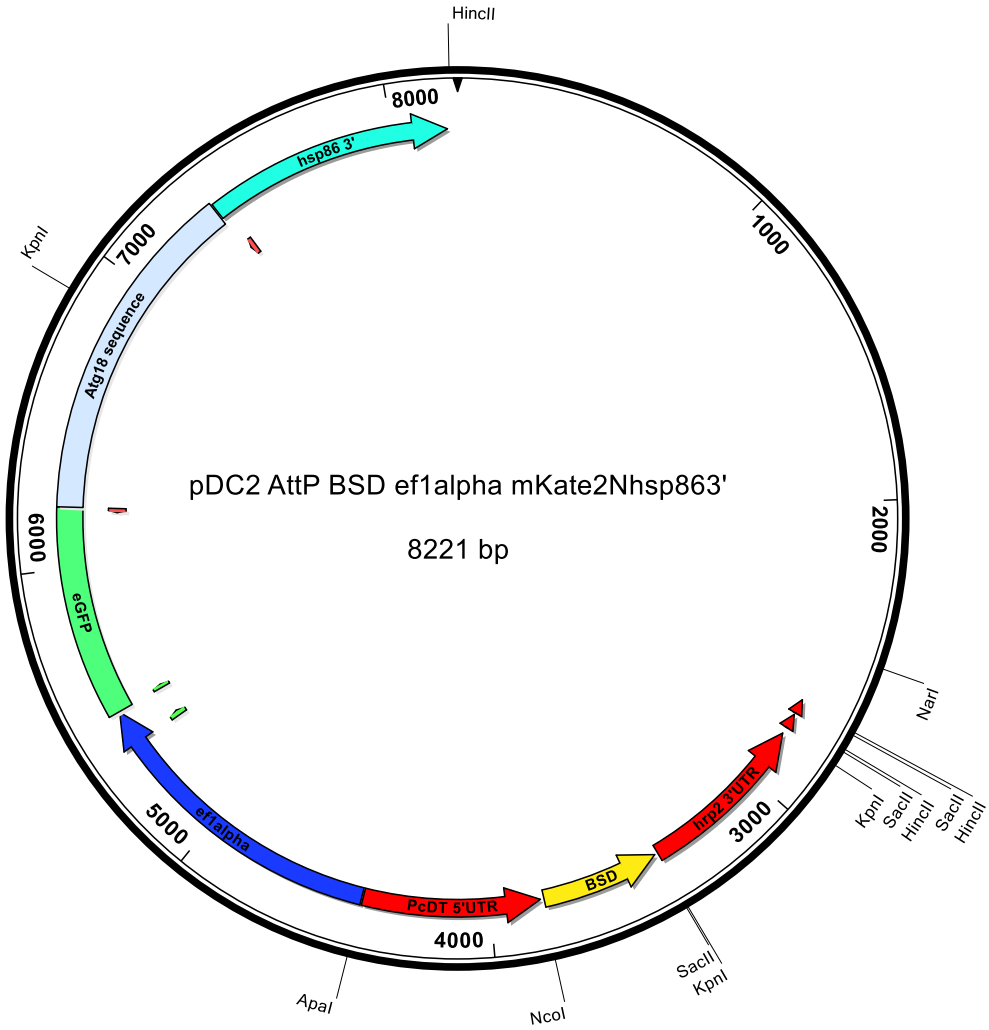


Figure 19: pDC2 AttP BSD plasmid for GFP tagging

This plasmid was used to tag PfAtg18 with GFP. The plasmid contains an ampicillin resistance gene for E. coli culture. The plasmid contains a resistance cassette against blasticidin (BSD) for selection in P. falciparum culture. The plasmid contains an ef1alpha promoter for expression in P. falciparum.

4.2.5 Confocal Microscope Imaging

Dd2^{R539T} lines with GFP-tagged Atg18 were used for confocal imaging studies. Antibodies were screened on Dd2^{R539T} lines with GFP-tagged Atg18 to determine co-localization of antibody signal with GFP-tagged Atg18. For the production of confocal slides, 400µL culture (5% Hct) was collected in a microcentrifuge tube, spun down in a tabletop centrifuge and washed three times with 500µL PBS. Cells were fixed with 1mL fixation buffer (0.0075% glutaraldehyde, 2% paraformaldehyde in PBS) at RT for 30 minutes on a rotator. Cells were spun down and washed three times with 500µL PBS, then permeabilized with 250µL permeabilization buffer (0.1% Triton X-100 in PBS) for

10 minutes on a rotator at RT. Cells were then spun down and washed three times with 500µL PBS and stained with the primary antibodies (Table 19) for testing or for staining against GFP overnight at 4ºC on a rotator. Anti-GFP antibodies were used to enhance the GFP signal for two reasons: (1) GFP signal is quenched in acidic conditions as might be present in an autophagolysosome or DV(Morishita et al., 2017) and (2) GFP does not fluoresce well following fixation by glutaraldehyde. Cells were washed three times with PBS and then stained for the secondary antibody (Table 19) for 2 hours on a rotator at RT. Cells were washed three times with PBS then approximately 10-20µL of packed RBCs were used to make a thin smear on a labeled glass slide. This slide was allowed to dry for several minutes before 1 drop of Prolong Gold mounting solution with DAPI was added to the smear. Coverslips were placed on top of each slide, slides were covered with tin foil, and left to dry overnight at RT. Slides were stored at 4ºC before imaging.

Images were collected on a Leica SP5 inverted confocal microscope with a 63x oil immersion objective NA 1.4 and 10x eyepiece. Post-processing and image analysis were performed using Huygens (SVI imaging) and Imaris software (Bitplane Inc).

Table 19: Antibody Testing for Confocal Imaging

Primary		**Secondary**	**Fluorochrome**
Anti-GFP anti bodies	Thermofisher OSE00003G rabbit polyclonal (1:20)	Abcam ab150079, goat polyclonal to rabbit (1:100)	AF647
		goat polyclonal to rabbit (1:100)	APC
	MAI-92, clone F56-gA1.2.3 mouse monoclonal (1:200)	goat polyclonal to mouse (1:100)	AF647
		donkey polyclonal to mouse (1:100)	AF568
	CST#2956 rabbit monoclonal (1:75)	Abcam ab150079, goat polyclonal to rabbit (1:100)	AF647
		goat polyclonal to rabbit (1:100)	APC
	Abcam ab290 rabbit polyclonal (1:500)	Abcam ab150079, goat polyclonal to rabbit (1:100)	AF647
		goat polyclonal to rabbit (1:100)	APC
LT antibodies: monoclonal anti-Atg18	SUNE monoclonal Atg18 #1	Abcam ab150113, goat anti-mouse (1:200)	AF488
	SUNE monoclonal Atg18 #2		

	SUNE monoclonal Atg18 #3		
	SUNE monoclonal Atg18 #4		
	SUNE monoclonal Atg18 #5		
LT antibodies: polyclonal anti-Atg18	LS 1316	Abcam ab150113, goat anti-mouse (1:200)	AF488
	LS 1317		
	LS 1318		
	LS heart bleed		
VR antibodies: polyclonal anti-Atg18	Y255 0	Abcam ab150113, goat anti-mouse (1:200)	AF488
	Y255 1		
	Y255 2		
	Y255 3		
	Y255 4		
	W450 1		
	W450 2		
	W450 4		

Three sets of primary antibodies were created in a two settings as detailed in the text. The LT antibodies: monoclonal anti-Atg18 and LT antibodies: polyclonal anti-Atg18 antibodies were produced by Dr. Louise Turner. The VR antibodies: polyclonal anti-Atg18 were made by me.

4.2.6 PIP binding assay

The ability of Dd2^{R539T} Atg18 to bind to various lipids, including PI3P, was assessed using a PIP Strip from Echelon. A GFP-trap_M by Chromotek was used to isolate GFP-tagged Atg18. Approximately 1000µL Dd2^{R539T} Atg18-GFP culture at 5% Hct and approximately 1% parasitemia was harvested. Cells were spun down and washed twice with cold PBS. Cells were then re-suspended in 200µL cold lysis buffer (Table 20), pipette mixed, and placed on ice for 30 minutes. The contents were mixed by pipette every 10 minutes during this incubation. The sample was then centrifuged in an Eppendorf Centrifuge 5427R at 20,000xg for 10 minutes at 4^{o}C. The lysate was transferred to a tube and 300µL dilution buffer (Table 20) was added. The magnetic beads were then equilibrated by adding 25µL beads to 500µL cold dilution buffer and magnetically separated by applying a magnet to the side of the tube until the supernatant appeared clear. This process was repeated twice and then the beads were added to the sample and placed on a rotator at 4^{o}C for one hour. The beads were then magnetically separated from the mixture by applying a magnet to the side of the tube, supernatant was discarded, and the beads were re-suspended in 500µL dilution buffer. The beads were magnetically separated by applying a magnet to the side of the tube and washed twice.

A PIP Strip membrane (Echelon) was blocked at room temperature on a rotator for one hour with 5mL of blocking buffer (Table 20). The magnetic beads (with GFP-tagged PfAtg18 protein bound) were added to the membrane in 5mL blocking buffer then incubated for one hour at room temperature on a rotator. The membrane was then washed three times with 5mL PBS-T for 10 minutes each. Abcam ab290 rabbit polyclonal (1:2000) in blocking buffer was added and then incubated for one hour at room temperature on a rotator. The membrane was then washed three times with 5mL PBS-T for 10 minutes each. Anti-rabbit HRP secondary antibody (1:2000) in blocking buffer and incubated for one hour at room temperature on a rotator. The membrane was then washed three times with 5mL PBS-T for 10 minutes each. For detection, 1mL K-TMBP was added and the membrane was placed on a rotator for 10 minutes. The beads, sized 0.5-1µm, were present throughout the process, though beads alone demonstrated no binding to the PIP Strip. The membrane was imaged to detect binding. The resulting image was processed using ImageJ. Briefly, the image was converted to 32-bit grayscale, background was subtracted with a radius set to 25 pixels, and the image was inverted. A circular selection was created and the integrated density of the center of each dot on the

membrane was measured. The value of the blank on the membrane was subtracted out and anything below the blank was recorded as zero.

Table 20: Buffer compositions for PfAtg18 lipid binding assay

Buffer	**Composition**
Lysis buffer	10mM Tris/Cl pH 7.5; 150mM NaCl; 0.5mM EDTA; 0.5% NP-40, 0.09% Na-Azide
Dilution/wash buffer	10mM Tris/Cl pH 7.5; 150mM NaCl; 0.5mM EDTA, 0.018% Na-Azide
Blocking buffer	PBS 0.1% tween-20, 3% BSA

4.2.7 PI3P measurements

Levels of PI3P were measured in early (0-3 hour) rings, late (9-12 hour) rings, and early (27-30 hour) trophozoites in two different parasite lines, 967^{R539T} and 967^{WTrev} at least in triplicate. Cultures were spun down and enriched, via saponin lysis for ring stages as previously described. Parasitemia was assessed via FACS as described in Chapter 5. Cells were frozen at -80^{o}C and shipped to the laboratory of Dr. Bernard Payrastre for PI3P analysis.

Lipids were extracted by the Bligh and Dyer protocol (Bligh and Dyer, 1959) by the Payrastre laboratory. Lipids not being analyzed immediately were stored at -80^{o}C. PI3P levels were measured through thin layer chromatography, the conversion of PI3P into PI3,5P2, followed by HPLC as detailed in (Chicanne et al., 2012). Raw data was normalized based on parasitemia, cells/µL, and volume analyzed. Statistical analysis was performed using multiple, unpaired t-tests, correcting for multiple comparisons using the Holm-Sidak method.

4.2.8 Electron microscopy

Parasite cultures 967^{WTrev}, 967^{R539T}, and KH002-009 were exposed to 700nM DHA for 10 minutes, 1 hour, 6 hours or were unexposed and then were synchronized to trophozoite and schizont stages using a Percoll gradient separation as previously described. Cultures

were spun down and washed with PBS then spun down a second time and re-suspended in 2.5% glutaraldehyde in sodium cacodylate buffer for fixation. Samples were stored at 4^{o}C before being shipped to Rocky Mountain Laboratories for processing and imaging. Dr. David Dorward performed a standard fixation protocol followed by post-fixation with osmium tetroxide and then staining with uranyl acetate then epoxy resin. The samples were then sectioned and exposed to lead citrate in section. Samples were examined using a model H-7500 transmission electron microscope (Hitachi High Technologies). Images were captured with a model XR100 CCD camera.

Parasite culture Dd2^{R539T} with GFP-labeled Atg18 was exposed to 700nM DHA for 10 minutes, 1 hour, 6 hours or was unexposed and then were synchronized to trophozoite and schizont stages using a Percoll gradient separation as previously described. Cultures were spun down and washed with PBS then spun down a second time and re-suspended in 4% paraformaldehyde and 0.1% glutaraldehyde. Samples were stored at 4^{o}C before being shipped to Rocky Mountain Laboratories for processing and imaging.

For transmission electron microscopy of immune-labeled sections, samples were prepared essentially as previously described (Faris et al., 2017) with several adaptations as follows. For embedment, LR White acrylic resin (Electron Microscopy Sciences) was used rather than Araldite epoxy resin. Silver sections were mounted on nickel grids, then dried overnight at 45^{o}C. The treatments with formic acid and sodium meta-periodate were omitted. Before labeling, grids were immersed in 100% ethanol for 10 seconds, then quickly rinsed with deionized water, and placed into blocking buffer. Primary and secondary antibodies were used at 1:50 dilution in blocking buffer. A rabbit anti-eGFP polyclonal primary antibody (Thermofisher OSE00003G) was used overnight at 4^{o}C following microwave irradiation.

4.2.9 Drug screen Dd2$^{R539T/T38I}$

Isogenic parasite lines Dd2^{R539T} and Dd2$^{R539T/T38I}$ were screened at NCATS against Mechanism Interrogation Plate (MIPE) 4.1 library and NPACT library by Dr. Richard Eastman. MIPE 4.1 contained 1978 compounds which were screened against the lines in single wells at 11 concentrations. NPACT contained 5632 compounds which were screened at 7 concentrations. Concentrations screened were three-fold dilutions for MIPE from 29µM to 0.5nM or five-fold dilutions for NPACT from 29µM to 1.86nM. Parasite lines were diluted to 0.3% parasitemia at 4% Hct and dispensed using a Multidrop Combi

in 5µL volume and 3µL complete media into 1536-well black clear cyclo-olefin polymer plate plates for a final hematocrit of 2.5%. Compounds were plated with 23nL of each compound using a pin tool (Inglese et al., 2006). Plates were incubated for 72 hours at 37ºC to allow for 1.5 generations of intraerythrocytic parasite growth (Yuan et al., 2009).

Cells were lysed by adding 2µL SYBR Green I in lysis buffer (Table 21) to each well and incubating overnight (approximately 18 hours) in the dark (Smilkstein et al., 2004, Bennett et al., 2004). Fluorescence was measured using an EnVision plate reader at 485/14nm excitation and 535/25 emission. AC50 values and curve classes were determined using quantitative High-Throughput Screening (qHTS). Statistical analysis for maximum response (MaxR) between lines was done using ANOVA followed by Tukey post-hoc test. Determination of class enrichment was assessed using Fishers test with Benjamini-Hochberg correction for multiple comparisons.

Table 21: Composition of SYBR Green I lysis buffer

Buffer	**Composition**
Lysis buffer	Tris (20mM; pH 7.5), EDTA (10mM), saponin (0.16%), Triton X-100 (1.6%)
SYBR Green I lysis buffer	10X SYBR Green I to lysis buffer, shake for 25 seconds

These screens use specific panels of drugs at varying concentrations to create a concentration-response curve and determine half-maximal activity concentration (AC50) for each compound. These concentration-response curves were fitted into four categories, utilizing criteria based on the quality of the calculated curve fit to the actual data points (r^2 value), the efficacy (magnitude of the response), and the presence and number of asymptotes to the curve (upper and/or lower) (Inglese et al., 2006) (Figure 20).

Compounds with curve classes 1-3 were categorized as active while those with class 4 designations were inactive. Class 1 designation is based on a well-fitting curve ($r^2 \geq 0.9\%$) with both upper and lower asymptotes. Class 1 was subcategorized to class 1a and class 1b based on either a complete response (1a), with more than 80% efficacy, or a partial response (1b), with 30-80% efficacy. The efficacy cut-off (30%) originated from three standard deviations above the mean basal activity. Class 2 curves have an incomplete

curve and are similarly subcategorized as class 2a or class 2b based on a good response and good fit (2a) or an insufficient response and poor fit (2b). Class 3 curves show activity at the highest concentrations only and have efficacy above 30%. Class 4 curves showed no response or efficacy less than 30% (Inglese et al., 2006).

Table 22: Curve class criteria description

Curve class	Description	Efficacy	r^2	Asymptotes	Inflection
1	(a) Complete response (b) Partial response	(a) > 80% (b) ≤ 80%	≥ 0.9%	2	Yes
2	Incomplete curve	(a) > 80% (b) ≤ 80%	(a) > 0.9% (b) < 0.9%	1	Yes
3	Single point activity	> 30%	N/A	1	No
4	Inactive	< 30%	N/A	0	No

This table was reproduced with modifications from Inglese et al. 2006.

It is important to note that AC50 values take into account the idea that compounds can either be activating or inhibiting; however, for the purpose of this thesis work, only inhibiting compounds were considered. Therefore, the half-maximal inhibitory concentration (IC50) nomenclature will be used.

Susceptibility is measured by changes in the drug response curve, where the response, in this case, parasite survival, is measured on the Y-axis and the drug concentration is measured on the X-axis. The curve shifts to the left it takes less drug to kill the parasite, and therefore the parasite population is deemed more susceptible to that particular compound than another parasite population. Conversely, a curve shifted to the right signals that more drug is needed to kill the same percentage of parasites, and therefore, this represents a decrease in susceptibility.

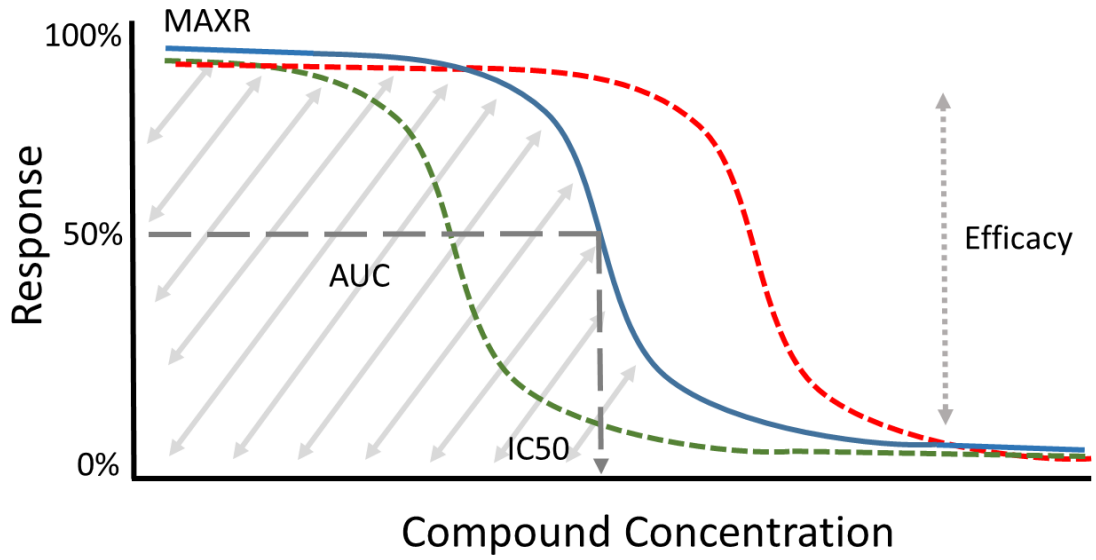


Figure 20: Drug response curve parameters

The solid curve in blue and dashed curves in green and red represent dose response curves. The green dashed curve represents a left shift from the blue curve, signifying that the green population is more susceptible to a given concentration of a compound than the blue population. Likewise, the red dashed curve represents a right shift from the blue curve, signifying that the red population is less susceptible to a given concentration of a compound than the blue population. The half-maximal inhibitory concentration (IC50) is the concentration of drug that inhibits half the population. The maximum response (MaxR) is the response at the maximum dose. The efficacy represents the difference between the top and bottom asymptotes of the dose response curve. Finally, the area under the curve (AUC) is the sum of the area from the curve bounded by the X- and Y-axes.

Several parameters can be calculated from the drug response curve (Figure 20). First, IC50, as described above, is the compound concentration at which half of the parasite population is inhibited. Efficacy is the absolute difference between the top and bottom of the curve for drug response curves that have two asymptotes. The MAXR is the response at the maximum dose, which is independent of the curve fit, but nonetheless derived from the drug response curve. AUC is the integral of the drug response curve. These parameters are best when they are used together for a full picture of the comparison between two compounds or between two populations. A understanding of MAXR and efficacy can be important in determining the maximal response generated from a given compound; meanwhile, comparisons of susceptibility are best expressed using AUC or IC50 values. Thus, the potency of a compound to a given line is the IC50 value. The lines were

considered to have differential susceptibility to a given compound if the potency was more than 5x different between the two.

4.2.10 Nutrient deprivation assays

The ability of parasite lines Dd2, Dd2^{R539T}, and Dd2$^{R539T/T38I}$ to survive under nutrient deprivation was assessed using growth studies. Parasitemia of the three lines were assessed by FACS and then diluted to approximately 0.5% parasitemia. Lines were then plated in flat-bottomed plates in various nutrient restriction conditions at 5% Hct and incubated in a gassed incubator. Complete media was titrated with a basal salt solution (Table 23) to create 100%, 85%, 75%, 65%, 50%, and 20% complete media with and without glucose. Parasitemia was assessed at 48 hours by FACS.

Table 23: Nutrient deprivation media compositions

Reagent	Complete	Basal salt solution with glucose	Basal salt solution
10x Inorganic Salts*	50mL	50mL	50mL
10x Na_2HPO_4 **	50mL	50mL	50mL
(Na)HCO_3	1.125g	1.125g	1.125g
Glucose	2g	2g	------
100x RPMI 1640 Vitamins	5mL	------	------
Glutathione (reduced) (1mg/mL)	500µL	500µL	500µL
HEPES	3g	3g	3g
Phenol Red	2.5mg	2.5mg	2.5mg
Hypoxanthine	25mg	25mg	25mg
Gentamicin (15mg/mL)	100µL	100µL	100µL
50x RPMI 1640 Amino Acid Solution without L-Glutathione	10mL	------	------
L-Glutamine	300mg	------	------
Albumax II	2.5g	------	------
ddH_2O	to 500mL final volume	to 500mL final volume	to 500mL final volume

**10X Inorganic salts mix (1L): 1g Ca(NO3)2•4H2O, 4g KCl, 0.5g MgSO4 (anhydrous), 60g NaCl, ddH2O to 1L final volume*

***10x Na_2HPO (1L): 8g Na_2HPO, ddH2O to 1L final volume*

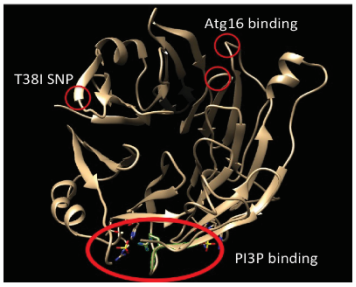
4.3 RESULTS

4.3.1 *P. falciparum* Atg18 protein characterization

4.3.1.1 PfAtg18 protein structure

A model for PfAtg18 protein was made using Chimera and the homologous yeast protein Hsv2, revealing multiple putative blades on the protein (Figure 21A). An alignment with the human WIPI proteins confirmed that sequences important for the WIPI proteins' functions are also present in the PfAtg18 protein (Figure 21B). The interaction of WIPI with PI3P is one of the principle functions of WIPI and is facilitated by the FRRG domain. This sequence, highlighted in yellow in Figure 21B, is also present in PfAtg18. WIPI also interacts with Atg16 using its two arginine domains sixteen amino acids apart, also highlighted in Figure 21A. Although PfAtg18 only has one arginine, the function of the second arginine is likely performed by lysine, which is another basic amino acid. These two amino acids are both charged aliphatic amino acids. Both amino acids have an amino group that is protonated at physiologic pH. They each have a carboxylic acid group, although lysine has a lysyl side chain and arginine has a guanidine group. In PfAtg18, these arginine/lysine and FRRG motifs are circled in Figure 21A, where the FRRG domain is shown to form a pocket, and the arginine/lysine domains are on adjacent blades for protein binding.

A



B

```
Majority              M-NLASQSGEAGAGQLLFA--NFNQDNT-----------------SLAVGSKSGYKFFSLSSVDKLEQIYECTDTE---
                                10        20        30        40        50        60        70        80
XP_001347411.1_PfAtg18 MVSLRLDNNR---------YISFNQDYG-----------------CLCWANEKGFKIYN---TNPFTQTYSRDLTDRNK 50
NP_056425.1_WIPI2a     M-NLASQSGEAGAGQLLFA--NFNQDNTEVKGASRAAGLGRRAVVWSLAVGSKSGYKFFSLSSVDKLEQIYECTDTE--- 74
NP_057087.2_WIPI2b     M-NLASQSGEAGAGQLLFA--NFNQDNT-----------------SLAVGSKSGYKFFSLSSVDKLEQIYECTDTE--- 56
NP_001028690.1_WIPI2c  M-NLASQSGEAGAGQLLFA--NFNQDNTEVKGASRAAGLGRRAVVWSLAVGSKSGYKFFSLSSVDKLEQIYECTDTE--- 74
NP_001028691.1_WIPI2d  M-NLASQSGEAGAGQLLFA--NFNQDNT-----------------SLAVGSKSGYKFFSLSSVDKLEQIYECTDTE--- 56
AAH39867.1_WIPI1       M-EAEAADAPPGGVESALSCFSFNQDCT-----------------SLAIGTKAGYKLFSLSSVEQLDQVHGSNEIP--- 58

Majority              -DVCIVERLFSSSLVAIVSLKAPRK-------LKVCHFKKGTEICNYSYSNTILAVKLNRQRLIVCLEESLYIHNIRDMK
                                90        100       110       120       130       140       150       160
XP_001347411.1_PfAtg18 NGLYLAEMLYRCNILAITGNKNDKKGKWAKNVLIIWDDRQMREIAKLTFSSNIIGVRLLREIIVVILEYKLCIYRLKDII 130
NP_056425.1_WIPI2a     -DVCIVERLFSSSLVAIVSLKAPRK-------LKVCHFKKGTEICNYSYSNTILAVKLNRQRLIVCLEESLYIHNIRDMK 146
NP_057087.2_WIPI2b     -DVCIVERLFSSSLVAIVSLKAPRK-------LKVCHFKKGTEICNYSYSNTILAVKLNRQRLIVCLEESLYIHNIRDMK 128
NP_001028690.1_WIPI2c  -DVCIVERLFSSSLVAIVSLKAPRK-------LKVCHFKKGTEICNYSYSNTILAVKLNRQRLIVCLEESLYIHNIRDMK 146
NP_001028691.1_WIPI2d  -DVCIVERLFSSSLVAIVSLKAPRK-------LKVCHFKKGTEICNYSYSNTILAVKLNRQRLIVCLEESLYIHNIRDMK 128
AAH39867.1_WIPI1       -DVYIVERLFSSSLVVVVSHTKPRQ-------MNVYHFKKGTEICNYSYSSNILSIRLNRQRLLVCLEESIYIHNIKDMK 130

Majority              VLHTIRETPPNPAGLCALSINNDNCYLAYPGSAT-IGEVQVFDT------------INLRAANMIPAHDSPLAALAFDAS
                                170       180       190       200       210       220       230       240
XP_001347411.1_PfAtg18 LLETL-NTSKNVSGLCCLSNIDKNIIIAYLSPIKGRVNIHIFEINSSENIHEELPYINFKTNLSIYAHDNSIGCINLSND 209
NP_056425.1_WIPI2a     VLHTIRETPPNPAGLCALSINNDNCYLAYPGSAT-IGEVQVFDT------------INLRAANMIPAHDSPLAALAFDAS 213
NP_057087.2_WIPI2b     VLHTIRETPPNPAGLCALSINNDNCYLAYPGSAT-IGEVQVFDT------------INLRAANMIPAHDSPLAALAFDAS 195
NP_001028690.1_WIPI2c  VLHTIRETPPNPAGLCALSINNDNCYLAYPGSAT-IGEVQVFDT------------INLRAANMIPAHDSPLAALAFDAS 213
NP_001028691.1_WIPI2d  VLHTIRETPPNPAGLCALSINNDNCYLAYPGSAT-IGEVQVFDT------------INLRAANMIPAHDSPLAALAFDAS 195
AAH39867.1_WIPI1       LLKTLLDIPANPTGLCALSINHSNSYLAYPGSLT-SGEIVLYDG------------NSLKTVCTIAAHEGTLAAITFNAS 197

Majority              GTKLATASEKGTVIRVFSIPEGQKLFEFRRGVKRCVSICSLAFSMDGMFLSASSNTETVHIFKLETVKEKPPEEPTTWTG
                                250       260       270       280       290       300       310       320
XP_001347411.1_PfAtg18 GKLLVTSSTKGTIIRLFNTFDGTLLNEFRRGTKN-AKILSLNISEDNNWLCLTSSRNTVHVFSI---------------- 272
NP_056425.1_WIPI2a     GTKLATASEKGTVIRVFSIPEGQKLFEFRRGVKRCVSICSLAFSMDGMFLSASSNTETVHIFKLETVKEKPPEEPTTWTG 293
NP_057087.2_WIPI2b     GTKLATASEKGTVIRVFSIPEGQKLFEFRRGVKRCVSICSLAFSMDGMFLSASSNTETVHIFKLETVKEKPPEEPTTWTG 275
NP_001028690.1_WIPI2c  GTKLATASEKGTVIRVFSIPEGQKLFEFRRGVKRCVSICSLAFSMDGMFLSASSNTETVHIFKLETVKEKPPEEPTTWTG 293
NP_001028691.1_WIPI2d  GTKLATASEKGTVIRVFSIPEGQKLFEFRRGVKRCVSICSLAFSMDGMFLSASSNTETVHIFKLETVKEKPPEEPTTWTG 275
AAH39867.1_WIPI1       GSKLASASEKGTVIRVFSVPDGQKLYEFRRGMKRYVTISSLVFSMDSQFLCASSNTETVHIFKLEQVTNSRPEEPSTWSG 277

Majority              YFGKVLMASTSYLPSQVTEMFNQGRAFATVRLPFCGHKNICSLATIQKIPRLLVGAADGYLYMYNLDPQEGGECALMKQH
                                330       340       350       360       370       380       390       400
XP_001347411.1_PfAtg18 ---------------------YKKKRPLRKVDI-ICKGKNVSP-------PALLN---------YEKESKN-------KKS 308
NP_056425.1_WIPI2a     YFGKVLMASTSYLPSQVTEMFNQGRAFATVRLPFCGHKNICSLATIQKIPRLLVGAADGYLYMYNLDPQEGGECALMKQH 373
NP_057087.2_WIPI2b     YFGKVLMASTSYLPSQVTEMFNQGRAFATVRLPFCGHKNICSLATIQKIPRLLVGAADGYLYMYNLDPQEGGECALMKQH 355
NP_001028690.1_WIPI2c  YFGKVLMASTSYLPSQVTEMFNQGRAFATVRLPFCGHKNICSLATIQKIPRLLVGAADGYLYMYNLDPQEGGECALMKQH 373
NP_001028691.1_WIPI2d  YFGKVLMASTSYLPSQVTEMFNQGRAFATVRLPFCGHKNICSLATIQKIPRLLVGAADGYLYMYNLDPQEGGECALMKQH 355
AAH39867.1_WIPI1       YMGKMFMAATNYLPTQVSDMMHQDRAFATARLNFSGQRNICTLSTIQKLPRLLVASSSGHLYMYNLDPQDGGECVLIKTH 357

Majority              RLDGSLETTNEILDSASHDCPLVTQTYGAAAGKXX-XXX--X--AYTDDLGAVGGACLEDE---ASALRLDEDSEHPPMI
                                410       420       430       440       450       460       470       480
XP_001347411.1_PfAtg18 SLK-CLLPCHPYLNSEWS-----FASYKLPGKKISSIC------AFVNDQNCIIVICSNGIIYK---LRFNEHIGGDMFK 373
NP_056425.1_WIPI2a     RLDGSLETTNEILDSASHDCPLVTQTYGAAAGKGTYVPSSPTRLAYTDDLGAVGGACLEDE---ASALRLDEDSEHPPMI 450
NP_057087.2_WIPI2b     RLDGSLETTNEILDSASHDCPLVTQTYGAAAGKGTYVPSSPTRLAYTDDLGAVGGACLEDE---ASALRLDEDSEHPPMI 432
NP_001028690.1_WIPI2c  RLDGSLETTNEILDSASHDCPLVTQTYGAAAGK-----------AYTDDLGAVGGACLEDE---ASALRLDEDSEHPPMI 439
NP_001028691.1_WIPI2d  RLDGSLETTNEILDSASHDCPLVTQTYGAAAGK-----------AYTDDLGAVGGACLEDE---ASALRLDEDSEHPPMI 421
AAH39867.1_WIPI1       SLLGS-GTTEENKENDLR--PSLPQSYAATVARPS-ASSASTVPGYSEDGGALRGEVIPEHEFATGPVCLDDENEFPPII 433

Majority              L---------RTD
                                490
XP_001347411.1_PfAtg18 I------SSHSFD                                                              380
NP_056425.1_WIPI2a     L---------RTD                                                              454
NP_057087.2_WIPI2b     L---------RTD                                                              436
NP_001028690.1_WIPI2c  L---------RTD                                                              443
NP_001028691.1_WIPI2d  L---------RTD                                                              425
AAH39867.1_WIPI1       LCRGNQKGKTKQS                                                              446
```

Figure 21: P. falciparum Atg18 modeling and alignment

(A) Image depicts P. falciparum Atg18 protein modeled based on homologous Hsv2 protein in yeast. Putative binding sites to PI3P and Atg16 are highlighted, as well as the location of the T38I SNP of interest (red circles). (B) The alignment of P. falciparum Atg18 protein sequence with several human WIPI protein homologues demonstrates conservation of binding sites (highlighted in yellow). WIPI protein FRRG sequence binds PI3P while two nearby arginine residues (sixteen amino acids apart) bind Atg16.

4.3.1.2 Imaging of PfAtg18

Homologs of Atg18 are important in the initiation of the autophagy cascade and denote the start of autophagy through the formation of puncta. Using $Dd2^{R539T}$ GFP-Atg18 parasites, PfAtg18 was imaged under different conditions. Under normal culture conditions, the protein appears diffuse throughout the cytoplasm of late-stage parasites by TEM (Figure 22A) and confocal (Figure 23A) imaging. However, following 700nM DHA treatment, PfAtg18 proteins start to coalesce within 10 minutes (Figure 22B, Figure 23B). After 1 hour of such treatment, PfAtg18 proteins have formed many puncta, scattered throughout the cytoplasm (Figure 22C, Figure 23C).

Seventeen anti-Atg18 antibodies (Table 19) were made, since transgenic parasites are time-consuming and technically difficult to create. Three approaches were undertaken to maximize the chance of being able to create a functional antibody suitable for imaging analysis. Following initial difficulties producing recombinant PfAtg18 protein, an anti-plasmid antibody was designed using the VR2001 system that has been extensively used for the production of anti-leishmanial antibodies (Oliveira et al., 2006). The plasmid is injected into mice, where it enters the bloodstream and is taken up by cells via transfection (Tang et al., 1992). The plasmid uses a CMV promoter, which functions in both human and other mammalian systems, to produce the encoded protein with a TPA peptide (Oliveira et al., 2006). The TPA signal-secretory peptide causes the protein of interest to be secreted. Secreted proteins are more likely to be presented using MHC class II to $CD4^+$ T cells, which then activate B cells for the production of antibodies (Williams, 2014). Thus, antibodies can be produced using this method without making recombinant protein. The second and third approaches were done by a collaborating lab, run by Dr. Louise Turner. The Turner laboratory was able to successfully create recombinant PfAtg18 and this protein was therefore used to create traditional anti-protein polyclonal antibodies.

The splenocytes from the spleens of the immunized mice were then fused to myeloma cells to create hybridomas, which were then screened for those capable of producing monoclonal antibodies against PfAtg18. These antibodies were screened against the GFP-Atg18 transgenic lines and those antibodies that co-localized with the GFP signal were utilized.

The antibodies were tested for co-localization with GFP-Atg18 signal by confocal microscopy. Of those tested, the LS1318 polyclonal from a recombinant protein and the

VR2001 Y255 #1 polyclonal from a plasmid were selected and these antibodies were used for Atg18 analysis in non-transfected lines.

Images collected of late-stage parasites from the Dd2 isogenic lines with VR2001 Y255 #1 anti-PfAtg18 antibody staining demonstrated similar staining patterns, with localization near the DV (as seen by hemozoin on DIC) and the nucleus (Figure 24).

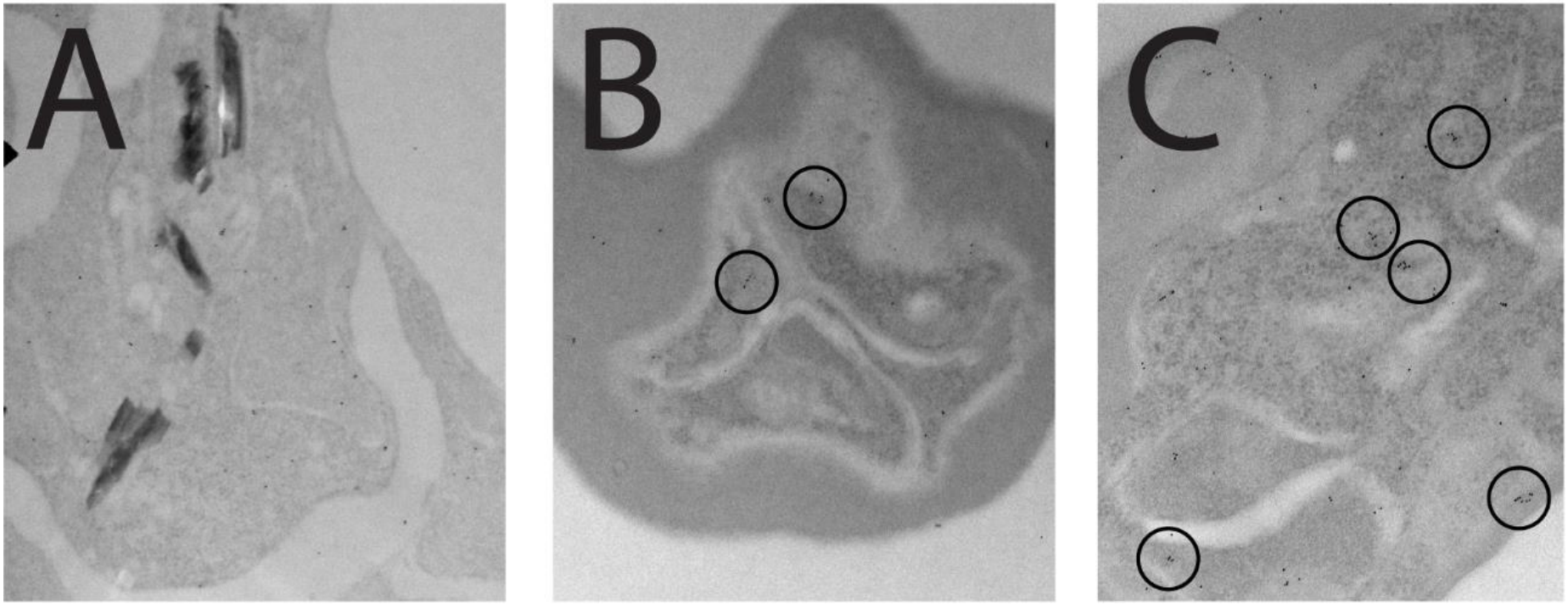


Figure 22: Transmission electron microscopy images of Dd2R539T GFP-Atg18 following DHA treatment

Transmission electron microscopy images of untreated (A) Dd2^{R539T} GFP-Atg18 parasites and following exposure to 700nM DHA for (B) 10 minutes and (C) 1 hour. Antibodies to GFP were gold-labeled (dots). Labels that congregate to form puncta are highlighted (black circles).

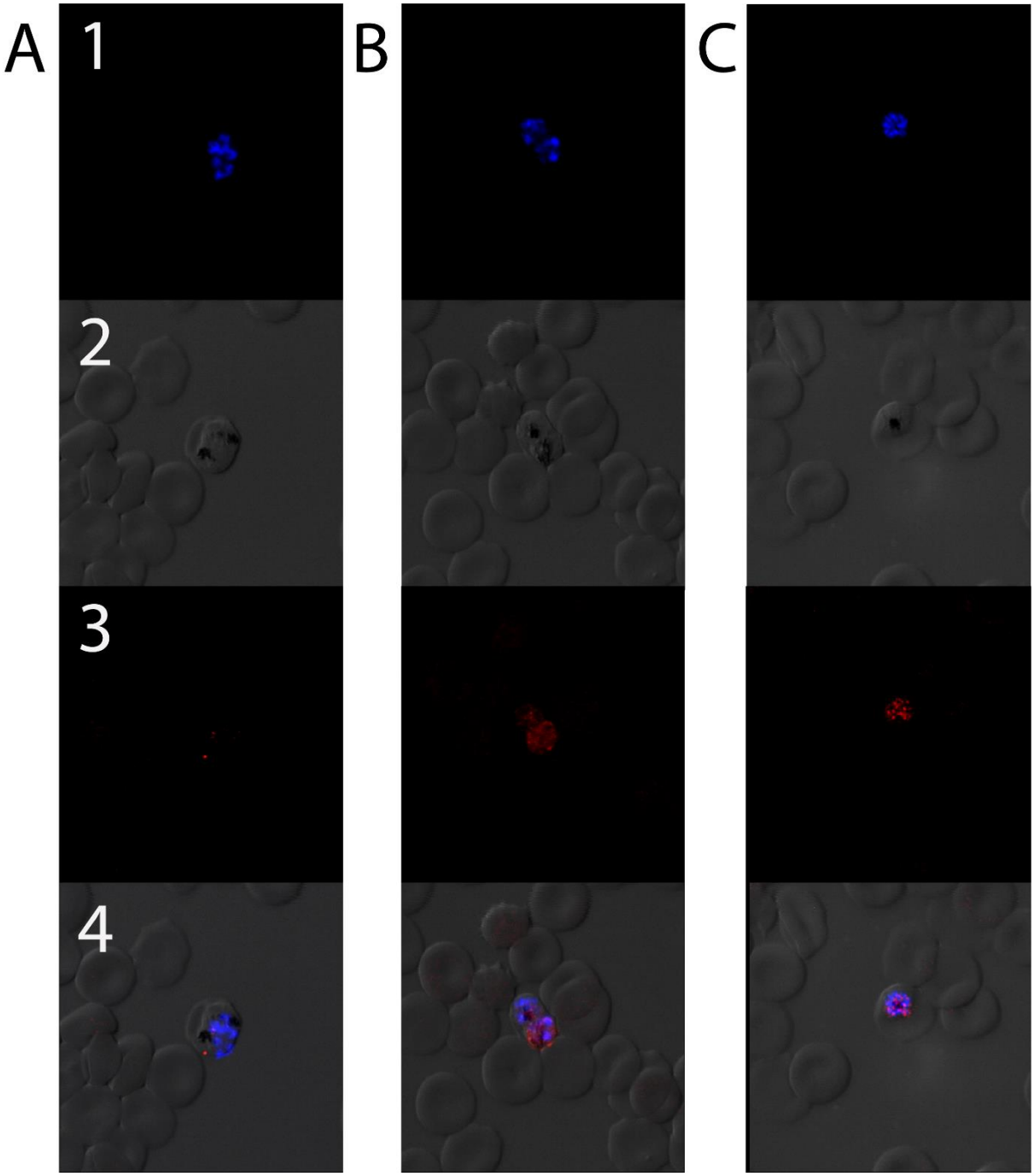


Figure 23: Confocal microscopy images of Dd2^{R539T} Atg18-GFP following DHA treatment

Late stage Dd2^{R539T} GFP-Atg18 parasites stained with DAPI (blue) and anti-GFP antibody (red). Rows depict images with (1) DAPI only (2) Differential inference contrast (DIC) only (3) anti-GFP only and (4) a merged image with all channels. Columns depict untreated (A) parasites as well as treatment with 700nM DHA for 10 minutes (B) and 1 hour (C).

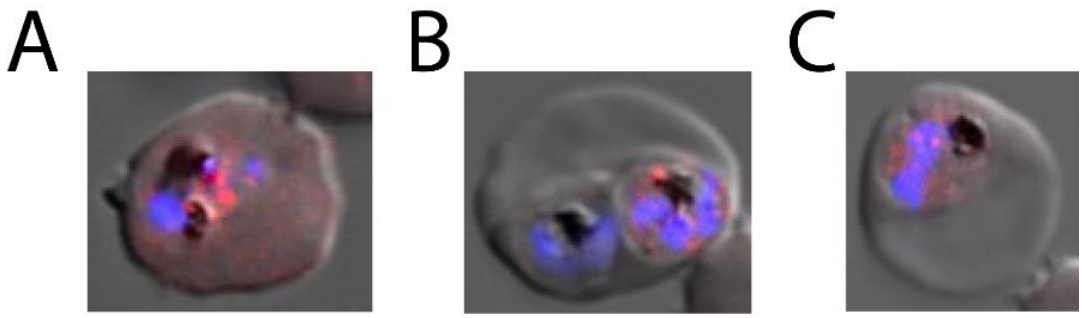


Figure 24: Dd2 isogenic lines with anti-PfAtg18 antibody staining

(A) Dd2, (B) Dd2^{R539T}, and (C) Dd2$^{R539T/T38I}$ isogenic lines were synchronized to late stages using Percoll and imaged using VR2001 anti-PfAtg18 antibody Y225 #1. Anti-PfAtg18 antibody staining in red, DAPI in blue, and DIC in grayscale. Imaging demonstrates similar localization near hemozoin (representing the DV) and the nucleus.

4.3.1.3 Phosphotidylinositol 3-phosphate interactions and levels

Homologous Atg18 proteins bind PI3P as one of the first steps in initiating an autophagy cascade; therefore, in determining possible functions of PfAtg18, it is important to assess if the plasmodial protein also has these binding capabilities. An Echelon PIP strip membrane was used to assess binding of PfAtg18 with eight phosphoinositides and seven other lipids. The protein was detected in 10 of the 15 spots, including seven of the eight phosphoinositides (Figure 25A). Similarly to other Atg18 proteins, PfAtg18 bound PI5P and PI3P at high levels (Vicinanza et al., 2015).

Given the interaction between PfAtg18 and PI3P, as well as previous evidence that PI3P levels may be important for resistance, PI3P quantification was performed on isogenic clinical isolates from Cambodia. Using the novel application of an approach to quantify PI3P in other systems, it was determined that PI3P levels were not different between isogenic 967 parasites, differing only in *k13* mutations, at any time point tested including at the early ring stage (0-3 hpi) (Figure 25B).

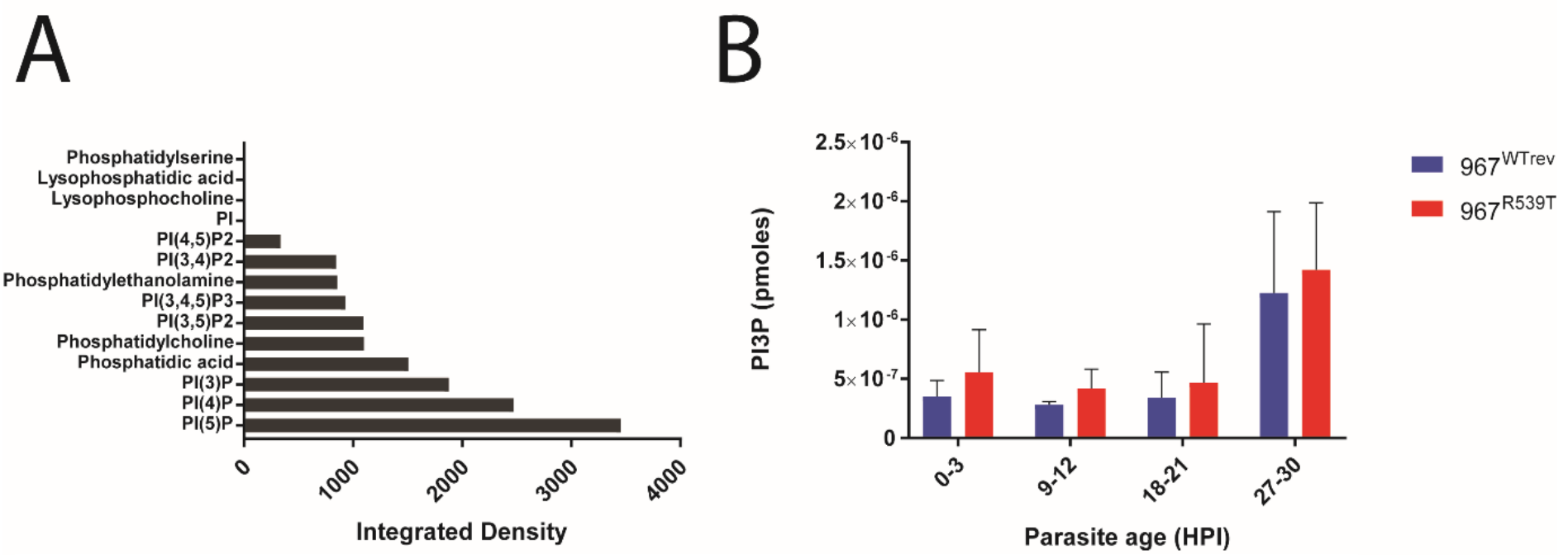


Figure 25: Lipid interactions and levels in P. falciparum

(A) Binding of Atg18 from Dd2^{R539T} GFP-tagged Atg18 parasite line to various lipids based on integrated density from Echelon PIP strip membrane. (B) Quantification of PI3P from samples of 967^{WTrev} (blue) versus 967^{R539T} (red) at four time points in the intraerythrocytic lifecycle: 0-3, 9-12, 18-21, and 27-30 hours post-invasion (HPI). Shown is mean with SD.

4.3.2 Phenotypic changes in parasites with T38I Atg18 SNP

4.3.2.1 Drug screen of Dd2^{R539T} vs. Dd2$^{R539T/T38I}$

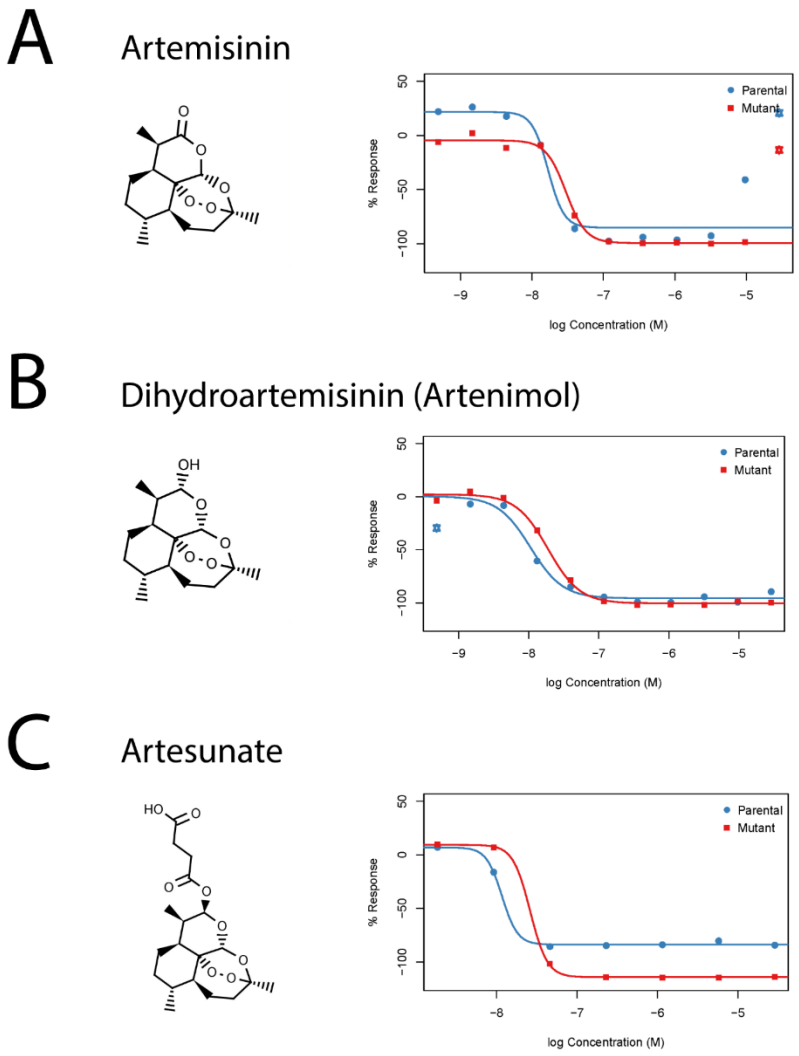


Figure 26: Drug response curves for artemisinins against Dd2^{R539T} vs. Dd2$^{R539T/T38I}$

Dose response curves from (A) artemisinin and two derivatives, (B) DHA and (C) artesunate, which are in use in Cambodia and Southeast Asia. Parent displayed in blue, mutant in red. Drug structures also shown.

The question of whether the T38I SNP modulates antimalarial drug resistance is central to this thesis project. Dd2^{R539T} and Dd2$^{R539T/T38I}$ isogenic lines were screened against a total of 6349 unique compounds, including 36 antimalarials, at multiple concentrations. The maximum response (MaxR) was not different between these two lines for any of the antimalarial compounds tested (Figure 28). The results from drug screens of 12 other isogenic lines, including some isogenic lines differing in *k13* mutations, were also

compared to Dd2^{R539T} and Dd2$^{R539T/T38I}$ to determine any drug response patterns that might have been missed in using just two lines. The MaxR was not different for any two lines (Figure 28). Given that artemisinin derivatives are of specific interest, artemisinin and its two derivatives in use in Southeast Asia, DHA and artesunate, are highlighted in Figure 26 and show no difference in IC50s. Similarly, three partner drugs of interest, chloroquine, mefloquine, and piperaquine, have no differences in drug response curves (Figure 27).

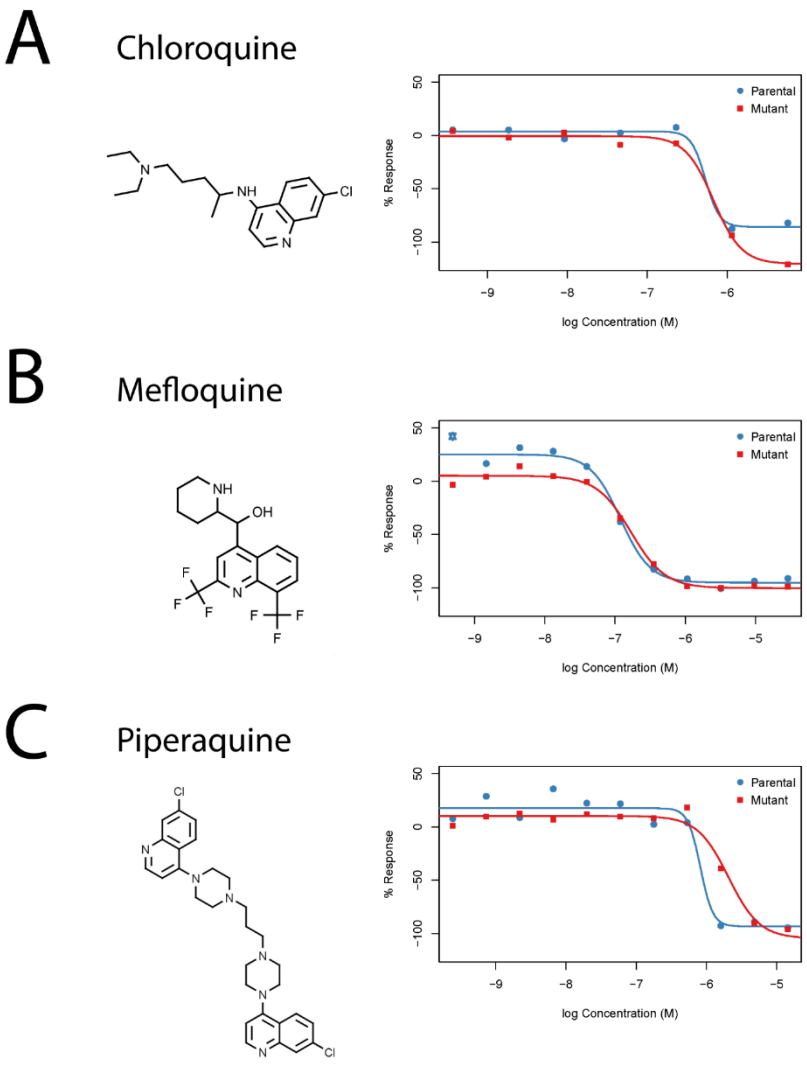


Figure 27: Drug response curves for antimalarial partner drugs against Dd2^{R539T} vs. Dd2$^{R539T/T38I}$
Dose response curves from (A) chloroquine (B) mefloquine and (C) piperaquine, long lasting partner drugs which have been recently inn use in Cambodia and Southeast Asia. Parent displayed in blue, mutant in red. Drug structures also shown.

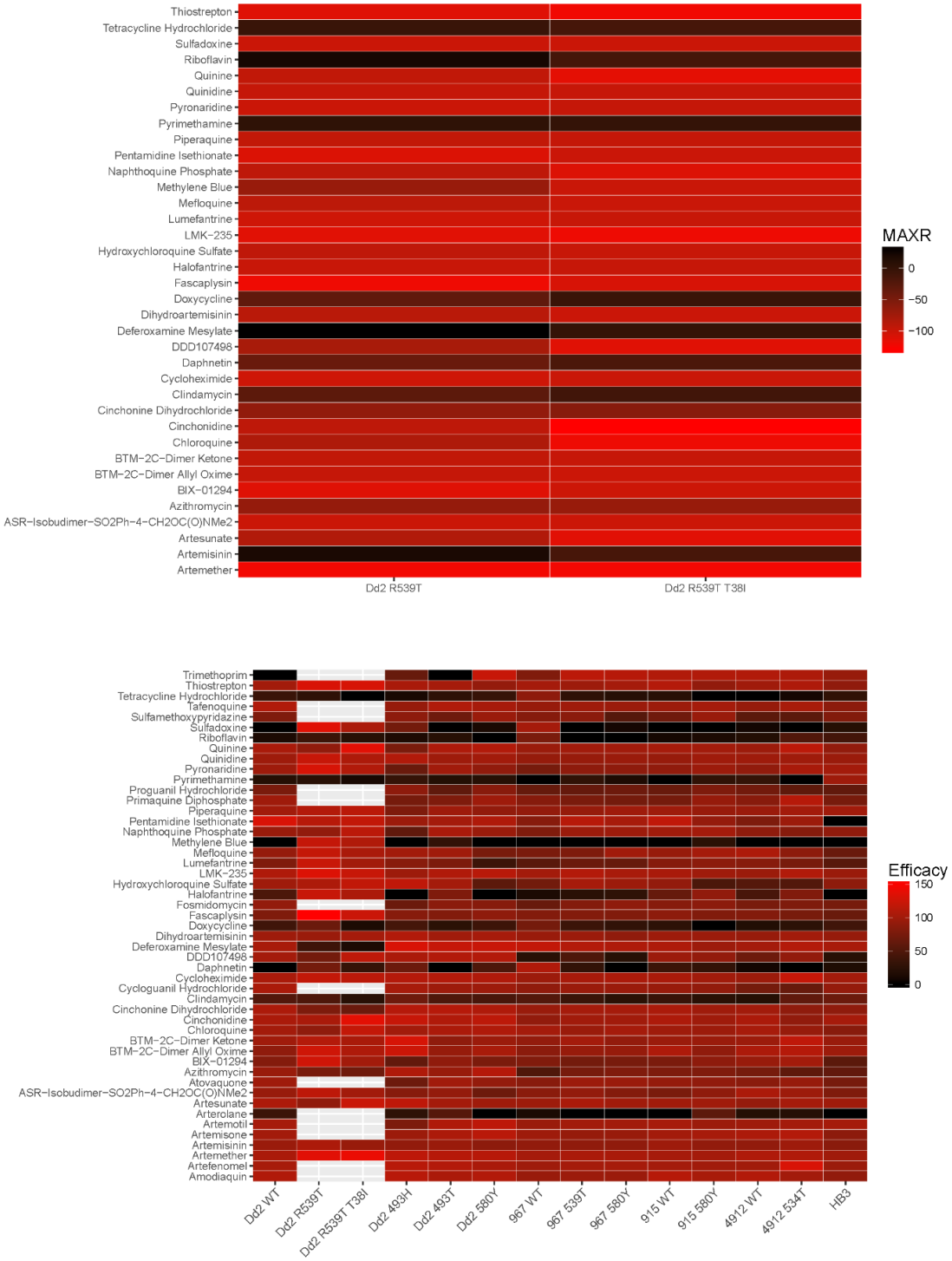


Figure 28: Heat map of antimalarial drug efficacy against kelch and atg18 isogenic lines
(A) Comparison of max response (MaxR) between parent Dd2^{R539T} and mutant Dd2$^{R539T/T38I}$. (B) Comparison of efficacy for six isogenic Dd2 lines, three isogenic 967 lines, two isogenic 915 lines, two isogenic 4912 lines, and HB3.

As there are seemingly no differences in IC50 or MaxR values for antimalarial compounds within the drug screen library, the rest of the over 6000 unique compounds in the drug screen were analyzed for susceptibility differences that could elucidate the contribution of the *atg18* SNP. The annotated drug library was organized based on mechanism of action, and demonstrated no differences in area under the curve (AUC) between Dd2^{R539T} and Dd2$^{R539T/T38I}$ for any superclass or class of mechanism of action (Figure 29).

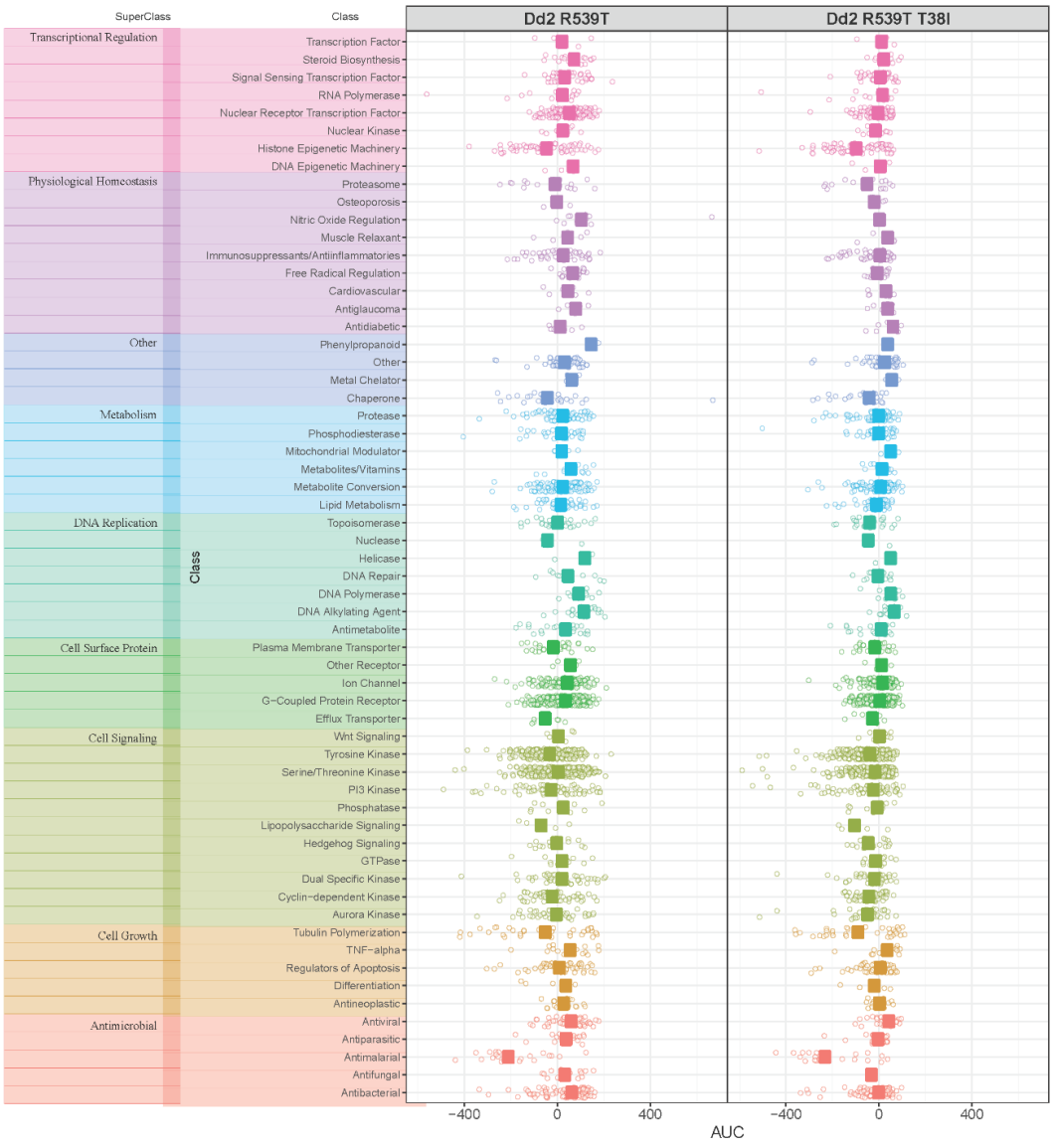


Figure 29: Dd^{2R539T} vs. Dd2$^{R539T/T38I}$ area under the curve by compound mechanism of action

Area under the curve for parent (Dd2^{R539T}) and mutant (Dd2$^{R539T/T38I}$) lines organized by superclasses: transcriptional regulation (pink), physiological homeostasis (purple), other (periwinkle blue), metabolism (sky blue), DNA replication (aqua), cell surface protein (green), cell signaling (olive), cell growth (orange), and antimicrobial (coral). These are further broken down into classes by line.

Without any indication that a specific set of compounds with a shared mechanism of action were impacted by the SNP, individual compound response curves were examined. The IC50 values of all differential compounds are given in Appendix A: Differential compounds. Of the 6349 unique compounds, there were 90 that were more active against the mutant ($Dd2^{R539T/T38I}$) than the parent ($Dd2^{R539T}$) (Figure 30). The majority of these compounds were not active against $Dd2^{R539T}$ but were active against $Dd2^{R539T/T38I}$; however, 8 compounds had a shift in IC50 value. Two of these had unconvincing curves and were thus excluded, leaving 6 compounds that were active against both lines, but more active against the mutant line (Figure 31). A subset of the 90 differential compounds were annotated (n = 29). Of the compounds that were annotated, 41.4% acted on cell

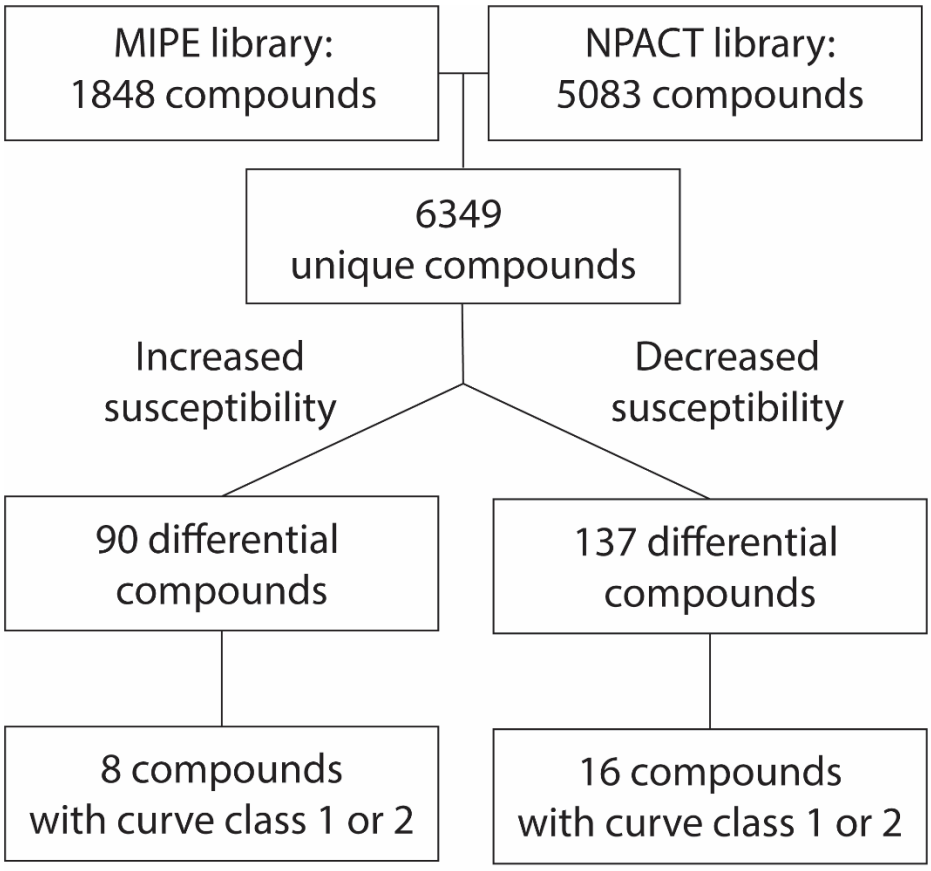


Figure 30: Drug screen compound flowchart

NCATS libraries MIPE and NPACT were used to screen a total of 6349 unique compounds. The T38I SNP in atg18 leads to increased susceptibility to 90 compounds, as defined by a change in IC50 value of 5x or more. Of these, 8 compounds demonstrated curves in curve class 1 or 2, demonstrating a shift in activity (Figure 31). On the other side, the SNP leads to decreased activity to 137 compounds, with 16 compounds demonstrating curve class 1 or 2 (Figure 32).

signaling, 20.7% acted on transcriptional regulation, 13.8% acted on a cell surface protein, and 10.3% (n = 3) were traditional antimicrobial compounds (Figure 32A).

Conversely, a total of 137 compounds were less efficacious against $Dd2^{R539T/T38I}$ than $Dd2^{R539T}$. Sixteen of these had a shift in IC50 value (Figure 33). Again, a subset of the compounds were annotated (n = 62). Of the differential compounds that were annotated, 46.8% acted on cell signaling, representing statistically relevant enrichment (p = 0.006) 16.1% acted on a cell surface protein, 8.1% acted on metabolism, 8.1% acted on physiological homeostasis and again, three compounds were traditional antimicrobial compounds (Figure 32B).

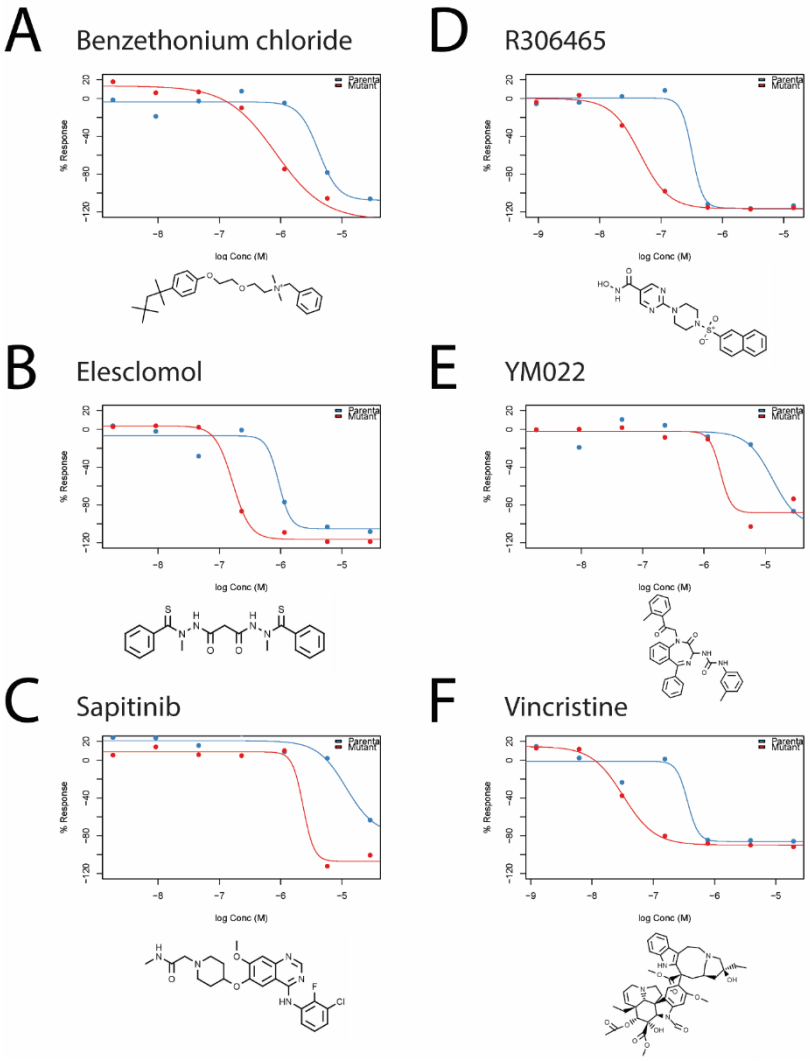


Figure 31: Drug response curves for compounds favoring Dd2R539T

Dose response curves from (A) benzethonium chloride (B) elesclomol (C) sapitinib (D) R306465 (E) YM022 and (F) vincristine. Parent displayed in blue, mutant in red. Drug structures also shown.

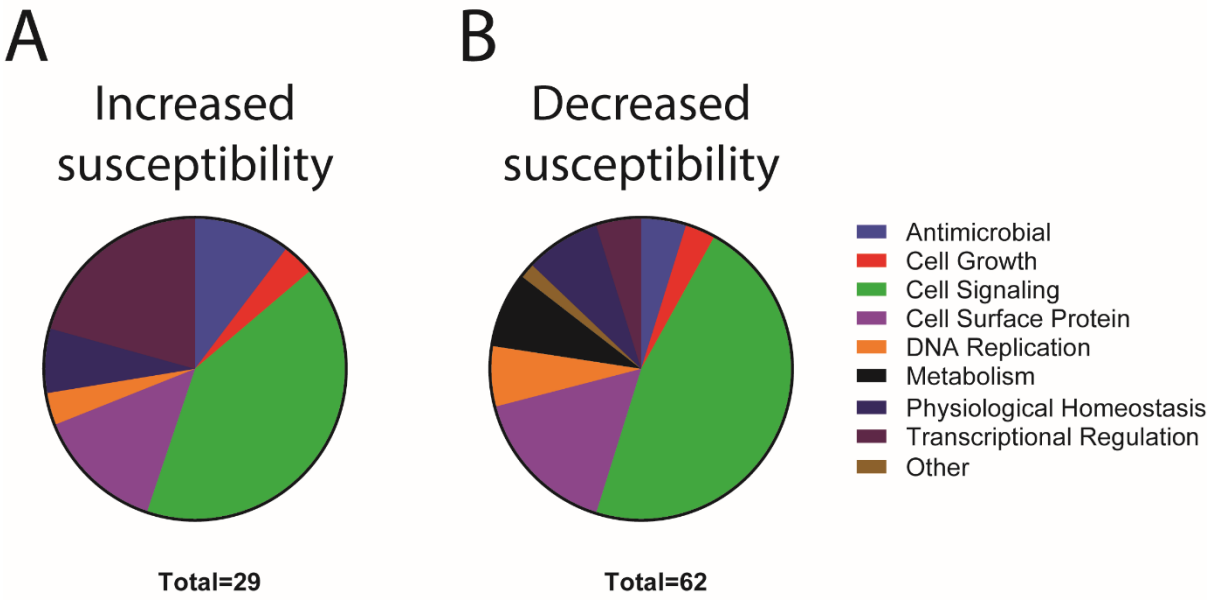


Figure 32: Mechanism of action of differential compounds against Dd2R539T/T38I vs. Dd2R539T

The atg18 T38I SNP caused (A) increased susceptibility to 90 compounds, a subset of which (n = 29) have known mechanisms of action. The SNP caused (B) decreased susceptibility to 137 compounds, of which 62 were annotated. Drugs are categorized into antimicrobial (blue), cell growth (red), cell signaling (green), cell surface protein (purple), DNA replication (orange), metabolism (black), physiological homeostasis (navy), transcriptional regulation (crimson), or other (tan).

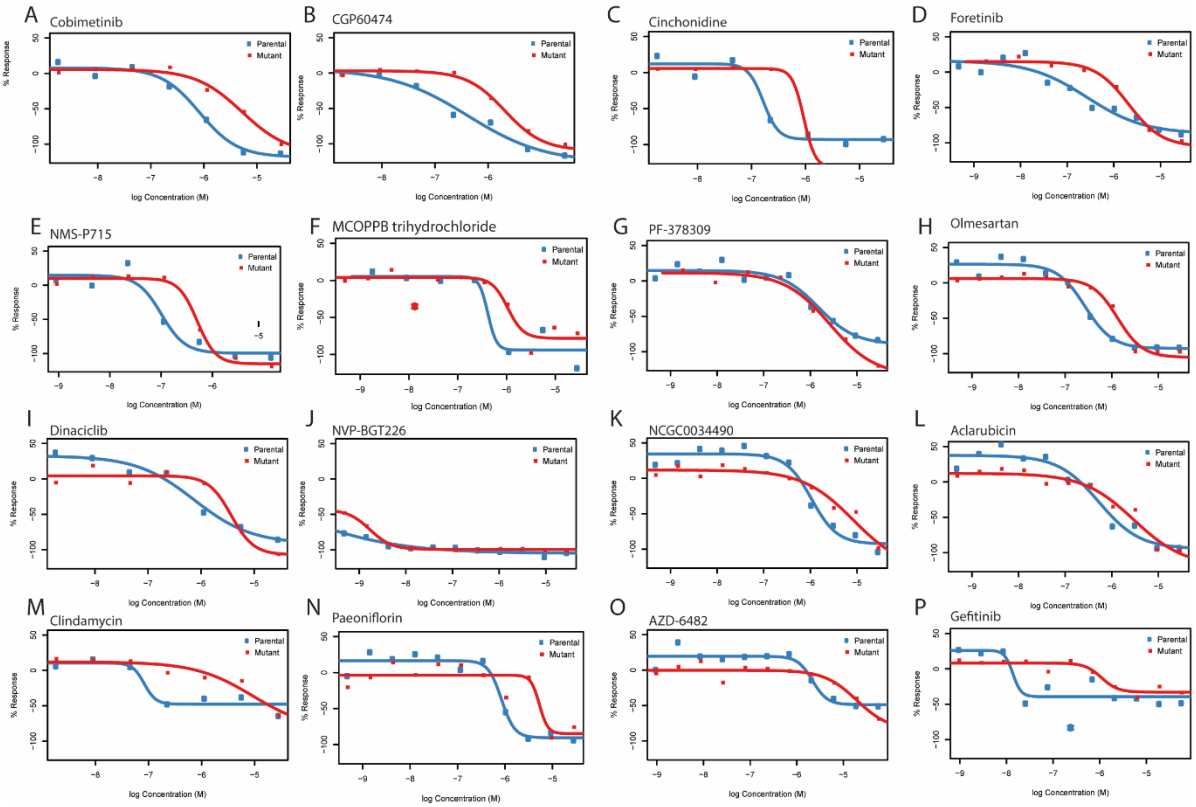


Figure 33: Drug response curves for compounds favoring Dd2R539T/T38I

Dose response curves from (A) cobimetinib, (B) CGP60474, (C) cinchonidine, (D) foretinib, (E) NMS-P715, (F) MCOPPB trihydrochloride, (G) PF-378309, (H) olmesartan, (I) dinaciclib, (J) NVP-BGT226, (K) NCGC0034490, (L) aclarubicin, (M) clindamycin, (N) paeoniflorin, (O) AZD-6482, and (P) gefitinib. Parent displayed in blue, mutant in red.

4.3.2.2 Parasite growth in response to nutrient deprivation

Growth rates of Dd2, Dd2^{R539T}, and Dd2$^{R539T/T38I}$ were assessed in a 48-hour flow cytometry-based assay. A variety of nutrient-limited media were made by titrating complete media with a basal salt solution lacking amino acids, vitamins, and albumax, with and without glucose. Parasites were grown in these nutrient-restricted media and parasitemia was assessed at 48 hours (Figure 34). When glucose was not present in the basal salt solution, parasites struggled to survive at 65% and 50% complete media, and all died at 25% complete media (Figure 34A). At 50% complete media, Dd2$^{R539T/T38I}$ had near-normal growth, while Dd2 and Dd2^{R539T} each grew significantly slower ($p < 0.0001$ and $p < 0.0001$). When glucose was not titrated, Dd2$^{R539T/T38I}$ parasites again grew faster at 50% complete media (vs. Dd2^{R539T} $p = 0.02$; vs. Dd2 $p = 0.002$) and, since all parasite lines were able to grow at 25% complete media, Dd2$^{R539T/T38I}$ also outgrew the other lines at 25% complete media (vs. Dd2^{R539T} $p = 0.0002$; vs. Dd2 $p < 0.0001$) (Figure 34B).

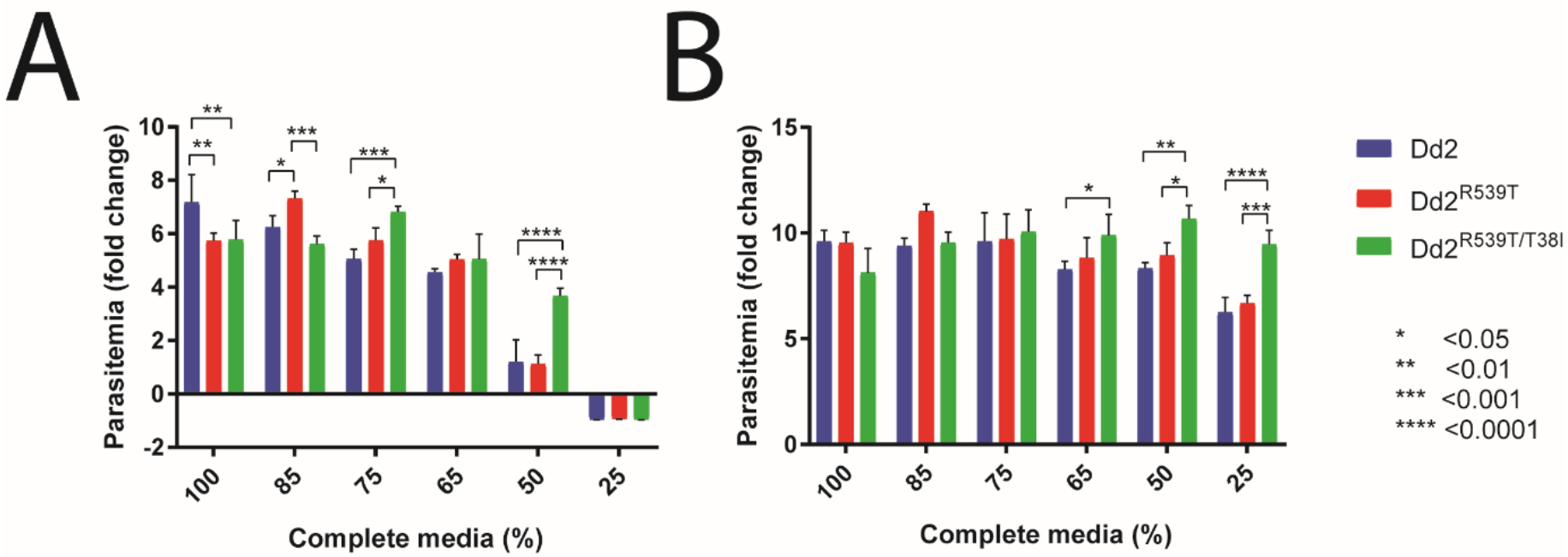


Figure 34: Growth rates of Dd2 isogenic lines in nutrient-limited conditions

Growth over 48 hours of isogenic lines Dd2 (blue), Dd2^{R539T} (red), Dd2$^{R539T/T38I}$ (green) in varying nutrient deprivation conditions with limiting glucose (A) and with glucose in normal (supra-physiologic) media concentration (B).

4.4 DISCUSSION

4.4.1 Understanding PfAtg18

Following the discovery of the T38I SNP in *atg18*, the central question became: what are the consequences of this SNP? To address this question, it was necessary to first understand the protein encoded by the *atg18* gene, *PF3D7_1012900*. Based on the modeling and alignment performed, it appears that this gene is homologous, and quite similar, to the WIPI proteins in humans. Proteins can use a number of motifs, including FRRG, PX, and FYVE to bind PI3P (Song et al., 2001, Kutateladze et al., 1999, Kutateladze, 2010). WIPI proteins use FRRG to bind PI3P; this domain is also present in PfAtg18. The dual arginines for Atg16 binding by WIPI proteins are conserved in the plasmodial protein as an arginine and a lysine, which is another basic amino acid. Based on the model, the residues for Atg16 binding are located on the tips of neighboring blades and therefore represent spatially feasible amino acids to bind a single protein. However, the SNP is located on the other side of the protein, not near either Atg16 or PIP3 binding sites; therefore, it is not likely to be directly involved in their binding. This is discussed further below. The high level of homology between the plasmodial protein and the WIPI proteins as well as conservation of these important residues suggests that the protein encoded by *PF3D7_1012900* can indeed be annotated as PfAtg18.

One primary function of WIPI/Atg18 is to bind PI3P to initiate autophagy (Obara and Ohsumi, 2008, Polson et al., 2010b). The WIPI/Atg18 proteins readily form puncta, much like LC3/Atg8, which can be detected by confocal microscopy and used as an autophagy assay (Proikas-Cezanne et al., 2007). Since GFP is sensitive to acidification, it will fluoresce when it is on the PAS or autophagosome, but will quench upon fusion with the lysosome. Therefore, the GFP tagged WIPI/Atg18 puncta assay allows for the detection of autophagic flux (Klionsky et al., 2016). There are several limitations of this assay. First, the ability for a cell to form detectable WIPI/Atg18 puncta upon the induction of autophagy is cell specific (Proikas-Cezanne et al., 2007, Polson et al., 2010a). Second, in some cell types, overexpression of GFP tagged WIPI/Atg18 can lead to aggregates that will appear as puncta, although they will be unrelated to autophagy (Klionsky et al., 2016). Despite these limitations, this assay represents a method to measure autophagic flux and, used in conjunction with already published LC3/Atg8 puncta assays, could be used as a second method of the autophagy detection. The use of two assays that each

measure the activity of different autophagy-related proteins would improve the likelihood of the assay to measure an autophagy-like mechanism.

To determine if PfAtg18 functionally behaves like WIPI/Atg18, it was necessary to determine if the protein readily formed puncta following cellular stressors. Because antibodies are not commercially available to most plasmodial proteins, transgenic parasites expressing GFP-Atg18 were created and several antibodies were made. There was some concern that GFP tags would hinder the functions of PfAtg18, hence both strategies were pursued concurrently. Upon obtaining GFP-Atg18 expressing parasites, transmission EM and confocal microscopy experiments were performed using DHA as a cellular stressor, as previous studies have demonstrated puncta formation of PfAtg8 following either starvation or DHA (Mott et al., 2015). Results of both transmission EM and confocal microscopy studies demonstrated the formation of puncta starting 10 minutes and peaking at 1 hour after the application of DHA. Parasites were also examined at 6 hours post-DHA treatment, but were largely dead at that time. These results were congruent with previous studies that demonstrated rapid puncta formation of WIPI/Atg18 following cellular stressors (Proikas-Cezanne et al., 2007), thus suggesting that GFP-Atg18 could be used as an autophagy measuring assay in *P. falciparum*. Further, it would appear that DHA induces puncta formation in both PfAtg8 and PfAtg18, thus suggesting that DHA may have a pro-autophagy effect on parasites.

A monoclonal antibody would be the ideal antibody, as hybridomas can produce an unlimited supply of identical antibody, rather than the relatively limited and heterogeneous antibodies produced in polyclonal antibody production. Unfortunately, the monoclonal antibodies did not detect GFP-Atg18 specifically and therefore are not useable. The diffuse nature of the monoclonal antibody staining pattern was likely due to the antibodies recognizing only one epitope of PfAtg18 which may have been shared between PfAtg18 and other plasmodial proteins. Nonetheless, several polyclonal antibodies were specific and these anti-PfAtg18 antibodies represent a powerful tool that can be utilized for future studies including co-localization studies as well as measurements of the autophagy-like pathway in any plasmodial line via puncta formation.

The results of the PIP strip membrane assay demonstrate that PfAtg18 can bind to PI3P. In addition to binding to PI3P, the results indicate that PfAtg18 can also bind to several other lipids, including PI5P and PI3,5P, as has been described in the general autophagic

literature (Vicinanza et al., 2015, Dove et al., 2004, Baskaran et al., 2012, Krick et al., 2012). The binding of PfAtg18 to PI3P has been confirmed by another group using a similar membrane detection assay (Bansal et al., 2017). Upon mutating the FRRG domain to FAAG, Bansal et al. demonstrated reduced binding of PfAtg18 to PI3P, thus confirming that the FRRG domain is the PI3P binding domain (Bansal et al., 2017). This group, however, did not demonstrate binding to PI3,5P or other phosphatidylinositols, although PI5P was not among those reported to have been tested. It is unlikely that PfAtg18 in the differing lines ($Dd2^{R539T}$ GFP-Atg18 used in this project vs. 3D7 GFP-Atg18 in Bansal et al.) truly bind phosphatidylinositols differently, given that the sequence of PfAtg18 is conserved between the lines. Further, both lines contain N-terminal GFP tags, which would likely cause steric hindrance in similar ways. It is possible that differences in phosphatidylinositol binding was caused by differing concentrations of PfAtg18 that were added to the membranes. This could have been due to differences in the lifecycle stages of the cultures, levels of expression of GFP-Atg18, or simply the amount of culture added to the assay. Bansal et al. demonstrated binding of TgAtg18 from *Toxoplasma gondii*, which is highly similar to PfAtg18, to PI3,5P, which would imply that PfAtg18 could also bind to PI3,5P. On the other hand, a different study was unable to detect PI3,5P in *Plasmodium* (Tawk et al., 2010), which suggests that PfAtg18 would have no need to bind PI3,5P. In order to determine if PfAtg18 truly binds other phosphatidylinositols or just PI3P, it would be necessary to repeat this experiment with other GFP-Atg18 lines in varying concentrations and lifecycle stages.

The ability of PfAtg18 to bind to PI3P holds significance for two reasons. The first is that homologous Atg18/WIPI proteins also bind PI3P and, therefore, the conservation of binding suggests potential preservation of part of the autophagy pathway. The second is that PI3P has been implicated in drug resistance in *P. falciparum*. Mbengue et al. determined that the kelch protein binds PI3-kinase (PI3K) and targets it for degradation. *K13* mutant, artemisinin-resistant parasites, however, are unable to bind PI3K, which thus accumulates, causing a buildup of its product, PI3P (Figure 11).

Given the evidence for the binding of PfAtg18 to PI3P and the aforementioned report that PI3P levels are important in resistance, PI3P levels were measured in a set of isogenic lines. The lines tested were isogenic Cambodian clinical isolates, 967^{Wtrev} and 967^{R539T}, which differ only in the presence or absence of a *k13* polymorphism. These lines were selected for several reasons. First, a contemporary Cambodian isolate that was

artemisinin-resistant was ideal as this parasite would better represent natural conditions in the circulating population rather than a laboratory line like Dd2. The 967^{R539T} parasite contains the genetic background that tends to accompany *k13* mutations in artemisinin-resistant parasites (Miotto et al., 2015). Second, isogenic lines were selected to isolate the impact of the *k13* polymorphism, R539T, on PI3P levels. Two polymorphisms, R539T and C580Y, which are both associated with artemisinin resistance, were used by Mbengue et al. Rather than using 967^{C580Y}, which has been edited using CRISPR to include the C580Y *k13* polymorphism, the original 967^{R539T} was used, since this was the naturally occurring mutation in the clinical isolate. Given that both R539T and C580Y correlate with artemisinin resistance (Straimer et al., 2015), preference was given to use R539T, the naturally occurring mutation.

This PI3P quantification experiment represents the novel application of an assay developed to quantify phosphatidylinositols in a variety of tissue and cell types. Although the Mbengue et al. paper used a commercially available Echelon PI3P Mass ELISA Kit for PI3P quantification, reproducible results have not been demonstrated by other groups with this method. Therefore, an alternative technique with more reliable results was sought that could effectively differentiate between PI3P and other phosphatidylinositols within parasites. The gold standard assay to quantify PI3P has been using radiolabeling followed by lipid extraction and HPLC (Payrastre, 2004); however, this method has several limitations. First, it has difficulty discriminating between similar phosphatidylinositols, such as PI3P vs. PI5P vs. PI3,5P2. Further, because the method uses radiolabeling, only PI3P that turned over and, therefore used radiolabeled inositol or phosphate, would be labeled and thus detected. Lipid pools in the cell that are not actively being turned over would remain undetected. The method used in this project, however, employed PIKfyve, an enzyme specific for PI3P, to convert PI3P to radiolabeled PI3,5P, which could then be isolated by TLC and quantified by HPLC. Not only does this method distinguish PI3P from PI3,5P or PI5P, it also quantifies the entire amount of PI3P rather than quantifying only the lipids that are turned over during labeling. This project represents the first time that this technique was applied to *Plasmodium*. PI3P has not been found in erythrocytes (Tawk et al., 2010); nevertheless, to reduce possible contributions, however small, from non-parasite lipids, parasites were lysed by saponin treatment prior to analysis. As phospholipid, and specifically PI3P, levels are known to increase over the course of the *Plasmodium* lifecycle (Jackson et al., 2004) (Tawk et al., 2010), four

different time points in the early part of the lifecycle were measured. There was a large jump in PI3P levels between 18-21 hpi and 27-30 hpi, consistent with a transition from mid-stage ring to trophozoite. In accordance with a previous study which reported a 3-fold increase in PI3P between rings and trophozoites (Tawk et al., 2010), this study found 2.9x the amount of PI3P in trophozoites as in rings. This demonstrated that the assay is capable of detecting changes in PI3P levels in *Plasmodium*.

The results revealed that there was no difference in PI3P levels in the isogenic set of Cambodian clinical isolates tested. This is in disagreement with the results of the study by Mbengue et al., which showed that the addition of *k13* polymorphisms led to an increase in PI3P levels. Although the results may be due to user variability to some extent, there are a number of other potential sources for these differences in the results. This discrepancy could be due to lack of sensitivity of the PIKfyve-HPLC assay. The results of the assay were variable between trials, possibly due to small changes in culture conditions or processing time that led to increased cellular stress and thus increased PI3P levels. However, the Mbengue et al. paper showed 2.7x more PI3P in a *k13* mutant parasite over the wild-type at 0-3 hpi (Mbengue et al., 2015), which would be expected to be detected in the PIKfyve-HPLC assay. These conflicting results could be resolved by measuring PI3P in the parasite lines tested by Mbengue et al. using the PIKfyve-HPLC assay or other lines using alternative methods. Some of these experiments are in progress.

Interestingly, PI3P has been shown to co-localize to the DV as well as the apicoplast (Tawk et al., 2010), which is consistent with the co-localization of both PfAtg8 (Kitamura et al., 2012, Tomlins et al., 2013) and PfAtg18 (Bansal et al., 2017). PI3P has also been found on vesicles (Tawk et al., 2010). The only known plasmodial protein with a FYVE domain, a motif that binds to PI3P (Kutateladze et al., 1999), termed the FYVE-domain containing protein (FCP), also localizes to the DV (McIntosh et al., 2007). PI3P has recently been shown to localize to the ER (Bhattacharjee et al., 2018), as would be expected for the formation of membranes in the early steps of autophagy initiation (Walker et al., 2008, Nascimbeni et al., 2017).

It is possible that autophagy machinery, PfAtg8, PfAtg18, and PI3P, have adapted the function of autophagy to include hemoglobin digestion. Given that the autophagic proteins are involved in organelle engulfment, trafficking to, and fusion with the lysosome, it would not represent a huge deviation for their plasmodial counterparts to be

involved in hemoglobin engulfment followed by trafficking to and fusion with the DV. Already, PI3K has been shown to be involved in hemoglobin transport. Blocking PI3K using wortmannin and LY294002 caused hemoglobin accumulation in the parasite cytoplasm, demonstrating that PI3K is an important part of the hemoglobin trafficking pathway (Vaid et al., 2010). Likewise, hemoglobin has been imaged within double-membraned vesicles, similar to autophagosomes, within the cytoplasm (Elliott et al., 2008). An autophagy-like mechanism may exist in *Plasmodium,* whereby parasites use autophagic machinery to provide a source of amino acids, but in this case from the host erythrocyte rather than from within the cell itself.

However, given that parasites are constantly remodeling their cytoplasm as they advance through the lifecycle, autophagy may exist in a classical sense as well. The transition from trophozoite through to merozoite followed by the ring stage sees the parasite segregate its cytoplasm and nucleus, then invade an erythrocyte to begin the cycle anew. Somewhere in this process, specialized organelles, including rhoptry and micronemes, are shed as the ring stage has just the essential organelles (Bannister et al., 2000a). Similarly, invasion of a liver cell by a sporozoite is accompanied by organelle clearance deemed "sporozoite metamorphosis" which is disrupted by overexpression of Atg8 (Jayabalasingham et al., 2014, Voss et al., 2016, Jayabalasingham et al., 2010). Furthermore, the commitment from the asexual intraerythrocytic parasite to the sexual gametocyte also involves shedding unnecessary organelles (Cervantes et al., 2014, Besteiro, 2017). The precise pathway of these organelles is poorly understood and could very well involve intracellular degradation and recycling. Although PI3P is important in autophagy, it has other uses and, therefore, a possible association of PI3P with artemisinin resistance does not necessarily implicate parasite autophagy. In other organisms, PI3P is also a marker of early endosomes (Gillooly et al., 2000) and is involved in membrane trafficking (Odorizzi et al., 2000). In *Plasmodium*, PI3P has also been implicated in protein export and pathogenesis through its association with Maurer's clefts and PfEMP1 export (Bhattacharjee et al., 2012, Bhattacharjee et al., 2018). However, there is enough circumstantial evidence to continue investigating the connection between PfAtg18, PI3P, and an autophagy-like pathway in *P. falciparum*.

4.4.2 Phenotypic changes associated with the T38I polymorphism in *atg18*

Upon determining that PfAtg18 is likely a homolog of WIPI/Atg18 with binding capacity and a similar pattern of behavior following stress, the consequence(s) of the T38I SNP could be better assessed. Through modeling PfAtg18, the location of the SNP was determined to be outside of the binding region for both PI3P and Atg16; however, this does not preclude the possibility that the SNP disrupts binding of PfAtg18 to another protein or lipid. It has been proposed that this area of the homologous WIPI protein binds to a number of regulatory proteins (Proikas-Cezanne et al., 2004). If the SNP does not impact binding, it may impact the function of PfAtg18 through phosphorylation, as a threonine can be phosphorylated and an isoleucine cannot. Protein analysis indicates that the T38 site has a low likelihood of being a phosphorylation site. Finally, a number of mutations in WIPI proteins have been described in numerous cancers including breast, colon, lung, skin, bone, pancreas, and esophagus cancers (Proikas-Cezanne et al., 2015). For a mutation to be advantageous in cancer, it may facilitate cancer cell growth, nutrient acquisition, or a number of other pro-survival mechanisms. The diversity of cancerous mutations found in WIPI proteins in cancer suggests that these mutations provide a survival advantage. Thus, the plasmodial *atg18* mutation may similarly offer a survival benefit of an unknown nature.

To address the impact of the SNP on antimalarial and other drug resistance, a compound screen was performed. Compound screens are routinely executed by the National Center for Translational Sciences (NCATS) at the NIH. There was no difference detected in IC50 values for the tested antimalarial compounds. This was surprising given the results of the *ex vivo* IC50 experiments reported in the previous chapter. There could be several reasons for this. First and foremost, this could indicate that the SNP is not in fact important in drug resistance. However, the *k13* polymorphisms, which have been clearly linked to drug resistance phenotypes (Ashley et al., 2014, Ariey et al., 2014, Straimer et al., 2015), do not cause differences in IC50 values in this same 72 hour assay used either (Witkowski et al., 2013c, Xie et al., 2014). Indeed, note the relative uniformity of the responses against all antimalarials for the entire set of isogenic lines for *k13* polymorphisms that were tested. Similarly, the 72-hour assay may not be ideal to elucidate the T38I SNP's contribution, as the effects may occur after a shorter or longer time course. Further, like kelch, the T38I SNP may be important only in a specific lifecycle stage. The assay utilized a mixed culture in all stages, which may mask the resistance phenotype, as there may be

too few parasites in a given stage to be detectable. Additionally, the effects of the SNP may be important only in the context of other background mutations, which are absent in the Dd2^{R539T} lines.

Despite having seemingly no effect on antimalarial IC50 values, the T38I SNP did change the susceptibility of the Dd2^{R539T} lines to several compounds. There were 90 compounds that showed more activity (more than 5x difference in the IC50 value) against the mutant than the parent line. Eighty two of these compounds were inactive against the parent, but the T38I SNP caused the parasite to become susceptible to the compound. Although eight of the compounds showed a shift of IC50 value, two of these curves were dubious and were therefore excluded. Thus the six compounds that the mutant was more susceptible to were benzethonium chloride, elesclomol, sapitinib, R306465, YM022, and vincristine.

Benzethonium chloride is a quaternary ammonium compound with antimicrobial and antifungal properties, used in a variety of wound care products, mouthwashes, and disinfectants (Serena et al., 2016, Said et al., 2014, Iwamura et al., 2016, Ichikawa et al., 2008). There is also some evidence that benzethonium chloride functions as an anticancer drug (Yip et al., 2006). Interestingly, benzethonium chloride has been shown to cause ER stress, activate the UPR (Rayess et al., 2018), form ROS (Gottardi, 1985), cause cell cycle arrest, and lead to apoptosis (Nomura et al., 2010) (Enomoto et al., 2007). The ability of ROS to induce autophagy (Azad et al., 2009) and the connection between autophagy and the UPR have been well-described (Benbrook and Long, 2012). Benzethonium has also been tied to eryptosis, apoptosis in the erythrocyte, and hemolysis through membrane disruption (Lang et al., 2011). Perhaps coincidentally, eryptosis is one mechanism of host survival during malaria infection (Foller et al., 2009).

Elesclomol, previously called STA-4783, is an anticancer drug that triggers apoptosis through oxidative stress (Kirshner et al., 2008, Hasinoff et al., 2015, Hasinoff et al., 2014). Although low levels of intracellular ROS can in themselves induce cancer, higher levels of ROS lead to apoptosis and thus the induction of ROS has been touted as an anticancer strategy (Huang et al., 2000). Elesclomol has shown success in clinical trials against melanoma cancers (O'Day et al., 2009), which is fitting given the role of ROS in the pathogenesis of melanoma (Denat et al., 2014). The interplay between elesclomol, ROS, and autophagy in melanoma has been discussed, including the induction of autophagy by

ROS and therefore the possible induction of autophagy by elesclomol (Hambright and Ghosh, 2017).

Sapitinib, also known as AZD8931, blocks epidermal growth factor receptor (EGFR), human epidermal growth factor receptor 2 (HER2) and human epidermal growth factor receptor 3 (HER3) (Hickinson et al., 2010). Sapitinib has also been shown to induce apoptosis (Morrison et al., 2014). It has been studied as an anticancer drug against breast cancer, ovarian cancer, and chordoma (Puvanenthiran et al., 2016, Mu et al., 2014, Scheipl et al., 2016). Growth factor inhibition leads to autophagy induction (Lum et al., 2005, Han et al., 2011, Fung et al., 2012), as growth factor reduction also causes downregulation of cell surface receptors needed for nutrient acquisition (Kan et al., 1994, Edinger and Thompson, 2002). Therefore, autophagy is induced to maintain cellular homeostasis in the absence of extrinsic nutrients (Lum et al., 2005). Since sapitinib blocks certain growth factors, it is likely to induce autophagy.

R306465 is an inhibitor of class I histone decetylase (HDAC) (Arts et al., 2007). Although it is often cell dependent, the inhibition of HDACs, specifically class I HDAC, has been shown to induce autophagy (Oh et al., 2008). While studies on R306465 are limited, another HDAC inhibitor, vorinostat (suberoylanilide hydroxamic acid, SAHA), induces autophagy by several mechanisms: the overexpression of autophagy related genes, inactivation of mTOR, and production of ROS (Li et al., 2010, Liu et al., 2010, Chiao et al., 2013).

YM022 is a selective antagonist of gastrin/cholecystokinin (CCK)-B receptors, which inhibits the secretion of gastrin and therefore inhibits the secretion of gastric acid (Nishida et al., 1994). Gastrin has been shown to induce autophagy (Rao et al., 2017, Kun et al., 2017). Therefore, this is the first of the compounds that would likely be an autophagy inhibitor.

Vincristine is a commonly used chemotherapeutic against acute lymphoblastic leukemia, lymphoma, and a number of other tumors (Said and Tsimberidou, 2014). Vincristine is a vinca alkaloid that acts on tubulin to destabilize microtubules and prevent mitosis (Jordan et al., 1991, Tangutur et al., 2017). Vincristine also appears to induce cell death, possibly by an alternative method given its ability to cause toxicity in postmitotic cells (Duflos et al., 2002). Cancer cells can die by alternative pathways facilitated by proteases including lysosomal cathepsins, which have increased expression in tumor cells and are dependent

on microtubules for their secretion (Kroemer and Jaattela, 2005, Joyce et al., 2004, Fehrenbacher et al., 2004). These cathepsins can then trigger apoptosis or apoptosis-like death pathways (Cirman et al., 2004). Vincristine has been shown to modulate lysosomes within a cancer cell by increasing both the size of individual lysosomes as well as total volume of lysosomes (Groth-Pedersen et al., 2007). Larger lysosomes are associated with increased disruption leading to cell death (Ono et al., 2003). Further, vincristine causes lysosomal membrane permeabilization allowing for cathepsins to escape into the cytoplasm (Groth-Pedersen et al., 2007).

The autophagy pathway is dependent on microtubules. Microtubules are needed for the production (Kochl et al., 2006, Punnonen and Reunanen, 1990) and movement of autophagosomes, as well as and their fusion to lysosomes (Fengsrud et al., 1995, Groth-Pedersen et al., 2007). Vinblastine, a closely related vinca alkaloid, causes an accumulation of autophagosomes which is thought to be due to the inhibition of autophagosome fusion to the lysosome (Fengsrud et al., 1995). Vincristine is therefore likely to have an autophagy inhibiting effect.

On the other side, the $Dd2^{R539T/T38I}$ parasite (mutant) decreased its susceptibility to a number of compounds. The parasite lost susceptibility to one hundred and twenty one compounds following the addition of the T38I SNP. Moreover, sixteen compounds had a shift of IC50 value, with a higher value in the T38I parasite.

The hits included a number of anticancer drugs that are either in development or current use. Foretinib, also called GSK1363089, is an anticancer drug that inhibits kinases including c-MET and vascular endothial growth factor receptor 2 (VGFR2) and induces apoptosis (Dufies et al., 2011). PF-3758309 is a p21-activated kinase (PAK) inhibitor that is being developed as an anticancer drug (Murray et al., 2010). CGP-60474 and dinaciclib are both cyclin dependent kinase (CDK) inhibitors which prevent cellular proliferation by causing cell cycle arrest (Ruetz et al., 2003, Kuo et al., 2005, Nemunaitis et al., 2013). Dinaciclib also inhibits the unfolded protein response (Nguyen and Grant, 2014). NMS-P715 inhibits the human monopolar spindle 1 (MPS1) kinase, a kinase important in mitosis, thus inhibiting cellular proliferation (Colombo et al., 2010). Cobimetinib, also called GDC-0973, inhibits mitogen-activated protein kinase (MAPK)/extracellular signal-regulated kinase (ERK) kinase (MEK) to prevent cellular proliferation and trigger apoptosis (Hoeflich et al., 2012).

MCOPPB trihydrochloride, a derivative of MCOPPB, is an agonist of nociception/orphanin FQ peptide (NOP) receptor which functions as an anxiolytic (Hirao et al., 2008).

Gefitinib is an anticancer drug that acts as an EGFR tyrosine kinase inhibitor (Xu et al., 2014b). Gefitinib has been show to induce autophagy (Xu et al., 2014b, Tan et al., 2015, Liu et al., 2015). It has also been shown to increase the sensitivity of *P. falciparum* parasites to chloroquine treatment by inhibiting chloroquine's efflux from the DV (Alcantara et al., 2013).

Aclarubicin is an anthracycline antibiotic and anticancer drug that inhibits topoisomerase II (Sørensen et al., 1992) and induces apoptosis (Gieseler et al., 1999). Aclarubicin has been shown to utilize cellular iron and to produce ROS (Richard et al., 2002). Aclarubicin and other anthracyclines can decrease DNA helicase activity in *P. falciparum* and have therefore been posited as novel antimalarial compounds (Suntornthiticharoen et al., 2006).

There were several other hits that also modulate the production of ROS. Olmesartan is an angiotension II receptor antagonist that is used to treat hypertension. Angiotensin II can produce ROS and induce autophagy, while angiotension II receptor blockers have been shown to inhibit the induction of autophagy (Yu et al., 2014). Paeoniflorin is a natural product with anti-inflammatory properties (Zhu et al., 2005). It has been shown to decrease ROS in a variety of cell types (Zhao et al., 2013, Wankun et al., 2011, Kong et al., 2016, Dong et al., 2015). The production of ROS is postulated mechanism of action for artemisinin derivatives (Klonis et al., 2011). Changes in the production of ROS would also alter autophagy levels and also kill parasites.

AZD-6482 and NVP-BGT226 are both PI3K inhibitors (Joshi et al., 2014). AZD-6282 is in clinical trials for several cancers including renal clear cell carcinoma and melanoma (Wang et al., 2015a, Shannan et al., 2016). NVP-BGT226 also inhibits mTOR, the master regulator of the autophagy pathway (Fan et al., 2006); however, there is no known homolog to mTOR in the plasmodial genome (Gardner et al., 2002, Serfontein et al., 2010). The nutrient functions of mTOR are potentially fulfilled by an AMPK kinase called KIN (Mancio-Silva et al., 2017). AZD-6482 inhibits class-I PI3K, while NVP-BGT226 inhibits both class-I and class-III PI3K (Hassett et al., 2017, Joshi et al., 2014). Class-I PI3K are important in signal transduction for cell proliferation and chemotaxis

through catalytic activities, typically by converting phosphatidylinositol-3,4-biphosphate (PIP2) to phosphatidylinositol-3,4,5-triphosphate (PIP3) (Jean and Kiger, 2014). Class-III PI3K plays a major role in the production of PI3P for autophagy (Jean and Kiger, 2014). *P. falciparum* only has class-III PI3K, dubbed Vps34 (Gardner et al., 2002). NVP-BGT226 has been shown to have potent activity against *P. falciparum* (Mott et al., 2015). NVP-BGT226 was also shown to decrease the PfAtg8 puncta response induced by artemisinin derivatives, suggesting that NVP-BGT226 may block the autophagy-like cascade in *P. falciparum* (Mott et al., 2015). The decreased susceptibility of the mutant line to NVP-BGT226 as compared to the parent is preliminary evidence that the SNP may modulate an autophagy-like pathway to some degree.

Two compounds with known antimalarial activities were among the hits. Clindamycin is an antibacterial that is active against many gram positive cocci and some gram negative rods. It can be used in the treatment of malaria, and is routinely used for the treatment of *P. falciparum* in pregnancy in combination with quinine (WHO, 2015a). It can also be used in combination with artesunate or quinine for the treatment of severe malaria (WHO, 2015a). Clindamycin inhibits protein synthesis by binding to the 50S ribosomal subunit (WHO, 2015a). The other antimalarial hit is cinchonidine, an alkaloid that has been isolated from *Cinchona officinalis*, the plant that also gives us quinine. It is not as effective against *P. falciparum* as quinine, but does have antimalarial activity (Warhurst, 1987, Wesche and Black, 1990). Interestingly, mutations in the plasmodial gene *crt*, which are important in chloroquine resistance, also appear to modulate susceptibility to various *Cinchona* alkaloids (Griffin et al., 2012). The mutant line was as susceptible as the parent after exposure to other *Cinchona* alkaloids, including quinine and quinidine; however, quinine was associated with an increase in *ex vivo* IC50s as reported earlier (Section 3.3.1.1). *Cinchona* alkaloids are not routinely used in Cambodia, though they had been used frequently in the past.

Many of the compounds that had differing susceptibility between the parent, $Dd2^{R539T}$, and mutant, $Dd2^{R539T/T38I}$, are known to induce apoptosis, ROS, or autophagy directly. The ability of a line to change its susceptibility to a drug that induces one of these processes suggests that the SNP is modifying one or all of those pathways.

Given that the results of the drug screen did not demonstrate a stark difference in the efficacy of the majority of antimalarials, the question remains as to why this SNP has

been selected. Given that autophagy is important in nutrient acquisition through the degradation of damaged cytoplasmic material, the T38I SNP may lead to an increase in metabolic functioning that could be enough for its selection.

The environment of culture media is designed to imitate the conditions of the human body in some ways, such as ion concentrations, but is supra-physiological in others (Trager and Jensen, 1976). Concentrations in RPMI 1640, one of the main ingredients in complete media, for the majority of amino acids, glucose, and several vitamins far exceed those measured in human blood (Desai, 2013). Studies vary in their findings as to which of these ingredients are essential to culture media. One study determined that L-cysteine, L-glutamic acid, L-glutamine, L-isoleucine, L-methionine, L-proline, L-tyrosine, D-pantothenic acid, glucose, and hypoxanthine were all essential to the growth of *P. falciparum* in culture (Divo et al., 1985). However, a later study determined that the only essential amino acid for parasite growth is L-isoleucine (Liu et al., 2006, Istvan et al., 2011). Interestingly, the source of nutrients (pooled human sera or albumax) has been shown to change parasite growth rates; specifically, parasites grown in pooled human sera grow more slowly than those grown in synthetic culture media (Pillai et al., 2012).

This supra-physiologic milieu may lead to parasites that do not accurately reflect *in vivo* conditions, since they are being selected for in an environment of abundance. When cultured, parasites rapidly adapt to the artificial conditions (Corcoran et al., 1986, Bhasin et al., 1985). Metabolic pathways that are essential *in vivo* could prove to be unnecessary or even energetically costly and undesirable *in vitro* as nutrients flood the cell. The remodeled genome of the cultured malaria parasite may not resemble the clinical isolate and therefore could lead to false conclusions regarding parasite biology or drug susceptibility.

Drug screens preformed in complete media may not give an accurate picture of clinical drug susceptibility. A previous high-throughput drug discovery study found that the use of standard complete culture media masked the effects of drugs and that utilizing a nutrient restricted media unmasked the susceptibility of the parasites to a variety of novel inhibitors (Pillai et al., 2012, Pillai et al., 2010). This could be an even bigger issue when the compounds target metabolic pathways (Desai, 2013). Autophagy is a metabolic pathway that is especially active under starvation conditions to provide an amino acid supply for a cell. However, in yeast an autophagy deficient cell grows normally within

supra-physiologic media (Tsukada and Ohsumi, 1993). Because of the potential for complete media to render metabolic pathways, including autophagy, unnecessary, studies are underway screening known antimalarials and other drugs of interest against the mutant ($Dd2^{R539T/T38I}$) and parent ($Dd2^{R539T}$) lines using a variety of growth restricted media.

In addition to performing drug screens, general growth phenotypes were assessed using nutrient-limited media. Interestingly, the $Dd2^{R539T/T38I}$ mutant appeared to survive better in nutrient-limited settings than either its parent, $Dd2^{R539T}$, or the original line, Dd2. The T38I SNP may therefore represent a fitness advantage by allowing the parasite to grow more effectively in the nutrient limited setting of the human body. This alone, rather than (or in addition to) a drug resistance phenotype, could allow for selection of the T38I SNP. Despite allowing for increased survival of early ring-stage parasites, *k13* polymorphisms have been shown to cause growth deficits *in vitro* (Straimer et al., 2017). The T38I mutation could therefore compensate for the loss of fitness caused by *k13* polymorphisms in the parasite population. On the other hand, DHA-resistant isolates have been shown to grow more rapidly in stressful conditions, as evidenced by a decreased growth rate for sensitive parasites at high parasitemia (Cui et al., 2012). At higher parasitemias, growth media, which is normally supra-physiologic, may become rapidly depleted, thus creating a nutrient-limited media. Therefore, these align with the finding that efficient growth in nutrient deprivation may be driving selection. Further, these stressful, oxidative stress inducing conditions would typically slow parasite growth (Becker et al., 2004). However, if a parasite is better equipped to handle damage by oxidative stress, perhaps by employing autophagy-like mechanisms, that parasite would likely outcompete other parasites in a population.

Drug resistance often comes with an associated fitness cost (Andersson and Hughes, 2010). *In vitro* studies of *P. falciparum* fitness use co-culture of two lines to determine which parasite line outcompetes the other. In the case of chloroquine resistance, a chloroquine-sensitive lines outcompeted the chloroquine-resistant lines, indicating a loss of fitness of 25% by several *mdr1* mutations (Hayward et al., 2005). Furthermore, copy-number variation of *mdr1* appears to have an associated fitness cost. Increased copy number of *mdr1* is associated with mefloquine resistance, but increased susceptibility to chloroquine (Veiga et al., 2011, Phompradit et al., 2011, Preechapornkul et al., 2009). Single-copy-number parasites had a fitness advantage over two parasites with increased

copy number in a competitive growth assay (Preechapornkul et al., 2009). Likewise, a study in mice demonstrated increased fitness in chloroquine-sensitive parasites, as they repeatedly outgrew chloroquine-resistant parasites *in vivo* (Rosario et al., 1978). In another study, pyrimethamine-sensitive parasites had a fitness advantage over pyrimethamine-resistant parasites; however, the resistant line eventually adapted to gain a fitness advantage over both other parasite lines (Walliker et al., 2005).

The repeated emergence of drug resistance in Southeast Asia has been at least partially attributed to fitness and competition inherent in a hypoendemic zone. In areas of low transmission, people are less likely to be highly immune to malaria and therefore, lower fitness parasites can persist (Rosenthal, 2013). Additionally, infections are more likely to be monoclonal in low transmission zones rather than polyclonal. Much like the *in vitro* assays, polyclonal infections allow for competition between two parasite strains, with the fit parasite winning and propagating forward in the population.

The reemergence of drug-susceptible parasites following high levels of drug resistance demonstrates the results of fitness costs in clinical studies. Despite the widespread prevalence of chloroquine-resistant parasites, chloroquine-sensitive parasites reemerged following the discontinuation of the use of chloroquine in Malawi (Kublin et al., 2003). Similarly, in Cambodia after the cessation of mefloquine pressure, parasites decreased *mdr1* copy number and again became susceptible to mefloquine (Lim et al., 2015).

A reduction in parasite fitness is an important sequela of drug resistance. However, as demonstrated, parasites can evolve additional mutations to offset the fitness cost of a resistance-causing mutation. The *atg18* T38I SNP is likely to be the result of a fitness mutation, as it appears to improve growth in nutrient-limited settings that better approximate its environment in the human bloodstream than normal supra-physiologic media.

Plasmodium parasites appear to be susceptible to changes in host diet. Dietary restrictions in mice have been shown to be protective against cerebral malaria by *P. berghei* (Mejia et al., 2015, Hunt et al., 1993). Refeeding of patients with *P. falciparum* in the hospital setting has been associated with an increase in parasitemia (Murray et al., 1975). In culture supplemented with sera from calorie-restricted mice as compared to fed mice, parasites formed fewer merozoites during schizogony, thus reducing overall parasitemia (Mancio-Silva et al., 2017). Thus parasitemia is intricately tied to host nutrition status.

The serine/threonine kinase KIN, which is putatively homologous to AMP-activated kinase (AMPK) has been implicated in nutrient sensing in *Plasmodium* in the absence of TOR proteins (Mancio-Silva et al., 2017). AMPK is another regulator of autophagy along with mTOR (Kim et al., 2011). An autophagy-like pathway may therefore play a role in nutrient sensing in *Plasmodium* and may modulate parasite virulence based on the ability of the parasite to obtain nutrients in a restricted setting.

Many antimalarial drugs target metabolic pathways (Delves et al., 2012). An improvement in a parasite's ability to survive low nutrient conditions not only benefits the parasite in terms of its growth rate, it also allows a parasite to evade drugs that may target varying metabolic pathways. While a drug may block one metabolic pathway, another pathway that was previously redundant may become essential. The ability to grow more efficiently in nutrient limited media suggests changes in the mutant's metabolism, which could allow the parasite to survive drug treatment. Again, the ability to survive a drug pulse based on the parasite's ability to employ alternate metabolic pathways may appear inconsequential in a drug screen in complete media, where nutrient limitation is not a factor.

The $Dd2^{R539T/T38I}$ parasite outgrew its parent parasites as assessed by independent cultures in nutrient limited conditions. It is possible that the T38I SNP leads to changes in the function of PfAtg18 to allow for more efficient nutrient acquisition through an autophagy-like pathway. This could allow for either increased fitness leading to expansion within the parasite population or the ability of a parasite to survive drug treatment by utilizing its autophagy-like pathway to survive in the absence of a blocked metabolic pathway. Further studies, including a more detailed characterization of the function of PfAtg18, are necessary to determine if this is indeed the case.

5 *PLASMODIUM FALCIPARUM* DORMANCY IN RESPONSE TO ARTEMISININ AS A MECHANISM OF RESISTANCE

5.1 INTRODUCTION AND AIMS

5.1.1 Introduction

The recommended dosing regimen for artemisinin consists of ACT, which pairs a short-acting artemisinin derivative with a longer acting partner drug. The artemisinin derivative quickly diminishes the parasitemia, but is rapidly cleared from a patient's system within a matter of hours. This leaves the patient with the partner drug, which stays above therapeutic levels for days to weeks, to prevent recrudescences and kill the remaining parasites. This has been the recommended treatment regimen since the development of artemisinin, as artemisinin monotherapy was associated with recrudescence even in the absence of any resistance (Li et al., 1984). As evidence, the same artemisinin derivative remained equally effective for a recrudescent infection as for the original infection (de Vries and Dien, 1996). The incidence of recrudescence decreases with longer drug regimens both *in vitro* (Bwijo et al., 1997) and in clinical studies (Looareesuwan, 1994, Nguyen et al., 1993). Despite this, there are still recrudescences with artemisinin monotherapy even after a prolonged seven day treatment (White, 1997), which confirms that artemisinin must be given as ACT. Due to the consistent failure of artemisinin monotherapy, the WHO has recommended artemisinin dosing as an ACT since 2001 (Paloque et al., 2016).

There are several theories regarding reason for the failure of artemisinin monotherapy. With any monotherapy, there is the risk that some parasites will evolve to evade the drug within a patient's parasite population and that these parasites will expand to cause the recrudescence. However, parasites remain equally susceptible to artemisinin following recrudescence after monotherapy, indicating that it is unlikely that resistance is the cause (de Vries and Dien, 1996). Because artemisinin derivatives act quickly but have a short half-life, it is possible that drug levels only remain above the minimum inhibitory concentration (MIC) for a short period of time, not allowing all parasites to be killed following a given dose (White, 1997, Giao et al., 2001). A theory proposed by Hoshen

and colleagues indicated that the incidence of clinical artemisinin recrudescences could be accounted for by a population of surviving parasites that go dormant to evade drug action and resume growth following drug clearance (Hoshen et al., 2000).

In a discussion of dormancy, it is important to note that nomenclature can be confusing. In general, dormant forms are metabolically inactive, as opposed to quiescent forms which have slowed or arrested growth but remain somewhat metabolically active (Rittershaus et al., 2013). Given that *P. falciparum* dormant parasites have been shown to maintain some metabolic activity (Shaw et al., 2015, Chen et al., 2014b), it may be more accurate to dub them "quiescent" forms rather than "dormant." However, given that the bulk of the literature refers to these plasmodial parasites as "dormant," this project will proceed with the historical nomenclature.

In vitro dormancy has been induced in response to artemisinin and a number of other compounds. Dormancy in *P. falciparum* was first described in an experiment in which a culture was treated with sorbitol every 12 hours for 96 hours and recrudesced (Nakazawa et al., 1995). Similarly, *in vitro* pyrimethamine treatment caused a ring-stage culture to ostensibly clear its parasites only to recrudesce days later (Nakazawa et al., 1995). At the time, Nakazawa and colleagues postulated that these recrudescences were due to a low number of dormant parasites that persisted in the culture at any given time, rather than an induced phenotype (Nakazawa et al., 1995). However, dormancy can be induced by artemisinin derivatives, as evidenced by morphologic cell cycle arrest at the ring-stage following treatment (Witkowski et al., 2010). Furthermore, dormancy was induced by nutrient specific starvation in ring-stage parasites that displayed cell cycle arrest when grown in the absence of isoleucine (Babbitt et al., 2012). These experiments demonstrated that dormant parasites can be induced in response to environmental stressors, although they do not preclude the ability of dormant forms to exist at low levels in the absence of stress. Further experiments have shown the induction of a dormancy phenotype following treatment by atovaquone (Peatey et al., 2015, Thapar et al., 2005), mefloquine (Nakazawa et al., 2002) and a number of artemisinin derivatives (Teuscher et al., 2010, Witkowski et al., 2010, Grobler et al., 2014).

Artemisinin-induced dormancy appears to relate to artemisinin resistance through the parasite's ability to arrest its cell cycle. Parasites are thought to stop passing through the cell cycle to prioritize cellular repair over replication (Wernsdorfer, 1994). Following

treatment with artemisinin, parasites remain in the ring stage until the drug is removed, when the culture continues to develop through the lifecycle (Witkowski et al., 2010). Artemisinin resistance seems to be modulated by the ability of parasites in the early ring stage (0-3 hours) to survive a short pulse of artemisinin (Witkowski et al., 2013a). Indeed, there is evidence that artemisinin-resistant isolates have a prolonged ring stage as compared to artemisinin-sensitive parasites (Mok et al., 2011). Given some evidence that artemisinin needs hemoglobin to exert its effects by the activation of the endoperoxide bridge, it is possible that parasites evolved to remain in the ring stage for longer in order to evade killing by artemisinin derivatives (Klonis et al., 2011). However, there is evidence that even in the absence of hemoglobin digestion in the early ring-stage, artemisinin is activated by the action of two falcipains (Xie et al., 2016).

Assays have been developed to isolate the artemisinin-induced dormant parasites from the dead and active parasites of a culture and have shown that artemisinin-resistant cultures recrudesce earlier than artemisinin-sensitive cultures (Teuscher et al., 2012, Tucker et al., 2012, Cui et al., 2012, Witkowski et al., 2013b). Recovery following artemisinin-induced dormancy occurs after a consistent duration and is thought to be dependent on parasite genetic background (Tucker et al., 2012, Teuscher et al., 2010). Kelch13 mutations are thought to modulate the dormancy phenotype (Paloque et al., 2016); however, this has not been proven. One theory postulates that artemisinin induces free radicals that stress a parasite and cause it to go dormant. The kelch mutation may help the parasite respond to and repair itself from this stressor and consequently keeps the parasite in this dormant state for longer, allowing it to survive the drug and eventually recrudesce (Winzeler and Manary, 2014). This theory runs counter to the observation that resistant parasites need higher concentrations of artemisinin derivatives to enter dormancy (Teuscher et al., 2012). The contribution of kelch mutations to the dormancy phenotype are assessed in this chapter.

Although dormant forms have not been detected in humans clinically, there is evidence that this is more than an *in vitro* phenotype. Dormant parasites have been described *in vivo* following artemisinin treatment in mice (LaCrue et al., 2011). Modeling studies, first by Nakazawa and colleagues, and later by Codd and colleagues, have also demonstrated that dormancy could account for discrepancies between previous models and clinical outcomes (Nakazawa et al., 1995, Codd et al., 2011). Despite these studies, a definitive finding of dormant *P. falciparum* parasites has not been confirmed in a human.

Despite the lack of evidence for dormancy in *P. falciparum* in people, there is plenty of proof that other *Plasmodium* species can exhibit a dormant phenotype in humans. Upon injection into humans via mosquito, *P. vivax* parasites infect the liver, much like *P. falciparum* parasites. However, a subset of these *P. vivax* sporozoites can become hypnozoites in the liver (Cogswell, 1992). Hypnozoites, deriving from the Greek "*hypnos*" (meaning sleep) and "*zoon*" (meaning animal) (Markus, 2011b), refer to dormant liver stage parasites that have the ability to reactivate days, weeks, or even years later to cause a malarial infection in their host (Markus, 2015). The recrudescence that occurs following reactivation of the hypnozoite can cause a disease relapse, either symptomatic or asymptomatic (Markus, 2015). There is also evidence of the formation of hypnozoites by *P. ovale* species (Markus, 2011a). Although hypnozoites have not been detected in *P. falciparum*, there is debate over whether relapses that have occurred decades after the original infection may be caused by dormant forms that subsequently reactivate (Richter et al., 2016).

The quiescent phenotype, as it should be referred to outside of *Plasmodium*, is a common phenotype in a wide variety of other species and cell types. In particular, bacteria, such as *Mycobacterium tuberculosis*, exhibit the quiescence phenotype in that they can remain latent in the human body for years before reactivating (Denis and Anthony, 2004, Betts et al., 2002). Long-lived cells, such as certain immune cells, can remain quiescent for years before the appropriate immunologic activation that causes exit from quiescence and proliferation (Di Rosa, 2016, Sprent and Surh, 2011). Stem cells exhibit quiescence as long-lived cells in a variety of tissues (Furutachi et al., 2015, Katayama et al., 2006, Wilson et al., 2008).

There is evidence for the connection between quiescence and autophagy in a number of different species and cell types. Autophagy is thought to be important in the entry and exit from quiescence in microbes, as it facilitates the procurement of amino acids needed for the increase in protein synthesis that accompanies the shift in metabolic functioning (Rittershaus et al., 2013, Shaikh et al., 2010). Autophagy is similarly required for the entry of yeast cells into their quiescent G_1/G_0 state (An et al., 2014). On the other hand, when autophagy was blocked in dormant ovarian cancer cells, cell regrowth was inhibited, indicating that autophagy helps cells survive and exit dormancy in certain tumor cells (Lu et al., 2008). Similarly, gastrointestinal tumors, which often have a sizeable fraction of dormant cells, were killed using RNAi ablation of autophagy related proteins

ATG7 and Autophagy-related protein 12 (ATG12) or the autophagy inhibiting drug chloroquine (Gupta et al., 2010). Autophagy is employed in the quiescence phenotype of long-lived cells, including hematopoietic stem cells (Warr et al., 2013, Watson et al., 2015) and cells involved in immunological memory (Xu et al., 2014a, Chen et al., 2014a). Given the typical plasmodial lifecycle of 36-50 hours, a parasite that remains dormant for several days or even weeks would qualify as a long-lived plasmodial parasite. The *Toxoplasma* bradyzoite, which is the quiescent cyst-like form, needs its autophagy-like metabolic pathway for long term survival (Di Cristina et al., 2017). *Toxoplasma* is closely related to *Plasmodium* and, therefore, this may be the best evidence to suggest that autophagy is involved in plasmodial dormancy.

In light of the connections between artemisinin resistance and plasmodial dormancy, as well as quiescence and autophagy, the possibility for a function of the T38I SNP in *atg18* in the dormancy phenotype came to light. In *C. elegans*, inhibition of Atg18 leads to a decrease in lifespan (Toth et al., 2008); therefore, *atg18* may have a role in lifecycle and lifespan in *Plasmodium* as well. Previous studies indicated that duration of dormancy and recrudescence are traits determined by genetic loci; therefore, I sought to determine if the T38I SNP modulated dormancy and recrudescence.

An important tool in elucidating genetic determinants of phenotypes in *P. falciparum* has been the genetic cross. A genetic cross uses the male and female gametocytes of two genetically distinct parent clones to create a set of genetically distinct progeny for the assessment of a particular phenotype. The gametocytes of the parents are fed to a mosquito and these sexual forms mate in the midgut of the mosquito to produce a number of sporozoites with genomes that have undergone genetic recombination between the two parents. The mosquito is then allowed to feed on a chimpanzee host, in which the genetically diverse sporozoites are injected, pass through the liver, and establish the intraerythrocytic life cycle. Blood is taken from the monkey, cultured, and parasites are cloned by limiting dilution to create clonal progeny isolates. The parents, along with the progeny, can be tested for a phenotype and the genetic determinants of the phenotype can be illuminated based on quantitative trait locus (QTL) analysis (Su et al., 2007). Based on the size of the 23Mb *P. falciparum* genome and the average recombination distance of approximately 15kb per centimorgan, it is estimated that between 30 to 100 progeny are needed to map a locus of interest within 15-50kb (Su et al., 1999, Su et al., 2007).

The first *P. falciparum* genetic cross mixed HB3, a pyrimethamine-resistant parasite from Honduras, with 3D7, a pyrimethamine-sensitive African parasite isolated from a person in the Netherlands (Walliker et al., 1987). This cross allowed researchers to identify the point mutations in the *dihydrofolate reductase-thymidylate synthase (DHFR-TS)* gene that mediate pyrimethamine resistance (Peterson et al., 1988). After the initial goal of finding the genetic determinants of pyrimethamine resistance was completed, the HB3x3D7 remained a useful tool. The HB3x3D7 cross aided in the understanding of *var* gene recombination (Freitas-Junior et al., 2000) and inheritance of histidine-rich proteins (HRPs) (Wellems et al., 1987). Since the original HB3x3D7 cross, three other crosses have been performed using non-human primates as intermediate hosts. The Dd2xHB3 cross mixed the genomes of chloroquine-resistant Dd2 from Indochina with chloroquine-sensitive HB3 to understand the genetics underlying chloroquine resistance. The results of the cross determined that *mdr* genes were the primary determinants of chloroquine resistance (Wellems et al., 1990) and instead implicated a region of the genome on chromosome 7 (Wellems et al., 1991, Su et al., 1997), which eventually led to the discovery of *crt* as a modulator of chloroquine resistance (Fidock et al., 2000). The progeny for the Dd2xHB3 cross were also used to understand parasite genomics, copy number variants and transcriptional regulation (Gonzales et al., 2008, Samarakoon et al., 2011), as well as to recognize the role of certain *clag* genes in plasmodial surface anion channel (PSAC) (Nguitragool et al., 2011). The 7G8xGB4 cross examined the ability of some parasites to infect *Aotus* monkeys, determining that polymorphisms in *RH5* were responsible species-specific virulence (Hayton et al., 2008). These same progeny were used to discover the role of *Pfs47* in allowing *P. falciparum* to infect mosquitoes without activation of the complement pathway, thus evading the mosquito's immune system and allowing for transmission (Molina-Cruz et al., 2013). The final cross examines the genetic determinants of artemisinin resistance using the artemisinin-sensitive GB4 from Ghana crossed with the artemisinin-resistant 803 from Cambodia. The results of this study have yet to be published at the time of this dissertation.

In this chapter, two different approaches were taken to determine if the *atg18* SNP is responsible for the dormancy phenotype in artemisinin-resistant isolates. The first is a reverse genetics method by determining the dormancy phenotype of the $Dd2^{R539T}$ and $Dd2^{R539T/T38I}$ isogenic parasite set. The second is a forward genetics method by using the

parents and progeny of the cross to determine if polymorphisms in *atg18* or another gene are responsible for the dormancy phenotype.

5.1.2 Aims

(1) The first aim is to determine if the T38I SNP in *atg18* modulates a dormancy phenotype.

(2) The second aim is to determine if differences in the dormancy phenotype between artemisinin-sensitive and resistant parasites can be attributed to polymorphisms in K13.

(3) The third and final aim is to determine if the 803xGB4 genetic cross can be used as a tool to elucidate the genetic determinants of the dormancy phenotype.

5.2 MATERIALS AND METHODS

5.2.1 Sorbitol lysis assay

This sorbitol assay was performed to measure culture lysis in response to sorbitol. It is not a sorbitol synchronization assay as was previously described (Section 2.1.3). Late stage parasites were synchronized using a modified Percoll method that differs substantially from the Percoll synchronization previously described (Section 2.1.4). Briefly, 4mL of 70% Percoll with sorbitol was added to a round-bottomed tube, then 4mL 40% Percoll with sorbitol was layered on top, followed by 4mL culture on top. This was centrifuged in an Avani J-E centrifuge at 3913xg for 5 minutes, then adjusted to 15,680xg for 25 minutes. Following the spin, the tube should have distinct layers. Media, hemozoin, and 40% Percoll were aspirated off, leaving only the schizonts, 70% Percoll mixture, and cell pellet. The schizont layer was carefully collected and 10mL wash (8mL media with 2mL 10X PBS) was added and incubated at RT for 5 minutes. The tube was then spun down and supernatant aspirated. The pellet was then re-suspended with 10mL of a second wash (27mL media + 3mL 10X PBS) and incubated at RT for 5 minutes. The tube was then spun down and supernatant aspirated. Then 500µL SDPBS (145mM NaCl, 20mM HEPES, pH 7.4, 0.1mg/mL BSA) was added to pellets and transferred to a microcentrifuge tube. The tube was spun in a microfuge and all supernatant was aspirated. Then 10µL cells were pipetted out and added to 400µL PBS/BSA. To make the blank, 50µL of this cell and PBS/BSA solution were added to 950µL sorbitol lysis buffer

(280mM sorbitol, 20mM Na-HEPES, 0.1mg/mL BSA, pH 7.4) and incubated at 37ºC for 12 minutes. To prepare cuvettes, 50µL cell mixture was added to the bottom of each cuvette. Cuvettes were read on a DU800 UV/vis spectrophotometer at 37ºC every 20 seconds for 60 minutes at 700nm. Cuvettes were manually pipetted to mix every 7 minutes for 60 minutes.

5.2.2 Dormancy induction

Parasites were cultured at 5% Hct in complete media. Experiments were performed in triplicate on independently cultured lines unless otherwise noted. Cultures were split at least two cycles prior to beginning experiments for biological replicates.

Parasites were synchronized to rings with sorbitol as previously described (Section 2.1.3) and parasitemia was adjusted to 2%. The cultures were spun down and pulsed with 700nM DHA in complete media for 6 hours at 37ºC. The culture was then washed twice and the parasites were returned to 37ºC. After 24 hours, the cultures were treated with sorbitol as previously described every 24 hours for three total treatments. Sorbitol lyses mature parasites and, therefore, consecutive treatments with sorbitol should isolate non-progressing or "dormant" ring stage parasites.

Parasitemia was measured by flow cytometry using dual staining with SYBR Green (DNA stain) and MitoTracker Deep Red (mitochondrial stain) as described below. Parasites were considered alive if they stained double positive with both SYBR and MitoTracker. Parasites were considered dormant if they remained in the culture flasks and stained double positive following three days of sorbitol treatment, as all replicating parasites would be lysed by sorbitol treatment daily over the course of three days. Blood (15µL) was added every other day to replace the loss due to the flow cytometry assay and fresh media was added every other day. Parasitemia was measured by flow cytometry and smears were taken daily until the parasitemia rose above 2%. Parasites were then cryopreserved and an aliquot was lysed by saponin to isolate DNA for future sequencing analysis. Growth controls without drug pressure or sorbitol were assessed by adding 30µL of infected RBCs at 2% parasitemia to 10mL complete media with 5% Hct. Media was changed daily and parasitemia was measured by FACS until parasitemia exceeded 2%.

5.2.3 Parasitemia by FACS

Approximately 20µL packed iRBCs were collected in a 96-well plate and washed with 100µL wash buffer (5mL HBSS, 1mL FBS, 44mL milliQ H_2O) then twice washed with 150µL wash buffer. Samples were incubated with 25µL staining solution (SYBR gree0.4x, MitoTracker Deep Red 0.6µM) for 30 minutes at 37ºC in the dark. Samples were again washed twice with 150µL wash buffer. After the final wash, samples were re-suspended with 150µL wash buffer. Samples were run on an Accuri flow cytometer until 200,000 events were obtained. An unstained sample and single stained samples were run each day as controls.

Cells were gated on side scatter vs. forward scatter (Figure 35A) to eliminate debris. Cells were then gated on forward scatter area vs. forward scatter height (Figure 35B) to eliminate duplets. Cells that stained double positive with SYBR and MitoTracker were considered live parasitized cells (Figure 35C).

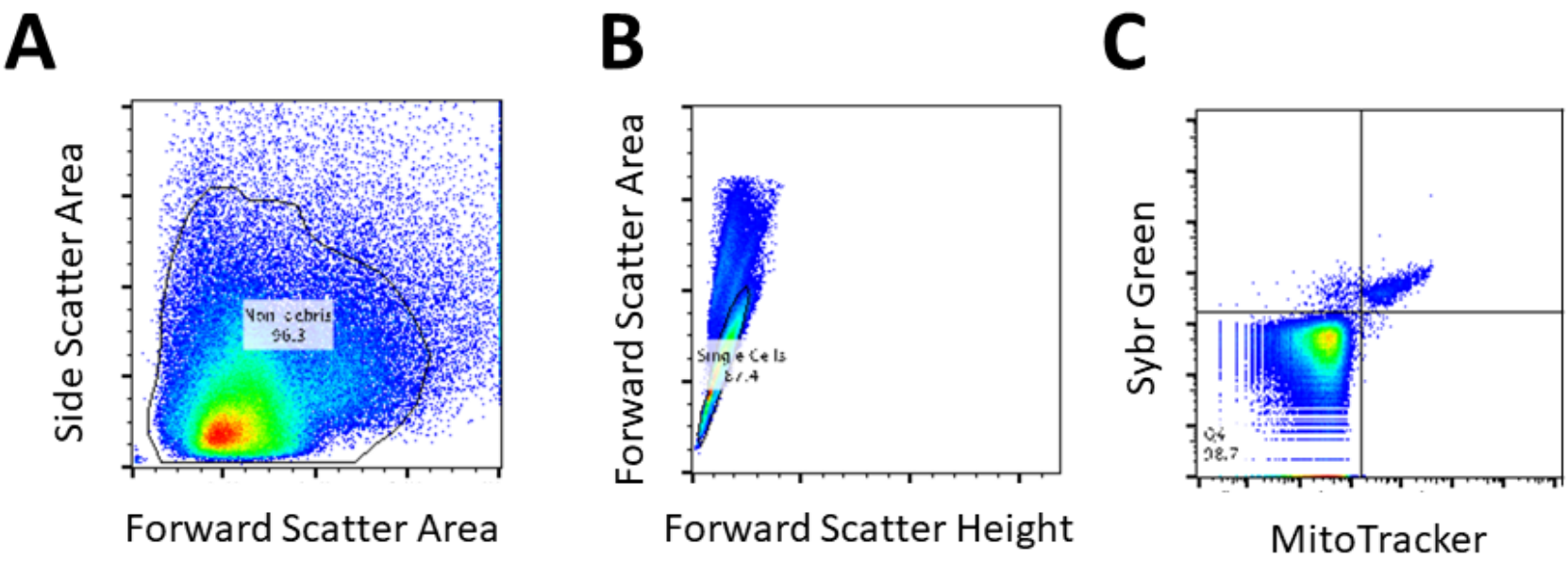


Figure 35: Gating strategy for FACS parasitemia assay

Stained cultures were run on a FACS Accuri until 200,000 events were obtained. Cells were gated on side scatter area to forward scatter area to eliminate debris (lower left corner). Remaining cells were gated to obtain singlets. Cells were then gated based on SYBR Green and Mitotracker Red.

5.3 RESULTS

5.3.1 Dormancy recrudescence assays

5.3.1.1 Sorbitol lysis assay

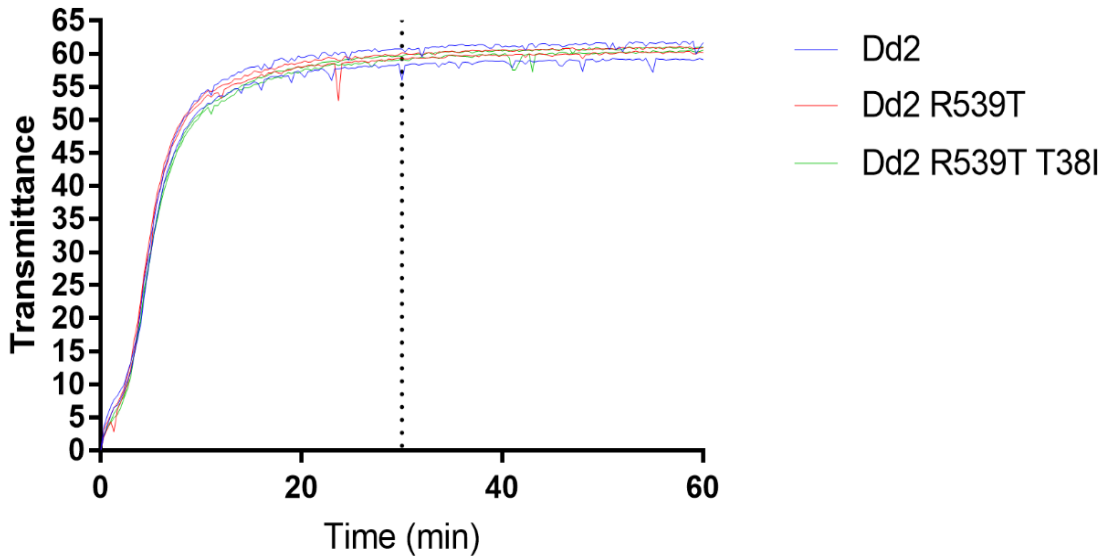


Figure 36: Sorbitol lysis assay for atg18 isogenic lines

Three isogenic Dd2 lines, Dd2 (blue), Dd2^{R539T} (red), and Dd2$^{R539T/T38I}$ (green), were tested in triplicate for susceptibility to sorbitol treatment over 60 minutes.

Mature Dd2 isogenic lines were subjected to sorbitol treatment for 60 minutes and transmittance was measured on a spectrophotometer every 20 seconds for 60 minutes. By 30 minutes, transmittance readings had leveled off for all three lines representing an average of 96.2%, 98.3%, and 97.8% of the maximum readings through 60 minutes for Dd2, Dd2^{R539T}, and Dd2$^{R539T/T38I}$ respectively (Figure 36).

5.3.1.2 Dormancy recrudescence assays on atg18 SNP isogenic lines

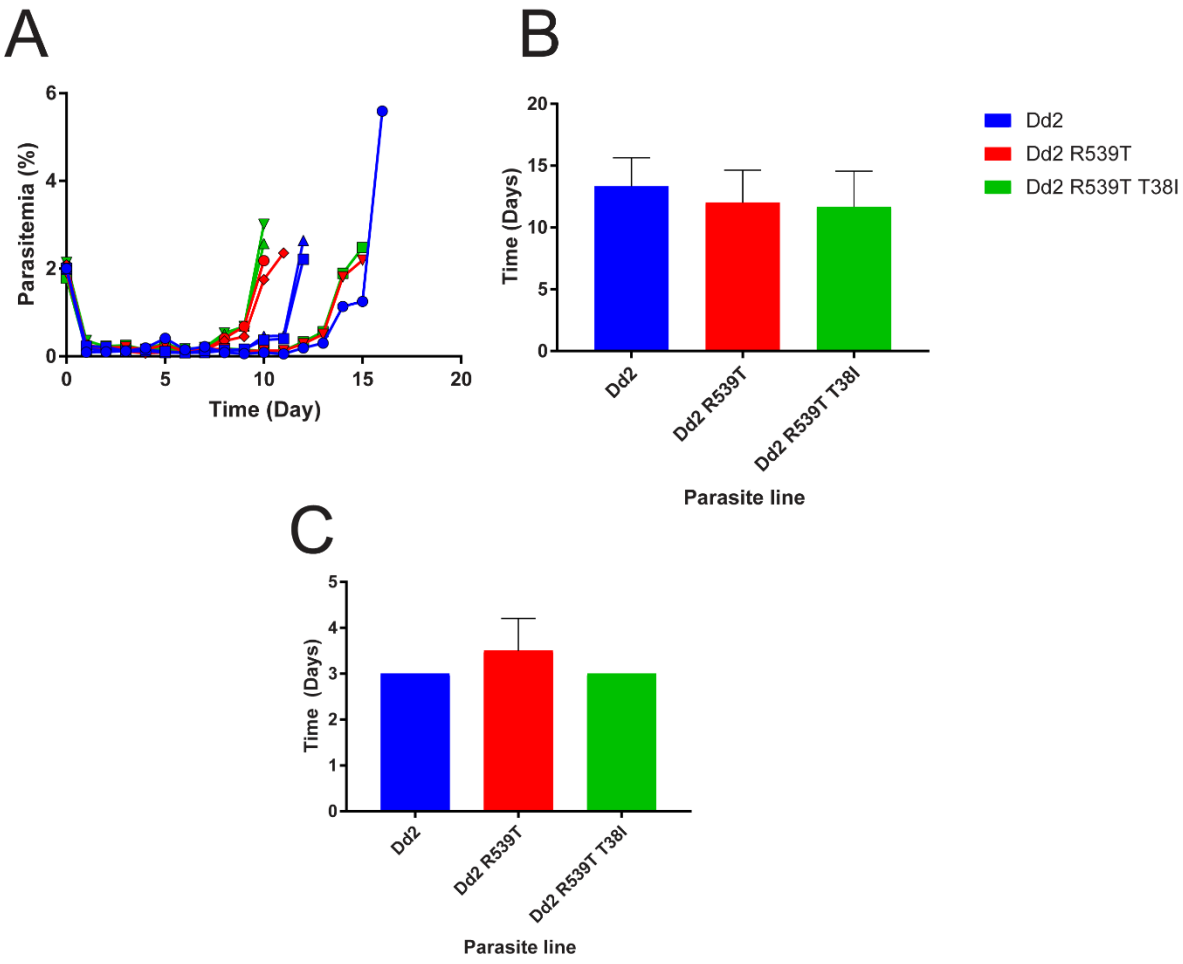


Figure 37: Dormancy and recrudescence in Dd2 atg18 isogenic lines

(A) Recrudescences after treatment of P. falciparum lines starting at 2% parasitemia with a 700nM DHA pulse for 6 hours followed by daily sorbitol treatments for 3 days. Replicates of the Dd2 recrudescences are shown in blue, $Dd2^{R539}$ in red, and $Dd2^{R539T/T38I}$ in green. (B) Time (days) to achieve 2% recrudescent parasitemia following dormancy (average ± standard deviation). (C) Growth control experiments show time to 2% parasitemia in the absence of drug pressure. Data are from experiments performed in triplicate on independently cultured lines.

Dormancy was induced by DHA and sorbitol, then time to recrudescence (2%) was tested in isogenic Dd2 parasites, differing in *K13* (R539T) and *atg18* (T38I) mutations. The time to recrudescence was not different for any of the lines (Figure 37A-B). To determine if this was an extended growth phenotype, time to 2% parasitemia in the absence of drug was also measured, but did not differ (Figure 37C).

5.3.1.3 Dormancy recrudescence assays on K13 isogenic lines

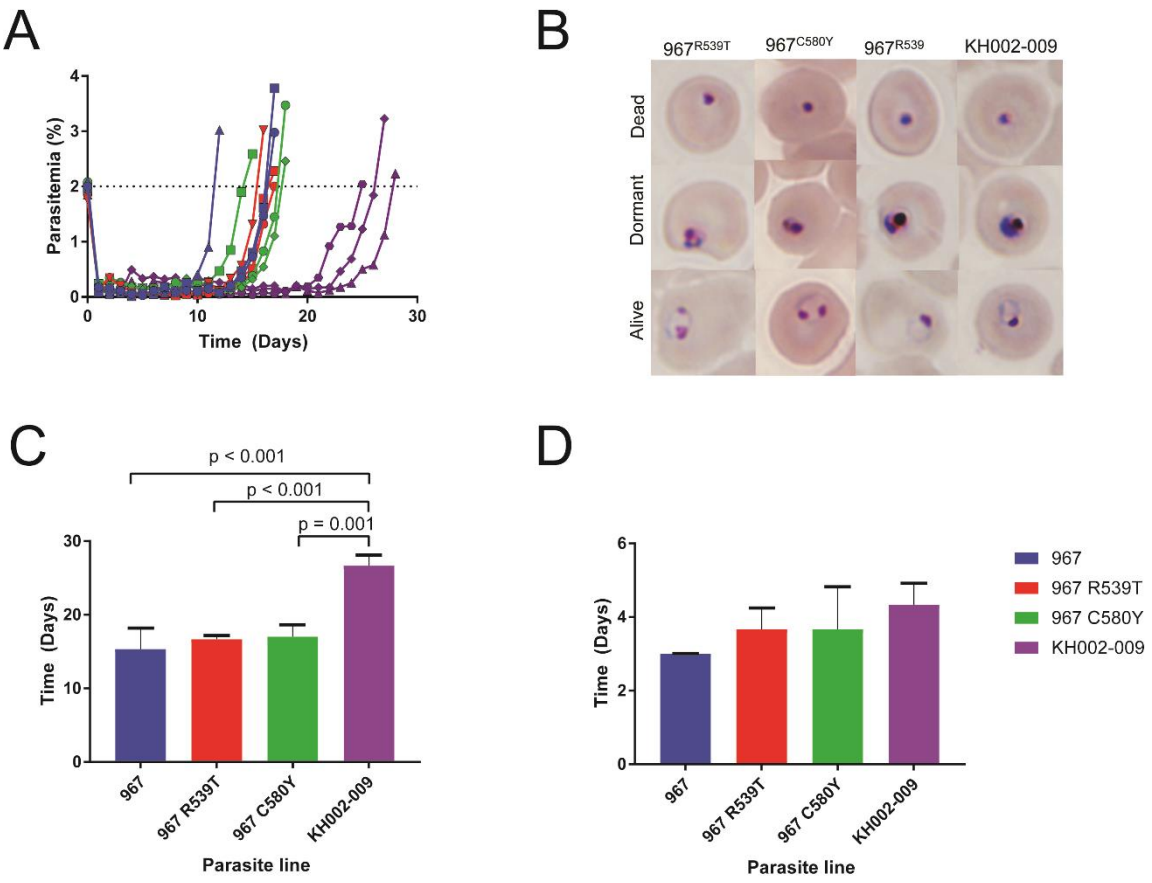


Figure 38: Dormancy and recrudescence in 967 K13 isogenic lines

(A) Recrudescences after treatment of P. falciparum lines starting at 2% parasitemia with a 700nM DHA pulse for 6 hours followed by daily sorbitol treatments for 3 days. Replicates of the 967^{R539T} recrudescences are shown in red, 967^{R539} in blue, 967^{C580Y} in green, and KH002-009 in purple. (B) Top two rows show images of dead and dormant parasites after exposure to a 700 nM DHA pulse for 6 hours followed by daily sorbitol treatments for 3 days; bottom row shows ring-stage parasites observed in recrudescencing populations. (C) Time (days) to achieve 2% recrudescent parasitemia following dormancy (average ± standard deviation). (D) Growth control experiments show time to 2% parasitemia in the absence of drug pressure. Data are from experiments performed in triplicate on independently cultured lines.

As with the Dd2 isogenic lines, two culture adapted Cambodian isolates and two isogenic lines were tested for dormancy recrudescence times. KH002-009 is a Cambodian isolate that is clinically sensitive to artemisinin and is wild-type for *atg18* as well as *arps10*, *mdr*, *crt*, and *fd* (Miotto et al., 2015). The Cambodian isolate 967^{R539T} is the mutant type for *atg18*, *arps10*, *mdr*, *crt*, and *fd* (Miotto et al., 2015). Its isogenic partners, 967^{WTrev} and 967^{C580Y}, differ in *K13* mutations. Dormancy was induced and the measured

recrudescence times were no different for the three isogenic lines differing in *K13* mutations (Figure 38A, C). However, KH002-009, the artemisinin sensitive parasite, recrudesced on day 26.7 as compared to 967^{WTrev} at 15.3 days ($p < 0.001$), 967^{R539T} at 16.7 days ($p < 0.001$), and 967^{C580Y} at 17 days ($p = 0.001$) (Figure 38C). The growth rates were not different between the four lines (Figure 38D). To determine if the parasites in culture after dormancy induction were indeed dormant forms, thin smears were examined on day 4 post-DHA treatment and compared to living parasites from the same culture on the day of 2% parasitemia (Figure 38B). All four lines had mostly pyknotic, dead parasites with scattered thickened ring forms surrounded by a halo, consistent with previously described dormant forms. All cultures looked phenotypically normal during their recrudescent periods.

5.3.1.4 Dormancy recrudescence assays on the GB4/803 genetic cross

To determine if the GB4/803 genetic cross would be a usable tool to elucidate the genetic determinants of a prolonged dormancy period, the parents were tested. GB4, a culture-adapted isolate from Ghana, is artemisinin sensitive. 803, a contemporary Cambodian isolate, is artemisinin resistant. GB4 is wild-type (T38) whereas 803 contains the T38I SNP in *atg18*. GB4 and 803 demonstrated different recrudescence times following DHA-sorbitol induced dormancy (Figure 39A-B) ($p = 0.002$). There was no difference in growth rates between the two lines (Figure 39C).

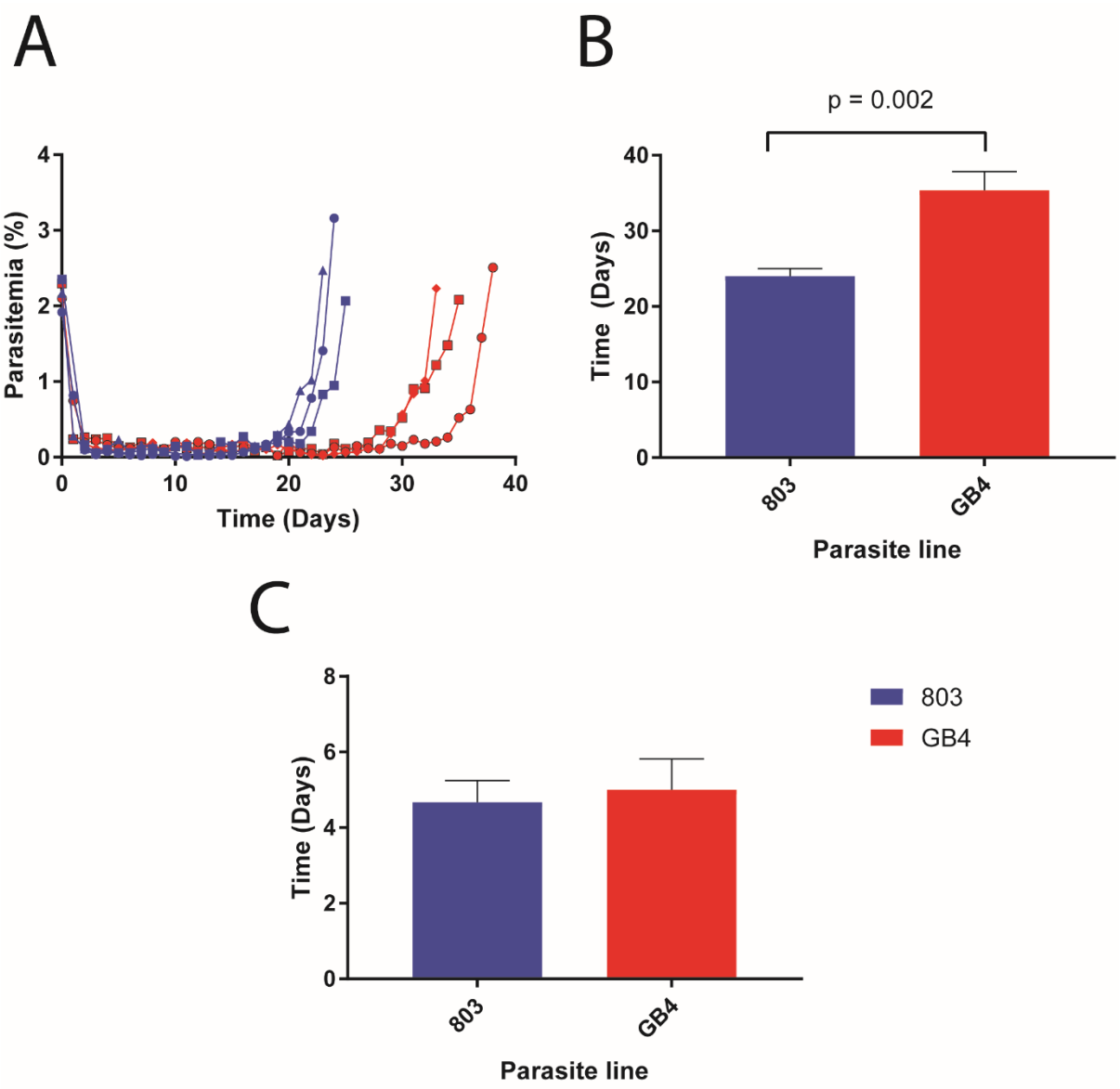


Figure 39: Dormancy and recrudescence in parents of the GB4x803 genetic cross (A) Recrudescences after treatment of P. falciparum lines starting at 2% parasitemia with a 700nM DHA pulse for 6 hours followed by daily sorbitol treatments for 3 days. Replicates of the 803 recrudescences are shown in blue and GB4 in red. (B) Time (days) to achieve 2% recrudescent parasitemia following dormancy (average ± standard deviation). (C) Growth control experiments show time to 2% parasitemia in the absence of drug pressure. Data are from experiments performed in triplicate on independently cultured lines.

A specific isogenic set of interest is progeny 76H10, which inherited a C580Y *K13* mutation from 803, and its *K13* wild-type reverted partner, 76H10^{WTrev}. These isogenic lines were produced by the Fidock lab (manuscript in preparation). These isogenic lines did not demonstrate a difference in recrudescence times following DHA-sorbitol induced dormancy (Figure 40A-B) nor did they differ in their growth rates (Figure 40C).

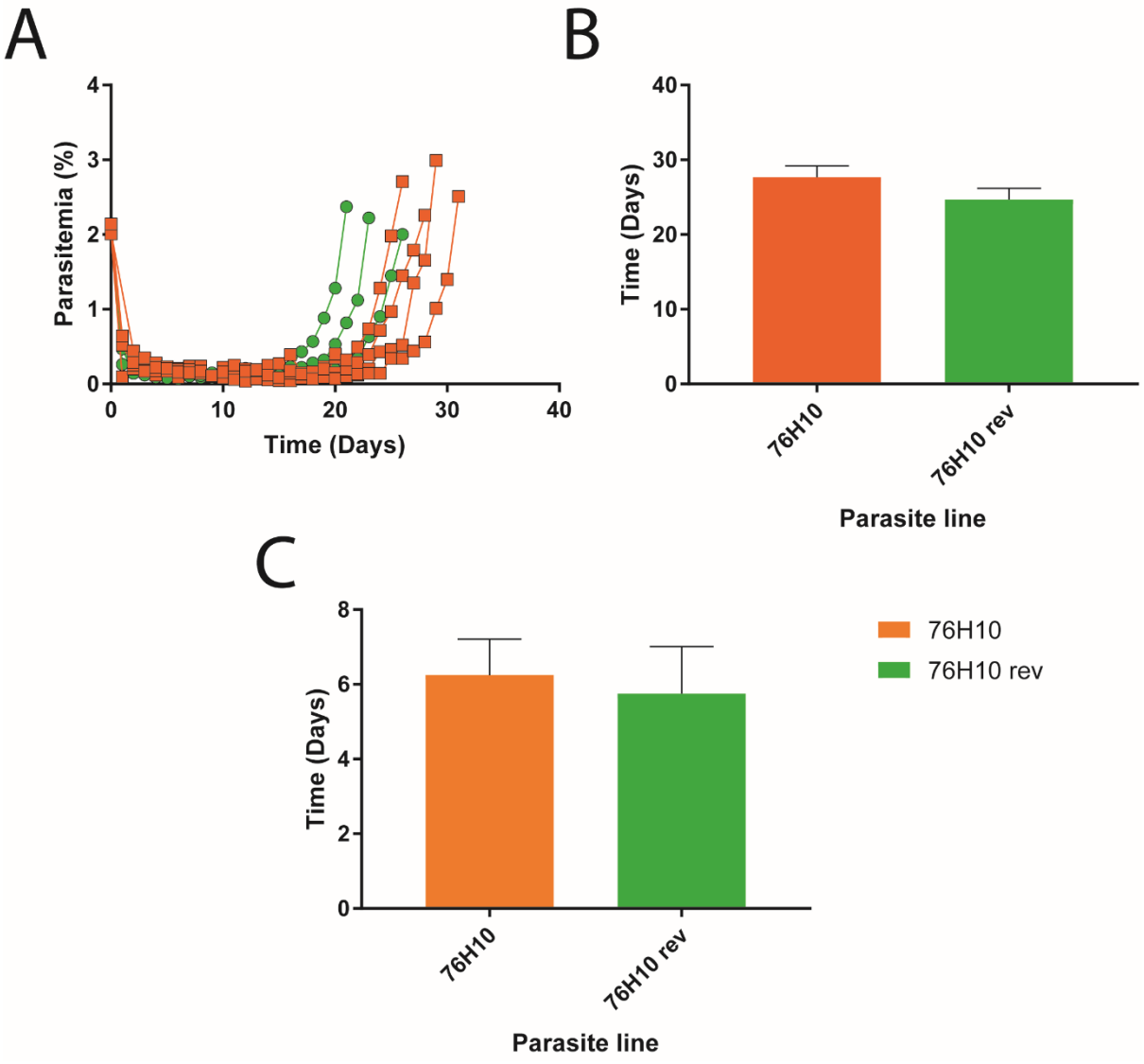


Figure 40: Dormancy and recrudescence in isogenic progeny 76H10 of the GB4x803 genetic cross
(A) Recrudescences after treatment of P. falciparum lines starting at 2% parasitemia with a 700nM DHA pulse for 6 hours followed by daily sorbitol treatments for 3 days. Replicates of the 76H10 recrudescences are shown in orange and 76H10^{WTrev} in green. (B) Time (days) to achieve 2% recrudescent parasitemia following dormancy (average ± standard deviation). (C) Growth control experiments show time to 2% parasitemia in the absence of drug pressure. Data are from experiments performed in triplicate on independently cultured lines.

Next, another twelve progeny of the cross were examined for their recrudescences following DHA-induced dormancy. The phenotype was more gradual than expected, although 803 clearly recrudesced at the same time as 39C3, 38G5, and 76H10^{Rev}. 76H10

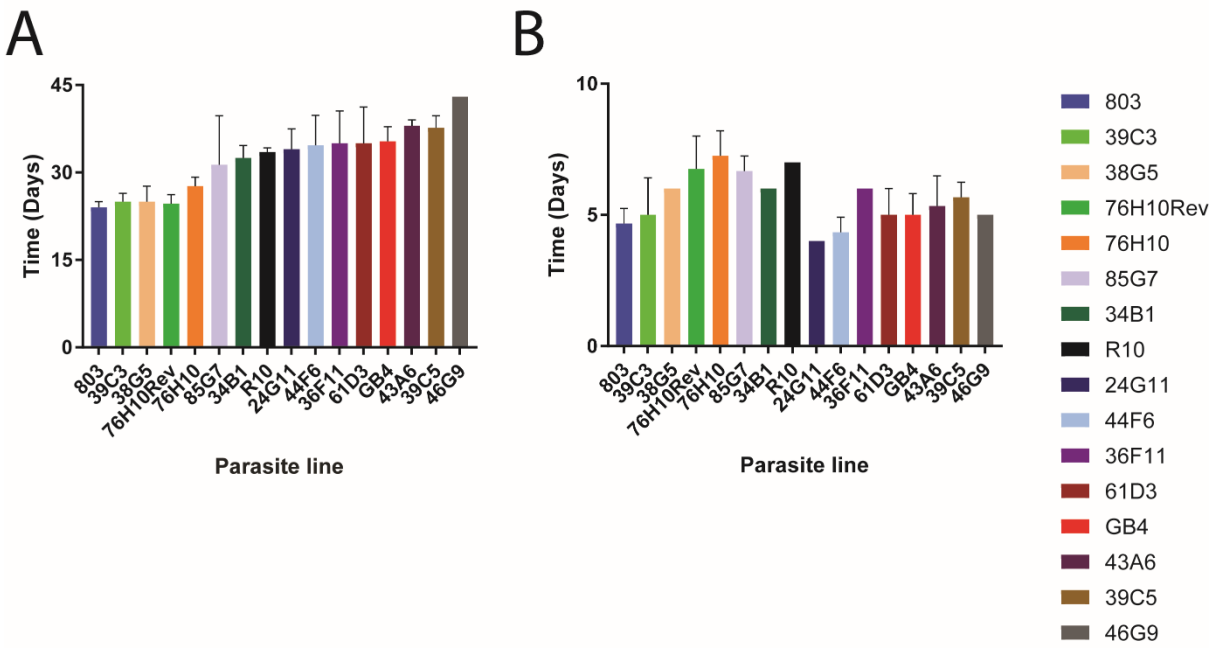


Figure 41: Dormancy and recrudescence in the GB4x803 genetic cross
(A) Time (days) to achieve 2% recrudescent parasitemia following treatment of P. falciparum lines starting at 2% parasitemia with a 700nM DHA pulse for 6 hours followed by daily sorbitol treatments for 3 days (average ± standard deviation). Note parents of the cross, 803 in blue and GB4 in red. Experiments performed in triplicate on independently cultured lines with the exception of (A) R10 (n = 2), 34B1 (n = 2), 39C3 (n = 2), 46G9 (n = 1) (B) Growth control experiments show time to 2% parasitemia in the absence of drug pressure. Data from experiments performed in triplicate on independently cultured lines with the exception of R10 (n = 2), 39C3 (n = 2), and 46G9 (n = 1).

(C580Y) recrudesced slightly later, which was unexpected since it contains a *K13* mutation, given that artemisinin-resistant parasites have been shown to recrudesce prior to artemisinin-sensitive parasites. Several of the lines recrudesced at the same time or after GB4: 44F6, 36F11, 61D3, 43A6, 39C5, and 46G9 (Figure 41).

Although the growth rates without drug exposure varied among the lines, there was no clear pattern to account for the early recrudescences. Further, there was no clear pattern in regards to length of dormancy and either *k13* polymorphism or *atg18* polymorphism (Table 24). While a formal QTL analysis has not yet been performed, these results confirm the previous findings that neither *k13* nor *atg18* polymorphisms are responsible for the duration of dormancy phenotype.

Table 24: Summary of kelch and atg18 polymorphisms in dormancy assays

Line	*K13* polymorphism	*atg18* polymorphism	Time to recrudescence (mean)
803	C580Y	T38I	24
39C3	C580	T38	25
38G5	C580Y	T38	25
76H10^{Rev}	C580	T38I	24.7
76H10	C580Y	T38I	27.7
85G7	C580Y	T38I	31.3
34B1	C580	T38	32.5
R10	C580	T38I	33.5
24G11	C580	T38	34
44F6	C580Y	T38	34.7
36F11	C580	T38I	35
61D3	C580	T38	35
GB4	C580	T38	35.3
43A6	C580	T38I	38
39C5	C580Y	T38	37.7
46G9	C580	T38	43

5.5 DISCUSSION

There are a variety of assays that have been used in the literature to assess parasite dormancy. The original dormancy assay was performed by Nakazawa and colleagues by incubating a ring-stage culture in sorbitol for 30 minutes every 12 hours, 8 times (Nakazawa et al., 1995). The results determined that approximately 0.001% of the culture recrudesced following this treatment, which was roughly the same level as following pyrimethamine only treatment. From these results, it is unclear whether there is a basal level of dormant parasites or if these dormant parasites are induced. Indeed, even after subsequent studies, the question of sorbitol's ability to induce dormancy remains.

Teuscher and colleagues developed the dormancy induction assay as it is commonly used *in vitro*. They used sorbitol-synchronized ring-stage parasites and exposed them to 200ng/mL DHA for 6 hours. Following the drug treatment, they selected for dormant parasites by removing late-stage parasites with a magnetic column daily for three days. The group then monitored the culture for recrudesce by microscopy. This assay has been used consistently to model dormancy *in vitro* (Teuscher et al., 2012, Chen et al., 2014b, Peatey et al., 2015, Gray et al., 2016).

Witkowski and colleagues coined terms for two similar assays to test for parasite dormancy. The first is the "recovery assay," which pulses a culture with 700nM DHA for six hours and then monitors it for recovery by microscopy without selection (Witkowski et al., 2013c). Variations on this assay have been used widely (Tucker et al., 2012, Klonis et al., 2011, Chavchich et al., 2016, Dembele et al., 2017, Duvalsaint and Kyle, 2018). It is important to note that this assay does not have a selection component and, therefore, live, replicating rings confound the dormancy findings. Even so, this assay can be important, especially when assessing artemisinin resistance, if one does not necessarily wish to differentiate the reason for growth (live rings vs. dormant rings).

The second assay by Witkowski and colleagues is the "ring-stage growth arrest assay," which treats a ring-stage culture with 700nM of DHA for 24 hours, then treats the culture with a single pulse of sorbitol. Recrudescence is monitored for by microscopy (Witkowski et al., 2013c). This assay is noteworthy for its long duration of DHA (or other artemisinin derivative) exposure. Several other studies have used a variation of this assay (Witkowski et al., 2010, Cui et al., 2012, Ménard et al., 2015, Hott et al., 2015b).

In addition to artemisinin derivatives, as performed in this project, a number of other compounds have also been tested for their abilities to induce dormancy. The initial studies by Nakazawa and colleagues used sorbitol only, as discussed, and pyrimethamine only (Nakazawa et al., 1995). Later studies showed dormancy induction by mefloquine (Nakazawa et al., 2002), atovaquone (Thapar et al., 2005, Ménard et al., 2015), amodiaquine, chloroquine, and quinine (Ménard et al., 2015). The dormancy phenotype has also been observed following nutrient starvation (Babbitt et al., 2012, McLean and Jacobs-Lorena, 2017). On the other hand, lumefantrine and KAE609, a novel spiroindolone, demonstrated a decreased parasitemia followed by recrudescence; however, no dormant forms were observed by microscopy prior to the recrudescence (Chavchich et al., 2016). Therefore, although the induction of dormancy is often only associated with artemisinin, studies have shown that this phenotype can be induced with myriad other, but not all, compounds.

Artemisinin derivatives are short-acting compounds. Despite this, dormancy studies range in the amount of time that the parasites are incubated with the drug. The concentration of DHA chosen for almost all assays was 200ng/mL or approximately 700nM, which is a physiologic concentration of DHA. This dose and duration of DHA treatment are thought to approximate clinical concentrations of DHA in the blood and are used in other artemisinin assays including the RSA (Witkowski et al., 2013a).

Following drug treatment, studies vary on how they select for dormant parasites. A number of studies assume that all parasites will either be killed or become dormant, thus perform no additional selection. However, some parasites are likely to continue through their lifecycles even following treatment with drug. In the absence of selection, these living parasites will be counted among the dormant parasites and will obfuscate calculations of the duration of dormancy. However, if parasites exit dormancy quickly, prior to selection, then the selection treatment will reduce the number of dormant parasites prematurely.

Two selection treatments have been used to remove developing parasites while retaining dormant parasites. The first is removal of late-stage parasites by magnetic column (Paul et al., 1981). Later stages, but not ring stages, take up hemoglobin and accumulate polymerized heme as hemozoin (Moore et al., 2006). When the culture passes through a magnetic column, hemozoin binds to the magnet, thus the magnet retains later stage

parasites and allows ring-stage parasites to pass through. Although the magnet is very effective at only allowing schizonts, and to some extent trophozoites, to adhere within its apparatus, it is not very efficient at removing these later stage parasites from culture (Ahn et al., 2008).

The second technique that has been used to select for dormant rings is sorbitol lysis. Sorbitol is a sugar alcohol that allows for culture synchronization through lysis of mature forms (Lambros and Vanderberg, 1979). It works by entering red blood cells via Plasmodial Surface Anion Channel (PSAC), which is expressed by parasites after the ring-stage, on the surface of red blood cells (Desai et al., 2000). Although highly effective, sorbitol treatment is stressful, which may not be ideal for a culture (Krugliak and Ginsburg, 2006). Further, sorbitol has possibly been implicated in dormancy induction on its own, so parsing out the contribution from the drug is more difficult in the presence of sorbitol selection. The goal of the selection process is to remove the maximal amount of late-stage parasites from the culture. Therefore, sorbitol selection is preferred over magnetic separation. There are a number of other synchronization techniques, including plasmagel, colchicine, Percoll, aphidicolin, and plasmoin (Hui et al., 1983, Inselburg and Banyal, 1984, Lelievre et al., 2005, Lambros and Vanderberg, 1979), but none of these have been used as selectors in a dormancy assay.

The time to recrudescence has been monitored in two ways: microscopy and FACS. By microscopy, the dormant forms appear rounded with some blue cytoplasm and reddish chromatin (Tucker et al., 2012, Chen et al., 2014b, Teuscher et al., 2012), which allows for subtle differentiation from other forms by Giemsa staining and microscopic evaluation. There have also been reports of rings appearing morphologically normal during artemisinin exposure (Witkowski et al., 2010). The morphology of dormant parasites in this study appeared as a red nucleus surrounded by a halo of blue cytoplasm, in accordance with the majority of the literature.

To remove the subjectivity of microscopy, a better method of detecting dormant forms is through the use of mitochondrial specific dyes, such as rhodamine 123 or MitoTracker (Witkowski et al., 2010). Parasites that stain positive for these dyes have functioning mitochondria, a quality of dormant parasites, as they appear to use mitochondria for metabolism during dormancy (Peatey et al., 2015). These mitochondrial dyes can be used to follow parasites by FACS or to identify specific dormant parasites by confocal

microscopy (Peatey et al., 2015, Dembele et al., 2017). The other benefit of FACS over microscopy is the ability to examine more cells quickly. In this project, 200,000 events were recorded for each culture each day. It would be wastefully time-consuming to examine this many cells by microscopy and, therefore, FACS provides a less biased estimate of parasitemia by sampling a larger number of cells.

Conflicting evidence exists regarding whether dormancy is a dose-dependent phenomenon. One study found that repeated DHA dosing delayed recrudescence as compared to a single DHA dose (Teuscher et al., 2010). However, another study demonstrated that there was no clear linear relationship between time of recrudescence and drug concentration in a study using pyrimethamine or mefloquine (Nakazawa et al., 2002). This suggests that perhaps there is a threshold drug concentration to induce dormancy, above which there is no effect on time of recrudescence. Recrudescence time remained fixed even after six successive drug treatments following recrudescence (Nakazawa et al., 2002). Other studies have noted reproducibility in day of recovery from dormancy as well (Teuscher et al., 2010, Tucker et al., 2012, Chavchich et al., 2016, Teuscher et al., 2012, Cui et al., 2012), signaling that recrudescence from dormancy is an inherent property encoded by the parasitic genome.

Multiple studies have shown that the addition of a second drug following dormancy induction can modulate the dormancy phenotype. The addition of mefloquine following DHA dormancy induction delayed culture recovery (Teuscher et al., 2010). Adding either KAE609 or lumefantrine prevented recrudescence following DHA-induced dormancy (Chavchich et al., 2016), although a later study showed relative resistance of dormant rings to lumefantrine treatment (Dembele et al., 2017). The PI4K inhibitor KDU691 was 20-fold more effective against DHA-induced dormant rings than against a not dormant culture (Dembele et al., 2017). Similarly, atovaquone killed more DHA-induced dormant rings than not dormant rings at the same concentration (Dembele et al., 2017). Cyclin dependent kinases WR636638, olomoucine, and roscovitine all delayed recrudescence following DHA treatment as compared to DHA treatment alone (Gray et al., 2016). One hypothesis is that dormancy is evolutionarily protective, allowing parasites to evade drug by becoming dormant. However, the ability of some drugs to change the duration to recrudescence indicates that dormant parasites continue to be susceptible to killing by some drugs. It is possible that these parasites are somewhat less susceptible than live, replicating parasites, although that is yet to be proven.

Interestingly, the timing of the second drug appears to impact its ability to delay recrudescence. When given on the same day as DHA treatment, olomoucine did not change the day of recrudescence as compared to DHA only treatment (Gray et al., 2016). However, when given on day 2, the culture did not recrudesce (followed until day 21). Unexpectedly, when given on either day 4 or 6, the recrudescence was delayed as compared to DHA only. This suggests that different processes are likely involved in the early dormancy phase as parasites are entering dormancy versus later dormancy or recovery.

While dormant cultures may be susceptible to certain drugs, other drugs can cause the dormancy phenotype to be cut short. Plant phytohormones abscisic acid and gibberellic acid, which signal plants to come out of dormancy, cause DHA-induced dormant cultures to recrudesce sooner than those treated with DHA alone (Duvalsaint and Kyle, 2018). As further evidence for a role of phytohormones in dormancy, the herbicide fluridone, which acts to inhibit abscisic acid synthesis, delayed dormancy recrudescence (Duvalsaint and Kyle, 2018). The ability of a compound to prevent dormancy would be a helpful characteristic in a combination therapy, to keep parasites replicating and therefore susceptible to drug treatment.

Although there have not been reports of direct evidence for dormant parasites in humans, modeling clinical data has suggested that dormancy exists in patients. Two models of dormancy have been put forth. The original model by Hoshen and colleagues was based on the assumption that artemisinins work in a stage-specific manner (Geary et al., 1989) and demonstrated that clinical data implicated a dormancy phenotype in response to artemisinin treatment (Hoshen et al., 2000). When the model added 0.2% of parasites becoming dormant, its ability to model the clinical data improved greatly and accounted for the high incidence of treatment failures following artemisinin usage (Hoshen et al., 2000). The next model by Codd and colleagues used quantifications of dormancy performed *in vitro* (Teuscher et al., 2010) to estimate the rates of dormancy in parasites of patients treated with either single-day or three-day artemisinin monotherapy (Codd et al., 2011). Assuming that dormancy rates were higher for single-day than three-day treatment helped account for more recrudesces in clinical data following in single-day treatment.

Several pathways have been associated with dormancy. Parasites with a mutation in *Maf1*, a regulator of RNA polymerase III, do not recrudesce following dormancy induction by amino acid starvation (McLean and Jacobs-Lorena, 2017). Cyclin-dependent kinases (cdks) are differentially expressed following DHA-induced dormancy and cdk inhibitors have been shown to delay or prevent recrudescences *in vitro* (Gray et al., 2016). The ability of PI4K inhibitors to prevent recrudescences in DHA-induced dormant cultures indicates that membrane trafficking may be important in dormancy. Similarly, the ability of phytohormones to induce recrudescences suggest that plasmodial phytohormones (if present) may control the dormancy state at least in part.

The energy source of dormant parasites is still largely unknown. Transcriptomics evidence has indicated that fatty acid synthesis and mitochondrial functioning continue during dormancy, despite their downregulation (Chen et al., 2014b). Glycolytic and protein synthesis-related genes are downregulated during dormancy (Shaw et al., 2015, Babbitt et al., 2012). The apicoplast has also been implicated in dormancy, as cultures lacking an apicoplast cannot recrudesce from dormancy without the presence of IPP (Duvalsaint and Kyle, 2018). Understanding the mechanism of dormancy is important so that specific compounds to prevent or induce recovery can be developed. A dormancy modulating compound could prove an invaluable tool in eliminating any dormant reservoir that may remain in a patient following artemisinin treatment.

In designing the optimal dormancy assay for this project, it was important to determine if sorbitol was the proper method of selection. Sorbitol, which uses PSAC to enter red blood cells, lyses mature stages as previously described. PSAC has been implicated in nutrient uptake, as demonstrated by the inhibition of uptake of alanine and proline after PSAC was blocked with an inhibitor compound, isolate-specific PSAC antagonist (ISPA-28) (Nguitragool et al., 2011). Many solutes enter the infected red blood cell from the sera via PSAC and then enter the parasite via the parasitophorous vacuolar membrane (Desai et al., 1993, Desai and Rosenberg, 1997). PSAC can be differentially expressed on different parasite lines and measuring its permeability was important for this project for two reasons: (1) to determine the ideal conditions to sorbitol lysis for the dormancy assay and (2) to determine if these isogenic lines might different in their ability to take up nutrients via PSAC.

The sorbitol lysis assay was performed to determine the amount of time to incubate cultures with sorbitol in order to lyse mature forms (Wagner et al., 2003), thus keeping the culture with ring forms only for the dormancy selection process. Because sorbitol is a relatively harsh treatment that can cause stress in a culture and therefore trigger the production of gametocytes, the time for sorbitol lysis was chosen based on the shortest time that would still cause the vast majority of the culture to lyse. Gametocytes are not lysed by sorbitol (Saul et al., 1990). Given the diminishing returns of incubating the culture in sorbitol for longer than 30 minutes based on the results of the sorbitol lysis assay, it was determined that 30 minutes was sufficient time for the sorbitol selection of dormant parasites. Sorbitol lysis times did not differ between the three tested lines and therefore the sorbitol incubation time was used for all dormancy experiments.

The results of the sorbitol lysis assay indicated that transgenic Dd2$^{R539T/T38I}$ parasites were not different from its isogenic lines Dd2^{R539T} and Dd2. In the previous chapter, Dd2$^{R539T/T38I}$ outgrew its isogenic partners in various nutrient-limited media. This ability to flourish in nutrient-depleted settings could be due to the parasite's ability to change its uptake of solutes from the media or its ability to use the solutes more efficiently within the cell. The finding that the sorbitol lysis assay was the same between the three lines also provided evidence that the permeability of the PSAC channel did not differ. This finding indicates that the T38I mutation is not involved in PSAC permeability, hinting that it is uninvolved in nutrient acquisition via this pathway. While PSAC allows for uptake of a variety of nutrients actively, glucose is taken up by an alternative equilibrative pathway (Kirk et al., 1996). Therefore, the finding that PSAC is not different would not implicate glucose uptake. However, in the growth experiments in the previous chapter, when glucose was not a limiting reagent, Dd2$^{R59T/T38I}$ continued to grow faster than the other two isogenic lines. This indicates that glucose is not involved in the Dd2$^{R539T/T38I}$ parasite's ability to outgrow its isogenic lines.

Although PSAC activity is not different between the Dd2$^{R539T/T38I}$ isogenic lines, that does not preclude uptake of different nutrients via a different pathway. However, this finding does suggest that the T38I SNP is involved in changing metabolic pathways within the cell rather than nutrient uptake, consistent with a change in the autophagy-like pathway. To make this assertion, further studies on nutrient uptake would be warranted.

Given the need for autophagy during dormancy in other cell types, including cancer and immune cells, it was hypothesized that the *atg18* T38I SNP may be involved in the dormancy phenotype of *P. falciparum* parasites. A number of previous studies have demonstrated that artemisinin-resistant lines recrudesce earlier than artemisinin-sensitive lines (Witkowski et al., 2010, Tucker et al., 2012, Cui et al., 2012, Witkowski et al., 2013c, Ménard et al., 2015). Since a parasite line will consistently recrudesce at a similar time following DHA treatment, it is believed that the dormancy phenotype is genetically modulated (Tucker et al., 2012). Therefore, a number of genetic polymorphisms associated with resistance are candidates for controlling dormancy and recrudescence. Although it was a promising candidate, the results of the dormancy assay indicate it is unlikely that the T38I SNP in *atg18* modulates parasite dormancy. The assay was performed on the Dd2 transgenic lines demonstrate no difference between the recrudescence times or growth rates of the parasites. Therefore, other genetic modulators of dormancy were pursued.

The next likely genetic determinant of dormancy was *k13*. The plasmodial kelch protein shares homology with the human protein Keap1. Keap1 can facilitate cell cycle arrest by postponing S phase, thus keeping the cell in a suspended state akin to dormancy (Hu et al., 2014). An additional function of Keap1 is to ubiquitinate the transcription factor NRF2, thus targeting it for degradation and repressing the antioxidant functions of NRF2 (Ma, 2013). Because artemisinin damages by ROS, it causes oxidative stress for parasites and would need to induce transcription factors such as NRF2 to combat that stress. It is hypothesized that polymorphisms in *k13* could modulate the stress response and force more parasites to go dormant to survive the drug insult, then ultimately recrudesce and replicate (Winzeler and Manary, 2014). Furthermore, artemisinin-resistant parasites display an altered cell cycle with a prolonged ring-stage, which could be due to the decreased susceptibility of ring-stage parasites to artemisinins as compared to later stage parasites (Mok et al., 2011). This cell cycle modulation has been associated with *k13* mutations, but have not been proven by using isogenic lines.

In order to test the contribution of *k13* polymorphisms to the dormancy phenotype, isogenic lines with and without *k13* polymorphisms, 967^{R539T} and 967^{C580Y}, were tested for their dormancy durations against wild-type *k13* parasites 967^{WTrev} and KH002-009. Unexpectedly, all 967 isogenic lines recrudesced at approximately the same time following DHA-induced dormancy regardless of their *k13* polymorphism. Consistent

with previous data that demonstrated earlier recrudescence in artemisinin-resistant lines as compared to artemisinin-sensitive lines, the KH002-009 line (artemisinin-sensitive) recrudesced far later than the 967 isogenic lines. These experiments demonstrated that *k13* polymorphisms do not modulate the dormancy phenotype as previously supposed, although they do confirm that artemisinin-resistant isolates consistently recrudesce before artemisinin-sensitive isolates. These results have recently been published in (Breglio et al., 2018).

The genetic determinant of the shorter dormancy duration is likely in one of the polymorphisms that differ between the 967 isogenic lines and KH002-009. There are a number of differences between these two lines, as the KH002-009 was chosen because it is wild-type for the top four background mutations (*arps10*, *fd*, *mdr2*, and *crt*) that are being selected for in Southeast Asia (Miotto et al., 2015). Additionally, KH002-009 is wild-type for *atg18* and, although the Dd2 isogenic lines provided evidence that *atg18* is not the genetic determinant of the dormancy phenotype.

Because there are a number of differences between KH002-009 and the 967 isogenic lines, there are a number of candidate genes that may contribute to or modulate the dormancy phenotype. In order to narrow down the genetic determinant(s), the GB4x803 cross was examined. Crosses are an extremely helpful tool in determining the region of the genome that contains a polymorphism associated with a given phenotype, as they can assess many polymorphisms concurrently. In order to use the cross effectively, the parents must have differential phenotypes. In order to confirm the negative findings regarding the *atg18* T38I SNP, it was important that one of the parents contains the SNP and that the other is wild-type at that locus: indeed, 803 contains a T38I SNP, whereas GB4 is wild-type. Following DHA-induced dormancy, GB4 had a long duration of dormancy whereas 803 had a short duration. This differential phenotype is necessary so that the cross can be used to determine the genetic contribution to dormancy.

In order to confirm the earlier results that *k13* does not modulate DHA-induced dormancy, the 76H10 isogenic lines were also tested in the dormancy assay. 76H10 is one of the progeny of the cross, which has a C580Y mutation in *k13*. The 76H10 revertant parasite is an edited isogenic line that is C580 (wild-type) in *k13*. In accordance with earlier results, the presence of the *k13* mutation did not change the duration to dormancy. This confirms the finding that *k13* polymorphisms do not modulate the dormancy phenotype.

In order to begin isolating the genetic determinants of dormancy, fourteen of the progeny of the GB4x803 cross were tested for their durations of dormancy. Although ideally there would be two clear groups, one segregating with the quickly-recrudescing 803 and the other with slowly-recrudescing GB4, the progeny have a more gradual change in their phenotypes. Three progeny obviously recrudesced with 803, while six progeny recrudesced with or after GB4. The progeny in the middle present a problem as they do not necessarily share the dormancy phenotype with one parent or the other. This gradation of phenotype suggests that the dormancy phenotype may be multifocal and may be modulated by multiple loci. More progeny are currently being tested to determine if they will segregate with one parent or the other. Eventually a QTL analysis will be performed to determine if any of the loci appear to modulate the early recovery from dormancy phenotype.

Elucidating the genetic contributions of dormancy has a number of implications. Dormancy appears to be important in artemisinin-resistance and artemisinin monotherapy recrudescences. Therefore, understanding the genetic determinants could shed light into ways to manipulate dormant parasites to improve treatment. Dormant parasites could be targeted for death by blocking metabolic pathways important in dormant parasites. Conversely, dormant parasites could be forced to reawaken and then killed with an existing antimalarial.

Understanding dormancy in *P. falciparum* could further the knowledge of hypnozoites in *P. vivax* and vice versa. Hypnozoites, or the dormant liver stage in *P. vivax* infections, represent a human reservoir of malaria that will make eradication difficult if not impossible. Although primaquine and several other antimalarials effectively treat hypnozoites, they often come with serious side effects including hemolytic anemia in patients with G6PD deficiency. These potentially deadly side effects make mass drug administration with primaquine risky in areas such as Cambodia that have a high rate of G6PD. This, combined with the relatively low burden of malaria, perpetuates the continued presence of *P. vivax* in such areas. An added bonus in understanding *P. falciparum* dormancy may be the ability to apply novel treatments to *P. vivax* and eliminate dormant parasites of both species.

6 SUMMARY OF FINDINGS

This thesis work investigated a possible role of an autophagy-like pathway in the mechanism of artemisinin resistance in *Plasmodium falciparum*. Autophagy is an intracellular, pro-survival, recycling pathway that cells use to degrade waste and damaged cytoplasmic material. It is highly conserved among eukaryotes, but poorly characterized in *P. falciparum.*

This work began with a sub-analysis of the TRAC WGS database to query for polymorphisms in putative autophagy-related genes that associated with different metrics of drug resistance. Several polymorphisms associated with artemisinin resistance phenotypes and partner drug resistance phenotypes; however, a non-synonymous SNP in *autophagy-related gene 18* (*atg18*) was the only SNP that rose to the level of significance. This T38I *atg18* polymorphism became the central subject of this thesis work.

An investigation into *atg18* revealed its sequence homology to yeast Atg18 and the human WIPI proteins. The protein encoded by *atg18*, PfAtg18, was tagged with GFP and found to form puncta on EM and confocal microscopy upon DHA treatment, as would be expected with homologous Atg18 proteins. PfAtg18 was found to bind PI3P and PI5P, again as would be expected with homologous Atg18 proteins.

The T38I *atg18* SNP was CRISPR edited into a laboratory line with an existing *k13* R539T mutation, a polymorphism that is associated with artemisinin resistance in clinical and *in vitro* studies. Two drug screens were performed with over 6000 unique compounds, including a number of antimalarial drugs, at a variety of concentrations. As compared to the parent line, the T38I SNP line did not have differential susceptibility to any artemisinin derivative or any of the partner drugs commonly used in the Greater Mekong Subregion. While the T38I SNP line showed differential susceptibility (either increased or decreased) to a number of compounds, no clear pattern can be ascertained as to the mechanism of action of these drugs. Further investigation is required.

While the results of the drug screen could not confirm the reason for the selection of this SNP in the parasite population, it was found that this SNP confers a fitness advantage. The T38I SNP parasite line grows similarly to its parent line(s) under nutrient-rich conditions; however, it outgrows these other lines in nutrient-deprived conditions. The

ability to outgrow competing parasites under nutrient-limited and stressful conditions may represent the reason for selection of the T38I polymorphism in *atg18*.

The dormancy phenotype was investigated due to the relationship between dormancy and autophagy in many other organisms and cell types. The *atg18* SNP was not found to modulate the dormancy phenotype, neither in the isogenic lines created nor in the progeny of the 803xGB4 genetic cross that were tested. Further, neither the *k13* R539T nor C580Y mutations were found to modify the dormancy phenotype. The literature had suggested that *k13* mutations may modulate this phenotype; however, these results reject that claim and have been published in (Breglio et al., 2018). Further progeny are being phenotyped to elucidate the genetic determinant(s) of the dormancy phenotype; however, it is clear that neither *atg18* nor *kelch* mutations are responsible for the observed dormancy phenotype.

7 REFERENCES

ABBOTT, A. 2001. Earliest malaria DNA found in Roman baby graveyard. *Nature,* 412**,** 847.

ABU BAKAR, N., KLONIS, N., HANSSEN, E., CHAN, C. & TILLEY, L. 2010. Digestive-vacuole genesis and endocytic processes in the early intraerythrocytic stages of Plasmodium falciparum. *J Cell Sci,* 123**,** 441-50.

ADAMS, J., KELSO, R. & COOLEY, L. 2000. The kelch repeat superfamily of proteins: propellers of cell function. *Trends Cell Biol,* 10**,** 17-24.

ADJALLEY, S. H., JOHNSTON, G. L., LI, T., EASTMAN, R. T., EKLAND, E. H., EAPPEN, A. G., RICHMAN, A., SIM, B. K., LEE, M. C., HOFFMAN, S. L. & FIDOCK, D. A. 2011. Quantitative assessment of Plasmodium falciparum sexual development reveals potent transmission-blocking activity by methylene blue. *Proc Natl Acad Sci U S A,* 108**,** E1214-23.

ADJUIK, M., BABIKER, A., GARNER, P., OLLIARO, P., TAYLOR, W. & WHITE, N. 2004. Artesunate combinations for treatment of malaria: meta-analysis. *Lancet,* 363**,** 9-17.

AHN, S.-Y., SHIN, M.-Y., KIM, Y.-A., YOO, J.-A., KWAK, D.-H., JUNG, Y.-J., JUN, G., RYU, S.-H., YEOM, J.-S., AHN, J.-Y., CHAI, J.-Y. & PARK, J.-W. 2008. Magnetic separation: a highly effective method for synchronization of cultured erythrocytic Plasmodium falciparum. *Parasitology Research,* 102**,** 1195-1200.

AIKAWA, M., UNI, Y., ANDRUTIS, A. T. & HOWARD, R. J. 1986. Membrane-associated electron-dense material of the asexual stages of Plasmodium falciparum: evidence for movement from the intracellular parasite to the erythrocyte membrane. *Am J Trop Med Hyg,* 35**,** 30-6.

AITA, V. M., LIANG, X. H., MURTY, V. V. V. S., PINCUS, D. L., YU, W., CAYANIS, E., KALACHIKOV, S., GILLIAM, T. C. & LEVINE, B. 1999. Cloning and Genomic Organization of Beclin 1, a Candidate Tumor Suppressor Gene on Chromosome 17q21. *Genomics,* 59**,** 59-65.

ALCANTARA, L. M., KIM, J., MORAES, C. B., FRANCO, C. H., FRANZOI, K. D., LEE, S., FREITAS-JUNIOR, L. H. & AYONG, L. S. 2013. Chemosensitization potential of P-glycoprotein inhibitors in malaria parasites. *Exp Parasitol,* 134**,** 235-43.

ALVERS, A. L., FISHWICK, L. K., WOOD, M. S., HU, D., CHUNG, H. S., DUNN, W. A., JR. & ARIS, J. P. 2009. Autophagy and amino acid homeostasis are required for chronological longevity in Saccharomyces cerevisiae. *Aging Cell,* 8**,** 353-69.

AMARATUNGA, C., LIM, P., SUON, S., SRENG, S., MAO, S., SOPHA, C., SAM, B., DEK, D., TRY, V., AMATO, R., BLESSBORN, D., SONG, L., TULLO, G. S., FAY, M. P., ANDERSON, J. M., TARNING, J. & FAIRHURST, R. M. 2016. Dihydroartemisinin-piperaquine resistance in Plasmodium falciparum malaria in Cambodia: a multisite prospective cohort study. *Lancet Infect Dis,* 16**,** 357-65.

AMARATUNGA, C., SRENG, S., SUON, S., PHELPS, E. S., STEPNIEWSKA, K., LIM, P., ZHOU, C., MAO, S., ANDERSON, J. M., LINDEGARDH, N., JIANG, H., SONG, J., SU, X. Z., WHITE, N. J., DONDORP, A. M., ANDERSON, T. J., FAY, M. P., MU, J., DUONG, S. & FAIRHURST, R. M. 2012. Artemisinin-resistant Plasmodium falciparum in Pursat province, western Cambodia: a parasite clearance rate study. *Lancet Infect Dis,* 12**,** 851-8.

AMARATUNGA, C., WITKOWSKI, B., DEK, D., TRY, V., KHIM, N., MIOTTO, O., MENARD, D. & FAIRHURST, R. M. 2014. Plasmodium falciparum founder populations in western Cambodia have reduced artemisinin sensitivity in vitro. *Antimicrob Agents Chemother,* 58**,** 4935-7.

AMATO, R., LIM, P., MIOTTO, O., AMARATUNGA, C., DEK, D., PEARSON, R. D., ALMAGRO-GARCIA, J., NEAL, A. T., SRENG, S., SUON, S., DRURY, E., JYOTHI, D., STALKER, J., KWIATKOWSKI, D. P. & FAIRHURST, R. M. 2017. Genetic markers associated with dihydroartemisinin-piperaquine failure in Plasmodium falciparum malaria in Cambodia: a genotype-phenotype association study. *Lancet Infect Dis,* 17**,** 164-173.

AMM, I., SOMMER, T. & WOLF, D. H. 2014. Protein quality control and elimination of protein waste: the role of the ubiquitin-proteasome system. *Biochim Biophys Acta,* 1843**,** 182-96.

AN, Z., TASSA, A., THOMAS, C., ZHONG, R., XIAO, G., FOTEDAR, R., TU, B. P., KLIONSKY, D. J. & LEVINE, B. 2014. Autophagy is required for G(1)/G(0) quiescence in response to nitrogen starvation in Saccharomyces cerevisiae. *Autophagy,* 10**,** 1702-11.

ANDERS, C., NIEWOEHNER, O., DUERST, A. & JINEK, M. 2014. Structural basis of PAM-dependent target DNA recognition by the Cas9 endonuclease. *Nature,* 513**,** 569-73.

ANDERSSON, D. I. & HUGHES, D. 2010. Antibiotic resistance and its cost: is it possible to reverse resistance? *Nat Rev Microbiol,* 8**,** 260-71.

ANNEAR, P. L., GRUNDY, J., IR, P., JACOBS, B., MEN, C., NACHTNEBEL, M., OUM, S., ROBINS, A. & ROS, C. E. 2015. The Kingdom of Cambodia Health System Review. *In:* ANNEAR, P. L. (ed.). World Health Organization.

ANTOINE, T., FISHER, N., AMEWU, R., O'NEILL, P. M., WARD, S. A. & BIAGINI, G. A. 2014. Rapid kill of malaria parasites by artemisinin and semi-synthetic endoperoxides involves ROS-dependent depolarization of the membrane potential. *Journal of Antimicrobial Chemotherapy,* 69**,** 1005-1016.

ARIEY, F., WITKOWSKI, B., AMARATUNGA, C., BEGHAIN, J., LANGLOIS, A. C., KHIM, N., KIM, S., DURU, V., BOUCHIER, C., MA, L., LIM, P., LEANG, R., DUONG, S., SRENG, S., SUON, S., CHUOR, C. M., BOUT, D. M., MENARD, S., ROGERS, W. O., GENTON, B., FANDEUR, T., MIOTTO, O., RINGWALD, P., LE BRAS, J., BERRY, A., BARALE, J. C., FAIRHURST, R. M., BENOIT-VICAL, F., MERCEREAU-PUIJALON, O. & MENARD, D. 2014. A molecular marker of artemisinin-resistant Plasmodium falciparum malaria. *Nature,* 505**,** 50-5.

ARSTILA, A. U. & TRUMP, B. F. 1968. Studies on cellular autophagocytosis. The formation of autophagic vacuoles in the liver after glucagon administration. *Am J Pathol,* 53**,** 687-733.

ARTS, J., ANGIBAUD, P., MARIEN, A., FLOREN, W., JANSSENS, B., KING, P., VAN DUN, J., JANSSEN, L., GEERTS, T., TUMAN, R. W., JOHNSON, D. L., ANDRIES, L., JUNG, M., JANICOT, M. & VAN EMELEN, K. 2007. R306465 is a novel potent inhibitor of class I histone deacetylases with broad-spectrum antitumoral activity against solid and haematological malignancies. *Br J Cancer,* 97**,** 1344-53.

ASAWAMAHASAKDA, W., ITTARAT, I., PU, Y. M., ZIFFER, H. & MESHNICK, S. R. 1994. Reaction of antimalarial endoperoxides with specific parasite proteins. *Antimicrobial Agents and Chemotherapy,* 38**,** 1854-1858.

ASHLEY, E. A., DHORDA, M., FAIRHURST, R. M., AMARATUNGA, C., LIM, P., SUON, S., SRENG, S., ANDERSON, J. M., MAO, S., SAM, B., SOPHA, C.,

CHUOR, C. M., NGUON, C., SOVANNAROTH, S., PUKRITTAYAKAMEE, S., JITTAMALA, P., CHOTIVANICH, K., CHUTASMIT, K., SUCHATSOONTHORN, C., RUNCHAROEN, R., HIEN, T. T., THUY-NHIEN, N. T., THANH, N. V., PHU, N. H., HTUT, Y., HAN, K. T., AYE, K. H., MOKUOLU, O. A., OLAOSEBIKAN, R. R., FOLARANMI, O. O., MAYXAY, M., KHANTHAVONG, M., HONGVANTHONG, B., NEWTON, P. N., ONYAMBOKO, M. A., FANELLO, C. I., TSHEFU, A. K., MISHRA, N., VALECHA, N., PHYO, A. P., NOSTEN, F., YI, P., TRIPURA, R., BORRMANN, S., BASHRAHEIL, M., PESHU, J., FAIZ, M. A., GHOSE, A., HOSSAIN, M. A., SAMAD, R., RAHMAN, M. R., HASAN, M. M., ISLAM, A., MIOTTO, O., AMATO, R., MACINNIS, B., STALKER, J., KWIATKOWSKI, D. P., BOZDECH, Z., JEEYAPANT, A., CHEAH, P. Y., SAKULTHAEW, T., CHALK, J., INTHARABUT, B., SILAMUT, K., LEE, S. J., VIHOKHERN, B., KUNASOL, C., IMWONG, M., TARNING, J., TAYLOR, W. J., YEUNG, S., WOODROW, C. J., FLEGG, J. A., DAS, D., SMITH, J., VENKATESAN, M., PLOWE, C. V., STEPNIEWSKA, K., GUERIN, P. J., DONDORP, A. M., DAY, N. P. & WHITE, N. J. 2014. Spread of artemisinin resistance in Plasmodium falciparum malaria. *N Engl J Med,* 371**,** 411-23.

ATKINSON, C. T. & AIKAWA, M. 1990. Ultrastructure of malaria-infected erythrocytes. *Blood Cells,* 16**,** 351-68.

AXE, E. L., WALKER, S. A., MANIFAVA, M., CHANDRA, P., RODERICK, H. L., HABERMANN, A., GRIFFITHS, G. & KTISTAKIS, N. T. 2008. Autophagosome formation from membrane compartments enriched in phosphatidylinositol 3-phosphate and dynamically connected to the endoplasmic reticulum. *J Cell Biol,* 182**,** 685-701.

AZAD, M. B., CHEN, Y. & GIBSON, S. B. 2009. Regulation of autophagy by reactive oxygen species (ROS): implications for cancer progression and treatment. *Antioxid Redox Signal,* 11**,** 777-90.

BABA, M., OSUMI, M. & OHSUMI, Y. 1995. Analysis of the membrane structures involved in autophagy in yeast by freeze-replica method. *Cell Struct Funct,* 20**,** 465-71.

BABA, M., TAKESHIGE, K., BABA, N. & OHSUMI, Y. 1994. Ultrastructural analysis of the autophagic process in yeast: detection of autophagosomes and their characterization. *J Cell Biol,* 124**,** 903-13.

BABBITT, S. E., ALTENHOFEN, L., COBBOLD, S. A., ISTVAN, E. S., FENNELL, C., DOERIG, C., LLINAS, M. & GOLDBERG, D. E. 2012. Plasmodium falciparum responds to amino acid starvation by entering into a hibernatory state. *Proc Natl Acad Sci U S A,* 109**,** E3278-87.

BACKUES, S. K. & KLIONSKY, D. J. 2012. Atg11: A Rab-dependent, coiled-coil membrane protein that acts as a tether for autophagy. *Autophagy,* 8**,** 1275-1278.

BACON, D. J., LATOUR, C., LUCAS, C., COLINA, O., RINGWALD, P. & PICOT, S. 2007. Comparison of a SYBR green I-based assay with a histidine-rich protein II enzyme-linked immunosorbent assay for in vitro antimalarial drug efficacy testing and application to clinical isolates. *Antimicrob Agents Chemother,* 51**,** 1172-8.

BAKULA, D., MÜLLER, A. J., ZULEGER, T., TAKACS, Z., FRANZ-WACHTEL, M., THOST, A.-K., BRIGGER, D., TSCHAN, M. P., FRICKEY, T., ROBENEK, H., MACEK, B. & PROIKAS-CEZANNE, T. 2017. WIPI3 and WIPI4 β-propellers are scaffolds for LKB1-AMPK-TSC signalling circuits in the control of autophagy. *Nature Communications,* 8**,** 15637.

BALLA, T. 2005. Inositol-lipid binding motifs: signal integrators through protein-lipid and protein-protein interactions. *Journal of Cell Science,* 118**,** 2093-2104.

BANNISTER, L. & MITCHELL, G. 2003. The ins, outs and roundabouts of malaria. *Trends in Parasitology,* 19**,** 209-213.

BANNISTER, L. H., HOPKINS, J. M., FOWLER, R. E., KRISHNA, S. & MITCHELL, G. H. 2000a. A brief illustrated guide to the ultrastructure of Plasmodium falciparum asexual blood stages. *Parasitol Today,* 16**,** 427-33.

BANNISTER, L. H., HOPKINS, J. M., FOWLER, R. E., KRISHNA, S. & MITCHELL, G. H. 2000b. Ultrastructure of rhoptry development in Plasmodium falciparum erythrocytic schizonts. *Parasitology,* 121 (Pt 3)**,** 273-87.

BANSAL, P., TRIPATHI, A., THAKUR, V., MOHMMED, A. & SHARMA, P. 2017. Autophagy-Related Protein ATG18 Regulates Apicoplast Biogenesis in Apicomplexan Parasites. *MBio,* 8.

BARNES, K. I., CHANDA, P. & AB BARNABAS, G. 2009. Impact of the large-scale deployment of artemether/lumefantrine on the malaria disease burden in Africa: case studies of South Africa, Zambia and Ethiopia. *Malar J,* 8 Suppl 1**,** S8.

BARRANGOU, R., FREMAUX, C., DEVEAU, H., RICHARDS, M., BOYAVAL, P., MOINEAU, S., ROMERO, D. A. & HORVATH, P. 2007. CRISPR provides acquired resistance against viruses in prokaryotes. *Science,* 315**,** 1709-12.

BASCO, L. K., LE BRAS, J., RHOADES, Z. & WILSON, C. M. 1995. Analysis of pfmdr1 and drug susceptibility in fresh isolates of Plasmodium falciparum from subsaharan Africa. *Mol Biochem Parasitol,* 74**,** 157-66.

BASKARAN, S., RAGUSA, M. J., BOURA, E. & HURLEY, J. H. 2012. Two-site recognition of phosphatidylinositol 3-phosphate by PROPPINs in autophagy. *Mol Cell,* 47**,** 339-48.

BEADLE, C., LONG, G. W., WEISS, W. R., MCELROY, P. D., MARET, S. M., OLOO, A. J. & HOFFMAN, S. L. 1994. Diagnosis of malaria by detection of Plasmodium falciparum HRP-2 antigen with a rapid dipstick antigen-capture assay. *Lancet,* 343**,** 564-8.

BECKER, K., TILLEY, L., VENNERSTROM, J. L., ROBERTS, D., ROGERSON, S. & GINSBURG, H. 2004. Oxidative stress in malaria parasite-infected erythrocytes: host–parasite interactions. *International Journal for Parasitology,* 34**,** 163-189.

BEHRENDS, C., SOWA, M. E., GYGI, S. P. & HARPER, J. W. 2010. Network organization of the human autophagy system. *Nature,* 466**,** 68-76.

BELLOT, G., GARCIA-MEDINA, R., GOUNON, P., CHICHE, J., ROUX, D., POUYSSEGUR, J. & MAZURE, N. M. 2009. Hypoxia-induced autophagy is mediated through hypoxia-inducible factor induction of BNIP3 and BNIP3L via their BH3 domains. *Mol Cell Biol,* 29**,** 2570-81.

BENBROOK, D. M. & LONG, A. 2012. Integration of autophagy, proteasomal degradation, unfolded protein response and apoptosis. *Exp Oncol,* 34**,** 286-97.

BENNETT, T. N., PAGUIO, M., GLIGORIJEVIC, B., SEUDIEU, C., KOSAR, A. D., DAVIDSON, E. & ROEPE, P. D. 2004. Novel, Rapid, and Inexpensive Cell-Based Quantification of Antimalarial Drug Efficacy. *Antimicrobial Agents and Chemotherapy,* 48**,** 1807-1810.

BERNARD, A., JIN, M., GONZALEZ-RODRIGUEZ, P., FULLGRABE, J., DELORME-AXFORD, E., BACKUES, S. K., JOSEPH, B. & KLIONSKY, D.

J. 2015. Rph1/KDM4 mediates nutrient-limitation signaling that leads to the transcriptional induction of autophagy. *Curr Biol,* 25**,** 546-55.

BESTEIRO, S. 2017. Autophagy in apicomplexan parasites. *Current Opinion in Microbiology,* 40**,** 14-20.

BESTEIRO, S., BROOKS, C. F., STRIEPEN, B. & DUBREMETZ, J.-F. 2011. Autophagy Protein Atg3 is Essential for Maintaining Mitochondrial Integrity and for Normal Intracellular Development of Toxoplasma gondii Tachyzoites. *PLOS Pathogens,* 7**,** e1002416.

BETTS, J. C., LUKEY, P. T., ROBB, L. C., MCADAM, R. A. & DUNCAN, K. 2002. Evaluation of a nutrient starvation model of Mycobacterium tuberculosis persistence by gene and protein expression profiling. *Molecular Microbiology,* 43**,** 717-731.

BHASIN, V. K., CLAYTON, C., TRAGER, W. & CROSS, G. A. 1985. Variations in the organization of repetitive DNA sequences in the genomes of Plasmodium falciparum clones. *Mol Biochem Parasitol,* 15**,** 149-58.

BHATTACHARJEE, S., COPPENS, I., MBENGUE, A., SURESH, N., GHORBAL, M., SLOUKA, Z., SAFEUKUI, I., TANG, H. Y., SPEICHER, D. W., STAHELIN, R. V., MOHANDAS, N. & HALDAR, K. 2018. Remodeling of the malaria parasite and host human red cell by vesicle amplification that induces artemisinin resistance. *Blood*.

BHATTACHARJEE, S., STAHELIN, R. V., SPEICHER, K. D., SPEICHER, D. W. & HALDAR, K. 2012. Endoplasmic reticulum PI(3)P lipid binding targets malaria proteins to the host cell. *Cell,* 148**,** 201-12.

BILLKER, O., LINDO, V., PANICO, M., ETIENNE, A. E., PAXTON, T., DELL, A., ROGERS, M., SINDEN, R. E. & MORRIS, H. R. 1998. Identification of xanthurenic acid as the putative inducer of malaria development in the mosquito. *Nature,* 392**,** 289.

BIRKELAND, H. C. & STENMARK, H. 2004. Protein targeting to endosomes and phagosomes via FYVE and PX domains. *Curr Top Microbiol Immunol,* 282**,** 89-115.

BLIGH, E. G. & DYER, W. J. 1959. A RAPID METHOD OF TOTAL LIPID EXTRACTION AND PURIFICATION. *Canadian Journal of Biochemistry and Physiology,* 37**,** 911-917.

BRAY, P. G., MUNGTHIN, M., HASTINGS, I. M., BIAGINI, G. A., SAIDU, D. K., LAKSHMANAN, V., JOHNSON, D. J., HUGHES, R. H., STOCKS, P. A., O'NEILL, P. M., FIDOCK, D. A., WARHURST, D. C. & WARD, S. A. 2006. PfCRT and the trans-vacuolar proton electrochemical gradient: regulating the access of chloroquine to ferriprotoporphyrin IX. *Mol Microbiol,* 62**,** 238-51.

BREGLIO, K. F., RAHMAN, R. S., SA, J. M., ROBERTS, D. J. & WELLEMS, T. E. 2018. Kelch mutations in Plasmodium falciparum protein K13 do not modulate dormancy after artemisinin exposure and sorbitol selection in vitro. *Antimicrob Agents Chemother*.

BRUCE-CHUVATT, L. J. 1981. Alphonse Laveran's discovery 100 years ago and today's global fight against malaria. *Journal of the Royal Society of Medicine,* 74**,** 531-536.

BRUCE-CHWATT, L. J. 1965. PALEOGENESIS AND PALEO-EPIDEMIOLOGY OF PRIMATE MALARIA. *Bull World Health Organ,* 32**,** 363-87.

BURD, C. G. & EMR, S. D. 1998. Phosphatidylinositol(3)-phosphate signaling mediated by specific binding to RING FYVE domains. *Mol Cell,* 2**,** 157-62.

BUSHELL, E., GOMES, A. R., SANDERSON, T., ANAR, B., GIRLING, G., HERD, C., METCALF, T., MODRZYNSKA, K., SCHWACH, F., MARTIN, R. E., MATHER, M. W., MCFADDEN, G. I., PARTS, L., RUTLEDGE, G. G., VAIDYA, A. B., WENGELNIK, K., RAYNER, J. C. & BILLKER, O. 2017. Functional Profiling of a Plasmodium Genome Reveals an Abundance of Essential Genes. *Cell,* 170**,** 260-272.e8.

BWIJO, B., ALIN, M. H., ABBAS, N., WERNSDORFER, W. & BJORKMAN, A. 1997. Efficacy of artemisinin and mefloquine combinations against Plasmodium falciparum. In vitro simulation of in vivo pharmacokinetics. *Trop Med Int Health,* 2**,** 461-7.

CABRERA, M., PAGUIO, M. F., XIE, C. & ROEPE, P. D. 2009. Reduced digestive vacuolar accumulation of chloroquine is not linked to resistance to chloroquine toxicity. *Biochemistry,* 48**,** 11152-4.

CARRARA, V. I., SIRILAK, S., THONGLAIRUAM, J., ROJANAWATSIRIVET, C., PROUX, S., GILBOS, V., BROCKMAN, A., ASHLEY, E. A., MCGREADY, R., KRUDSOOD, S., LEEMINGSAWAT, S., LOOAREESUWAN, S., SINGHASIVANON, P., WHITE, N. & NOSTEN, F. 2006. Deployment of early

diagnosis and mefloquine-artesunate treatment of falciparum malaria in Thailand: the Tak Malaria Initiative. *PLoS Med,* 3**,** e183.

CERVANTES, S., BUNNIK, E. M., SARAF, A., CONNER, C. M., ESCALANTE, A., SARDIU, M. E., PONTS, N., PRUDHOMME, J., FLORENS, L. & LE ROCH, K. G. 2014. The multifunctional autophagy pathway in the human malaria parasite, Plasmodium falciparum. *Autophagy,* 10**,** 80-92.

CHAN, E. Y. 2009. mTORC1 Phosphorylates the ULK1-mAtg13-FIP200 Autophagy Regulatory Complex. *Science Signaling,* 2**,** pe51-pe51.

CHANG, J. T., KUMSTA, C., HELLMAN, A. B., ADAMS, L. M. & HANSEN, M. 2017. Spatiotemporal regulation of autophagy during Caenorhabditis elegans aging. *Elife,* 6.

CHAORATTANAKAWEE, S., SAUNDERS, D. L., SEA, D., CHANARAT, N., YINGYUEN, K., SUNDRAKES, S., SAINGAM, P., BUATHONG, N., SRIWICHAI, S., CHANN, S., SE, Y., YOM, Y., HENG, T. K., KONG, N., KUNTAWUNGINN, W., TANGTHONGCHAIWIRIYA, K., JACOB, C., TAKALA-HARRISON, S., PLOWE, C., LIN, J. T., CHUOR, C. M., PROM, S., TYNER, S. D., GOSI, P., TEJA-ISAVADHARM, P., LON, C. & LANTERI, C. A. 2015. Ex Vivo Drug Susceptibility Testing and Molecular Profiling of Clinical Plasmodium falciparum Isolates from Cambodia from 2008 to 2013 Suggest Emerging Piperaquine Resistance. *Antimicrob Agents Chemother,* 59**,** 4631-43.

CHAVCHICH, M., VAN BREDA, K., ROWCLIFFE, K., DIAGANA, T. T. & EDSTEIN, M. D. 2016. The Spiroindolone KAE609 Does Not Induce Dormant Ring Stages in Plasmodium falciparum Parasites. *Antimicrob Agents Chemother,* 60**,** 5167-74.

CHEESEMAN, I. H., MILLER, B. A., NAIR, S., NKHOMA, S., TAN, A., TAN, J. C., AL SAAI, S., PHYO, A. P., MOO, C. L., LWIN, K. M., MCGREADY, R., ASHLEY, E., IMWONG, M., STEPNIEWSKA, K., YI, P., DONDORP, A. M., MAYXAY, M., NEWTON, P. N., WHITE, N. J., NOSTEN, F., FERDIG, M. T. & ANDERSON, T. J. 2012. A major genome region underlying artemisinin resistance in malaria. *Science,* 336**,** 79-82.

CHEN, C., LIU, Y., LIU, R., IKENOUE, T., GUAN, K.-L., LIU, Y. & ZHENG, P. 2008. TSC–mTOR maintains quiescence and function of hematopoietic stem

cells by repressing mitochondrial biogenesis and reactive oxygen species. *The Journal of Experimental Medicine,* 205**,** 2397-2408.

CHEN, M., HONG, M. J., SUN, H., WANG, L., SHI, X., GILBERT, B. E., CORRY, D. B., KHERADMAND, F. & WANG, J. 2014a. Essential role for autophagy in the maintenance of immunological memory against influenza infection. *Nat Med,* 20**,** 503-10.

CHEN, N., LACRUE, A. N., TEUSCHER, F., WATERS, N. C., GATTON, M. L., KYLE, D. E. & CHENG, Q. 2014b. Fatty acid synthesis and pyruvate metabolism pathways remain active in dihydroartemisinin-induced dormant ring stages of Plasmodium falciparum. *Antimicrob Agents Chemother,* 58**,** 4773-81.

CHENG, J., FUJITA, A., YAMAMOTO, H., TATEMATSU, T., KAKUTA, S., OBARA, K., OHSUMI, Y. & FUJIMOTO, T. 2014. Yeast and mammalian autophagosomes exhibit distinct phosphatidylinositol 3-phosphate asymmetries. *Nat Commun,* 5**,** 3207.

CHIAO, M. T., CHENG, W. Y., YANG, Y. C., SHEN, C. C. & KO, J. L. 2013. Suberoylanilide hydroxamic acid (SAHA) causes tumor growth slowdown and triggers autophagy in glioblastoma stem cells. *Autophagy,* 9**,** 1509-26.

CHICANNE, G., SEVERIN, S., BOSCHERON, C., TERRISSE, A. D., GRATACAP, M. P., GAITS-IACOVONI, F., TRONCHERE, H. & PAYRASTRE, B. 2012. A novel mass assay to quantify the bioactive lipid PtdIns3P in various biological samples. *Biochem J,* 447**,** 17-23.

CHINAPPI, M., VIA, A., MARCATILI, P. & TRAMONTANO, A. 2010. On the mechanism of chloroquine resistance in Plasmodium falciparum. *PLoS One,* 5**,** e14064.

CHUANG, L. Y., CHENG, Y. H. & YANG, C. H. 2013. Specific primer design for the polymerase chain reaction. *Biotechnol Lett,* 35**,** 1541-9.

CHYLINSKI, K., MAKAROVA, K. S., CHARPENTIER, E. & KOONIN, E. V. 2014. Classification and evolution of type II CRISPR-Cas systems. *Nucleic Acids Res,* 42**,** 6091-105.

CIRMAN, T., OREŠIĆ, K., MAZOVEC, G. D., TURK, V., REED, J. C., MYERS, R. M., SALVESEN, G. S. & TURK, B. 2004. Selective Disruption of Lysosomes in HeLa Cells Triggers Apoptosis Mediated by Cleavage of Bid by Multiple Papain-like Lysosomal Cathepsins. *Journal of Biological Chemistry,* 279**,** 3578-3587.

CLARK, S. L., JR. 1957. Cellular differentiation in the kidneys of newborn mice studies with the electron microscope. *J Biophys Biochem Cytol,* 3**,** 349-62.

CLARKE, A. J., RIFFELMACHER, T., BRAAS, D., CORNALL, R. J. & SIMON, A. K. 2018. B1a B cells require autophagy for metabolic homeostasis and self-renewal. *J Exp Med,* 215**,** 399-413.

CODD, A., TEUSCHER, F., KYLE, D. E., CHENG, Q. & GATTON, M. L. 2011. Artemisinin-induced parasite dormancy: a plausible mechanism for treatment failure. *Malar J,* 10**,** 56.

CODOGNO, P., MEHRPOUR, M. & PROIKAS-CEZANNE, T. 2011. Canonical and non-canonical autophagy: variations on a common theme of self-eating? *Nat Rev Mol Cell Biol,* 13**,** 7-12.

COGSWELL, F. B. 1992. The hypnozoite and relapse in primate malaria. *Clin Microbiol Rev,* 5**,** 26-35.

COLOMBO, R., CALDARELLI, M., MENNECOZZI, M., GIORGINI, M. L., SOLA, F., CAPPELLA, P., PERRERA, C., DEPAOLINI, S. R., RUSCONI, L., CUCCHI, U., AVANZI, N., BERTRAND, J. A., BOSSI, R. T., PESENTI, E., GALVANI, A., ISACCHI, A., COLOTTA, F., DONATI, D. & MOLL, J. 2010. Targeting the Mitotic Checkpoint for Cancer Therapy with NMS-P715, an Inhibitor of MPS1 Kinase. *Cancer Research,* 70**,** 10255-10264.

CONG, L., RAN, F. A., COX, D., LIN, S., BARRETTO, R., HABIB, N., HSU, P. D., WU, X., JIANG, W., MARRAFFINI, L. A. & ZHANG, F. 2013. Multiplex genome engineering using CRISPR/Cas systems. *Science,* 339**,** 819-23.

COOPER, R. A., CONRAD, M. D., WATSON, Q. D., HUEZO, S. J., NINSIIMA, H., TUMWEBAZE, P., NSOBYA, S. L. & ROSENTHAL, P. J. 2015. Lack of Artemisinin Resistance in Plasmodium falciparum in Uganda Based on Parasitological and Molecular Assays. *Antimicrob Agents Chemother,* 59**,** 5061-4.

COOPER, R. A., FERDIG, M. T., SU, X. Z., URSOS, L. M., MU, J., NOMURA, T., FUJIOKA, H., FIDOCK, D. A., ROEPE, P. D. & WELLEMS, T. E. 2002. Alternative mutations at position 76 of the vacuolar transmembrane protein PfCRT are associated with chloroquine resistance and unique stereospecific quinine and quinidine responses in Plasmodium falciparum. *Mol Pharmacol,* 61**,** 35-42.

COPPLE, I. M. 2012. The Keap1-Nrf2 cell defense pathway--a promising therapeutic target? *Adv Pharmacol,* 63**,** 43-79.

CORCORAN, L. M., FORSYTH, K. P., BIANCO, A. E., BROWN, G. V. & KEMP, D. J. 1986. Chromosome size polymorphisms in Plasmodium falciparum can involve deletions and are frequent in natural parasite populations. *Cell,* 44**,** 87-95.

COUNIHAN, N. A., KALANON, M., COPPEL, R. L. & DE KONING-WARD, T. F. 2013. Plasmodium rhoptry proteins: why order is important. *Trends Parasitol,* 29**,** 228-36.

COWMAN, A. F. & FOOTE, S. J. 1990. Chemotherapy and drug resistance in malaria. *Int J Parasitol,* 20**,** 503-13.

CUDD, A., LABBE, H., GERVAIS, M. & NICOLAU, C. 1984. Liposomes injected intravenously into mice associate with liver mitochondria. *Biochim Biophys Acta,* 774**,** 169-80.

CUI, L. & SU, X.-Z. 2009. Discovery, mechanisms of action and combination therapy of artemisinin. *Expert review of anti-infective therapy,* 7**,** 999-1013.

CUI, L., WANG, Z., MIAO, J., MIAO, M., CHANDRA, R., JIANG, H., SU, X.-Z. & CUI, L. 2012. Mechanisms of in vitro resistance to dihydroartemisinin in Plasmodium falciparum. *Molecular microbiology,* 86**,** 111-128.

CULLINAN, S. B., ZHANG, D., HANNINK, M., ARVISAIS, E., KAUFMAN, R. J. & DIEHL, J. A. 2003. Nrf2 is a direct PERK substrate and effector of PERK-dependent cell survival. *Mol Cell Biol,* 23**,** 7198-209.

CUNHA, C. B. & CUNHA, B. A. 2008. Brief history of the clinical diagnosis of malaria: from Hippocrates to Osler. *J Vector Borne Dis,* 45**,** 194-9.

D'ACREMONT, V., LANDRY, P., MUELLER, I., PECOUD, A. & GENTON, B. 2002. Clinical and laboratory predictors of imported malaria in an outpatient setting: an aid to medical decision making in returning travelers with fever. *Am J Trop Med Hyg,* 66**,** 481-6.

DATSENKO, K. A., POUGACH, K., TIKHONOV, A., WANNER, B. L., SEVERINOV, K. & SEMENOVA, E. 2012. Molecular memory of prior infections activates the CRISPR/Cas adaptive bacterial immunity system. *Nat Commun,* 3**,** 945.

DE DUVE, C., PRESSMAN, B. C., GIANETTO, R., WATTIAUX, R. & APPELMANS, F. 1955. Tissue fractionation studies. 6. Intracellular distribution patterns of enzymes in rat-liver tissue. *Biochem J,* 60**,** 604-17.

DE KONING-WARD, T. F., JANSE, C. J. & WATERS, A. P. 2000. The development of genetic tools for dissecting the biology of malaria parasites. *Annu Rev Microbiol,* 54**,** 157-85.

DE KONING-WARD, T. F., WATERS, A. P. & CRABB, B. S. 2001. Puromycin-N-acetyltransferase as a selectable marker for use in Plasmodium falciparum. *Mol Biochem Parasitol,* 117**,** 155-60.

DE VRIES, P. J. & DIEN, T. K. 1996. Clinical pharmacology and therapeutic potential of artemisinin and its derivatives in the treatment of malaria. *Drugs,* 52**,** 818-36.

DEITSCH, K. W., DRISKILL, C. L. & WELLEMS, T. E. 2001. Transformation of malaria parasites by the spontaneous uptake and expression of DNA from human erythrocytes. *Nucleic Acids Research,* 29**,** 850-853.

DELTCHEVA, E., CHYLINSKI, K., SHARMA, C. M., GONZALES, K., CHAO, Y., PIRZADA, Z. A., ECKERT, M. R., VOGEL, J. & CHARPENTIER, E. 2011. CRISPR RNA maturation by trans-encoded small RNA and host factor RNase III. *Nature,* 471**,** 602-7.

DELVES, M., PLOUFFE, D., SCHEURER, C., MEISTER, S., WITTLIN, S., WINZELER, E. A., SINDEN, R. E. & LEROY, D. 2012. The activities of current antimalarial drugs on the life cycle stages of Plasmodium: a comparative study with human and rodent parasites. *PLoS Med,* 9**,** e1001169.

DEMBELE, L., ANG, X., CHAVCHICH, M., BONAMY, G. M. C., SELVA, J. J., LIM, M. Y., BODENREIDER, C., YEUNG, B. K. S., NOSTEN, F., RUSSELL, B. M., EDSTEIN, M. D., STRAIMER, J., FIDOCK, D. A., DIAGANA, T. T. & BIFANI, P. 2017. The Plasmodium PI(4)K inhibitor KDU691 selectively inhibits dihydroartemisinin-pretreated Plasmodium falciparum ring-stage parasites. *Sci Rep,* 7**,** 2325.

DENAT, L., KADEKARO, A. L., MARROT, L., LEACHMAN, S. A. & ABDEL-MALEK, Z. A. 2014. Melanocytes as Instigators and Victims of Oxidative Stress. *Journal of Investigative Dermatology,* 134**,** 1512-1518.

DENIS, A. M. & ANTHONY, R. M. C. 2004. Predictive In Vitro Models of the Sterilizing Activity of Anti-Tuberculosis Drugs. *Current Pharmaceutical Design,* 10**,** 3285-3295.

DEPRISTO, M. A., ZILVERSMIT, M. M. & HARTL, D. L. 2006. On the abundance, amino acid composition, and evolutionary dynamics of low-complexity regions in proteins. *Gene,* 378**,** 19-30.

DESAI, S. A. 2013. Insights Gained from P. falciparum Cultivation in Modified Media. *The Scientific World Journal,* 2013**,** 363505.

DESAI, S. A., BEZRUKOV, S. M. & ZIMMERBERG, J. 2000. A voltage-dependent channel involved in nutrient uptake by red blood cells infected with the malaria parasite. *Nature,* 406**,** 1001-5.

DESAI, S. A., KROGSTAD, D. J. & MCCLESKEY, E. W. 1993. A nutrient-permeable channel on the intraerythrocytic malaria parasite. *Nature,* 362**,** 643-6.

DESAI, S. A. & ROSENBERG, R. L. 1997. Pore size of the malaria parasite's nutrient channel. *Proc Natl Acad Sci U S A,* 94**,** 2045-9.

DETER, R. L., BAUDHUIN, P. & DE DUVE, C. 1967. Participation of lysosomes in cellular autophagy induced in rat liver by glucagon. *J Cell Biol,* 35**,** C11-6.

DEVEAU, H., BARRANGOU, R., GARNEAU, J. E., LABONTE, J., FREMAUX, C., BOYAVAL, P., ROMERO, D. A., HORVATH, P. & MOINEAU, S. 2008. Phage response to CRISPR-encoded resistance in Streptococcus thermophilus. *J Bacteriol,* 190**,** 1390-400.

DHEDA, K., GUMBO, T., GANDHI, N. R., MURRAY, M., THERON, G., UDWADIA, Z., MIGLIORI, G. B. & WARREN, R. 2014. Global control of tuberculosis: from extensively drug-resistant to untreatable tuberculosis. *The Lancet. Respiratory medicine,* 2**,** 321-338.

DI CRISTINA, M., DOU, Z., LUNGHI, M., KANNAN, G., HUYNH, M.-H., MCGOVERN, O. L., SCHULTZ, T. L., SCHULTZ, A. J., MILLER, A. J., HAYES, B. M., VAN DER LINDEN, W., EMILIANI, C., BOGYO, M., BESTEIRO, S., COPPENS, I. & CARRUTHERS, V. B. 2017. Toxoplasma depends on lysosomal consumption of autophagosomes for persistent infection. *Nature Microbiology,* 2**,** 17096.

DI PAOLO, G. & DE CAMILLI, P. 2006. Phosphoinositides in cell regulation and membrane dynamics. *Nature,* 443**,** 651.

DI ROSA, F. 2016. Two Niches in the Bone Marrow: A Hypothesis on Life-long T Cell Memory. *Trends Immunol,* 37**,** 503-12.

DIVO, A. A., GEARY, T. G., DAVIS, N. L. & JENSEN, J. B. 1985. Nutritional requirements of Plasmodium falciparum in culture. I. Exogenously supplied dialyzable components necessary for continuous growth. *J Protozool,* 32**,** 59-64.

DJIMDE, A., DOUMBO, O. K., CORTESE, J. F., KAYENTAO, K., DOUMBO, S., DIOURTE, Y., COULIBALY, D., DICKO, A., SU, X. Z., NOMURA, T., FIDOCK, D. A., WELLEMS, T. E. & PLOWE, C. V. 2001. A molecular marker for chloroquine-resistant falciparum malaria. *N Engl J Med,* 344**,** 257-63.

DOGOVSKI, C., XIE, S. C., BURGIO, G., BRIDGFORD, J., MOK, S., MCCAW, J. M., CHOTIVANICH, K., KENNY, S., GNADIG, N., STRAIMER, J., BOZDECH, Z., FIDOCK, D. A., SIMPSON, J. A., DONDORP, A. M., FOOTE, S., KLONIS, N. & TILLEY, L. 2015. Targeting the cell stress response of Plasmodium falciparum to overcome artemisinin resistance. *PLoS Biol,* 13**,** e1002132.

DONDORP, A., NOSTEN, F., STEPNIEWSKA, K., DAY, N. & WHITE, N. 2005. Artesunate versus quinine for treatment of severe falciparum malaria: a randomised trial. *Lancet,* 366**,** 717-25.

DONDORP, A. M., FAIRHURST, R. M., SLUTSKER, L., MACARTHUR, J. R., BREMAN, J. G., GUERIN, P. J., WELLEMS, T. E., RINGWALD, P., NEWMAN, R. D. & PLOWE, C. V. 2011. The threat of artemisinin-resistant malaria. *N Engl J Med,* 365**,** 1073-5.

DONDORP, A. M., FANELLO, C. I., HENDRIKSEN, I. C., GOMES, E., SENI, A., CHHAGANLAL, K. D., BOJANG, K., OLAOSEBIKAN, R., ANUNOBI, N., MAITLAND, K., KIVAYA, E., AGBENYEGA, T., NGUAH, S. B., EVANS, J., GESASE, S., KAHABUKA, C., MTOVE, G., NADJM, B., DEEN, J., MWANGA-AMUMPAIRE, J., NANSUMBA, M., KAREMA, C., UMULISA, N., UWIMANA, A., MOKUOLU, O. A., ADEDOYIN, O. T., JOHNSON, W. B., TSHEFU, A. K., ONYAMBOKO, M. A., SAKULTHAEW, T., NGUM, W. P., SILAMUT, K., STEPNIEWSKA, K., WOODROW, C. J., BETHELL, D., WILLS, B., ONEKO, M., PETO, T. E., VON SEIDLEIN, L., DAY, N. P. & WHITE, N. J. 2010. Artesunate versus quinine in the treatment of severe falciparum malaria in African children (AQUAMAT): an open-label, randomised trial. *Lancet,* 376**,** 1647-57.

DONDORP, A. M., LEE, S. J., FAIZ, M. A., MISHRA, S., PRICE, R., TJITRA, E., THAN, M., HTUT, Y., MOHANTY, S., YUNUS, E. B., RAHMAN, R.,

NOSTEN, F., ANSTEY, N. M., DAY, N. P. J. & WHITE, N. J. 2008. The Relationship between Age and the Manifestations of and Mortality Associated with Severe Malaria. *Clinical Infectious Diseases,* 47**,** 151-157.

DONDORP, A. M., NOSTEN, F., YI, P., DAS, D., PHYO, A. P., TARNING, J., LWIN, K. M., ARIEY, F., HANPITHAKPONG, W., LEE, S. J., RINGWALD, P., SILAMUT, K., IMWONG, M., CHOTIVANICH, K., LIM, P., HERDMAN, T., AN, S. S., YEUNG, S., SINGHASIVANON, P., DAY, N. P., LINDEGARDH, N., SOCHEAT, D. & WHITE, N. J. 2009. Artemisinin resistance in Plasmodium falciparum malaria. *N Engl J Med,* 361**,** 455-67.

DONG, H., LI, R., YU, C., XU, T., ZHANG, X. & DONG, M. 2015. Paeoniflorin inhibition of 6-hydroxydopamine-induced apoptosis in PC12 cells via suppressing reactive oxygen species-mediated PKCdelta/NF-kappaB pathway. *Neuroscience,* 285**,** 70-80.

DOOLEY, H. C., RAZI, M., POLSON, H. E., GIRARDIN, S. E., WILSON, M. I. & TOOZE, S. A. 2014. WIPI2 links LC3 conjugation with PI3P, autophagosome formation, and pathogen clearance by recruiting Atg12-5-16L1. *Mol Cell,* 55**,** 238-52.

DOOLEY, H. C., WILSON, M. I. & TOOZE, S. A. 2015. WIPI2B links PtdIns3P to LC3 lipidation through binding ATG16L1. *Autophagy,* 11**,** 190-191.

DORN, B. R., DUNN, W. A., JR. & PROGULSKE-FOX, A. 2001. Porphyromonas gingivalis traffics to autophagosomes in human coronary artery endothelial cells. *Infect Immun,* 69**,** 5698-708.

DOVE, S. K., PIPER, R. C., MCEWEN, R. K., YU, J. W., KING, M. C., HUGHES, D. C., THURING, J., HOLMES, A. B., COOKE, F. T., MICHELL, R. H., PARKER, P. J. & LEMMON, M. A. 2004. Svp1p defines a family of phosphatidylinositol 3,5-bisphosphate effectors. *Embo j,* 23**,** 1922-33.

DUFIES, M., JACQUEL, A., ROBERT, G., CLUZEAU, T., PUISSANT, A., FENOUILLE, N., LEGROS, L., RAYNAUD, S., CASSUTO, J. P., LUCIANO, F. & AUBERGER, P. 2011. Mechanism of action of the multikinase inhibitor Foretinib. *Cell Cycle,* 10**,** 4138-48.

DUFLOS, A., KRUCZYNSKI, A. & BARRET, J. M. 2002. Novel Aspects of Natural and Modified Vinca Alkaloids. *Current Medicinal Chemistry - Anti-Cancer Agents,* 2**,** 55-70.

DURAISINGH, M. T., TRIGLIA, T. & COWMAN, A. F. 2002. Negative selection of Plasmodium falciparum reveals targeted gene deletion by double crossover recombination. *Int J Parasitol,* 32**,** 81-9.

DURAN, A., LINARES, J. F., GALVEZ, A. S., WIKENHEISER, K., FLORES, J. M., DIAZ-MECO, M. T. & MOSCAT, J. 2008. The Signaling Adaptor p62 Is an Important NF-κB Mediator in Tumorigenesis. *Cancer Cell,* 13**,** 343-354.

DURU, V., KHIM, N., LEANG, R., KIM, S., DOMERGUE, A., KLOEUNG, N., KE, S., CHY, S., EAM, R., KHEAN, C., LOCH, K., KEN, M., LEK, D., BEGHAIN, J., ARIEY, F., GUERIN, P. J., HUY, R., MERCEREAU-PUIJALON, O., WITKOWSKI, B. & MENARD, D. 2015. Plasmodium falciparum dihydroartemisinin-piperaquine failures in Cambodia are associated with mutant K13 parasites presenting high survival rates in novel piperaquine in vitro assays: retrospective and prospective investigations. *BMC Med,* 13**,** 305.

DUVALSAINT, M. & KYLE, D. E. 2018. Phytohormones, isoprenoids and role of the apicoplast in recovery from dihydroartemisinin-induced dormancy of Plasmodium falciparum. *Antimicrob Agents Chemother*.

ECKSTEIN-LUDWIG, U., WEBB, R. J., VAN GOETHEM, I. D. A., EAST, J. M., LEE, A. G., KIMURA, M., O'NEILL, P. M., BRAY, P. G., WARD, S. A. & KRISHNA, S. 2003. Artemisinins target the SERCA of Plasmodium falciparum. *Nature,* 424**,** 957.

EDINGER, A. L. & THOMPSON, C. B. 2002. Akt maintains cell size and survival by increasing mTOR-dependent nutrient uptake. *Mol Biol Cell,* 13**,** 2276-88.

ELLIOTT, D. A., MCINTOSH, M. T., HOSGOOD, H. D., CHEN, S., ZHANG, G., BAEVOVA, P. & JOINER, K. A. 2008. Four distinct pathways of hemoglobin uptake in the malaria parasite Plasmodium falciparum. *Proceedings of the National Academy of Sciences,* 105**,** 2463-2468.

ENOMOTO, R., SUZUKI, C., OHNO, M., OHASI, T., FUTAGAMI, R., ISHIKAWA, K., KOMAE, M., NISHINO, T., KONISHI, Y. & LEE, E. 2007. Cationic surfactants induce apoptosis in normal and cancer cells. *Ann N Y Acad Sci,* 1095**,** 1-6.

ERMAK, G., SOJITRA, S., YIN, F., CADENAS, E., CUERVO, A. M. & DAVIES, K. J. 2012. Chronic expression of RCAN1-1L protein induces mitochondrial autophagy and metabolic shift from oxidative phosphorylation to glycolysis in neuronal cells. *J Biol Chem,* 287**,** 14088-98.

FAIRHURST, R. M. & DONDORP, A. M. 2016. Artemisinin-Resistant Plasmodium falciparum Malaria. *Microbiol Spectr,* 4.

FALKENBURGER, B. H., JENSEN, J. B., DICKSON, E. J., SUH, B.-C. & HILLE, B. 2010. Phosphoinositides: lipid regulators of membrane proteins. *The Journal of Physiology,* 588**,** 3179-3185.

FAN, Q. W., KNIGHT, Z. A., GOLDENBERG, D. D., YU, W., MOSTOV, K. E., STOKOE, D., SHOKAT, K. M. & WEISS, W. A. 2006. A dual PI3 kinase/mTOR inhibitor reveals emergent efficacy in glioma. *Cancer Cell,* 9**,** 341-9.

FARIS, R., MOORE, R. A., WARD, A., RACE, B., DORWARD, D. W., HOLLISTER, J. R., FISCHER, E. R. & PRIOLA, S. A. 2017. Cellular prion protein is present in mitochondria of healthy mice. *Sci Rep,* 7**,** 41556.

FEHRENBACHER, N., GYRD-HANSEN, M., POULSEN, B., FELBOR, U., KALLUNKI, T., BOES, M., WEBER, E., LEIST, M. & JÄÄTTELÄ, M. 2004. Sensitization to the Lysosomal Cell Death Pathway upon Immortalization and Transformation. *Cancer Research,* 64**,** 5301-5310.

FELGNER, P. L., GADEK, T. R., HOLM, M., ROMAN, R., CHAN, H. W., WENZ, M., NORTHROP, J. P., RINGOLD, G. M. & DANIELSEN, M. 1987. Lipofection: a highly efficient, lipid-mediated DNA-transfection procedure. *Proc Natl Acad Sci U S A,* 84**,** 7413-7.

FENGSRUD, M., ROOS, N., BERG, T., LIOU, W., SLOT, J. W. & SEGLEN, P. O. 1995. Ultrastructural and immunocytochemical characterization of autophagic vacuoles in isolated hepatocytes: effects of vinblastine and asparagine on vacuole distributions. *Exp Cell Res,* 221**,** 504-19.

FIDOCK, D. A., NOMURA, T., TALLEY, A. K., COOPER, R. A., DZEKUNOV, S. M., FERDIG, M. T., URSOS, L. M., SIDHU, A. B., NAUDE, B., DEITSCH, K. W., SU, X. Z., WOOTTON, J. C., ROEPE, P. D. & WELLEMS, T. E. 2000. Mutations in the P. falciparum digestive vacuole transmembrane protein PfCRT and evidence for their role in chloroquine resistance. *Mol Cell,* 6**,** 861-71.

FIDOCK, D. A. & WELLEMS, T. E. 1997. Transformation with human dihydrofolate reductase renders malaria parasites insensitive to WR99210 but does not affect the intrinsic activity of proguanil. *Proc Natl Acad Sci U S A,* 94**,** 10931-6.

FINK, A. L. 1998. Protein aggregation: folding aggregates, inclusion bodies and amyloid. *Fold Des,* 3**,** R9-23.

FITCH, C. D., CHEVLI, R., BANYAL, H. S., PHILLIPS, G., PFALLER, M. A. & KROGSTAD, D. J. 1982. Lysis of Plasmodium falciparum by ferriprotoporphyrin IX and a chloroquine-ferriprotoporphyrin IX complex. *Antimicrobial Agents and Chemotherapy,* 21**,** 819-822.

FLEISCHER, B. 2004. Editorial: 100 years ago: Giemsa's solution for staining of plasmodia. *Tropical Medicine & International Health,* 9**,** 755-756.

FOLLER, M., BOBBALA, D., KOKA, S., HUBER, S. M., GULBINS, E. & LANG, F. 2009. Suicide for survival--death of infected erythrocytes as a host mechanism to survive malaria. *Cell Physiol Biochem,* 24**,** 133-40.

FREITAS-JUNIOR, L. H., BOTTIUS, E., PIRRIT, L. A., DEITSCH, K. W., SCHEIDIG, C., GUINET, F., NEHRBASS, U., WELLEMS, T. E. & SCHERF, A. 2000. Frequent ectopic recombination of virulence factor genes in telomeric chromosome clusters of P. falciparum. *Nature,* 407**,** 1018-22.

FU, Y., FODEN, J. A., KHAYTER, C., MAEDER, M. L., REYON, D., JOUNG, J. K. & SANDER, J. D. 2013. High-frequency off-target mutagenesis induced by CRISPR-Cas nucleases in human cells. *Nat Biotechnol,* 31**,** 822-6.

FUNG, C., CHEN, X., GRANDIS, J. R. & DUVVURI, U. 2012. EGFR tyrosine kinase inhibition induces autophagy in cancer cells. *Cancer Biology & Therapy,* 13**,** 1417-1424.

FURUTACHI, S., MIYA, H., WATANABE, T., KAWAI, H., YAMASAKI, N., HARADA, Y., IMAYOSHI, I., NELSON, M., NAKAYAMA, K. I., HIRABAYASHI, Y. & GOTOH, Y. 2015. Slowly dividing neural progenitors are an embryonic origin of adult neural stem cells. *Nat Neurosci,* 18**,** 657-65.

GACESA, R., DUNLAP, W. C. & LONG, P. F. 2015. Bioinformatics analyses provide insight into distant homology of the Keap1-Nrf2 pathway. *Free Radic Biol Med,* 88**,** 373-380.

GANESAN, S. M., MORRISEY, J. M., KE, H., PAINTER, H. J., LAROIYA, K., PHILLIPS, M. A., RATHOD, P. K., MATHER, M. W. & VAIDYA, A. B. 2011. Yeast dihydroorotate dehydrogenase as a new selectable marker for Plasmodium falciparum transfection. *Mol Biochem Parasitol,* 177**,** 29-34.

GANLEY, IAN G., WONG, P.-M., GAMMOH, N. & JIANG, X. 2011. Distinct Autophagosomal-Lysosomal Fusion Mechanism Revealed by Thapsigargin-Induced Autophagy Arrest. *Molecular Cell,* 42**,** 731-743.

GARDNER, M. J., HALL, N., FUNG, E., WHITE, O., BERRIMAN, M., HYMAN, R. W., CARLTON, J. M., PAIN, A., NELSON, K. E., BOWMAN, S., PAULSEN, I. T., JAMES, K., EISEN, J. A., RUTHERFORD, K., SALZBERG, S. L., CRAIG, A., KYES, S., CHAN, M. S., NENE, V., SHALLOM, S. J., SUH, B., PETERSON, J., ANGIUOLI, S., PERTEA, M., ALLEN, J., SELENGUT, J., HAFT, D., MATHER, M. W., VAIDYA, A. B., MARTIN, D. M., FAIRLAMB, A. H., FRAUNHOLZ, M. J., ROOS, D. S., RALPH, S. A., MCFADDEN, G. I., CUMMINGS, L. M., SUBRAMANIAN, G. M., MUNGALL, C., VENTER, J. C., CARUCCI, D. J., HOFFMAN, S. L., NEWBOLD, C., DAVIS, R. W., FRASER, C. M. & BARRELL, B. 2002. Genome sequence of the human malaria parasite Plasmodium falciparum. *Nature,* 419**,** 498-511.

GAVIRIA, D., PAGUIO, M. F., TURNBULL, L. B., TAN, A., SIRIWARDANA, A., GHOSH, D., FERDIG, M. T., SINAI, A. P. & ROEPE, P. D. 2013. A process similar to autophagy is associated with cytocidal chloroquine resistance in Plasmodium falciparum. *PLoS One,* 8**,** e79059.

GBD 2015. Global Burden of Disease (GBD) country profile: Cambodia. Institute for Health Metrics and Evaluation.

GEARY, T. G., DIVO, A. A. & JENSEN, J. B. 1989. Stage specific actions of antimalarial drugs on Plasmodium falciparum in culture. *Am J Trop Med Hyg,* 40**,** 240-4.

GEARY, T. G., DIVO, A. D., JENSEN, J. B., ZANGWILL, M. & GINSBURG, H. 1990. Kinetic modelling of the response of Plasmodium falciparum to chloroquine and its experimental testing in vitro. Implications for mechanism of action of and resistance to the drug. *Biochem Pharmacol,* 40**,** 685-91.

GENTON, B. & D'ACREMONT, V. 2001. Clinical features of malaria in returning travelers and migrants. *In:* P, S. (ed.) *Travelers' malaria.* Hamilton: BC Decker.

GHORBAL, M., GORMAN, M., MACPHERSON, C. R., MARTINS, R. M., SCHERF, A. & LOPEZ-RUBIO, J. J. 2014. Genome editing in the human malaria parasite Plasmodium falciparum using the CRISPR-Cas9 system. *Nat Biotechnol,* 32**,** 819-21.

GHOSH, D., WALTON, J. L., ROEPE, P. D. & SINAI, A. P. 2012. Autophagy is a cell death mechanism in Toxoplasma gondii. *Cellular Microbiology,* 14**,** 589-607.

GIAO, P. T., BINH, T. Q., KAGER, P. A., LONG, H. P., VAN THANG, N., VAN NAM, N. & DE VRIES, P. J. 2001. Artemisinin for treatment of uncomplicated

falciparum malaria: is there a place for monotherapy? *Am J Trop Med Hyg,* 65**,** 690-5.

GIEMSA, G. 1904. Eine Vereinfachung und Vervollkommnung meiner Methylenblau-Eosin-Färbemethode zur Erzielung der Romanowsky-Nocht'schen Chromatinfärbung. *Centralblatt für Bakteriologie,* 32**,** 307-313.

GIESELER, F., BAUER, E., NUESSLER, V., CLARK, M. & VALSAMAS, S. 1999. Molecular effects of topoisomerase II inhibitors in AML cell lines: correlation of apoptosis with topoisomerase II activity but not with DNA damage. *Leukemia,* 13**,** 1859.

GILLOOLY, D. J., MORROW, I. C., LINDSAY, M., GOULD, R., BRYANT, N. J., GAULLIER, J. M., PARTON, R. G. & STENMARK, H. 2000. Localization of phosphatidylinositol 3-phosphate in yeast and mammalian cells. *Embo j,* 19**,** 4577-88.

GLIGORIJEVIC, B., PURDY, K., ELLIOTT, D. A., COOPER, R. A. & ROEPE, P. D. 2008. Stage independent chloroquine resistance and chloroquine toxicity revealed via spinning disk confocal microscopy. *Mol Biochem Parasitol,* 159**,** 7-23.

GOLDBERG, D. E., SLATER, A. F., CERAMI, A. & HENDERSON, G. B. 1990. Hemoglobin degradation in the malaria parasite Plasmodium falciparum: an ordered process in a unique organelle. *Proc Natl Acad Sci U S A,* 87**,** 2931-5.

GOLDSMITH, J., LEVINE, B. & DEBNATH, J. 2014. Chapter Two - Autophagy and Cancer Metabolism. *In:* GALLUZZI, L. & KROEMER, G. (eds.) *Methods in Enzymology.* Academic Press.

GONZALES, J. M., PATEL, J. J., PONMEE, N., JIANG, L., TAN, A., MAHER, S. P., WUCHTY, S., RATHOD, P. K. & FERDIG, M. T. 2008. Regulatory Hotspots in the Malaria Parasite Genome Dictate Transcriptional Variation. *PLOS Biology,* 6**,** e238.

GOSLINE, S. J., NASCIMENTO, M., MCCALL, L. I., ZILBERSTEIN, D., THOMAS, D. Y., MATLASHEWSKI, G. & HALLETT, M. 2011. Intracellular eukaryotic parasites have a distinct unfolded protein response. *PLoS One,* 6**,** e19118.

GOTTARDI, W. 1985. The influence of the chemical behaviour of iodine on the germicidal action of disinfectant solutions containing iodine. *Journal of Hospital Infection,* 6**,** 1-11.

GRAY, K. A., GRESTY, K. J., CHEN, N., ZHANG, V., GUTTERIDGE, C. E., PEATEY, C. L., CHAVCHICH, M., WATERS, N. C. & CHENG, Q. 2016. Correlation between Cyclin Dependent Kinases and Artemisinin-Induced Dormancy in Plasmodium falciparum In Vitro. *PLoS One,* 11**,** e0157906.

GRIFFIN, C. E., HOKE, J. M., SAMARAKOON, U., DUAN, J., MU, J., FERDIG, M. T., WARHURST, D. C. & COOPER, R. A. 2012. Mutation in the Plasmodium falciparum CRT protein determines the stereospecific activity of antimalarial cinchona alkaloids. *Antimicrob Agents Chemother,* 56**,** 5356-64.

GROBLER, L., CHAVCHICH, M., HAYNES, R. K., EDSTEIN, M. D. & GROBLER, A. F. 2014. Assessment of the induction of dormant ring stages in Plasmodium falciparum parasites by artemisone and artemisone entrapped in Pheroid vesicles in vitro. *Antimicrob Agents Chemother,* 58**,** 7579-82.

GROTEMEIER, A., ALERS, S., PFISTERER, S. G., PAASCH, F., DAUBRAWA, M., DIETERLE, A., VIOLLET, B., WESSELBORG, S., PROIKAS-CEZANNE, T. & STORK, B. 2010. AMPK-independent induction of autophagy by cytosolic Ca2+ increase. *Cell Signal,* 22**,** 914-25.

GROTH-PEDERSEN, L., OSTENFELD, M. S., HØYER-HANSEN, M., NYLANDSTED, J. & JÄÄTTELÄ, M. 2007. Vincristine Induces Dramatic Lysosomal Changes and Sensitizes Cancer Cells to Lysosome-Destabilizing Siramesine. *Cancer Research,* 67**,** 2217-2225.

GUPTA, A., ROY, S., LAZAR, A. J., WANG, W. L., MCAULIFFE, J. C., REYNOSO, D., MCMAHON, J., TAGUCHI, T., FLORIS, G., DEBIEC-RYCHTER, M., SCHOFFSKI, P., TRENT, J. A., DEBNATH, J. & RUBIN, B. P. 2010. Autophagy inhibition and antimalarials promote cell death in gastrointestinal stromal tumor (GIST). *Proc Natl Acad Sci U S A,* 107**,** 14333-8.

HAIN, A. U., BARTEE, D., SANDERS, N. G., MILLER, A. S., SULLIVAN, D. J., LEVITSKAYA, J., MEYERS, C. F. & BOSCH, J. 2014. Identification of an Atg8-Atg3 protein-protein interaction inhibitor from the medicines for Malaria Venture Malaria Box active in blood and liver stage Plasmodium falciparum parasites. *J Med Chem,* 57**,** 4521-31.

HAIN, A. U., MILLER, A. S., LEVITSKAYA, J. & BOSCH, J. 2016. Virtual Screening and Experimental Validation Identify Novel Inhibitors of the Plasmodium falciparum Atg8-Atg3 Protein-Protein Interaction. *ChemMedChem,* 11**,** 900-10.

HAIN, A. U., WELTZER, R. R., HAMMOND, H., JAYABALASINGHAM, B., DINGLASAN, R. R., GRAHAM, D. R., COLQUHOUN, D. R., COPPENS, I. & BOSCH, J. 2012. Structural characterization and inhibition of the Plasmodium Atg8-Atg3 interaction. *J Struct Biol,* 180**,** 551-62.

HAMBRIGHT, H. G. & GHOSH, R. 2017. Autophagy: In the cROSshairs of cancer. *Biochemical Pharmacology,* 126**,** 13-22.

HAMILTON, W. L., CLAESSENS, A., OTTO, T. D., KEKRE, M., FAIRHURST, R. M., RAYNER, J. C. & KWIATKOWSKI, D. 2017. Extreme mutation bias and high AT content in Plasmodium falciparum. *Nucleic Acids Res,* 45**,** 1889-1901.

HAN, W., PAN, H., CHEN, Y., SUN, J., WANG, Y., LI, J., GE, W., FENG, L., LIN, X., WANG, X., WANG, X. & JIN, H. 2011. EGFR tyrosine kinase inhibitors activate autophagy as a cytoprotective response in human lung cancer cells. *PLoS One,* 6**,** e18691.

HANADA, T., NODA, N. N., SATOMI, Y., ICHIMURA, Y., FUJIOKA, Y., TAKAO, T., INAGAKI, F. & OHSUMI, Y. 2007. The Atg12-Atg5 conjugate has a novel E3-like activity for protein lipidation in autophagy. *J Biol Chem,* 282**,** 37298-302.

HARA, T., NAKAMURA, K., MATSUI, M., YAMAMOTO, A., NAKAHARA, Y., SUZUKI-MIGISHIMA, R., YOKOYAMA, M., MISHIMA, K., SAITO, I., OKANO, H. & MIZUSHIMA, N. 2006. Suppression of basal autophagy in neural cells causes neurodegenerative disease in mice. *Nature,* 441**,** 885-9.

HARDING, T. M., MORANO, K. A., SCOTT, S. V. & KLIONSKY, D. J. 1995. Isolation and characterization of yeast mutants in the cytoplasm to vacuole protein targeting pathway. *J Cell Biol,* 131**,** 591-602.

HASENKAMP, S., RUSSELL, K. T. & HORROCKS, P. 2012. Comparison of the absolute and relative efficiencies of electroporation-based transfection protocols for Plasmodium falciparum. *Malaria Journal,* 11**,** 210-210.

HASINOFF, B. B., WU, X., YADAV, A. A., PATEL, D., ZHANG, H., WANG, D. S., CHEN, Z. S. & YALOWICH, J. C. 2015. Cellular mechanisms of the cytotoxicity of the anticancer drug elesclomol and its complex with Cu(II). *Biochem Pharmacol,* 93**,** 266-76.

HASINOFF, B. B., YADAV, A. A., PATEL, D. & WU, X. 2014. The cytotoxicity of the anticancer drug elesclomol is due to oxidative stress indirectly mediated through its complex with Cu(II). *J Inorg Biochem,* 137**,** 22-30.

HASSETT, M. R., STERNBERG, A. R. & ROEPE, P. D. 2017. Inhibition of Human Class I vs Class III Phosphatidylinositol 3′-Kinases. *Biochemistry,* 56**,** 4326-4334.

HASTY, P., RIVERA-PEREZ, J. & BRADLEY, A. 1991. The length of homology required for gene targeting in embryonic stem cells. *Mol Cell Biol,* 11**,** 5586-91.

HAWLEY, S. R., BRAY, P. G., O'NEILL, P. M., PARK, B. K. & WARD, S. A. 1996. The role of drug accumulation in 4-aminoquinoline antimalarial potency. The influence of structural substitution and physicochemical properties. *Biochem Pharmacol,* 52**,** 723-33.

HAYTON, K., GAUR, D., LIU, A., TAKAHASHI, J., HENSCHEN, B., SINGH, S., LAMBERT, L., FURUYA, T., BOUTTENOT, R., DOLL, M., NAWAZ, F., MU, J., JIANG, L., MILLER, L. H. & WELLEMS, T. E. 2008. Erythrocyte binding protein PfRH5 polymorphisms determine species-specific pathways of Plasmodium falciparum invasion. *Cell Host Microbe,* 4**,** 40-51.

HAYWARD, R., SALIBA, K. J. & KIRK, K. 2005. pfmdr1 mutations associated with chloroquine resistance incur a fitness cost in Plasmodium falciparum. *Molecular Microbiology,* 55**,** 1285-1295.

HE, C., SONG, H., YORIMITSU, T., MONASTYRSKA, I., YEN, W. L., LEGAKIS, J. E. & KLIONSKY, D. J. 2006. Recruitment of Atg9 to the preautophagosomal structure by Atg11 is essential for selective autophagy in budding yeast. *J Cell Biol,* 175**,** 925-35.

HELER, R., SAMAI, P., MODELL, J. W., WEINER, C., GOLDBERG, G. W., BIKARD, D. & MARRAFFINI, L. A. 2015. Cas9 specifies functional viral targets during CRISPR-Cas adaptation. *Nature,* 519**,** 199-202.

HERMAN, P. K. & EMR, S. D. 1990. Characterization of VPS34, a gene required for vacuolar protein sorting and vacuole segregation in Saccharomyces cerevisiae. *Mol Cell Biol,* 10**,** 6742-54.

HICKINSON, D. M., KLINOWSKA, T., SPEAKE, G., VINCENT, J., TRIGWELL, C., ANDERTON, J., BECK, S., MARSHALL, G., DAVENPORT, S., CALLIS, R., MILLS, E., GROSIOS, K., SMITH, P., BARLAAM, B., WILKINSON, R. W. & OGILVIE, D. 2010. AZD8931, an equipotent, reversible inhibitor of signaling by epidermal growth factor receptor, ERBB2 (HER2), and ERBB3: a unique agent for simultaneous ERBB receptor blockade in cancer. *Clin Cancer Res,* 16**,** 1159-69.

HIEN, T. T., THUY-NHIEN, N. T., PHU, N. H., BONI, M. F., THANH, N. V., NHA-CA, N. T., THAI LE, H., THAI, C. Q., TOI, P. V., THUAN, P. D., LONG LE, T., DONG LE, T., MERSON, L., DOLECEK, C., STEPNIEWSKA, K., RINGWALD, P., WHITE, N. J., FARRAR, J. & WOLBERS, M. 2012. In vivo susceptibility of Plasmodium falciparum to artesunate in Binh Phuoc Province, Vietnam. *Malar J,* 11**,** 355.

HIRAO, A., IMAI, A., SUGIE, Y., YAMADA, Y., HAYASHI, S. & TOIDE, K. 2008. Pharmacological Characterization of the Newly Synthesized Nociceptin/Orphanin FQ–Receptor Agonist 1-[1-(1-Methylcyclooctyl)-4-piperidinyl]-2-[(3R)-3-piperidinyl]-1H-benzimidazole as an Anxiolytic Agent. *Journal of Pharmacological Sciences,* 106**,** 361-368.

HOEFLICH, K. P., MERCHANT, M., ORR, C., CHAN, J., DEN OTTER, D., BERRY, L., KASMAN, I., KOEPPEN, H., RICE, K., YANG, N.-Y., ENGST, S., JOHNSTON, S., FRIEDMAN, L. S. & BELVIN, M. 2012. Intermittent Administration of MEK Inhibitor GDC-0973 plus PI3K Inhibitor GDC-0941 Triggers Robust Apoptosis and Tumor Growth Inhibition. *Cancer Research,* 72**,** 210-219.

HOMMELSHEIM, C. M., FRANTZESKAKIS, L., HUANG, M. & ULKER, B. 2014. PCR amplification of repetitive DNA: a limitation to genome editing technologies and many other applications. *Sci Rep,* 4**,** 5052.

HOSHEN, M. B., NA-BANGCHANG, K., STEIN, W. D. & GINSBURG, H. 2000. Mathematical modelling of the chemotherapy of Plasmodium falciparum malaria with artesunate: postulation of 'dormancy', a partial cytostatic effect of the drug, and its implication for treatment regimens. *Parasitology,* 121 (Pt 3)**,** 237-46.

HOTT, A., CASANDRA, D., SPARKS, K. N., MORTON, L. C., CASTANARES, G. G., RUTTER, A. & KYLE, D. E. 2015a. Artemisinin-resistant Plasmodium falciparum parasites exhibit altered patterns of development in infected erythrocytes. *Antimicrob Agents Chemother,* 59**,** 3156-67.

HOTT, A., TUCKER, M. S., CASANDRA, D., SPARKS, K. & KYLE, D. E. 2015b. Fitness of artemisinin-resistant Plasmodium falciparum in vitro. *Journal of Antimicrobial Chemotherapy,* 70**,** 2787-2796.

HOYER-HANSEN, M., BASTHOLM, L., SZYNIAROWSKI, P., CAMPANELLA, M., SZABADKAI, G., FARKAS, T., BIANCHI, K., FEHRENBACHER, N., ELLING, F., RIZZUTO, R., MATHIASEN, I. S. & JAATTELA, M. 2007.

Control of macroautophagy by calcium, calmodulin-dependent kinase kinase-beta, and Bcl-2. *Mol Cell,* 25**,** 193-205.

HSU, P. D., SCOTT, D. A., WEINSTEIN, J. A., RAN, F. A., KONERMANN, S., AGARWALA, V., LI, Y., FINE, E. J., WU, X., SHALEM, O., CRADICK, T. J., MARRAFFINI, L. A., BAO, G. & ZHANG, F. 2013. DNA targeting specificity of RNA-guided Cas9 nucleases. *Nat Biotechnol,* 31**,** 827-32.

HU, M., ZOU, Y., NAMBIAR, S. M., LEE, J., YANG, Y. & DAI, G. 2014. Keap1 modulates the redox cycle and hepatocyte cell cycle in regenerating liver. *Cell Cycle,* 13**,** 2349-58.

HUANG, F., TAKALA-HARRISON, S., JACOB, C. G., LIU, H., SUN, X., YANG, H., NYUNT, M. M., ADAMS, M., ZHOU, S., XIA, Z., RINGWALD, P., BUSTOS, M. D., TANG, L. & PLOWE, C. V. 2015. A Single Mutation in K13 Predominates in Southern China and Is Associated With Delayed Clearance of Plasmodium falciparum Following Artemisinin Treatment. *J Infect Dis,* 212**,** 1629-35.

HUANG, P., FENG, L., OLDHAM, E. A., KEATING, M. J. & PLUNKETT, W. 2000. Superoxide dismutase as a target for the selective killing of cancer cells. *Nature,* 407**,** 390-5.

HUGHES, A. L. 2004. The evolution of amino acid repeat arrays in Plasmodium and other organisms. *J Mol Evol,* 59**,** 528-35.

HUI, G. N., PALMER, K. L. & SIDDIQUI, W. A. 1983. Synchronization of Plasmodium falciparum in continuous in vitro culture: use of colchicine. *Am J Trop Med Hyg,* 32**,** 1451-3.

HUNT, N. H., MANDUCI, N. & THUMWOOD, C. M. 1993. Amelioration of murine cerebral malaria by dietary restriction. *Parasitology,* 107 (Pt 5)**,** 471-6.

ICHIKAWA, T., YANO, Y., FUJITA, Y., KASHIWABARA, T. & NAGAO, K. 2008. The enhancement effect of three sugar alcohols on the fungicidal effect of benzethonium chloride toward Candida albicans. *J Dent,* 36**,** 965-8.

ICHIMURA, Y., KIRISAKO, T., TAKAO, T., SATOMI, Y., SHIMONISHI, Y., ISHIHARA, N., MIZUSHIMA, N., TANIDA, I., KOMINAMI, E., OHSUMI, M., NODA, T. & OHSUMI, Y. 2000. A ubiquitin-like system mediates protein lipidation. *Nature,* 408**,** 488-92.

INGLESE, J., AULD, D. S., JADHAV, A., JOHNSON, R. L., SIMEONOV, A., YASGAR, A., ZHENG, W. & AUSTIN, C. P. 2006. Quantitative high-

throughput screening: A titration-based approach that efficiently identifies biological activities in large chemical libraries. *Proceedings of the National Academy of Sciences of the United States of America,* 103**,** 11473-11478.

INSELBURG, J. & BANYAL, H. S. 1984. Plasmodium falciparum: synchronization of asexual development with aphidicolin, a DNA synthesis inhibitor. *Exp Parasitol,* 57**,** 48-54.

ISTVAN, E. S., DHARIA, N. V., BOPP, S. E., GLUZMAN, I., WINZELER, E. A. & GOLDBERG, D. E. 2011. Validation of isoleucine utilization targets in Plasmodium falciparum. *Proc Natl Acad Sci U S A,* 108**,** 1627-32.

ITOH, K., WAKABAYASHI, N., KATOH, Y., ISHII, T., IGARASHI, K., ENGEL, J. D. & YAMAMOTO, M. 1999. Keap1 represses nuclear activation of antioxidant responsive elements by Nrf2 through binding to the amino-terminal Neh2 domain. *Genes Dev,* 13**,** 76-86.

ITOH, K., WAKABAYASHI, N., KATOH, Y., ISHII, T., O'CONNOR, T. & YAMAMOTO, M. 2003. Keap1 regulates both cytoplasmic-nuclear shuttling and degradation of Nrf2 in response to electrophiles. *Genes Cells,* 8**,** 379-91.

IWAMURA, Y., HAYASHI, J., SATO, T., SATO, S., MURAKAMI, T., FUJIMURA, T., SASAKI, Y., OKADA, K., TAKAHASHI, E., KIKUCHI, T., AINO, M., NOGUCHI, T., SHIMAZAKI, Y., MITANI, A. & FUKUDA, M. 2016. Assessment of oral malodor and tonsillar microbiota after gargling with benzethonium chloride. *J Oral Sci,* 58**,** 83-91.

JACKSON, K. E., KLONIS, N., FERGUSON, D. J., ADISA, A., DOGOVSKI, C. & TILLEY, L. 2004. Food vacuole-associated lipid bodies and heterogeneous lipid environments in the malaria parasite, Plasmodium falciparum. *Mol Microbiol,* 54**,** 109-22.

JANSE, C. J., FRANKE-FAYARD, B., MAIR, G. R., RAMESAR, J., THIEL, C., ENGELMANN, S., MATUSCHEWSKI, K., GEMERT, G. J. V., SAUERWEIN, R. W. & WATERS, A. P. 2006. High efficiency transfection of Plasmodium berghei facilitates novel selection procedures. *Molecular and Biochemical Parasitology,* 145**,** 60-70.

JANSE, C. J., PONNUDURAI, T., LENSEN, A. H., MEUWISSEN, J. H., RAMESAR, J., VAN DER PLOEG, M. & OVERDULVE, J. P. 1988. DNA synthesis in gametocytes of Plasmodium falciparum. *Parasitology,* 96 (Pt 1)**,** 1-7.

JAYABALASINGHAM, B., BANO, N. & COPPENS, I. 2010. Metamorphosis of the malaria parasite in the liver is associated with organelle clearance. *Cell Research,* 20**,** 1043.

JAYABALASINGHAM, B., VOSS, C., EHRENMAN, K., ROMANO, J. D., SMITH, M. E., FIDOCK, D. A., BOSCH, J. & COPPENS, I. 2014. Characterization of the ATG8-conjugation system in 2 Plasmodium species with special focus on the liver stage. *Autophagy,* 10**,** 269-284.

JEAN, S. & KIGER, A. A. 2014. Classes of phosphoinositide 3-kinases at a glance. *Journal of Cell Science,* 127**,** 923-928.

JIA, K. & LEVINE, B. 2007. Autophagy is required for dietary restriction-mediated life span extension in C. elegans. *Autophagy,* 3**,** 597-9.

JIN, M., HE, D., BACKUES, S. K., FREEBERG, M. A., LIU, X., KIM, J. K. & KLIONSKY, D. J. 2014. Transcriptional regulation by Pho23 modulates the frequency of autophagosome formation. *Curr Biol,* 24**,** 1314-1322.

JIN, S. & WHITE, E. 2007. Role of autophagy in cancer: management of metabolic stress. *Autophagy,* 3**,** 28-31.

JINEK, M., CHYLINSKI, K., FONFARA, I., HAUER, M., DOUDNA, J. A. & CHARPENTIER, E. 2012. A programmable dual-RNA-guided DNA endonuclease in adaptive bacterial immunity. *Science,* 337**,** 816-21.

JINEK, M., JIANG, F., TAYLOR, D. W., STERNBERG, S. H., KAYA, E., MA, E., ANDERS, C., HAUER, M., ZHOU, K., LIN, S., KAPLAN, M., IAVARONE, A. T., CHARPENTIER, E., NOGALES, E. & DOUDNA, J. A. 2014. Structures of Cas9 endonucleases reveal RNA-mediated conformational activation. *Science,* 343**,** 1247997.

JOHNSTON, J. C., SHAHIDI, N. C., SADATSAFAVI, M. & FITZGERALD, J. M. 2009. Treatment outcomes of multidrug-resistant tuberculosis: a systematic review and meta-analysis. *PLoS One,* 4**,** e6914.

JOMAA, H., WIESNER, J., SANDERBRAND, S., ALTINCICEK, B., WEIDEMEYER, C., HINTZ, M., TURBACHOVA, I., EBERL, M., ZEIDLER, J., LICHTENTHALER, H. K., SOLDATI, D. & BECK, E. 1999. Inhibitors of the nonmevalonate pathway of isoprenoid biosynthesis as antimalarial drugs. *Science,* 285**,** 1573-6.

JORDAN, M. A., THROWER, D. & WILSON, L. 1991. Mechanism of Inhibition of Cell Proliferation by Vinca Alkaloids. *Cancer Research,* 51**,** 2212-2222.

JOSHI, M. C., KUMAR, K. & KUMAR, V. 2014. Potent phosphatidylinositol 3-kinase inhibitors and their biology. *Curr Drug Discov Technol,* 11**,** 113-26.

JOSLING, G. A. & LLINÁS, M. 2015. Sexual development in Plasmodium parasites: knowing when it's time to commit. *Nature Reviews Microbiology,* 13**,** 573.

JOYCE, J. A., BARUCH, A., CHEHADE, K., MEYER-MORSE, N., GIRAUDO, E., TSAI, F. Y., GREENBAUM, D. C., HAGER, J. H., BOGYO, M. & HANAHAN, D. 2004. Cathepsin cysteine proteases are effectors of invasive growth and angiogenesis during multistage tumorigenesis. *Cancer Cell,* 5**,** 443-53.

JUNG, C. H., JUN, C. B., RO, S. H., KIM, Y. M., OTTO, N. M., CAO, J., KUNDU, M. & KIM, D. H. 2009. ULK-Atg13-FIP200 complexes mediate mTOR signaling to the autophagy machinery. *Mol Biol Cell,* 20**,** 1992-2003.

KABEYA, Y., MIZUSHIMA, N., UENO, T., YAMAMOTO, A., KIRISAKO, T., NODA, T., KOMINAMI, E., OHSUMI, Y. & YOSHIMORI, T. 2000. LC3, a mammalian homologue of yeast Apg8p, is localized in autophagosome membranes after processing. *Embo j,* 19**,** 5720-8.

KABEYA, Y., NODA, N. N., FUJIOKA, Y., SUZUKI, K., INAGAKI, F. & OHSUMI, Y. 2009. Characterization of the Atg17-Atg29-Atg31 complex specifically required for starvation-induced autophagy in Saccharomyces cerevisiae. *Biochem Biophys Res Commun,* 389**,** 612-5.

KAIN, K. C., HARRINGTON, M. A., TENNYSON, S. & KEYSTONE, J. S. 1998. Imported malaria: prospective analysis of problems in diagnosis and management. *Clin Infect Dis,* 27**,** 142-9.

KAISER, G., DE NIZ, M., BURDA, P.-C., NIKLAUS, L., STANWAY, R. L. & HEUSSLER, V. 2017. Generation of transgenic rodent malaria parasites by transfection of cell culture-derived merozoites. *Malaria Journal,* 16**,** 305.

KAMADA, Y., FUNAKOSHI, T., SHINTANI, T., NAGANO, K., OHSUMI, M. & OHSUMI, Y. 2000. Tor-mediated induction of autophagy via an Apg1 protein kinase complex. *J Cell Biol,* 150**,** 1507-13.

KAN, O., BALDWIN, S. A. & WHETTON, A. D. 1994. Apoptosis is regulated by the rate of glucose transport in an interleukin 3 dependent cell line. *The Journal of Experimental Medicine,* 180**,** 917-923.

KANNAN, R., SAHAL, D. & CHAUHAN, V. S. 2002. Heme-Artemisinin Adducts Are Crucial Mediators of the Ability of Artemisinin to Inhibit Heme Polymerization. *Chemistry & Biology,* 9**,** 321-332.

KATAYAMA, Y., BATTISTA, M., KAO, W.-M., HIDALGO, A., PEIRED, A. J., THOMAS, S. A. & FRENETTE, P. S. 2006. Signals from the Sympathetic Nervous System Regulate Hematopoietic Stem Cell Egress from Bone Marrow. *Cell,* 124**,** 407-421.

KAZADI MULOMBO, W. Updates of the Greater Mekong Subregion Elimination Strategy. Malaria Policy Advisory Committee (MPAC), 2015 Geneva.

KHEANG, S. T., SOVANNAROTH, S., EK, S., CHY, S., CHHUN, P., MAO, S., NGUON, S., LEK, D. S., MENARD, D. & KAK, N. 2017. Prevalence of K13 mutation and Day-3 positive parasitaemia in artemisinin-resistant malaria endemic area of Cambodia: a cross-sectional study. *Malaria Journal,* 16**,** 372.

KIHARA, A., NODA, T., ISHIHARA, N. & OHSUMI, Y. 2001. Two distinct Vps34 phosphatidylinositol 3-kinase complexes function in autophagy and carboxypeptidase Y sorting in Saccharomyces cerevisiae. *J Cell Biol,* 152**,** 519-30.

KIM, J., KUNDU, M., VIOLLET, B. & GUAN, K.-L. 2011. AMPK and mTOR regulate autophagy through direct phosphorylation of Ulk1. *Nature Cell Biology,* 13**,** 132.

KIRISAKO, T., BABA, M., ISHIHARA, N., MIYAZAWA, K., OHSUMI, M., YOSHIMORI, T., NODA, T. & OHSUMI, Y. 1999. Formation Process of Autophagosome Is Traced with Apg8/Aut7p in Yeast. *The Journal of Cell Biology,* 147**,** 435-446.

KIRK, K., HORNER, H. A. & KIRK, J. 1996. Glucose uptake in Plasmodium falciparum-infected erythrocytes is an equilibrative not an active process. *Molecular and Biochemical Parasitology,* 82**,** 195-205.

KIRSHNER, J. R., HE, S., BALASUBRAMANYAM, V., KEPROS, J., YANG, C.-Y., ZHANG, M., DU, Z., BARSOUM, J. & BERTIN, J. 2008. Elesclomol induces cancer cell apoptosis through oxidative stress. *Molecular Cancer Therapeutics,* 7**,** 2319-2327.

KITADA, T., ASAKAWA, S., HATTORI, N., MATSUMINE, H., YAMAMURA, Y., MINOSHIMA, S., YOKOCHI, M., MIZUNO, Y. & SHIMIZU, N. 1998. Mutations in the parkin gene cause autosomal recessive juvenile parkinsonism. *Nature,* 392**,** 605-8.

KITAMURA, K., KISHI-ITAKURA, C., TSUBOI, T., SATO, S., KITA, K., OHTA, N. & MIZUSHIMA, N. 2012. Autophagy-related Atg8 localizes to the apicoplast of the human malaria parasite Plasmodium falciparum. *PLoS One,* 7**,** e42977.

KLIONSKY, D. J., ABDELMOHSEN, K., ABE, A., ABEDIN, M. J., ABELIOVICH, H., ACEVEDO AROZENA, A., ADACHI, H., ADAMS, C. M., ADAMS, P. D., ADELI, K., ADHIHETTY, P. J., ADLER, S. G., AGAM, G., AGARWAL, R., AGHI, M. K., AGNELLO, M., AGOSTINIS, P., AGUILAR, P. V., AGUIRRE-GHISO, J., AIROLDI, E. M., AIT-SI-ALI, S., AKEMATSU, T., AKPORIAYE, E. T., AL-RUBEAI, M., ALBAICETA, G. M., ALBANESE, C., ALBANI, D., ALBERT, M. L., ALDUDO, J., ALGÜL, H., ALIREZAEI, M., ALLOZA, I., ALMASAN, A., ALMONTE-BECERIL, M., ALNEMRI, E. S., ALONSO, C., ALTAN-BONNET, N., ALTIERI, D. C., ALVAREZ, S., ALVAREZ-ERVITI, L., ALVES, S., AMADORO, G., AMANO, A., AMANTINI, C., AMBROSIO, S., AMELIO, I., AMER, A. O., AMESSOU, M., AMON, A., AN, Z., ANANIA, F. A., ANDERSEN, S. U., ANDLEY, U. P., ANDREADI, C. K., ANDRIEU-ABADIE, N., ANEL, A., ANN, D. K., ANOOPKUMAR-DUKIE, S., ANTONIOLI, M., AOKI, H., APOSTOLOVA, N., AQUILA, S., AQUILANO, K., ARAKI, K., ARAMA, E., ARANDA, A., ARAYA, J., ARCARO, A., ARIAS, E., ARIMOTO, H., ARIOSA, A. R., ARMSTRONG, J. L., ARNOULD, T., ARSOV, I., ASANUMA, K., ASKANAS, V., ASSELIN, E., ATARASHI, R., ATHERTON, S. S., ATKIN, J. D., ATTARDI, L. D., AUBERGER, P., AUBURGER, G., AURELIAN, L., AUTELLI, R., AVAGLIANO, L., AVANTAGGIATI, M. L., AVRAHAMI, L., AWALE, S., AZAD, N., BACHETTI, T., BACKER, J. M., BAE, D.-H., BAE, J.-S., BAE, O.-N., BAE, S. H., BAEHRECKE, E. H., BAEK, S.-H., BAGHDIGUIAN, S., BAGNIEWSKA-ZADWORNA, A., et al. 2016. Guidelines for the use and interpretation of assays for monitoring autophagy (3rd edition). *Autophagy,* 12**,** 1-222.

KLONIS, N., CREEK, D. J. & TILLEY, L. 2013a. Iron and heme metabolism in Plasmodium falciparum and the mechanism of action of artemisinins. *Current Opinion in Microbiology,* 16**,** 722-727.

KLONIS, N., CRESPO-ORTIZ, M. P., BOTTOVA, I., ABU-BAKAR, N., KENNY, S., ROSENTHAL, P. J. & TILLEY, L. 2011. Artemisinin activity against Plasmodium falciparum requires hemoglobin uptake and digestion. *Proc Natl Acad Sci U S A,* 108**,** 11405-10.

KLONIS, N., XIE, S. C., MCCAW, J. M., CRESPO-ORTIZ, M. P., ZALOUMIS, S. G., SIMPSON, J. A. & TILLEY, L. 2013b. Altered temporal response of malaria parasites determines differential sensitivity to artemisinin. *Proc Natl Acad Sci U S A,* 110**,** 5157-62.

KOBAYASHI, A., KANG, M. I., OKAWA, H., OHTSUJI, M., ZENKE, Y., CHIBA, T., IGARASHI, K. & YAMAMOTO, M. 2004. Oxidative stress sensor Keap1 functions as an adaptor for Cul3-based E3 ligase to regulate proteasomal degradation of Nrf2. *Mol Cell Biol,* 24**,** 7130-9.

KOCHL, R., HU, X. W., CHAN, E. Y. & TOOZE, S. A. 2006. Microtubules facilitate autophagosome formation and fusion of autophagosomes with endosomes. *Traffic,* 7**,** 129-45.

KOMATSU, M., KUROKAWA, H., WAGURI, S., TAGUCHI, K., KOBAYASHI, A., ICHIMURA, Y., SOU, Y.-S., UENO, I., SAKAMOTO, A., TONG, K. I., KIM, M., NISHITO, Y., IEMURA, S.-I., NATSUME, T., UENO, T., KOMINAMI, E., MOTOHASHI, H., TANAKA, K. & YAMAMOTO, M. 2010. The selective autophagy substrate p62 activates the stress responsive transcription factor Nrf2 through inactivation of Keap1. *Nature Cell Biology,* 12**,** 213.

KON, M., KIFFIN, R., KOGA, H., CHAPOCHNICK, J., MACIAN, F., VARTICOVSKI, L. & CUERVO, A. M. 2011. Chaperone-Mediated Autophagy Is Required for Tumor Growth. *Science Translational Medicine,* 3**,** 109ra117-109ra117.

KONG-HAP, M. A., MOUAMMINE, A., DAHER, W., BERRY, L., LEBRUN, M., DUBREMETZ, J.-F. & BESTEIRO, S. 2013. Regulation of ATG8 membrane association by ATG4 in the parasitic protist Toxoplasma gondii. *Autophagy,* 9**,** 1334-1348.

KONG, L., WANG, S., WU, X., ZUO, F., QIN, H. & WU, J. 2016. Paeoniflorin attenuates ultraviolet B-induced apoptosis in human keratinocytes by inhibiting the ROS-p38-p53 pathway. *Mol Med Rep,* 13**,** 3553-8.

KOUROKU, Y., FUJITA, E., TANIDA, I., UENO, T., ISOAI, A., KUMAGAI, H., OGAWA, S., KAUFMAN, R. J., KOMINAMI, E. & MOMOI, T. 2007. ER stress (PERK/eIF2alpha phosphorylation) mediates the polyglutamine-induced LC3 conversion, an essential step for autophagy formation. *Cell Death Differ,* 14**,** 230-9.

KRICK, R., BUSSE, R. A., SCACIOC, A., STEPHAN, M., JANSHOFF, A., THUMM, M. & KUHNEL, K. 2012. Structural and functional characterization of the two phosphoinositide binding sites of PROPPINs, a beta-propeller protein family. *Proc Natl Acad Sci U S A,* 109**,** E2042-9.

KRISHNA, S., PULCINI, S., FATIH, F. & STAINES, H. 2010. Artemisinins and the biological basis for the PfATP6/SERCA hypothesis. *Trends in Parasitology*, 26**,** 517-523.

KROEMER, G. & JAATTELA, M. 2005. Lysosomes and autophagy in cell death control. *Nat Rev Cancer,* 5**,** 886-97.

KRUGLIAK, M. & GINSBURG, H. 2006. The evolution of the new permeability pathways in Plasmodium falciparum—infected erythrocytes—a kinetic analysis. *Experimental Parasitology,* 114**,** 253-258.

KUBLIN, J. G., CORTESE, J. F., NJUNJU, E. M., G. MUKADAM, R. A., WIRIMA, J. J., KAZEMBE, P. N., DJIMDÉ, A. A., KOURIBA, B., TAYLOR, T. E. & PLOWE, C. V. 2003. Reemergence of Chloroquine-Sensitive Plasmodium falciparum Malaria after Cessation of Chloroquine Use in Malawi. *The Journal of Infectious Diseases,* 187**,** 1870-1875.

KUILMAN, T., MICHALOGLOU, C., MOOI, W. J. & PEEPER, D. S. 2010. The essence of senescence. *Genes Dev,* 24**,** 2463-79.

KUN, Z., HANQING, G., HAILING, T., YUAN, Y., JUN, Z., LINGXIA, Z., KUN, H. & XIN, Z. 2017. Gastrin Enhances Autophagy and Promotes Gastric Carcinoma Proliferation via Inducing AMPKalpha. *Oncol Res,* 25**,** 1399-1407.

KUNKEL, T. A. & BEBENEK, K. 2000. DNA replication fidelity. *Annu Rev Biochem,* 69**,** 497-529.

KUO, G.-H., DEANGELIS, A., EMANUEL, S., WANG, A., ZHANG, Y., CONNOLLY, P. J., CHEN, X., GRUNINGER, R. H., RUGG, C., FUENTES-

PESQUERA, A., MIDDLETON, S. A., JOLLIFFE, L. & MURRAY, W. V. 2005. Synthesis and Identification of [1,3,5]Triazine-pyridine Biheteroaryl as a Novel Series of Potent Cyclin-Dependent Kinase Inhibitors. *Journal of Medicinal Chemistry,* 48**,** 4535-4546.

KUTATELADZE, T. G. 2010. Translation of the phosphoinositide code by PI effectors. *Nat Chem Biol,* 6**,** 507-13.

KUTATELADZE, T. G., OGBURN, K. D., WATSON, W. T., DE BEER, T., EMR, S. D., BURD, C. G. & OVERDUIN, M. 1999. Phosphatidylinositol 3-phosphate recognition by the FYVE domain. *Mol Cell,* 3**,** 805-11.

KYAW, M. P., NYUNT, M. H., CHIT, K., AYE, M. M., AYE, K. H., AYE, M. M., LINDEGARDH, N., TARNING, J., IMWONG, M., JACOB, C. G., RASMUSSEN, C., PERIN, J., RINGWALD, P. & NYUNT, M. M. 2013. Reduced susceptibility of Plasmodium falciparum to artesunate in southern Myanmar. *PLoS One,* 8**,** e57689.

LACRUE, A. N., SCHEEL, M., KENNEDY, K., KUMAR, N. & KYLE, D. E. 2011. Effects of artesunate on parasite recrudescence and dormancy in the rodent malaria model Plasmodium vinckei. *PLoS One,* 6**,** e26689.

LAKSHMANAN, V., BRAY, P. G., VERDIER-PINARD, D., JOHNSON, D. J., HORROCKS, P., MUHLE, R. A., ALAKPA, G. E., HUGHES, R. H., WARD, S. A., KROGSTAD, D. J., SIDHU, A. B. & FIDOCK, D. A. 2005. A critical role for PfCRT K76T in Plasmodium falciparum verapamil-reversible chloroquine resistance. *Embo j,* 24**,** 2294-305.

LAMBROS, C. & VANDERBERG, J. P. 1979. Synchronization of Plasmodium falciparum erythrocytic stages in culture. *J Parasitol,* 65**,** 418-20.

LANDIER, J., PARKER, D. M., THU, A. M., CARRARA, V. I., LWIN, K. M., BONNINGTON, C. A., PUKRITTAYAKAMEE, S., DELMAS, G. & NOSTEN, F. H. 2016. The role of early detection and treatment in malaria elimination. *Malar J,* 15**,** 363.

LANG, E., JILANI, K., ZELENAK, C., PASHAM, V., BOBBALA, D., QADRI, S. M. & LANG, F. 2011. Stimulation of suicidal erythrocyte death by benzethonium. *Cell Physiol Biochem,* 28**,** 347-54.

LANGRETH, S. G., JENSEN, J. B., REESE, R. T. & TRAGER, W. 1978. Fine structure of human malaria in vitro. *J Protozool,* 25**,** 443-52.

LAZARUS, M. D., SCHNEIDER, T. G. & TARASCHI, T. F. 2008. A new model for hemoglobin ingestion and transport by the human malaria parasite Plasmodium falciparum. *Journal of Cell Science,* 121**,** 1937-1949.

LEHANE, A. M., HAYWARD, R., SALIBA, K. J. & KIRK, K. 2008. A verapamil-sensitive chloroquine-associated H+ leak from the digestive vacuole in chloroquine-resistant malaria parasites. *J Cell Sci,* 121**,** 1624-32.

LEHANE, A. M. & KIRK, K. 2008. Chloroquine resistance-conferring mutations in pfcrt give rise to a chloroquine-associated H+ leak from the malaria parasite's digestive vacuole. *Antimicrob Agents Chemother,* 52**,** 4374-80.

LELIEVRE, J., BERRY, A. & BENOIT-VICAL, F. 2005. An alternative method for Plasmodium culture synchronization. *Exp Parasitol,* 109**,** 195-7.

LEONG, F. J., ZHAO, R., ZENG, S., MAGNUSSON, B., DIAGANA, T. T. & PERTEL, P. 2014. A first-in-human randomized, double-blind, placebo-controlled, single- and multiple-ascending oral dose study of novel Imidazolopiperazine KAF156 to assess its safety, tolerability, and pharmacokinetics in healthy adult volunteers. *Antimicrob Agents Chemother,* 58**,** 6437-43.

LEVEQUE, M. F., BERRY, L., CIPRIANO, M. J., NGUYEN, H. M., STRIEPEN, B. & BESTEIRO, S. 2015. Autophagy-Related Protein ATG8 Has a Noncanonical Function for Apicoplast Inheritance in Toxoplasma gondii. *MBio,* 6**,** e01446-15.

LEVINE, B. & KROEMER, G. 2008. Autophagy in the Pathogenesis of Disease. *Cell,* 132**,** 27-42.

LI, G., GUO, X., ARNOLD, K., JIAN, H. & FU, L. 1984. Randomised comparative study of mefloquine, qinghaosu, and pyrimethamine-sulfadoxine in patients with falciparum malaria. *The Lancet,* 324**,** 1360-1361.

LI, H., O'DONOGHUE, A. J., VAN DER LINDEN, W. A., XIE, S. C., YOO, E., FOE, I. T., TILLEY, L., CRAIK, C. S., DA FONSECA, P. C. & BOGYO, M. 2016. Structure- and function-based design of Plasmodium-selective proteasome inhibitors. *Nature,* 530**,** 233-6.

LI, J., LIU, R., LEI, Y., WANG, K., LAU, Q. C., XIE, N., ZHOU, S., NIE, C., CHEN, L., WEI, Y. & HUANG, C. 2010. Proteomic analysis revealed association of aberrant ROS signaling with suberoylanilide hydroxamic acid-induced autophagy in Jurkat T-leukemia cells. *Autophagy,* 6**,** 711-24.

LI, J. & ZHOU, B. 2010. Biological actions of artemisinin: insights from medicinal chemistry studies. *Molecules,* 15**,** 1378-97.

LI, Q. G., PEGGINS, J. O., FLECKENSTEIN, L. L., MASONIC, K., HEIFFER, M. H. & BREWER, T. G. 1998. The pharmacokinetics and bioavailability of dihydroartemisinin, arteether, artemether, artesunic acid and artelinic acid in rats. *J Pharm Pharmacol,* 50**,** 173-82.

LIANG, X. H., JACKSON, S., SEAMAN, M., BROWN, K., KEMPKES, B., HIBSHOOSH, H. & LEVINE, B. 1999. Induction of autophagy and inhibition of tumorigenesis by beclin 1. *Nature,* 402**,** 672.

LIM, P., DEK, D., TRY, V., EASTMAN, R. T., CHY, S., SRENG, S., SUON, S., MAO, S., SOPHA, C., SAM, B., ASHLEY, E. A., MIOTTO, O., DONDORP, A. M., WHITE, N. J., SU, X. Z., CHAR, M. C., ANDERSON, J. M., AMARATUNGA, C., MENARD, D. & FAIRHURST, R. M. 2013. Ex vivo susceptibility of Plasmodium falciparum to antimalarial drugs in western, northern, and eastern Cambodia, 2011-2012: association with molecular markers. *Antimicrob Agents Chemother,* 57**,** 5277-83.

LIM, P., DEK, D., TRY, V., SRENG, S., SUON, S. & FAIRHURST, R. M. 2015. Decreasing pfmdr1 copy number suggests that Plasmodium falciparum in Western Cambodia is regaining in vitro susceptibility to mefloquine. *Antimicrob Agents Chemother,* 59**,** 2934-7.

LIU, J., ISTVAN, E. S., GLUZMAN, I. Y., GROSS, J. & GOLDBERG, D. E. 2006. Plasmodium falciparum ensures its amino acid supply with multiple acquisition pathways and redundant proteolytic enzyme systems. *Proceedings of the National Academy of Sciences,* 103**,** 8840-8845.

LIU, J. T., LI, W. C., GAO, S., WANG, F., LI, X. Q., YU, H. Q., FAN, L. L., WEI, W., WANG, H. & SUN, G. P. 2015. Autophagy Inhibition Overcomes the Antagonistic Effect Between Gefitinib and Cisplatin in Epidermal Growth Factor Receptor Mutant Non--Small-Cell Lung Cancer Cells. *Clin Lung Cancer,* 16**,** e55-66.

LIU, Y. L., YANG, P. M., SHUN, C. T., WU, M. S., WENG, J. R. & CHEN, C. C. 2010. Autophagy potentiates the anti-cancer effects of the histone deacetylase inhibitors in hepatocellular carcinoma. *Autophagy,* 6**,** 1057-65.

LOOAREESUWAN, S. 1994. Overview of clinical studies on artemisinin derivatives in Thailand. *Trans R Soc Trop Med Hyg,* 88 Suppl 1**,** S9-11.

LOYTER, A., SCANGOS, G., JURICEK, D., KEENE, D. & RUDDLE, F. H. 1982. Mechanisms of DNA entry into mammalian cells. II. Phagocytosis of calcium phosphate DNA co-precipitate visualized by electron microscopy. *Exp Cell Res,* 139**,** 223-34.

LU, Q., YANG, P., HUANG, X., HU, W., GUO, B., WU, F., LIN, L., KOVACS, A. L., YU, L. & ZHANG, H. 2011. The WD40 repeat PtdIns(3)P-binding protein EPG-6 regulates progression of omegasomes to autophagosomes. *Dev Cell,* 21**,** 343-57.

LU, Z., LUO, R. Z., LU, Y., ZHANG, X., YU, Q., KHARE, S., KONDO, S., KONDO, Y., YU, Y., MILLS, G. B., LIAO, W. S. & BAST, R. C., JR. 2008. The tumor suppressor gene ARHI regulates autophagy and tumor dormancy in human ovarian cancer cells. *J Clin Invest,* 118**,** 3917-29.

LUM, J. J., BAUER, D. E., KONG, M., HARRIS, M. H., LI, C., LINDSTEN, T. & THOMPSON, C. B. 2005. Growth factor regulation of autophagy and cell survival in the absence of apoptosis. *Cell,* 120**,** 237-48.

MA, Q. 2013. Role of nrf2 in oxidative stress and toxicity. *Annu Rev Pharmacol Toxicol,* 53**,** 401-26.

MAIER, A. G., BRAKS, J. A., WATERS, A. P. & COWMAN, A. F. 2006. Negative selection using yeast cytosine deaminase/uracil phosphoribosyl transferase in Plasmodium falciparum for targeted gene deletion by double crossover recombination. *Mol Biochem Parasitol,* 150**,** 118-21.

MAMOUN, C. B., GLUZMAN, I. Y., GOYARD, S., BEVERLEY, S. M. & GOLDBERG, D. E. 1999a. A set of independent selectable markers for transfection of the human malaria parasite Plasmodium falciparum. *Proc Natl Acad Sci U S A,* 96**,** 8716-20.

MAMOUN, C. B., TRUONG, R., GLUZMAN, I., AKOPYANTS, N. S., OKSMAN, A. & GOLDBERG, D. E. 1999b. Transfer of genes into Plasmodium falciparum by polyamidoamine dendrimers. *Mol Biochem Parasitol,* 103**,** 117-21.

MANCIO-SILVA, L., SLAVIC, K., GRILO RUIVO, M. T., GROSSO, A. R., MODRZYNSKA, K. K., VERA, I. M., SALES-DIAS, J., GOMES, A. R., MACPHERSON, C. R., CROZET, P., ADAMO, M., BAENA-GONZALEZ, E., TEWARI, R., LLINAS, M., BILLKER, O. & MOTA, M. M. 2017. Nutrient sensing modulates malaria parasite virulence. *Nature,* 547**,** 213-216.

MANSON, P. 1894. On the Nature and Significance of the Crescentic and Flagellated Bodies in Malarial Blood. *British Medical Journal,* 2**,** 1306-1308.

MARKUS, M. B. 2011a. The hypnozoite concept, with particular reference to malaria. *Parasitology Research,* 108**,** 247-252.

MARKUS, M. B. 2011b. Malaria: origin of the term "hypnozoite". *J Hist Biol,* 44**,** 781-6.

MARKUS, M. B. 2015. Do hypnozoites cause relapse in malaria? *Trends in Parasitology,* 31**,** 239-245.

MARTI, M., GOOD, R. T., RUG, M., KNUEPFER, E. & COWMAN, A. F. 2004. Targeting malaria virulence and remodeling proteins to the host erythrocyte. *Science,* 306**,** 1930-3.

MARTIN, R. E. & KIRK, K. 2004. The malaria parasite's chloroquine resistance transporter is a member of the drug/metabolite transporter superfamily. *Mol Biol Evol,* 21**,** 1938-49.

MARTIN, R. E., MARCHETTI, R. V., COWAN, A. I., HOWITT, S. M., BROER, S. & KIRK, K. 2009. Chloroquine transport via the malaria parasite's chloroquine resistance transporter. *Science,* 325**,** 1680-2.

MASIERO, E., AGATEA, L., MAMMUCARI, C., BLAAUW, B., LORO, E., KOMATSU, M., METZGER, D., REGGIANI, C., SCHIAFFINO, S. & SANDRI, M. 2009. Autophagy is required to maintain muscle mass. *Cell Metab,* 10**,** 507-15.

MAUTHE, M., JACOB, A., FREIBERGER, S., HENTSCHEL, K., STIERHOF, Y. D., CODOGNO, P. & PROIKAS-CEZANNE, T. 2011. Resveratrol-mediated autophagy requires WIPI-1-regulated LC3 lipidation in the absence of induced phagophore formation. *Autophagy,* 7**,** 1448-61.

MBENGUE, A., BHATTACHARJEE, S., PANDHARKAR, T., LIU, H., ESTIU, G., STAHELIN, R. V., RIZK, S. S., NJIMOH, D. L., RYAN, Y., CHOTIVANICH, K., NGUON, C., GHORBAL, M., LOPEZ-RUBIO, J. J., PFRENDER, M., EMRICH, S., MOHANDAS, N., DONDORP, A. M., WIEST, O. & HALDAR, K. 2015. A molecular mechanism of artemisinin resistance in Plasmodium falciparum malaria. *Nature,* 520**,** 683-7.

MCCUTCHAN, J. H. & PAGANO, J. S. 1968. Enchancement of the infectivity of simian virus 40 deoxyribonucleic acid with diethylaminoethyl-dextran. *J Natl Cancer Inst,* 41**,** 351-7.

MCCUTCHAN, T. F., DAME, J. B., MILLER, L. H. & BARNWELL, J. 1984. Evolutionary relatedness of Plasmodium species as determined by the structure of DNA. *Science,* 225**,** 808-11.

MCINTOSH, M. T., VAID, A., HOSGOOD, H. D., VIJAY, J., BHATTACHARYA, A., SAHANI, M. H., BAEVOVA, P., JOINER, K. A. & SHARMA, P. 2007. Traffic to the Malaria Parasite Food Vacuole: A NOVEL PATHWAY INVOLVING A PHOSPHATIDYLINOSITOL 3-PHOSPHATE-BINDING PROTEIN. *Journal of Biological Chemistry,* 282**,** 11499-11508.

MCLEAN, K. J. & JACOBS-LORENA, M. 2017. Plasmodium falciparum Maf1 Confers Survival upon Amino Acid Starvation. *MBio,* 8.

MCNAMARA, C. W., LEE, M. C. S., LIM, C. S., LIM, S. H., ROLAND, J., NAGLE, A., SIMON, O., YEUNG, B. K. S., CHATTERJEE, A. K., MCCORMACK, S. L., MANARY, M. J., ZEEMAN, A.-M., DECHERING, K. J., KUMAR, T. R. S., HENRICH, P. P., GAGARING, K., IBANEZ, M., KATO, N., KUHEN, K. L., FISCHLI, C., ROTTMANN, M., PLOUFFE, D. M., BURSULAYA, B., MEISTER, S., RAMEH, L., TRAPPE, J., HAASEN, D., TIMMERMAN, M., SAUERWEIN, R. W., SUWANARUSK, R., RUSSELL, B., RENIA, L., NOSTEN, F., TULLY, D. C., KOCKEN, C. H. M., GLYNNE, R. J., BODENREIDER, C., FIDOCK, D. A., DIAGANA, T. T. & WINZELER, E. A. 2013. Targeting Plasmodium PI(4)K to eliminate malaria. *Nature,* 504**,** 248-253.

MEISTER, S., PLOUFFE, D. M., KUHEN, K. L., BONAMY, G. M., WU, T., BARNES, S. W., BOPP, S. E., BORBOA, R., BRIGHT, A. T., CHE, J., COHEN, S., DHARIA, N. V., GAGARING, K., GETTAYACAMIN, M., GORDON, P., GROESSL, T., KATO, N., LEE, M. C., MCNAMARA, C. W., FIDOCK, D. A., NAGLE, A., NAM, T. G., RICHMOND, W., ROLAND, J., ROTTMANN, M., ZHOU, B., FROISSARD, P., GLYNNE, R. J., MAZIER, D., SATTABONGKOT, J., SCHULTZ, P. G., TUNTLAND, T., WALKER, J. R., ZHOU, Y., CHATTERJEE, A., DIAGANA, T. T. & WINZELER, E. A. 2011. Imaging of Plasmodium liver stages to drive next-generation antimalarial drug discovery. *Science,* 334**,** 1372-7.

MEJIA, P., TREVINO-VILLARREAL, J. H., HINE, C., HARPUTLUGIL, E., LANG, S., CALAY, E., ROGERS, R., WIRTH, D., DURAISINGH, M. T. & MITCHELL, J. R. 2015. Dietary restriction protects against experimental

cerebral malaria via leptin modulation and T-cell mTORC1 suppression. *Nat Commun,* 6**,** 6050.

MENARD, D., KHIM, N., BEGHAIN, J., ADEGNIKA, A. A., SHAFIUL-ALAM, M., AMODU, O., RAHIM-AWAB, G., BARNADAS, C., BERRY, A., BOUM, Y., BUSTOS, M. D., CAO, J., CHEN, J. H., COLLET, L., CUI, L., THAKUR, G. D., DIEYE, A., DJALLE, D., DORKENOO, M. A., EBOUMBOU-MOUKOKO, C. E., ESPINO, F. E., FANDEUR, T., FERREIRA-DA-CRUZ, M. F., FOLA, A. A., FUEHRER, H. P., HASSAN, A. M., HERRERA, S., HONGVANTHONG, B., HOUZE, S., IBRAHIM, M. L., JAHIRUL-KARIM, M., JIANG, L., KANO, S., ALI-KHAN, W., KHANTHAVONG, M., KREMSNER, P. G., LACERDA, M., LEANG, R., LEELAWONG, M., LI, M., LIN, K., MAZARATI, J. B., MENARD, S., MORLAIS, I., MUHINDO-MAVOKO, H., MUSSET, L., NA-BANGCHANG, K., NAMBOZI, M., NIARE, K., NOEDL, H., OUEDRAOGO, J. B., PILLAI, D. R., PRADINES, B., QUANG-PHUC, B., RAMHARTER, M., RANDRIANARIVELOJOSIA, M., SATTABONGKOT, J., SHEIKH-OMAR, A., SILUE, K. D., SIRIMA, S. B., SUTHERLAND, C., SYAFRUDDIN, D., TAHAR, R., TANG, L. H., TOURE, O. A., TSHIBANGU-WA-TSHIBANGU, P., VIGAN-WOMAS, I., WARSAME, M., WINI, L., ZAKERI, S., KIM, S., EAM, R., BERNE, L., KHEAN, C., CHY, S., KEN, M., LOCH, K., CANIER, L., DURU, V., LEGRAND, E., BARALE, J. C., STOKES, B., STRAIMER, J., WITKOWSKI, B., FIDOCK, D. A., ROGIER, C., RINGWALD, P., ARIEY, F. & MERCEREAU-PUIJALON, O. 2016. A Worldwide Map of Plasmodium falciparum K13-Propeller Polymorphisms. *N Engl J Med,* 374**,** 2453-64.

MÉNARD, S., BEN HADDOU, T., RAMADANI, A. P., ARIEY, F., IRIART, X., BEGHAIN, J., BOUCHIER, C., WITKOWSKI, B., BERRY, A., MERCEREAU-PUIJALON, O. & BENOIT-VICAL, F. 2015. Induction of Multidrug Tolerance in Plasmodium falciparum by Extended Artemisinin Pressure. *Emerging Infectious Diseases,* 21**,** 1733-1741.

MESHNICK, S. R., YANG, Y. Z., LIMA, V., KUYPERS, F., KAMCHONWONGPAISAN, S. & YUTHAVONG, Y. 1993. Iron-dependent free radical generation from the antimalarial agent artemisinin (qinghaosu). *Antimicrobial Agents and Chemotherapy,* 37**,** 1108-1114.

MEUNIER, B. & ROBERT, A. 2010. Heme as Trigger and Target for Trioxane-Containing Antimalarial Drugs. *Accounts of Chemical Research,* 43**,** 1444-1451.

MICHELL, R. H., HEATH, V. L., LEMMON, M. A. & DOVE, S. K. 2006. Phosphatidylinositol 3,5-bisphosphate: metabolism and cellular functions. *Trends Biochem Sci,* 31**,** 52-63.

MIOTTO, O., ALMAGRO-GARCIA, J., MANSKE, M., MACINNIS, B., CAMPINO, S., ROCKETT, K. A., AMARATUNGA, C., LIM, P., SUON, S., SRENG, S., ANDERSON, J. M., DUONG, S., NGUON, C., CHUOR, C. M., SAUNDERS, D., SE, Y., LON, C., FUKUDA, M. M., AMENGA-ETEGO, L., HODGSON, A. V., ASOALA, V., IMWONG, M., TAKALA-HARRISON, S., NOSTEN, F., SU, X. Z., RINGWALD, P., ARIEY, F., DOLECEK, C., HIEN, T. T., BONI, M. F., THAI, C. Q., AMAMBUA-NGWA, A., CONWAY, D. J., DJIMDE, A. A., DOUMBO, O. K., ZONGO, I., OUEDRAOGO, J. B., ALCOCK, D., DRURY, E., AUBURN, S., KOCH, O., SANDERS, M., HUBBART, C., MASLEN, G., RUANO-RUBIO, V., JYOTHI, D., MILES, A., O'BRIEN, J., GAMBLE, C., OYOLA, S. O., RAYNER, J. C., NEWBOLD, C. I., BERRIMAN, M., SPENCER, C. C., MCVEAN, G., DAY, N. P., WHITE, N. J., BETHELL, D., DONDORP, A. M., PLOWE, C. V., FAIRHURST, R. M. & KWIATKOWSKI, D. P. 2013. Multiple populations of artemisinin-resistant Plasmodium falciparum in Cambodia. *Nat Genet,* 45**,** 648-55.

MIOTTO, O., AMATO, R., ASHLEY, E. A., MACINNIS, B., ALMAGRO-GARCIA, J., AMARATUNGA, C., LIM, P., MEAD, D., OYOLA, S. O., DHORDA, M., IMWONG, M., WOODROW, C., MANSKE, M., STALKER, J., DRURY, E., CAMPINO, S., AMENGA-ETEGO, L., THANH, T. N., TRAN, H. T., RINGWALD, P., BETHELL, D., NOSTEN, F., PHYO, A. P., PUKRITTAYAKAMEE, S., CHOTIVANICH, K., CHUOR, C. M., NGUON, C., SUON, S., SRENG, S., NEWTON, P. N., MAYXAY, M., KHANTHAVONG, M., HONGVANTHONG, B., HTUT, Y., HAN, K. T., KYAW, M. P., FAIZ, M. A., FANELLO, C. I., ONYAMBOKO, M., MOKUOLU, O. A., JACOB, C. G., TAKALA-HARRISON, S., PLOWE, C. V., DAY, N. P., DONDORP, A. M., SPENCER, C. C., MCVEAN, G., FAIRHURST, R. M., WHITE, N. J. & KWIATKOWSKI, D. P. 2015. Genetic architecture of artemisinin-resistant Plasmodium falciparum. *Nat Genet,* 47**,** 226-34.

MIRANDA, K., PACE, D. A., CINTRON, R., RODRIGUES, J. C. F., FANG, J., SMITH, A., ROHLOFF, P., COELHO, E., DE HAAS, F., DE SOUZA, W., COPPENS, I., SIBLEY, L. D. & MORENO, S. N. J. 2010. Characterization of a novel organelle in Toxoplasma gondii with similar composition and function to the plant vacuole. *Molecular Microbiology,* 76**,** 1358-1375.

MISRA, S. & HURLEY, J. H. 1999. Crystal structure of a phosphatidylinositol 3-phosphate-specific membrane-targeting motif, the FYVE domain of Vps27p. *Cell,* 97**,** 657-66.

MIZUSHIMA, N. & LEVINE, B. 2010. Autophagy in mammalian development and differentiation. *Nature cell biology,* 12**,** 823-830.

MIZUSHIMA, N., NODA, T., YOSHIMORI, T., TANAKA, Y., ISHII, T., GEORGE, M. D., KLIONSKY, D. J., OHSUMI, M. & OHSUMI, Y. 1998. A protein conjugation system essential for autophagy. *Nature,* 395**,** 395-8.

MOEHRLE, J. J., DUPARC, S., SIETHOFF, C., VAN GIERSBERGEN, P. L., CRAFT, J. C., ARBE-BARNES, S., CHARMAN, S. A., GUTIERREZ, M., WITTLIN, S. & VENNERSTROM, J. L. 2013. First-in-man safety and pharmacokinetics of synthetic ozonide OZ439 demonstrates an improved exposure profile relative to other peroxide antimalarials. *Br J Clin Pharmacol,* 75**,** 524-37.

MOJICA, F. J., DIEZ-VILLASENOR, C., GARCIA-MARTINEZ, J. & ALMENDROS, C. 2009. Short motif sequences determine the targets of the prokaryotic CRISPR defence system. *Microbiology,* 155**,** 733-40.

MOK, S., ASHLEY, E. A., FERREIRA, P. E., ZHU, L., LIN, Z., YEO, T., CHOTIVANICH, K., IMWONG, M., PUKRITTAYAKAMEE, S., DHORDA, M., NGUON, C., LIM, P., AMARATUNGA, C., SUON, S., HIEN, T. T., HTUT, Y., FAIZ, M. A., ONYAMBOKO, M. A., MAYXAY, M., NEWTON, P. N., TRIPURA, R., WOODROW, C. J., MIOTTO, O., KWIATKOWSKI, D. P., NOSTEN, F., DAY, N. P., PREISER, P. R., WHITE, N. J., DONDORP, A. M., FAIRHURST, R. M. & BOZDECH, Z. 2015. Drug resistance. Population transcriptomics of human malaria parasites reveals the mechanism of artemisinin resistance. *Science,* 347**,** 431-5.

MOK, S., IMWONG, M., MACKINNON, M. J., SIM, J., RAMADOSS, R., YI, P., MAYXAY, M., CHOTIVANICH, K., LIONG, K.-Y., RUSSELL, B., SOCHEAT, D., NEWTON, P. N., DAY, N. P. J., WHITE, N. J., PREISER, P.

R., NOSTEN, F., DONDORP, A. M. & BOZDECH, Z. 2011. Artemisinin resistance in Plasmodium falciparum is associated with an altered temporal pattern of transcription. *BMC Genomics,* 12**,** 391-391.

MOLINA-CRUZ, A., GARVER, L. S., ALABASTER, A., BANGIOLO, L., HAILE, A., WINIKOR, J., ORTEGA, C., VAN SCHAIJK, B. C., SAUERWEIN, R. W., TAYLOR-SALMON, E. & BARILLAS-MURY, C. 2013. The human malaria parasite Pfs47 gene mediates evasion of the mosquito immune system. *Science,* 340**,** 984-7.

MOORE, L. R., FUJIOKA, H., WILLIAMS, P. S., CHALMERS, J. J., GRIMBERG, B., ZIMMERMAN, P. A. & ZBOROWSKI, M. 2006. Hemoglobin degradation in malaria-infected erythrocytes determined from live cell magnetophoresis. *Faseb j,* 20**,** 747-9.

MORISHITA, H., KAIZUKA, T., HAMA, Y. & MIZUSHIMA, N. 2017. A new probe to measure autophagic flux in vitro and in vivo. *Autophagy,* 13**,** 757-758.

MORRISON, G., FU, X., SHEA, M., NANDA, S., GIULIANO, M., WANG, T., KLINOWSKA, T., OSBORNE, C. K., RIMAWI, M. F. & SCHIFF, R. 2014. Therapeutic potential of the dual EGFR/HER2 inhibitor AZD8931 in circumventing endocrine resistance. *Breast Cancer Res Treat,* 144**,** 263-72.

MORTENSEN, M., FERGUSON, D. J., EDELMANN, M., KESSLER, B., MORTEN, K. J., KOMATSU, M. & SIMON, A. K. 2010. Loss of autophagy in erythroid cells leads to defective removal of mitochondria and severe anemia in vivo. *Proc Natl Acad Sci U S A,* 107**,** 832-7.

MORTIMORE, G. E., HUTSON, N. J. & SURMACZ, C. A. 1983. Quantitative correlation between proteolysis and macro- and microautophagy in mouse hepatocytes during starvation and refeeding. *Proc Natl Acad Sci U S A,* 80**,** 2179-83.

MORTIMORE, G. E. & WARD, W. F. 1976. Behavior of the lysosomal system during organ perfusion. An inquiry into the mechanism of hepatic proteolysis. *Front Biol,* 45**,** 157-84.

MOTT, B. T., EASTMAN, R. T., GUHA, R., SHERLACH, K. S., SIRIWARDANA, A., SHINN, P., MCKNIGHT, C., MICHAEL, S., LACERDA-QUEIROZ, N., PATEL, P. R., KHINE, P., SUN, H., KASBEKAR, M., AGHDAM, N., FONTAINE, S. D., LIU, D., MIERZWA, T., MATHEWS-GRINER, L. A., FERRER, M., RENSLO, A. R., INGLESE, J., YUAN, J., ROEPE, P. D., SU, X.

Z. & THOMAS, C. J. 2015. High-throughput matrix screening identifies synergistic and antagonistic antimalarial drug combinations. *Sci Rep,* 5**,** 13891.

MU, Z., KLINOWSKA, T., DONG, X., FOSTER, E., WOMACK, C., FERNANDEZ, S. V. & CRISTOFANILLI, M. 2014. AZD8931, an equipotent, reversible inhibitor of signaling by epidermal growth factor receptor (EGFR), HER2, and HER3: preclinical activity in HER2 non-amplified inflammatory breast cancer models. *J Exp Clin Cancer Res,* 33**,** 47.

MUKHERJEE, A., BOPP, S., MAGISTRADO, P., WONG, W., DANIELS, R., DEMAS, A., SCHAFFNER, S., AMARATUNGA, C., LIM, P., DHORDA, M., MIOTTO, O., WOODROW, C., ASHLEY, E. A., DONDORP, A. M., WHITE, N. J., WIRTH, D., FAIRHURST, R. & VOLKMAN, S. K. 2017. Artemisinin resistance without pfkelch13 mutations in Plasmodium falciparum isolates from Cambodia. *Malaria Journal,* 16**,** 195.

MURRAY, B. W., GUO, C., PIRAINO, J., WESTWICK, J. K., ZHANG, C., LAMERDIN, J., DAGOSTINO, E., KNIGHTON, D., LOI, C. M., ZAGER, M., KRAYNOV, E., POPOFF, I., CHRISTENSEN, J. G., MARTINEZ, R., KEPHART, S. E., MARAKOVITS, J., KARLICEK, S., BERGQVIST, S. & SMEAL, T. 2010. Small-molecule p21-activated kinase inhibitor PF-3758309 is a potent inhibitor of oncogenic signaling and tumor growth. *Proc Natl Acad Sci U S A,* 107**,** 9446-51.

MURRAY, M. J., MURRAY, N. J., MURRAY, A. B. & MURRAY, M. B. 1975. Refeeding-malaria and hyperferraemia. *Lancet,* 1**,** 653-4.

MUWANGUZI, J., HENRIQUES, G., SAWA, P., BOUSEMA, T., SUTHERLAND, C. J. & BESHIR, K. B. 2016. Lack of K13 mutations in Plasmodium falciparum persisting after artemisinin combination therapy treatment of Kenyan children. *Malar J,* 15**,** 36.

NAIR, U., CAO, Y., XIE, Z. & KLIONSKY, D. J. 2010. Roles of the lipid-binding motifs of Atg18 and Atg21 in the cytoplasm to vacuole targeting pathway and autophagy. *J Biol Chem,* 285**,** 11476-88.

NÁJERA, J. A., GONZÁLEZ-SILVA, M. & ALONSO, P. L. 2011. Some Lessons for the Future from the Global Malaria Eradication Programme (1955–1969). *PLOS Medicine,* 8**,** e1000412.

NAKAGAWA, I., AMANO, A., MIZUSHIMA, N., YAMAMOTO, A., YAMAGUCHI, H., KAMIMOTO, T., NARA, A., FUNAO, J., NAKATA, M.,

TSUDA, K., HAMADA, S. & YOSHIMORI, T. 2004. Autophagy defends cells against invading group A Streptococcus. *Science,* 306**,** 1037-40.

NAKAZAWA, S., KANBARA, H. & AIKAWA, M. 1995. Plasmodium falciparum: recrudescence of parasites in culture. *Exp Parasitol,* 81**,** 556-63.

NAKAZAWA, S., MAOKA, T., UEMURA, H., ITO, Y. & KANBARA, H. 2002. Malaria parasites giving rise to recrudescence in vitro. *Antimicrob Agents Chemother,* 46**,** 958-65.

NARA, A., MIZUSHIMA, N., YAMAMOTO, A., KABEYA, Y., OHSUMI, Y. & YOSHIMORI, T. 2002. SKD1 AAA ATPase-dependent endosomal transport is involved in autolysosome formation. *Cell Struct Funct,* 27**,** 29-37.

NASCIMBENI, A. C., CODOGNO, P. & MOREL, E. 2017. Phosphatidylinositol-3-phosphate in the regulation of autophagy membrane dynamics. *Febs j,* 284**,** 1267-1278.

NAUDE, B., BRZOSTOWSKI, J. A., KIMMEL, A. R. & WELLEMS, T. E. 2005. Dictyostelium discoideum expresses a malaria chloroquine resistance mechanism upon transfection with mutant, but not wild-type, Plasmodium falciparum transporter PfCRT. *J Biol Chem,* 280**,** 25596-603.

NAVALE, R., ATUL, ALLANKI, A. D. & SIJWALI, P. S. 2014. Characterization of the autophagy marker protein Atg8 reveals atypical features of autophagy in Plasmodium falciparum. *PLoS One,* 9**,** e113220.

NELSON, A. L., PURFIELD, A., MCDANIEL, P., UTHAIMONGKOL, N., BUATHONG, N., SRIWICHAI, S., MILLER, R. S., WONGSRICHANALAI, C. & MESHNICK, S. R. 2005. pfmdr1 genotyping and in vivo mefloquine resistance on the Thai-Myanmar border. *Am J Trop Med Hyg,* 72**,** 586-92.

NEMUNAITIS, J. J., SMALL, K. A., KIRSCHMEIER, P., ZHANG, D., ZHU, Y., JOU, Y. M., STATKEVICH, P., YAO, S. L. & BANNERJI, R. 2013. A first-in-human, phase 1, dose-escalation study of dinaciclib, a novel cyclin-dependent kinase inhibitor, administered weekly in subjects with advanced malignancies. *J Transl Med,* 11**,** 259.

NEWTON, C. R., TAYLOR, T. E. & WHITTEN, R. O. 1998. Pathophysiology of fatal falciparum malaria in African children. *Am J Trop Med Hyg,* 58**,** 673-83.

NGUITRAGOOL, W., BOKHARI, ABDULLAH A. B., PILLAI, AJAY D., RAYAVARA, K., SHARMA, P., TURPIN, B., ARAVIND, L. & DESAI,

SANJAY A. 2011. Malaria Parasite clag3 Genes Determine Channel-Mediated Nutrient Uptake by Infected Red Blood Cells. *Cell,* 145**,** 665-677.

NGUYEN, D. S., DAO, B. H., NGUYEN, P. D., NGUYEN, V. H., LE, N. B., MAI, V. S. & MESHNICK, S. R. 1993. Treatment of malaria in Vietnam with oral artemisinin. *Am J Trop Med Hyg,* 48**,** 398-402.

NGUYEN, H. M., BERRY, L., SULLIVAN, J. W. J. & BESTEIRO, S. 2017. Autophagy participates in the unfolded protein response in Toxoplasma gondii. *FEMS Microbiology Letters,* 364**,** fnx153-fnx153.

NGUYEN, T. K. & GRANT, S. 2014. Dinaciclib (SCH727965) inhibits the unfolded protein response through a CDK1- and 5-dependent mechanism. *Mol Cancer Ther,* 13**,** 662-74.

NICKLIN, P., BERGMAN, P., ZHANG, B., TRIANTAFELLOW, E., WANG, H., NYFELER, B., YANG, H., HILD, M., KUNG, C., WILSON, C., MYER, V. E., MACKEIGAN, J. P., PORTER, J. A., WANG, Y. K., CANTLEY, L. C., FINAN, P. M. & MURPHY, L. O. 2009. Bidirectional transport of amino acids regulates mTOR and autophagy. *Cell,* 136**,** 521-34.

NIKBAKHT, H., XIA, X. & HICKEY, D. A. 2014. The evolution of genomic GC content undergoes a rapid reversal within the genus Plasmodium. *Genome,* 57**,** 507-11.

NISHIDA, A., MIYATA, K., TSUTSUMI, R., YUKI, H., AKUZAWA, S., KOBAYASHI, A., KAMATO, T., ITO, H., YAMANO, M., KATUYAMA, Y. & ET AL. 1994. Pharmacological profile of (R)-1-[2,3-dihydro-1-(2'-methylphenacyl)-2-oxo- 5-phenyl-1H-1,4-benzodiazepin-3-yl]-3-(3-methylphenyl)urea (YM022), a new potent and selective gastrin/cholecystokinin-B receptor antagonist, in vitro and in vivo. *J Pharmacol Exp Ther,* 269**,** 725-31.

NISHIMASU, H., CONG, L., YAN, W. X., RAN, F. A., ZETSCHE, B., LI, Y., KURABAYASHI, A., ISHITANI, R., ZHANG, F. & NUREKI, O. 2015. Crystal Structure of Staphylococcus aureus Cas9. *Cell,* 162**,** 1113-26.

NISHIMASU, H., RAN, F. A., HSU, P. D., KONERMANN, S., SHEHATA, S. I., DOHMAE, N., ISHITANI, R., ZHANG, F. & NUREKI, O. 2014. Crystal structure of Cas9 in complex with guide RNA and target DNA. *Cell,* 156**,** 935-49.

NODA, T. & KLIONSKY, D. J. 2008. The quantitative Pho8Delta60 assay of nonspecific autophagy. *Methods Enzymol,* 451**,** 33-42.

NOMURA, Y., BHAWAL, U. K., NISHIKIORI, R., SAWAJIRI, M., MAEDA, T. & OKAZAKI, M. 2010. Effects of high-dose major components in oral disinfectants on the cell cycle and apoptosis in primary human gingival fibroblasts in vitro. *Dent Mater J,* 29**,** 75-83.

NOSTEN, F., TER KUILE, F., CHONGSUPHAJAISIDDHI, T., LUXEMBURGER, C., WEBSTER, H. K., EDSTEIN, M., PHAIPUN, L., THEW, K. L. & WHITE, N. J. 1991. Mefloquine-resistant falciparum malaria on the Thai-Burmese border. *Lancet,* 337**,** 1140-3.

NOVIKOFF, A. B., BEAUFAY, H. & DE DUVE, C. 1956. Electron microscopy of lysosomerich fractions from rat liver. *J Biophys Biochem Cytol,* 2**,** 179-84.

O'DAY, S., GONZALEZ, R., LAWSON, D., WEBER, R., HUTCHINS, L., ANDERSON, C., HADDAD, J., KONG, S., WILLIAMS, A. & JACOBSON, E. 2009. Phase II, Randomized, Controlled, Double-Blinded Trial of Weekly Elesclomol Plus Paclitaxel Versus Paclitaxel Alone for Stage IV Metastatic Melanoma. *Journal of Clinical Oncology,* 27**,** 5452-5458.

OBARA, K., NODA, T., NIIMI, K. & OHSUMI, Y. 2008. Transport of phosphatidylinositol 3-phosphate into the vacuole via autophagic membranes in Saccharomyces cerevisiae. *Genes Cells,* 13**,** 537-47.

OBARA, K. & OHSUMI, Y. 2008. Dynamics and function of PtdIns(3)P in autophagy. *Autophagy,* 4**,** 952-4.

OBARA, K. & OHSUMI, Y. 2011. Atg14: a key player in orchestrating autophagy. *Int J Cell Biol,* 2011**,** 713435.

OBARA, K., SEKITO, T. & OHSUMI, Y. 2006. Assortment of phosphatidylinositol 3-kinase complexes--Atg14p directs association of complex I to the pre-autophagosomal structure in Saccharomyces cerevisiae. *Mol Biol Cell,* 17**,** 1527-39.

ODORIZZI, G., BABST, M. & EMR, S. D. 2000. Phosphoinositide signaling and the regulation of membrane trafficking in yeast. *Trends Biochem Sci,* 25**,** 229-35.

OH, M., CHOI, I. K. & KWON, H. J. 2008. Inhibition of histone deacetylase1 induces autophagy. *Biochem Biophys Res Commun,* 369**,** 1179-83.

OHSUMI, Y. 2014. Historical landmarks of autophagy research. *Cell Research,* 24**,** 9-23.

OLIVEIRA, F., KAMHAWI, S., SEITZ, A. E., PHAM, V. M., GUIGAL, P. M., FISCHER, L., WARD, J. & VALENZUELA, J. G. 2006. From transcriptome to immunome: Identification of DTH inducing proteins from a Phlebotomus ariasi salivary gland cDNA library. *Vaccine,* 24**,** 374-390.

ONO, K., KIM, S. O. & HAN, J. 2003. Susceptibility of lysosomes to rupture is a determinant for plasma membrane disruption in tumor necrosis factor alpha-induced cell death. *Mol Cell Biol,* 23**,** 665-76.

OUATTARA, A., KONE, A., ADAMS, M., FOFANA, B., MAIGA, A. W., HAMPTON, S., COULIBALY, D., THERA, M. A., DIALLO, N., DARA, A., SAGARA, I., GIL, J. P., BJORKMAN, A., TAKALA-HARRISON, S., DOUMBO, O. K., PLOWE, C. V. & DJIMDE, A. A. 2015. Polymorphisms in the K13-propeller gene in artemisinin-susceptible Plasmodium falciparum parasites from Bougoula-Hameau and Bandiagara, Mali. *Am J Trop Med Hyg,* 92**,** 1202-6.

PALOQUE, L., RAMADANI, A. P., MERCEREAU-PUIJALON, O., AUGEREAU, J. M. & BENOIT-VICAL, F. 2016. Plasmodium falciparum: multifaceted resistance to artemisinins. *Malar J,* 15**,** 149.

PAPANDREOU, I., LIM, A. L., LADEROUTE, K. & DENKO, N. C. 2008. Hypoxia signals autophagy in tumor cells via AMPK activity, independent of HIF-1, BNIP3, and BNIP3L. *Cell Death And Differentiation,* 15**,** 1572.

PARUSSINI, F., COPPENS, I., SHAH, P. P., DIAMOND, S. L. & CARRUTHERS, V. B. 2010. Cathepsin L occupies a vacuolar compartment and is a protein maturase within the endo/exocytic system of Toxoplasma gondii. *Molecular Microbiology,* 76**,** 1340-1357.

PATEL, J. J., THACKER, D., TAN, J. C., PLEETER, P., CHECKLEY, L., GONZALES, J. M., DENG, B., ROEPE, P. D., COOPER, R. A. & FERDIG, M. T. 2010. Chloroquine susceptibility and reversibility in a Plasmodium falciparum genetic cross. *Mol Microbiol,* 78**,** 770-87.

PAUL, F., ROATH, S., MELVILLE, D., WARHURST, D. C. & OSISANYA, J. O. 1981. Separation of malaria-infected erythrocytes from whole blood: use of a selective high-gradient magnetic separation technique. *Lancet,* 2**,** 70-1.

PAYNE, D. 1987. Spread of chloroquine resistance in Plasmodium falciparum. *Parasitol Today,* 3**,** 241-6.

PAYRASTRE, B. 2004. Phosphoinositides: lipid kinases and phosphatases. *Methods Mol Biol,* 273**,** 201-12.

PAYRASTRE, B., GAITS-IACOVONI, F., SANSONETTI, P. & TRONCHERE, H. 2012. Phosphoinositides and cellular pathogens. *Subcell Biochem,* 59**,** 363-88.

PEATEY, C. L., CHAVCHICH, M., CHEN, N., GRESTY, K. J., GRAY, K.-A., GATTON, M. L., WATERS, N. C. & CHENG, Q. 2015. Mitochondrial Membrane Potential in a Small Subset of Artemisinin-Induced Dormant Plasmodium falciparum Parasites In Vitro. *The Journal of Infectious Diseases,* 212**,** 426-434.

PETERSON, D. S., WALLIKER, D. & WELLEMS, T. E. 1988. Evidence that a point mutation in dihydrofolate reductase-thymidylate synthase confers resistance to pyrimethamine in falciparum malaria. *Proceedings of the National Academy of Sciences,* 85**,** 9114-9118.

PFEIFER, U. & WARMUTH-METZ, M. 1983. Inhibition by insulin of cellular autophagy in proximal tubular cells of rat kidney. *Am J Physiol,* 244**,** E109-14.

PHADWAL, K., ALEGRE-ABARRATEGUI, J., WATSON, A. S., PIKE, L., ANBALAGAN, S., HAMMOND, E. M., WADE-MARTINS, R., MCMICHAEL, A., KLENERMAN, P. & SIMON, A. K. 2012. A novel method for autophagy detection in primary cells: impaired levels of macroautophagy in immunosenescent T cells. *Autophagy,* 8**,** 677-89.

PHOMPRADIT, P., WISEDPANICHKIJ, R., MUHAMAD, P., CHAIJAROENKUL, W. & NA-BANGCHANG, K. 2011. Molecular analysis of pfatp6 and pfmdr1 polymorphisms and their association with in vitro sensitivity in Plasmodium falciparum isolates from the Thai-Myanmar border. *Acta Trop,* 120**,** 130-5.

PHYO, A. P., JITTAMALA, P., NOSTEN, F. H., PUKRITTAYAKAMEE, S., IMWONG, M., WHITE, N. J., DUPARC, S., MACINTYRE, F., BAKER, M. & MOHRLE, J. J. 2016. Antimalarial activity of artefenomel (OZ439), a novel synthetic antimalarial endoperoxide, in patients with Plasmodium falciparum and Plasmodium vivax malaria: an open-label phase 2 trial. *Lancet Infect Dis,* 16**,** 61-69.

PHYO, A. P., NKHOMA, S., STEPNIEWSKA, K., ASHLEY, E. A., NAIR, S., MCGREADY, R., LER MOO, C., AL-SAAI, S., DONDORP, A. M., LWIN, K. M., SINGHASIVANON, P., DAY, N. P., WHITE, N. J., ANDERSON, T. J. &

NOSTEN, F. 2012. Emergence of artemisinin-resistant malaria on the western border of Thailand: a longitudinal study. *Lancet,* 379**,** 1960-6.

PILLAI, A. D., NGUITRAGOOL, W., LYKO, B., DOLINTA, K., BUTLER, M. M., NGUYEN, S. T., PEET, N. P., BOWLIN, T. L. & DESAI, S. A. 2012. Solute restriction reveals an essential role for clag3-associated channels in malaria parasite nutrient acquisition. *Mol Pharmacol,* 82**,** 1104-14.

PILLAI, A. D., PAIN, M., SOLOMON, T., BOKHARI, A. A. & DESAI, S. A. 2010. A cell-based high-throughput screen validates the plasmodial surface anion channel as an antimalarial target. *Mol Pharmacol,* 77**,** 724-33.

PIMENTA, P. F., TOURAY, M. & MILLER, L. 1994. The journey of malaria sporozoites in the mosquito salivary gland. *J Eukaryot Microbiol,* 41**,** 608-24.

PIZARRO-CERDA, J., MORENO, E. & GORVEL, J. P. 2000. Invasion and intracellular trafficking of Brucella abortus in nonphagocytic cells. *Microbes Infect,* 2**,** 829-35.

PIZZI, E. & FRONTALI, C. 2001. Low-complexity regions in Plasmodium falciparum proteins. *Genome Res,* 11**,** 218-29.

PLANNING, M. O. 2008. General Population Census of Cambodia 2008. Phnom Penh, Cambodia: National Institute of Statistics

POLSON, H. E., DE LARTIGUE, J., RIGDEN, D. J., REEDIJK, M., URBE, S., CLAGUE, M. J. & TOOZE, S. A. 2010a. Mammalian Atg18 (WIPI2) localizes to omegasome-anchored phagophores and positively regulates LC3 lipidation. *Autophagy,* 6**,** 506-22.

POLSON, H. E. J., DE LARTIGUE, J., RIGDEN, D. J., REEDIJK, M., URBÉ, S., CLAGUE, M. J. & TOOZE, S. A. 2010b. Mammalian Atg18 (WIPI2) localizes to omegasome-anchored phagophores and positively regulates LC3 lipidation. *Autophagy,* 6**,** 506-522.

PONTING, C. P. 1996. Novel domains in NADPH oxidase subunits, sorting nexins, and PtdIns 3-kinases: binding partners of SH3 domains? *Protein Sci,* 5**,** 2353-7.

POTTER, H., WEIR, L. & LEDER, P. 1984. Enhancer-dependent expression of human kappa immunoglobulin genes introduced into mouse pre-B lymphocytes by electroporation. *Proc Natl Acad Sci U S A,* 81**,** 7161-5.

PREECHAPORNKUL, P., IMWONG, M., CHOTIVANICH, K., PONGTAVORNPINYO, W., DONDORP, A. M., DAY, N. P., WHITE, N. J. & PUKRITTAYAKAMEE, S. 2009. Plasmodium falciparum pfmdr1

amplification, mefloquine resistance, and parasite fitness. *Antimicrob Agents Chemother,* 53**,** 1509-15.

PRICE, R. N., UHLEMANN, A. C., BROCKMAN, A., MCGREADY, R., ASHLEY, E., PHAIPUN, L., PATEL, R., LAING, K., LOOAREESUWAN, S., WHITE, N. J., NOSTEN, F. & KRISHNA, S. 2004. Mefloquine resistance in Plasmodium falciparum and increased pfmdr1 gene copy number. *Lancet,* 364**,** 438-447.

PROIKAS-CEZANNE, T. & ROBENEK, H. 2011. Freeze-fracture replica immunolabelling reveals human WIPI-1 and WIPI-2 as membrane proteins of autophagosomes. *J Cell Mol Med,* 15**,** 2007-10.

PROIKAS-CEZANNE, T., RUCKERBAUER, S., STIERHOF, Y. D., BERG, C. & NORDHEIM, A. 2007. Human WIPI-1 puncta-formation: a novel assay to assess mammalian autophagy. *FEBS Lett,* 581**,** 3396-404.

PROIKAS-CEZANNE, T., TAKACS, Z., DÖNNES, P. & KOHLBACHER, O. 2015. WIPI proteins: essential PtdIns3P effectors at the nascent autophagosome. *Journal of Cell Science,* 128**,** 207-217.

PROIKAS-CEZANNE, T., WADDELL, S., GAUGEL, A., FRICKEY, T., LUPAS, A. & NORDHEIM, A. 2004. WIPI-1alpha (WIPI49), a member of the novel 7-bladed WIPI protein family, is aberrantly expressed in human cancer and is linked to starvation-induced autophagy. *Oncogene,* 23**,** 9314-25.

PULESTON, D. J., ZHANG, H., POWELL, T. J., LIPINA, E., SIMS, S., PANSE, I., WATSON, A. S., CERUNDOLO, V., TOWNSEND, A. R., KLENERMAN, P. & SIMON, A. K. 2014. Autophagy is a critical regulator of memory CD8(+) T cell formation. *Elife,* 3.

PUNNONEN, E. L. & REUNANEN, H. 1990. Effects of vinblastine, leucine, and histidine, and 3-methyladenine on autophagy in Ehrlich ascites cells. *Exp Mol Pathol,* 52**,** 87-97.

PUVANENTHIRAN, S., ESSAPEN, S., SEDDON, A. M. & MODJTAHEDI, H. 2016. Impact of the putative cancer stem cell markers and growth factor receptor expression on the sensitivity of ovarian cancer cells to treatment with various forms of small molecule tyrosine kinase inhibitors and cytotoxic drugs. *Int J Oncol,* 49**,** 1825-1838.

RABINOWITZ, J. D. & WHITE, E. 2010. Autophagy and Metabolism. *Science,* 330**,** 1344-1348.

RAGUSA, M. J., STANLEY, R. E. & HURLEY, J. H. 2012. Architecture of the Atg17 complex as a scaffold for autophagosome biogenesis. *Cell,* 151**,** 1501-1512.

RALPH, S. A., VAN DOOREN, G. G., WALLER, R. F., CRAWFORD, M. J., FRAUNHOLZ, M. J., FOTH, B. J., TONKIN, C. J., ROOS, D. S. & MCFADDEN, G. I. 2004. Metabolic maps and functions of the Plasmodium falciparum apicoplast. *Nature Reviews Microbiology,* 2**,** 203.

RAMAKRISHNAN, S., DOCAMPO, M. D., MACRAE, J. I., PUJOL, F. M., BROOKS, C. F., VAN DOOREN, G. G., HILTUNEN, J. K., KASTANIOTIS, A. J., MCCONVILLE, M. J. & STRIEPEN, B. 2012. Apicoplast and endoplasmic reticulum cooperate in fatty acid biosynthesis in apicomplexan parasite Toxoplasma gondii. *J Biol Chem,* 287**,** 4957-71.

RAN, F. A., HSU, P. D., WRIGHT, J., AGARWALA, V., SCOTT, D. A. & ZHANG, F. 2013. Genome engineering using the CRISPR-Cas9 system. *Nat Protoc,* 8**,** 2281-2308.

RAO, S. V., SOLUM, G., NIEDERDORFER, B., NORSETT, K. G., BJORKOY, G. & THOMMESEN, L. 2017. Gastrin activates autophagy and increases migration and survival of gastric adenocarcinoma cells. *BMC Cancer,* 17**,** 68.

RAYESS, H. M., XI, Y., GARSHOTT, D. M., BROWNELL, A. L., YOO, G. H., CALLAGHAN, M. U. & FRIBLEY, A. M. 2018. Benzethonium chloride activates ER stress and reduces proliferation in HNSCC. *Oral Oncology,* 76**,** 27-33.

REGGIORI, F., TUCKER, K. A., STROMHAUG, P. E. & KLIONSKY, D. J. 2004. The Atg1-Atg13 complex regulates Atg9 and Atg23 retrieval transport from the pre-autophagosomal structure. *Dev Cell,* 6**,** 79-90.

RICHARD, D., MORJANI, H. & CHÉNAIS, B. T. 2002. Free radical production and labile iron pool decrease triggered by subtoxic concentration of aclarubicin in human leukemia cell lines. *Leukemia Research,* 26**,** 927-931.

RICHTER, J., FRANKEN, G., HOLTFRETER, M. C., WALTER, S., LABISCH, A. & MEHLHORN, H. 2016. Clinical implications of a gradual dormancy concept in malaria. *Parasitol Res,* 115**,** 2139-48.

RIFFELMACHER, T., CLARKE, A., RICHTER, F. C., STRANKS, A., PANDEY, S., DANIELLI, S., HUBLITZ, P., YU, Z., JOHNSON, E., SCHWERD, T., MCCULLAGH, J., UHLIG, H., JACOBSEN, S. E. W. & SIMON, A. K. 2017.

Autophagy-Dependent Generation of Free Fatty Acids Is Critical for Normal Neutrophil Differentiation. *Immunity,* 47**,** 466-480.e5.

RITTERSHAUS, EMILY S. C., BAEK, S.-H. & SASSETTI, CHRISTOPHER M. 2013. The Normalcy of Dormancy: Common Themes in Microbial Quiescence. *Cell Host & Microbe,* 13**,** 643-651.

ROCK, E. P., MARSH, K., SAUL, S. J., WELLEMS, T. E., TAYLOR, D. W., MALOY, W. L. & HOWARD, R. J. 1987. Comparative analysis of the Plasmodium falciparum histidine-rich proteins HRP1, HRP2 and HRP3 in malaria diagnosis of diverse origin. *Parasitology,* 95**,** 209–227.

ROEPE, P. D. 2009. Molecular and physiologic basis of quinoline drug resistance in Plasmodium falciparum malaria. *Future Microbiol,* 4**,** 441-55.

ROHMER, M. 1999. The discovery of a mevalonate-independent pathway for isoprenoid biosynthesis in bacteria, algae and higher plants. *Nat Prod Rep,* 16**,** 565-74.

RON, D. & WALTER, P. 2007. Signal integration in the endoplasmic reticulum unfolded protein response. *Nat Rev Mol Cell Biol,* 8**,** 519-29.

ROSARIO, V. E., HALL, R., WALLIKER, D. & BEALE, G. H. 1978. Persistence of drug-resistant malaria parasites. *Lancet,* 1**,** 185-7.

ROSENTHAL, P. J. 2013. The interplay between drug resistance and fitness in malaria parasites. *Molecular Microbiology,* 89**,** 1025-1038.

ROSS, R. 2002. The role of the mosquito in the evolution of the malarial parasite: the recent researches of Surgeon-Major Ronald Ross, I.M.S. 1898. *The Yale Journal of Biology and Medicine,* 75**,** 103-105.

RUBINSZTEIN, DAVID C., MARIÑO, G. & KROEMER, G. 2011. Autophagy and Aging. *Cell,* 146**,** 682-695.

RUETZ, S., FABBRO, D., ZIMMERMANN, J., MEYER, T. & GRAY, N. 2003. Chemical and biological profile of dual Cdk1 and Cdk2 inhibitors. *Curr Med Chem Anticancer Agents,* 3**,** 1-14.

SA, J. M., TWU, O., HAYTON, K., REYES, S., FAY, M. P., RINGWALD, P. & WELLEMS, T. E. 2009. Geographic patterns of Plasmodium falciparum drug resistance distinguished by differential responses to amodiaquine and chloroquine. *Proc Natl Acad Sci U S A,* 106**,** 18883-9.

SAID, J., WALKER, M., PARSONS, D., STAPLETON, P., BEEZER, A. E. & GAISFORD, S. 2014. An in vitro test of the efficacy of an anti-biofilm wound dressing. *Int J Pharm,* 474**,** 177-81.

SAID, R. & TSIMBERIDOU, A. M. 2014. Pharmacokinetic evaluation of vincristine for the treatment of lymphoid malignancies. *Expert Opin Drug Metab Toxicol,* 10**,** 483-94.

SAKOH-NAKATOGAWA, M., MATOBA, K., ASAI, E., KIRISAKO, H., ISHII, J., NODA, N. N., INAGAKI, F., NAKATOGAWA, H. & OHSUMI, Y. 2013. Atg12-Atg5 conjugate enhances E2 activity of Atg3 by rearranging its catalytic site. *Nat Struct Mol Biol,* 20**,** 433-9.

SALEM, A. F., WHITAKER-MENEZES, D., LIN, Z., MARTINEZ-OUTSCHOORN, U. E., TANOWITZ, H. B., AL-ZOUBI, M. S., HOWELL, A., PESTELL, R. G., SOTGIA, F. & LISANTI, M. P. 2012. Two-compartment tumor metabolism: Autophagy in the tumor microenvironment and oxidative mitochondrial metabolism (OXPHOS) in cancer cells. *Cell Cycle,* 11**,** 2545-2559.

SAMARAKOON, U., GONZALES, J. M., PATEL, J. J., TAN, A., CHECKLEY, L. & FERDIG, M. T. 2011. The landscape of inherited and de novo copy number variants in a plasmodium falciparum genetic cross. *BMC Genomics,* 12**,** 457-457.

SANCHEZ, C. P., MAYER, S., NURHASANAH, A., STEIN, W. D. & LANZER, M. 2011. Genetic linkage analyses redefine the roles of PfCRT and PfMDR1 in drug accumulation and susceptibility in Plasmodium falciparum. *Mol Microbiol,* 82**,** 865-78.

SASAKI, N., CHHENG, K., MIZOUE, N., ABE, I. & LOWE, A. J. 2016. Forest reference emission level and carbon sequestration in Cambodia. *Global Ecology and Conservation,* 7**,** 82-96.

SATO, S., CLOUGH, B., COATES, L. & WILSON, R. J. M. 2004. Enzymes for Heme Biosynthesis are Found in Both the Mitochondrion and Plastid of the Malaria Parasite Plasmodium falciparum. *Protist,* 155**,** 117-125.

SAUL, A., GRAVES, P. & EDSER, L. 1990. Refractoriness of erythrocytes infected with Plasmodium falciparum gametocytes to lysis by sorbitol. *Int J Parasitol,* 20**,** 1095-7.

SCHAEFER, K. A., WU, W.-H., COLGAN, D. F., TSANG, S. H., BASSUK, A. G. & MAHAJAN, V. B. 2017. Unexpected mutations after CRISPR-Cas9 editing in vivo. *Nat Meth,* 14**,** 547-548.

SCHAPIRA, A. 1984. Concomitant resistance to pyrimethamine and cycloguanil of chloroquine-resistant falciparum malaria from East Africa: an in vitro study of 12 isolates. *Trans R Soc Trop Med Hyg,* 78**,** 359-62.

SCHEIPL, S., BARNARD, M., COTTONE, L., JORGENSEN, M., DREWRY, D. H., ZUERCHER, W. J., TURLAIS, F., YE, H., LEITE, A. P., SMITH, J. A., LEITHNER, A., MOLLER, P., BRUDERLEIN, S., GUPPY, N., AMARY, F., TIRABOSCO, R., STRAUSS, S. J., PILLAY, N. & FLANAGAN, A. M. 2016. EGFR inhibitors identified as a potential treatment for chordoma in a focused compound screen. *J Pathol,* 239**,** 320-34.

SCHERZ-SHOUVAL, R. & ELAZAR, Z. 2007. ROS, mitochondria and the regulation of autophagy. *Trends Cell Biol,* 17**,** 422-7.

SCHLAGENHAUF, P. 2004. Malaria: from prehistory to present. *Infectious Disease Clinics of North America,* 18**,** 189-205.

SCHU, P. V., TAKEGAWA, K., FRY, M. J., STACK, J. H., WATERFIELD, M. D. & EMR, S. D. 1993. Phosphatidylinositol 3-kinase encoded by yeast VPS34 gene essential for protein sorting. *Science,* 260**,** 88-91.

SCHWACH, F., BUSHELL, E., GOMES, A. R., ANAR, B., GIRLING, G., HERD, C., RAYNER, J. C. & BILLKER, O. 2015. PlasmoGEM, a database supporting a community resource for large-scale experimental genetics in malaria parasites. *Nucleic Acids Res,* 43**,** D1176-82.

SEEBER, F. 2002. Biogenesis of iron–sulphur clusters in amitochondriate and apicomplexan protists. *International Journal for Parasitology,* 32**,** 1207-1217.

SEGLEN, P. O., GORDON, P. B. & POLI, A. 1980. Amino acid inhibition of the autophagic/lysosomal pathway of protein degradation in isolated rat hepatocytes. *Biochim Biophys Acta,* 630**,** 103-18.

SERENA, T., CONNELL, H., MCCONNELL, S., PATEL, K., DONER, B., SABO, M., MILLER, M., SERENA, L., LE, L. T., GOLDSMITH, D. & CHUNG, J. 2016. Novel Multivalent Wound-Healing Ointment Provides Bioburden Control and Moisture Management: A Retrospective Registry Data Analysis. *Adv Skin Wound Care,* 29**,** 461-8.

SERFONTEIN, J., NISBET, R. E., HOWE, C. J. & DE VRIES, P. J. 2010. Evolution of the TSC1/TSC2-TOR signaling pathway. *Sci Signal,* 3**,** ra49.

SERRANO, M. 2010. Shifting senescence into quiescence by turning up p53. *Cell Cycle,* 9**,** 4256-7.

SEYDEL, K. B., KAMPONDENI, S. D., VALIM, C., POTCHEN, M. J., MILNER, D. A., MUWALO, F. W., BIRBECK, G. L., BRADLEY, W. G., FOX, L. L., GLOVER, S. J., HAMMOND, C. A., HEYDERMAN, R. S., CHILINGULO, C. A., MOLYNEUX, M. E. & TAYLOR, T. E. 2015. Brain Swelling and Death in Children with Cerebral Malaria. *New England Journal of Medicine,* 372**,** 1126-1137.

SHAIKH, A. S., TANG, Y. J., MUKHOPADHYAY, A., MARTIN, H. G., GIN, J., BENKE, P. I. & KEASLING, J. D. 2010. Study of stationary phase metabolism via isotopomer analysis of amino acids from an isolated protein. *Biotechnol Prog,* 26**,** 52-6.

SHANNAN, B., WATTERS, A., CHEN, Q., MOLLIN, S., DORR, M., MEGGERS, E., XU, X., GIMOTTY, P. A., PEREGO, M., LI, L., BENCI, J., KREPLER, C., BRAFFORD, P., ZHANG, J., WEI, Z., ZHANG, G., LIU, Q., YIN, X., NATHANSON, K. L., HERLYN, M. & VULTUR, A. 2016. PIM kinases as therapeutic targets against advanced melanoma. *Oncotarget,* 7**,** 54897-54912.

SHAW, P. J., CHAOTHEING, S., KAEWPROMMAL, P., PIRIYAPONGSA, J., WONGSOMBAT, C., SUWANNAKITTI, N., KOONYOSYING, P., UTHAIPIBULL, C., YUTHAVONG, Y. & KAMCHONWONGPAISAN, S. 2015. Plasmodium parasites mount an arrest response to dihydroartemisinin, as revealed by whole transcriptome shotgun sequencing (RNA-seq) and microarray study. *BMC Genomics,* 16**,** 830.

SHEEN, J. H., ZONCU, R., KIM, D. & SABATINI, D. M. 2011. Defective regulation of autophagy upon leucine deprivation reveals a targetable liability of human melanoma cells in vitro and in vivo. *Cancer Cell,* 19**,** 613-28.

SHINDE, D., LAI, Y., SUN, F. & ARNHEIM, N. 2003. Taq DNA polymerase slippage mutation rates measured by PCR and quasi-likelihood analysis: (CA/GT)(n) and (A/T)(n) microsatellites. *Nucleic Acids Research,* 31**,** 974-980.

SIDHU, A. B., VERDIER-PINARD, D. & FIDOCK, D. A. 2002. Chloroquine resistance in Plasmodium falciparum malaria parasites conferred by pfcrt mutations. *Science,* 298**,** 210-3.

SINDEN, R. E. 1983. The cell biology of sexual development in plasmodium. *Parasitology,* 86 (Pt 4)**,** 7-28.

SINDEN, R. E. 1999. Plasmodium differentiation in the mosquito. *Parassitologia,* 41**,** 139-48.

SKINNER-ADAMS, T. S., LAWRIE, P. M., HAWTHORNE, P. L., GARDINER, D. L. & TRENHOLME, K. R. 2003. Comparison of Plasmodium falciparum transfection methods. *Malaria Journal,* 2**,** 19-19.

SKINNER, T. S., MANNING, L. S., JOHNSTON, W. A. & DAVIS, T. M. E. 1996. In vitro stage-specific sensitivity of Plasmodium falciparum to quinine and artemisinin drugs. *International Journal for Parasitology,* 26**,** 519-525.

SLATER, A. F., SWIGGARD, W. J., ORTON, B. R., FLITTER, W. D., GOLDBERG, D. E., CERAMI, A. & HENDERSON, G. B. 1991. An iron-carboxylate bond links the heme units of malaria pigment. *Proc Natl Acad Sci U S A,* 88**,** 325-9.

SMILKSTEIN, M., SRIWILAIJAROEN, N., KELLY, J. X., WILAIRAT, P. & RISCOE, M. 2004. Simple and Inexpensive Fluorescence-Based Technique for High-Throughput Antimalarial Drug Screening. *Antimicrobial Agents and Chemotherapy,* 48**,** 1803-1806.

SOHAL, R. S. & SOHAL, B. H. 1991. Hydrogen peroxide release by mitochondria increases during aging. *Mech Ageing Dev,* 57**,** 187-202.

SONG, X., XU, W., ZHANG, A., HUANG, G., LIANG, X., VIRBASIUS, J. V., CZECH, M. P. & ZHOU, G. W. 2001. Phox homology domains specifically bind phosphatidylinositol phosphates. *Biochemistry,* 40**,** 8940-4.

SØRENSEN, B. S., SINDING, J., ANDERSEN, A. H., ALSNER, J., JENSEN, P. B. & WESTERGAARD, O. 1992. Mode of action of topoisomerase II-targeting agents at a specific DNA sequence: Uncoupling the DNA binding, cleavage and religation events. *Journal of Molecular Biology,* 228**,** 778-786.

SPRENT, J. & SURH, C. D. 2011. Normal T cell homeostasis: the conversion of naive cells into memory-phenotype cells. *Nature Immunology,* 12**,** 478.

STEINBERG, M. H., FORGET, B. G., HIGGS, D. R. & WEATHERALL, D. J. 2009. *Disorders of Hemoglobin: Genetics, Pathophysiology, and Clinical Management,* Cambridge University Press.

STRAIMER, J., GNÄDIG, N. F., STOKES, B. H., EHRENBERGER, M., CRANE, A. A. & FIDOCK, D. A. 2017. Plasmodium falciparum K13 Mutations

Differentially Impact Ozonide Susceptibility and Parasite Fitness In Vitro. *mBio,* 8**,** e00172-17.

STRAIMER, J., GNADIG, N. F., WITKOWSKI, B., AMARATUNGA, C., DURU, V., RAMADANI, A. P., DACHEUX, M., KHIM, N., ZHANG, L., LAM, S., GREGORY, P. D., URNOV, F. D., MERCEREAU-PUIJALON, O., BENOIT-VICAL, F., FAIRHURST, R. M., MENARD, D. & FIDOCK, D. A. 2015. Drug resistance. K13-propeller mutations confer artemisinin resistance in Plasmodium falciparum clinical isolates. *Science,* 347**,** 428-31.

STRAIMER, J., LEE, M. C., LEE, A. H., ZEITLER, B., WILLIAMS, A. E., PEARL, J. R., ZHANG, L., REBAR, E. J., GREGORY, P. D., LLINAS, M., URNOV, F. D. & FIDOCK, D. A. 2012. Site-specific genome editing in Plasmodium falciparum using engineered zinc-finger nucleases. *Nat Methods,* 9**,** 993-8.

STROHECKER, A. M., GUO, J. Y., KARSLI-UZUNBAS, G., PRICE, S. M., CHEN, G. J., MATHEW, R., MCMAHON, M. & WHITE, E. 2013. Autophagy Sustains Mitochondrial Glutamine Metabolism and Growth of Braf^{V600E}–Driven Lung Tumors. *Cancer Discovery,* 3**,** 1272-1285.

STROMHAUG, P. E., REGGIORI, F., GUAN, J., WANG, C. W. & KLIONSKY, D. J. 2004. Atg21 is a phosphoinositide binding protein required for efficient lipidation and localization of Atg8 during uptake of aminopeptidase I by selective autophagy. *Mol Biol Cell,* 15**,** 3553-66.

SU, X.-Z., KIRKMAN, L. A., FUJIOKA, H. & WELLEMS, T. E. 1997. Complex Polymorphisms in an ~330 kDa Protein Are Linked to Chloroquine-Resistant P. falciparum in Southeast Asia and Africa. *Cell,* 91**,** 593-603.

SU, X., FERDIG, M. T., HUANG, Y., HUYNH, C. Q., LIU, A., YOU, J., WOOTTON, J. C. & WELLEMS, T. E. 1999. A genetic map and recombination parameters of the human malaria parasite Plasmodium falciparum. *Science,* 286**,** 1351-3.

SU, X., HAYTON, K. & WELLEMS, T. E. 2007. Genetic linkage and association analyses for trait mapping in Plasmodium falciparum. *Nature Reviews Genetics,* 8**,** 497.

SULLIVAN, J. S., J SULLIVAN, J., WILLIAMS, A., GRADY, K., BOUNNGASENG, A., S HUBER, C., NACE, D., WILLIAMS, T., GALE GALLAND, G., BARNWELL, J. & E COLLINS, W. 2004. *Adaptation of a strain of*

Plasmodium falciparum from Ghana to Aotus lemurinus griseimembra, A. nancymai, and A. vociferans monkeys.

SUNTORNTHITICHAROEN, P., PETMITR, S. & CHAVALITSHEWINKOON-PETMITR, P. 2006. Purification and characterization of a novel 3′-5′ DNA helicase from Plasmodium falciparum and its sensitivity to anthracycline antibiotics. *Parasitology,* 133**,** 389-398.

SUZUKI, T. & YAMAMOTO, M. 2017. Stress-sensing mechanisms and the physiological roles of the Keap1-Nrf2 system during cellular stress. *J Biol Chem,* 292**,** 16817-16824.

SWANSON, M. S. & ISBERG, R. R. 1995. Association of Legionella pneumophila with the macrophage endoplasmic reticulum. *Infect Immun,* 63**,** 3609-20.

TAKALA-HARRISON, S., CLARK, T. G., JACOB, C. G., CUMMINGS, M. P., MIOTTO, O., DONDORP, A. M., FUKUDA, M. M., NOSTEN, F., NOEDL, H., IMWONG, M., BETHELL, D., SE, Y., LON, C., TYNER, S. D., SAUNDERS, D. L., SOCHEAT, D., ARIEY, F., PHYO, A. P., STARZENGRUBER, P., FUEHRER, H. P., SWOBODA, P., STEPNIEWSKA, K., FLEGG, J., ARZE, C., CERQUEIRA, G. C., SILVA, J. C., RICKLEFS, S. M., PORCELLA, S. F., STEPHENS, R. M., ADAMS, M., KENEFIC, L. J., CAMPINO, S., AUBURN, S., MACINNIS, B., KWIATKOWSKI, D. P., SU, X. Z., WHITE, N. J., RINGWALD, P. & PLOWE, C. V. 2013. Genetic loci associated with delayed clearance of Plasmodium falciparum following artemisinin treatment in Southeast Asia. *Proc Natl Acad Sci U S A,* 110**,** 240-5.

TAKAMURA, A., KOMATSU, M., HARA, T., SAKAMOTO, A., KISHI, C., WAGURI, S., EISHI, Y., HINO, O., TANAKA, K. & MIZUSHIMA, N. 2011. Autophagy-deficient mice develop multiple liver tumors. *Genes Dev,* 25**,** 795-800.

TALUNDZIC, E., OKOTH, S. A., CONGPUONG, K., PLUCINSKI, M. M., MORTON, L., GOLDMAN, I. F., KACHUR, P. S., WONGSRICHANALAI, C., SATIMAI, W., BARNWELL, J. W. & UDHAYAKUMAR, V. 2015. Selection and spread of artemisinin-resistant alleles in Thailand prior to the global artemisinin resistance containment campaign. *PLoS Pathog,* 11**,** e1004789.

TAN, X., THAPA, N., SUN, Y. & ANDERSON, R. A. 2015. A kinase-independent role for EGF receptor in autophagy initiation. *Cell,* 160**,** 145-60.

TANG, D. C., DEVIT, M. & JOHNSTON, S. A. 1992. Genetic immunization is a simple method for eliciting an immune response. *Nature,* 356**,** 152-4.

TANG, M. X., REDEMANN, C. T. & SZOKA, F. C., JR. 1996. In vitro gene delivery by degraded polyamidoamine dendrimers. *Bioconjug Chem,* 7**,** 703-14.

TANGUTUR, A. D., KUMAR, D., KRISHNA, K. V. & KANTEVARI, S. 2017. Microtubule Targeting Agents as Cancer Chemotherapeutics: An Overview of Molecular Hybrids as Stabilizing and Destabilizing Agents. *Curr Top Med Chem,* 17**,** 2523-2537.

TAWK, L., CHICANNE, G., DUBREMETZ, J. F., RICHARD, V., PAYRASTRE, B., VIAL, H. J., ROY, C. & WENGELNIK, K. 2010. Phosphatidylinositol 3-phosphate, an essential lipid in Plasmodium, localizes to the food vacuole membrane and the apicoplast. *Eukaryot Cell,* 9**,** 1519-30.

TAYLOR, S. M., PAROBEK, C. M., DECONTI, D. K., KAYENTAO, K., COULIBALY, S. O., GREENWOOD, B. M., TAGBOR, H., WILLIAMS, J., BOJANG, K., NJIE, F., DESAI, M., KARIUKI, S., GUTMAN, J., MATHANGA, D. P., MÅRTENSSON, A., NGASALA, B., CONRAD, M. D., ROSENTHAL, P. J., TSHEFU, A. K., MOORMANN, A. M., VULULE, J. M., DOUMBO, O. K., TER KUILE, F. O., MESHNICK, S. R., BAILEY, J. A. & JULIANO, J. J. 2015. Absence of Putative Artemisinin Resistance Mutations Among Plasmodium falciparum in Sub-Saharan Africa: A Molecular Epidemiologic Study. *The Journal of Infectious Diseases,* 211**,** 680-688.

TAYLOR, T. E., FU, W. J., CARR, R. A., WHITTEN, R. O., MUELLER, J. G., FOSIKO, N. G., LEWALLEN, S., LIOMBA, N. G. & MOLYNEUX, M. E. 2004. Differentiating the pathologies of cerebral malaria by postmortem parasite counts. *Nature Medicine,* 10**,** 143.

TEUSCHER, F., CHEN, N., KYLE, D. E., GATTON, M. L. & CHENG, Q. 2012. Phenotypic changes in artemisinin-resistant Plasmodium falciparum lines in vitro: evidence for decreased sensitivity to dormancy and growth inhibition. *Antimicrob Agents Chemother,* 56**,** 428-31.

TEUSCHER, F., GATTON, M. L., CHEN, N., PETERS, J., KYLE, D. E. & CHENG, Q. 2010. Artemisinin induced dormancy in Plasmodium falciparum: Duration, recovery rates and implications in treatment failure. *The Journal of infectious diseases,* 202**,** 1362-1368.

THAPAR, M. M., GIL, J. P. & BJORKMAN, A. 2005. In vitro recrudescence of Plasmodium falciparum parasites suppressed to dormant state by atovaquone alone and in combination with proguanil. *Trans R Soc Trop Med Hyg,* 99**,** 62-70.

THOMAS, K. R., FOLGER, K. R. & CAPECCHI, M. R. 1986. High frequency targeting of genes to specific sites in the mammalian genome. *Cell,* 44**,** 419-28.

THORPE, G. W., FONG, C. S., ALIC, N., HIGGINS, V. J. & DAWES, I. W. 2004. Cells have distinct mechanisms to maintain protection against different reactive oxygen species: oxidative-stress-response genes. *Proc Natl Acad Sci U S A,* 101**,** 6564-9.

THRIEMER, K., HONG, N. V., ROSANAS-URGELL, A., PHUC, B. Q., HA DO, M., POCKELE, E., GUETENS, P., VAN, N. V., DUONG, T. T., AMAMBUA-NGWA, A., D'ALESSANDRO, U. & ERHART, A. 2014. Delayed parasite clearance after treatment with dihydroartemisinin-piperaquine in Plasmodium falciparum malaria patients in central Vietnam. *Antimicrob Agents Chemother,* 58**,** 7049-55.

THUMM, M., EGNER, R., KOCH, B., SCHLUMPBERGER, M., STRAUB, M., VEENHUIS, M. & WOLF, D. H. 1994. Isolation of autophagocytosis mutants of Saccharomyces cerevisiae. *FEBS Lett,* 349**,** 275-80.

TILLEY, L., STRAIMER, J., GNADIG, N. F., RALPH, S. A. & FIDOCK, D. A. 2016. Artemisinin Action and Resistance in Plasmodium falciparum. *Trends Parasitol,* 32**,** 682-96.

TOMLINS, A. M., BEN-RACHED, F., WILLIAMS, R. A., PROTO, W. R., COPPENS, I., RUCH, U., GILBERGER, T. W., COOMBS, G. H., MOTTRAM, J. C., MULLER, S. & LANGSLEY, G. 2013. Plasmodium falciparum ATG8 implicated in both autophagy and apicoplast formation. *Autophagy,* 9**,** 1540-52.

TOOZE, S. A., ABADA, A. & ELAZAR, Z. 2014. Endocytosis and autophagy: exploitation or cooperation? *Cold Spring Harb Perspect Biol,* 6**,** a018358.

TOTH, M. L., SIGMOND, T., BORSOS, E., BARNA, J., ERDELYI, P., TAKACS-VELLAI, K., OROSZ, L., KOVACS, A. L., CSIKOS, G., SASS, M. & VELLAI, T. 2008. Longevity pathways converge on autophagy genes to regulate life span in Caenorhabditis elegans. *Autophagy,* 4**,** 330-8.

TRAGER, W. & JENSEN, J. B. 1976. Human malaria parasites in continuous culture. *Science,* 193**,** 673-5.

TRAGER, W. & JENSON, J. B. 1978. Cultivation of malarial parasites. *Nature,* 273**,** 621-2.

TRAMPUZ, A., JEREB, M., MUZLOVIC, I. & PRABHU, R. M. 2003. Clinical review: Severe malaria. *Critical Care,* 7**,** 315-323.

TRENHOLME, C., WILLIAMS, R., DESJARDINS, R., FRISCHER, H., CARSON, P., RIECKMANN, K. & CANFIELD, C. 1975. Mefloquine (WR 142,490) in the treatment of human malaria. *Science,* 190**,** 792-794.

TSUKADA, M. & OHSUMI, Y. 1993. Isolation and characterization of autophagy-defective mutants of Saccharomyces cerevisiae. *FEBS Lett,* 333**,** 169-74.

TSUYUKI, S., TAKABAYASHI, M., KAWAZU, M., KUDO, K., WATANABE, A., NAGATA, Y., KUSAMA, Y. & YOSHIDA, K. 2014. Detection of WIPI1 mRNA as an indicator of autophagosome formation. *Autophagy,* 10**,** 497-513.

TU, Y. 2011. The discovery of artemisinin (qinghaosu) and gifts from Chinese medicine. *Nat Med,* 17**,** 1217-20.

TUCKER, M. S., MUTKA, T., SPARKS, K., PATEL, J. & KYLE, D. E. 2012. Phenotypic and genotypic analysis of in vitro-selected artemisinin-resistant progeny of Plasmodium falciparum. *Antimicrob Agents Chemother,* 56**,** 302-14.

VAID, A., RANJAN, R., SMYTHE, W. A., HOPPE, H. C. & SHARMA, P. 2010. PfPI3K, a phosphatidylinositol-3 kinase from Plasmodium falciparum, is exported to the host erythrocyte and is involved in hemoglobin trafficking. *Blood,* 115**,** 2500-7.

VALDERRAMOS, S. G., VALDERRAMOS, J. C., MUSSET, L., PURCELL, L. A., MERCEREAU-PUIJALON, O., LEGRAND, E. & FIDOCK, D. A. 2010. Identification of a mutant PfCRT-mediated chloroquine tolerance phenotype in Plasmodium falciparum. *PLoS Pathog,* 6**,** e1000887.

VANHAESEBROECK, B., GUILLERMET-GUIBERT, J., GRAUPERA, M. & BILANGES, B. 2010. The emerging mechanisms of isoform-specific PI3K signalling. *Nature Reviews Molecular Cell Biology,* 11**,** 329.

VEIGA, M. I., FERREIRA, P. E., JORNHAGEN, L., MALMBERG, M., KONE, A., SCHMIDT, B. A., PETZOLD, M., BJORKMAN, A., NOSTEN, F. & GIL, J. P. 2011. Novel polymorphisms in Plasmodium falciparum ABC transporter genes are associated with major ACT antimalarial drug resistance. *PLoS One,* 6**,** e20212.

VEIGA, M. I., FERREIRA, P. E., MALMBERG, M., JORNHAGEN, L., BJORKMAN, A., NOSTEN, F. & GIL, J. P. 2012. pfmdr1 amplification is related to increased Plasmodium falciparum in vitro sensitivity to the bisquinoline piperaquine. *Antimicrob Agents Chemother,* 56**,** 3615-9.

VELAYATI, A. A., MASJEDI, M. R., FARNIA, P., TABARSI, P., GHANAVI, J., ZIAZARIFI, A. H. & HOFFNER, S. E. 2009. Emergence of new forms of totally drug-resistant tuberculosis bacilli: super extensively drug-resistant tuberculosis or totally drug-resistant strains in iran. *Chest,* 136**,** 420-425.

VICINANZA, M., KOROLCHUK, VIKTOR I., ASHKENAZI, A., PURI, C., MENZIES, FIONA M., CLARKE, JONATHAN H. & RUBINSZTEIN, DAVID C. 2015. PI(5)P Regulates Autophagosome Biogenesis. *Molecular Cell,* 57**,** 219-234.

VOSS, C., EHRENMAN, K., MLAMBO, G., MISHRA, S., KUMAR, K. A., SACCI, J. B., JR., SINNIS, P. & COPPENS, I. 2016. Overexpression of Plasmodium berghei ATG8 by Liver Forms Leads to Cumulative Defects in Organelle Dynamics and to Generation of Noninfectious Merozoites. *MBio,* 7.

WAGNER, M. A., ANDEMARIAM, B. & DESAI, S. A. 2003. A Two-Compartment Model of Osmotic Lysis in Plasmodium falciparum-Infected Erythrocytes. *Biophysical Journal,* 84**,** 116-123.

WALCZAK, M., GANESAN, S. M., NILES, J. C. & YEH, E. 2018. ATG8 Is Essential Specifically for an Autophagy-Independent Function in Apicoplast Biogenesis in Blood-Stage Malaria Parasites. *MBio,* 9.

WALKER, D. M., MAHFOOZ, N., KEMME, K. A., PATEL, V. C., SPANGLER, M. & DREW, M. E. 2013. Plasmodium falciparum erythrocytic stage parasites require the putative autophagy protein PfAtg7 for normal growth. *PLoS One,* 8**,** e67047.

WALKER, S., CHANDRA, P., MANIFAVA, M., AXE, E. & KTISTAKIS, N. T. 2008. Making autophagosomes: localized synthesis of phosphatidylinositol 3-phosphate holds the clue. *Autophagy,* 4**,** 1093-6.

WALLIKER, D., HUNT, P. & BABIKER, H. 2005. Fitness of drug-resistant malaria parasites. *Acta Tropica,* 94**,** 251-259.

WALLIKER, D., QUAKYI, I., WELLEMS, T., MCCUTCHAN, T., SZARFMAN, A., LONDON, W., CORCORAN, L., BURKOT, T. & CARTER, R. 1987. Genetic

analysis of the human malaria parasite Plasmodium falciparum. *Science,* 236**,** 1661-1666.

WANG, J., WEN, J., YI, R., LIU, F., ZHOU, J., LIU, G., LI, Q., YANG, Z. & SU, X. 2015a. High selectivity of PI3Kbeta inhibitors in SETD2-mutated renal clear cell carcinoma. *J buon,* 20**,** 1267-75.

WANG, J., ZHANG, C.-J., CHIA, W. N., LOH, C. C. Y., LI, Z., LEE, Y. M., HE, Y., YUAN, L.-X., LIM, T. K., LIU, M., LIEW, C. X., LEE, Y. Q., ZHANG, J., LU, N., LIM, C. T., HUA, Z.-C., LIU, B., SHEN, H.-M., TAN, K. S. W. & LIN, Q. 2015b. Haem-activated promiscuous targeting of artemisinin in Plasmodium falciparum. *Nature Communications,* 6**,** 10111.

WANG, Z., CABRERA, M., YANG, J., YUAN, L., GUPTA, B., LIANG, X., KEMIREMBE, K., SHRESTHA, S., BRASHEAR, A., LI, X., PORCELLA, S. F., MIAO, J., YANG, Z., SU, X. Z. & CUI, L. 2016. Genome-wide association analysis identifies genetic loci associated with resistance to multiple antimalarials in Plasmodium falciparum from China-Myanmar border. *Sci Rep,* 6**,** 33891.

WANKUN, X., WENZHEN, Y., MIN, Z., WEIYAN, Z., HUAN, C., WEI, D., LVZHEN, H., XU, Y. & XIAOXIN, L. 2011. Protective effect of paeoniflorin against oxidative stress in human retinal pigment epithelium in vitro. *Mol Vis,* 17**,** 3512-22.

WARHURST, D. C. 1987. Cinchona alkaloids and malaria. *Acta Leiden,* 55**,** 53-64.

WARR, M. R., BINNEWIES, M., FLACH, J., REYNAUD, D., GARG, T., MALHOTRA, R., DEBNATH, J. & PASSEGUE, E. 2013. FOXO3A directs a protective autophagy program in haematopoietic stem cells. *Nature,* 494**,** 323-7.

WATANABE, Y., KOBAYASHI, T., YAMAMOTO, H., HOSHIDA, H., AKADA, R., INAGAKI, F., OHSUMI, Y. & NODA, N. N. 2012. Structure-based analyses reveal distinct binding sites for Atg2 and phosphoinositides in Atg18. *J Biol Chem,* 287**,** 31681-90.

WATERS, A. P., THOMAS, A. W., VAN DIJK, M. R. & JANSE, C. J. 1997. Transfection of malaria parasites. *Methods,* 13**,** 134-47.

WATKINS, W. M., SIXSMITH, D. G. & CHULAY, J. D. 1984. The activity of proguanil and its metabolites, cycloguanil and p-chlorophenylbiguanide, against Plasmodium falciparum in vitro. *Ann Trop Med Parasitol,* 78**,** 273-8.

WATSON, A. S., RIFFELMACHER, T., STRANKS, A., WILLIAMS, O., DE BOER, J., CAIN, K., MACFARLANE, M., MCGOURAN, J., KESSLER, B., KHANDWALA, S., CHOWDHURY, O., PULESTON, D., PHADWAL, K., MORTENSEN, M., FERGUSON, D., SOILLEUX, E., WOLL, P., JACOBSEN, S. E. & SIMON, A. K. 2015. Autophagy limits proliferation and glycolytic metabolism in acute myeloid leukemia. *Cell Death Discov,* 1.

WELLEMS, T. E., PANTON, L. J., GLUZMAN, I. Y., DO ROSARIO, V. E., GWADZ, R. W., WALKER-JONAH, A. & KROGSTAD, D. J. 1990. Chloroquine resistance not linked to mdr-like genes in a Plasmodium falciparum cross. *Nature,* 345**,** 253.

WELLEMS, T. E., WALKER-JONAH, A. & PANTON, L. J. 1991. Genetic mapping of the chloroquine-resistance locus on Plasmodium falciparum chromosome 7. *Proceedings of the National Academy of Sciences,* 88**,** 3382-3386.

WELLEMS, T. E., WALLIKER, D., SMITH, C. L., DO ROSARIO, V. E., MALOY, W. L., HOWARD, R. J., CARTER, R. & MCCUTCHAN, T. F. 1987. A histidine-rich protein gene marks a linkage group favored strongly in a genetic cross of Plasmodium falciparum. *Cell,* 49**,** 633-642.

WERNSDORFER, W. H. 1994. Epidemiology of drug resistance in malaria. *Acta Trop,* 56**,** 143-56.

WESCHE, D. L. & BLACK, J. 1990. A comparison of the antimalarial activity of the cinchona alkaloids against Plasmodium falciparum in vitro. *J Trop Med Hyg,* 93**,** 153-9.

WHITE, L. J., FLEGG, J. A., PHYO, A. P., WILADPAI-NGERN, J. H., BETHELL, D., PLOWE, C., ANDERSON, T., NKHOMA, S., NAIR, S., TRIPURA, R., STEPNIEWSKA, K., PAN-NGUM, W., SILAMUT, K., COOPER, B. S., LUBELL, Y., ASHLEY, E. A., NGUON, C., NOSTEN, F., WHITE, N. J. & DONDORP, A. M. 2015. Defining the in vivo phenotype of artemisinin-resistant falciparum malaria: a modelling approach. *PLoS Med,* 12**,** e1001823.

WHITE, N. J. 1997. Assessment of the pharmacodynamic properties of antimalarial drugs in vivo. *Antimicrob Agents Chemother,* 41**,** 1413-22.

WHITE, N. J. 2008. Qinghaosu (artemisinin): the price of success. *Science,* 320**,** 330-4.

WHITE, N. J. 2011. The parasite clearance curve. *Malaria Journal,* 10**,** 278.

WHITE, N. J., PUKRITTAYAKAMEE, S., HIEN, T. T., FAIZ, M. A., MOKUOLU, O. A. & DONDORP, A. M. 2014a. Malaria. *Lancet,* 383**,** 723-35.

WHITE, N. J., PUKRITTAYAKAMEE, S., PHYO, A. P., RUEANGWEERAYUT, R., NOSTEN, F., JITTAMALA, P., JEEYAPANT, A., JAIN, J. P., LEFEVRE, G., LI, R., MAGNUSSON, B., DIAGANA, T. T. & LEONG, F. J. 2014b. Spiroindolone KAE609 for falciparum and vivax malaria. *N Engl J Med,* 371**,** 403-10.

WHO 1990. Severe and complicated malaria. World Health Organization, Division of Control of Tropical Diseases. *Trans R Soc Trop Med Hyg,* 84 Suppl 2**,** 1-65.

WHO 2006. The impact of chronic disease in Cambodia. World Health Organization.

WHO 2011. Noncommunicable Diseases Country Profiles. France.

WHO 2015a. Guidelines for the Treatment of Malaria. Italy: World Health Organization.

WHO 2015b. Status report on artemisinin and ACT resistance. *Global Malaria Programme.*

WHO 2015c. Strategy for malaria elimination in the Greater Mekong Subregion (2015-2030). *In:* ORGANIZATION, W. H. (ed.).

WHO 2016a. Artemisinin and artemisinin-based combination therapy resistance. *Global Marlaia Programme.* World Health Organization.

WHO 2016b. World Malaria Report 2016. Geneva.

WILLIAMS, J. A. 2014. Improving DNA vaccine performance through vector design. *Curr Gene Ther,* 14**,** 170-89.

WILSON, A., LAURENTI, E., OSER, G., VAN DER WATH, R. C., BLANCO-BOSE, W., JAWORSKI, M., OFFNER, S., DUNANT, C. F., ESHKIND, L., BOCKAMP, E., LIÓ, P., MACDONALD, H. R. & TRUMPP, A. 2008. Hematopoietic Stem Cells Reversibly Switch from Dormancy to Self-Renewal during Homeostasis and Repair. *Cell,* 135**,** 1118-1129.

WILSON, C. M., VOLKMAN, S. K., THAITHONG, S., MARTIN, R. K., KYLE, D. E., MILHOUS, W. K. & WIRTH, D. F. 1993. Amplification of pfmdr 1 associated with mefloquine and halofantrine resistance in Plasmodium falciparum from Thailand. *Mol Biochem Parasitol,* 57**,** 151-60.

WINTERBOURN, C. C. 1995. Toxicity of iron and hydrogen peroxide: the Fenton reaction. *Toxicology Letters,* 82-83**,** 969-974.

WINZELER, E. A. & MANARY, M. J. 2014. Drug resistance genomics of the antimalarial drug artemisinin. *Genome Biology,* 15**,** 544.

WITKOWSKI, B., AMARATUNGA, C., KHIM, N., SRENG, S., CHIM, P., KIM, S., LIM, P., MAO, S., SOPHA, C., SAM, B., ANDERSON, J. M., DUONG, S., CHUOR, C. M., TAYLOR, W. R., SUON, S., MERCEREAU-PUIJALON, O., FAIRHURST, R. M. & MENARD, D. 2013a. Novel phenotypic assays for the detection of artemisinin-resistant Plasmodium falciparum malaria in Cambodia: in-vitro and ex-vivo drug-response studies. *Lancet Infect Dis,* 13**,** 1043-9.

WITKOWSKI, B., DURU, V., KHIM, N., ROSS, L. S., SAINTPIERRE, B., BEGHAIN, J., CHY, S., KIM, S., KE, S., KLOEUNG, N., EAM, R., KHEAN, C., KEN, M., LOCH, K., BOUILLON, A., DOMERGUE, A., MA, L., BOUCHIER, C., LEANG, R., HUY, R., NUEL, G., BARALE, J. C., LEGRAND, E., RINGWALD, P., FIDOCK, D. A., MERCEREAU-PUIJALON, O., ARIEY, F. & MENARD, D. 2017. A surrogate marker of piperaquine-resistant Plasmodium falciparum malaria: a phenotype-genotype association study. *Lancet Infect Dis,* 17**,** 174-183.

WITKOWSKI, B., KHIM, N., CHIM, P., KIM, S., KE, S., KLOEUNG, N., CHY, S., DUONG, S., LEANG, R., RINGWALD, P., DONDORP, A. M., TRIPURA, R., BENOIT-VICAL, F., BERRY, A., GORGETTE, O., ARIEY, F., BARALE, J.-C., MERCEREAU-PUIJALON, O. & MENARD, D. 2013b. Reduced Artemisinin Susceptibility of Plasmodium falciparum Ring Stages in Western Cambodia. *Antimicrobial Agents and Chemotherapy,* 57**,** 914-923.

WITKOWSKI, B., KHIM, N., CHIM, P., KIM, S., KE, S., KLOEUNG, N., CHY, S., DUONG, S., LEANG, R., RINGWALD, P., DONDORP, A. M., TRIPURA, R., BENOIT-VICAL, F., BERRY, A., GORGETTE, O., ARIEY, F., BARALE, J. C., MERCEREAU-PUIJALON, O. & MENARD, D. 2013c. Reduced artemisinin susceptibility of Plasmodium falciparum ring stages in western Cambodia. *Antimicrob Agents Chemother,* 57**,** 914-23.

WITKOWSKI, B., LELIEVRE, J., BARRAGAN, M. J., LAURENT, V., SU, X. Z., BERRY, A. & BENOIT-VICAL, F. 2010. Increased tolerance to artemisinin in Plasmodium falciparum is mediated by a quiescence mechanism. *Antimicrob Agents Chemother,* 54**,** 1872-7.

WOJTKOWIAK, J. W., ROTHBERG, J. M., KUMAR, V., SCHRAMM, K. J., HALLER, E., PROEMSEY, J. B., LLOYD, M. C., SLOANE, B. F. & GILLIES, R. J. 2012. Chronic Autophagy Is a Cellular Adaptation to Tumor Acidic pH Microenvironments. *Cancer Research,* 72**,** 3938-3947.

WONGSRICHANALAI, C. & MESHNICK, S. R. 2008. Declining artesunate-mefloquine efficacy against falciparum malaria on the Cambodia-Thailand border. *Emerg Infect Dis,* 14**,** 716-9.

WOOTTON, J. C. & FEDERHEN, S. 1993. Statistics of local complexity in amino acid sequences and sequence databases. *Computers & Chemistry,* 17**,** 149-163.

WORLD BANK, T. 2017. *The World Bank in Cambodia* [Online]. Available: http://www.worldbank.org/en/country/cambodia [Accessed].

WU, Y., SIFRI, C. D., LEI, H. H., SU, X. Z. & WELLEMS, T. E. 1995. Transfection of Plasmodium falciparum within human red blood cells. *Proc Natl Acad Sci U S A,* 92**,** 973-7.

WWARN. 2017. *Tracking resistance to artemisinin collaboration II* [Online]. Available: http://www.wwarn.org/working-together/partner-projects/tracking-resistance-artemisinin-collaboration-ii [Accessed].

XIE, S. C., DOGOVSKI, C., HANSSEN, E., CHIU, F., YANG, T., CRESPO, M. P., STAFFORD, C., BATINOVIC, S., TEGUH, S., CHARMAN, S., KLONIS, N. & TILLEY, L. 2016. Haemoglobin degradation underpins the sensitivity of early ring stage Plasmodium falciparum to artemisinins. *J Cell Sci,* 129**,** 406-16.

XIE, S. C., DOGOVSKI, C., KENNY, S., TILLEY, L. & KLONIS, N. 2014. Optimal assay design for determining the in vitro sensitivity of ring stage Plasmodium falciparum to artemisinins. *International Journal for Parasitology,* 44**,** 893-899.

XIE, Z., NAIR, U. & KLIONSKY, D. J. 2008. Atg8 controls phagophore expansion during autophagosome formation. *Mol Biol Cell,* 19**,** 3290-8.

XIONG, X., TAO, R., DEPINHO, R. A. & DONG, X. C. 2012. The autophagy-related gene 14 (Atg14) is regulated by forkhead box O transcription factors and circadian rhythms and plays a critical role in hepatic autophagy and lipid metabolism. *J Biol Chem,* 287**,** 39107-14.

XU, X., ARAKI, K., LI, S., HAN, J. H., YE, L., TAN, W. G., KONIECZNY, B. T., BRUINSMA, M. W., MARTINEZ, J., PEARCE, E. L., GREEN, D. R., JONES, D. P., VIRGIN, H. W. & AHMED, R. 2014a. Autophagy is essential for effector CD8(+) T cell survival and memory formation. *Nat Immunol,* 15**,** 1152-61.

XU, Z., HANG, J., HU, J. & GAO, B. 2014b. Gefitinib, an EGFR tyrosine kinase inhibitor, activates autophagy through AMPK in human lung cancer cells. *J buon,* 19**,** 466-73.

XUE, H. Y. & FORSDYKE, D. R. 2003. Low-complexity segments in Plasmodium falciparum proteins are primarily nucleic acid level adaptations. *Mol Biochem Parasitol,* 128**,** 21-32.

YANG, S., WANG, X., CONTINO, G., LIESA, M., SAHIN, E., YING, H., BAUSE, A., LI, Y., STOMMEL, J. M., DELL'ANTONIO, G., MAUTNER, J., TONON, G., HAIGIS, M., SHIRIHAI, O. S., DOGLIONI, C., BARDEESY, N. & KIMMELMAN, A. C. 2011. Pancreatic cancers require autophagy for tumor growth. *Genes Dev,* 25**,** 717-29.

YAO, G. 2014. Modelling mammalian cellular quiescence. *Interface Focus,* 4**,** 20130074.

YEH, E. & DERISI, J. L. 2011. Chemical Rescue of Malaria Parasites Lacking an Apicoplast Defines Organelle Function in Blood-Stage Plasmodium falciparum. *PLOS Biology,* 9**,** e1001138.

YIP, K. W., MAO, X., AU, P. Y., HEDLEY, D. W., CHOW, S., DALILI, S., MOCANU, J. D., BASTIANUTTO, C., SCHIMMER, A. & LIU, F. F. 2006. Benzethonium chloride: a novel anticancer agent identified by using a cell-based small-molecule screen. *Clin Cancer Res,* 12**,** 5557-69.

YORIMITSU, T. & KLIONSKY, D. J. 2005. Atg11 links cargo to the vesicle-forming machinery in the cytoplasm to vacuole targeting pathway. *Mol Biol Cell,* 16**,** 1593-605.

YOSEF, I., GOREN, M. G. & QIMRON, U. 2012. Proteins and DNA elements essential for the CRISPR adaptation process in Escherichia coli. *Nucleic Acids Res,* 40**,** 5569-76.

YOULE, R. J. & NARENDRA, D. P. 2010. Mechanisms of mitophagy. *Nature Reviews Molecular Cell Biology,* 12**,** 9.

YU, K. Y., WANG, Y. P., WANG, L. H., JIAN, Y., ZHAO, X. D., CHEN, J. W., MURAO, K., ZHU, W., DONG, L., WANG, G. Q. & ZHANG, G. X. 2014. Mitochondrial KATP channel involvement in angiotensin II-induced autophagy in vascular smooth muscle cells. *Basic Res Cardiol,* 109**,** 416.

YUAN, J., JOHNSON, R. L., HUANG, R., WICHTERMAN, J., JIANG, H., HAYTON, K., FIDOCK, D. A., WELLEMS, T. E., INGLESE, J., AUSTIN, C. P. & SU, X.-Z. 2009. Genetic mapping of targets mediating differential chemical phenotypes in Plasmodium falciparum. *Nature chemical biology,* 5**,** 765-771.

ZHAO, Y., ZHOU, G., WANG, J., JIA, L., ZHANG, P., LI, R., SHAN, L., LIU, B., SONG, X., LIU, S. & XIAO, X. 2013. Paeoniflorin protects against ANIT-induced cholestasis by ameliorating oxidative stress in rats. *Food Chem Toxicol,* 58**,** 242-8.

ZHU, L., WEI, W., ZHENG, Y. Q. & JIA, X. Y. 2005. Effects and mechanisms of total glucosides of paeony on joint damage in rat collagen-induced arthritis. *Inflamm Res,* 54**,** 211-20.

ZILVERSMIT, M. M., VOLKMAN, S. K., DEPRISTO, M. A., WIRTH, D. F., AWADALLA, P. & HARTL, D. L. 2010. Low-complexity regions in Plasmodium falciparum: missing links in the evolution of an extreme genome. *Mol Biol Evol,* 27**,** 2198-209.

APPENDIX A: DIFFERENTIAL COMPOUNDS

Table 25: Differential compounds favoring mutant (Dd2$^{R539T/T38I}$)

Sample ID	Parent (Dd2R539T)						Mutant (Dd2R539T/T38I)					
	CCLASS2	LAC50	MaxR	TAUC	EEF	klass	CCLASS2	LAC50	MaxR	TAUC	EEF	klass
NCGC00015501-07	4	NA	113.5232	602.1744	0	inactive	1.2	-9.07535	96.74674	572.6673	37.80774	active
NCGC00016564-07	4	-6.07535	69.1344	529.2449	28.04678	inactive	-2.2	-5.02535	61.07529	494.8381	52.26987	active
NCGC00017337-18	4	-8.18222	-21.4406	-65.2685	26.84911	inactive	-1.1	-8.53222	-4.2149	-50.0287	109.6466	active
NCGC00018100-02	4	-8.47535	103.4127	658.3412	27.66057	inactive	-2.2	-4.82535	76.88629	533.4987	44.50083	active
NCGC00018296-08	4	NA	108.079	608.0767	0	inactive	-2.2	-4.97535	60.17994	526.8526	53.37287	active
NCGC00090726-11	4	-6.77535	105.73	543.1998	18.85984	inactive	-2.2	-5.37535	103.4555	521.7306	63.90414	active
NCGC00095003-06	2.1	-4.67535	2021.154	1474.333	2329.109	active	1.2	-9.12535	115.4384	538.4643	47.14066	active
NCGC00095986-04	4	-4.78222	5.101416	83.98024	22.45213	inactive	1.2	-5.58222	18.23931	-16.7055	38.15834	active
NCGC00162383-02	4	NA	116.2177	604.8494	0	inactive	1.2	-8.27535	122.9265	560.6855	32.28923	active
NCGC00168785-02	4	-4.92535	98.37312	614.9305	26.68489	inactive	-2.2	-4.97535	69.99754	488.5579	31.45373	active
NCGC00168850-03	4	-5.24211	-12.7872	42.43601	26.206	inactive	-1.1	-8.69211	-38.944	-104.02	113.3432	active
NCGC00168921-03	4	-7.43222	-14.7456	-62.3577	24.83364	inactive	-1.1	-8.53222	-31.6593	-71.6909	119.5295	active
NCGC00169803-03	-1.1	-8.35469	-8.27948	11.00466	94.47788	active	-1.1	-9.10469	-35.684	-113.415	123.1747	active
NCGC00179265-08	4	-4.98222	-12.3117	14.73081	30.35233	inactive	-1.2	-8.38222	-19.5104	-67.4242	59.64774	active
NCGC00179711-03	4	-5.79211	-2.81768	29.75047	18.82381	inactive	2.1	-5.14211	77.38289	-49.4165	109.9795	active
NCGC00180312-03	4	-8.09211	9.251324	84.16985	17.5823	inactive	-2.2	-5.09211	-33.2813	-41.6779	40.37687	active
NCGC00180557-02	4	NA	-6.94722	-53.9729	0	inactive	2.2	-5.49345	39.79859	63.07475	36.71145	active
NCGC00182554-04	4	-7.88222	6.5095	-19.7811	23.58682	inactive	1.2	-5.63222	20.68275	-42.225	45.46975	active
NCGC00185071-02	4	NA	124.1016	582.6313	0	inactive	1.2	-9.02535	91.34392	499.296	32	active
NCGC00187906-01	4	-6.26412	91.03899	571.3059	27.68469	inactive	-2.2	-5.36412	96.15392	463.5652	43.68196	active
NCGC00188380-01	4	-7.57535	96.23	632.0402	27.01693	inactive	-2.2	-4.87535	62.53547	527.5918	53.4974	active
NCGC00242489-02	4	-5.73222	-1.18879	45.631	14.20754	inactive	-2.2	-6.03222	-18.1943	-82.3703	35.56204	active
NCGC00263160-01	4	-5.62535	92.06008	597.4116	21.51741	inactive	-2.2	-4.92535	81.51918	544.9591	34.73939	active
NCGC00345786-04	4	-6.78222	16.87656	-25.1995	28.87632	inactive	1.2	-6.23222	17.56027	101.7647	75.58727	active
NCGC00345797-01	4	-5.72535	91.90975	594.5607	29.94963	inactive	-2.2	-4.92535	85.05531	544.3987	42.12022	active
NCGC00345808-01	4	-4.67535	84.89139	561.1201	35.62877	inactive	-2.2	-4.87535	60.35689	522.4401	52.96247	active
NCGC00345848-01	4	-5.37535	87.91852	554.7201	34.38419	inactive	-2.2	-5.12535	68.8732	500.2538	46.46151	active
NCGC00346557-02	4	-6.73222	-3.96583	68.89652	17.97775	inactive	-1.2	-5.38222	-25.7036	-4.48041	33.18415	active
NCGC00346573-05	4	-5.98222	36.04504	69.89332	20.89379	inactive	1.2	-5.48222	37.99636	-63.1023	68.48376	active
NCGC00346619-07	4	-5.38222	17.8573	65.28645	27.19993	inactive	1.2	-5.68222	25.39385	-51.0317	65.78463	active
NCGC00346681-11	4	-5.98222	-15.8819	45.72998	29.79371	inactive	-1.2	-7.98222	0.517759	87.61022	68.37114	active
NCGC00346697-01	4	-6.27535	92.93589	553.0024	20.71417	inactive	1.2	-8.97535	99.60604	459.2331	32.18018	active
NCGC00346716-14	4	-7.83222	20.37947	44.16311	20.9369	inactive	1.1	-5.58222	46.89048	-43.0584	84.22773	active
NCGC00346889-03	4	NA	-30.1367	-107.614	0	inactive	-1.1	-8.53222	77.65562	-31.4641	110.249	active
NCGC00347495-02	4	NA	-6.63024	-33.6494	0	inactive	-1.1	-8.84345	66.93981	-112.218	121.0513	active
NCGC00347572-02	4	-8.34345	33.0595	258.3712	24.5	inactive	1.2	-8.29345	44.36651	317.2142	40.3658	active
NCGC00347941-04	4	-6.03222	38.38977	2.059574	19	inactive	1.2	-5.68222	48.12669	31.62971	79.19968	active
NCGC00347944-06	4	-5.38222	-16.9768	-59.3718	32.29486	inactive	1.1	-5.53222	82.49822	43.75108	101.7968	active
NCGC00351570-01	4	-6.98222	-1.14924	-21.6219	23.56319	inactive	-1.1	-8.33222	-39.6559	-53.0089	108.3153	active
NCGC00356145-11	-2.2	-5.27643	36.57699	445.7754	81.54878	active	-1.2	-6.02643	70.81211	466.3044	32.13463	active
NCGC00370916-01	4	-8.63222	6.619893	80.3757	18.28235	inactive	-1.1	-6.33222	-20.4593	112.7041	89.70773	active
NCGC00378664-01	4	-4.88222	-19.4422	3.946824	30.57757	inactive	-1.2	-7.28222	-26.8164	-75.1986	32.9523	active
NCGC00378879-01	4	-7.43222	-7.31277	-57.9394	27	inactive	1.2	-5.63222	-1.41698	-84.6899	35.21108	active
NCGC00379171-01	4	-6.83222	15.24703	98.31618	11.29519	inactive	1.2	-5.78222	20.26206	-13.4307	46.01204	active
NCGC00380175-01	4	-5.54211	18.95683	61.53499	29.11431	inactive	-1.1	-8.69211	-16.6628	-68.6918	96.23381	active
NCGC00380477-01	-1.1	-7.94345	79.03933	37.53054	81.48715	active	-1.1	-8.84345	-37.2662	-108.308	128.9028	active
NCGC00380798-01	4	-8.11017	1.171787	11.63488	19.63212	inactive	1.1	-6.81017	-0.22233	54.83746	103.4282	active
NCGC00380868-01	4	NA	-16.7015	-87.0786	0	inactive	-1.1	-8.84345	-27.9914	-72.9139	111.0402	active
NCGC00380901-01	4	-5.69345	2.766936	-27.3674	19.83525	inactive	-1.1	-7.99345	-32.3739	-39.5575	108.2489	active
NCGC00380918-01	4	-7.19345	25.89261	107.5867	21.11543	inactive	-1.1	-8.84345	-1.77167	-12.1508	87.86934	active
NCGC00380941-01	4	-7.13222	32.04694	146.3624	18	inactive	1.2	-7.08222	59.11337	192.056	53.72954	active
NCGC00381138-01	4	-8.29211	18.16125	25.30506	22	inactive	-1.1	-8.69211	-35.6547	-81.3432	127.0046	active
NCGC00381186-01	4	-7.29345	8.311729	98.29879	17.4469	inactive	-1.2	-6.44345	-40.5662	39.9654	79.62357	active
NCGC00381234-01	4	-7.40469	25.41203	70.0708	8.74916	inactive	-1.1	-8.85469	-29.5475	-96.5376	111.9366	active
NCGC00381293-01	4	-8.35469	13.26483	37.86244	16.32682	inactive	1.2	-9.15469	-4.66575	-44.963	30.5	active
NCGC00381408-02	4	-8.18222	-30.9768	-98.859	21.92701	inactive	2.2	-5.23222	13.92569	-69.1179	51.11025	active
NCGC00384195-05	4	-7.68222	-18.4885	-64.892	17.3618	inactive	-1.2	-7.88222	-24.3733	-59.0712	32.60667	active
NCGC00384201-02	4	-6.93222	-8.10983	26.77197	20.88162	inactive	-2.2	-5.28222	-35.1893	-42.5673	45.69108	active
NCGC00384707-01	4	-8.65469	2.661862	-59.7233	26.73911	inactive	-1.1	-9.10469	-17.4141	-77.2434	109.9078	active
NCGC00384794-01	4	-8.80535	20.03783	27.51708	28.5131	inactive	-1.1	-9.30535	-11.5069	-73.4979	100.7301	active
NCGC00384797-01	-1.2	-8.20469	0.913987	7.330408	72.27948	active	-1.1	-9.15469	-10.5222	-71.8292	86.57999	active
NCGC00384800-01	4	-7.09345	-8.3388	-48.4923	25.65733	inactive	-1.2	-8.84345	1.172835	12.8502	79.31448	active
NCGC00384838-01	4	-4.99345	13.93314	27.10471	11.13024	inactive	2.2	-5.29345	45.40439	69.10951	56.20589	active
NCGC00385053-01	4	-7.89211	-20.4312	-91.5593	11.04948	inactive	1.2	-8.39211	-5.02573	-33.1766	33.03516	active
NCGC00385189-01	4	-6.50469	-12.024	11.38346	28.68709	inactive	2.2	-5.75469	11.61812	-56.2886	33.40307	active
NCGC00385294-01	1.1	-5.89345	80.62193	41.56598	109.5557	active	-1.1	-8.84345	-17.0263	-86.5359	114.4502	active
NCGC00385343-01	4	-5.90535	29.20319	45.04896	27.45507	inactive	2.2	-5.85535	48.63414	56.33548	54.20234	active
NCGC00385400-01	4	-7.93222	24.39041	-20.1422	18.24675	inactive	1.1	-5.68222	69.23712	20.13464	96.15177	active
NCGC00385655-01	4	-8.74211	0.468443	-26.2025	23	inactive	-1.1	-5.74211	-31.633	176.1792	108.4179	active
NCGC00386111-01	4	-4.73222	17.59838	-13.9408	26.1452	inactive	2.2	-5.08222	18.54279	-25.9498	38.09371	active
NCGC00386190-05	4	NA	-5.07755	-22.0238	0	inactive	2.1	-4.98222	74.44022	-58.581	133.7159	active

NCGC00386280-01	4	-6.03222	-0.97836	3.907185	27.65194	inactive	2.2	-5.43222	37.04612	-22.0945	68.12612	active
NCGC00386584-02	4	-8.58222	41.36819	78.41417	24.63494	inactive	1.1	-5.78222	63.54892	46.47354	89.6521	active
NCGC00386753-04	4	-6.63222	-1.17447	-22.6941	17.86951	inactive	-1.2	-7.68222	-8.11287	12.59299	77.10337	active
NCGC00386831-01	-2.2	-5.48222	-20.6034	77.16308	68.85411	active	-1.1	-8.23222	72.45506	-31.2616	85.54978	active
NCGC00386861-01	4	NA	-17.9465	-38.5531	0	inactive	1.1	-5.58222	69.7951	49.27906	90.75219	active
NCGC00386908-01	4	-7.93222	-17.6078	-11.2049	24.35235	inactive	1.1	-5.58222	53.79868	-36.5521	88.22742	active
NCGC00386992-01	4	-8.58222	-11.8253	-1.4084	20.1619	inactive	1.1	-5.68222	76.50574	68.22438	94.0497	active
NCGC00387156-01	4	-7.04345	29.52183	67.11627	18.95103	inactive	-2.2	-5.24345	39.63094	322.5265	45.8796	active
NCGC00387470-01	4	NA	33.68534	55.05373	0	inactive	1.1	-5.63222	47.51146	-29.9708	90.95496	active
NCGC00389445-01	2.2	-5.13222	73.29916	49.41195	87.40772	active	-2.2	-5.83222	-41.7651	-101.537	46.73693	active
NCGC00390222-01	4	-7.03222	-3.38668	78.39287	15.13301	inactive	1.2	-5.63222	9.174487	-63.8542	47.7865	active
NCGC00390369-01	4	-6.28222	11.422	5.668701	15.77126	inactive	2.1	-4.83222	70.51918	-17.9221	107.1871	active
NCGC00480894-01	4	-7.63222	0.226561	111.8937	21.95553	inactive	-2.2	-5.23222	-15.7251	62.59746	40.2812	active
NCGC00483922-01	4	-4.73222	7.588348	133.5358	26.67891	inactive	-2.2	-5.13222	3.864838	225.3271	58.81326	active
NCGC00485518-01	4	NA	24.56623	79.41848	0	inactive	1.2	-6.28222	25.91554	22.85992	54.18399	active
NCGC00485585-01	4	-8.82098	6.054071	77.14856	29.45569	inactive	2.2	-5.72098	21.04815	-23.5382	41.38252	active
NCGC00485884-01	4	-5.53222	11.9177	9.126238	14.47077	inactive	-1.1	-8.38222	-23.3369	-15.1768	101.7197	active
NCGC00485923-01	4	-5.43222	-2.62584	87.55944	28.17708	inactive	1.1	-5.58222	69.93628	7.036324	101.2612	active
NCGC00485938-01	4	NA	59.98474	71.71547	0	inactive	1.1	-5.53222	67.08051	56.62897	80.09129	active

CCLASS2 denotes curve class 2 as described in the text. LAC50 is the logAC50 value. TAUC is the total area under the curve. EFF is efficacy. Klass denotes whether the compound was active or inactive against the line based on the curve class. Compounds of interest include: NCGC00016373-09 (benzethonium chloride), NCGC00183656-09 (elesclomol), NCGC00242498-03 (D-4476), NCGC00345800-05 (CVT-6883), NCGC00346573-05 (sapitinib), NCGC00351481-01 (R306465), NCGC00371098-01 (YM022), and NCGC00386339-01 (vincristine).

Table 26: Differential compounds favoring parent (Dd2^{R539T})

Sample ID	Parent (Dd2R539T)						Mutant (Dd2R539T/T38I)					
	CCLASS2	LAC50	MaxR	TAUC	EEF	klass	CCLASS2	LAC50	MaxR	TAUC	EEF	klass
NCGC00015122-09	-1.2	-5.47535	-26.2707	26.82453	46.08846	active	4	-5.27535	-0.72119	42.66092	11.36543	inactive
NCGC00015205-07	1.2	-9.07535	-22.7486	88.31787	49.98103	active	4	-4.87535	-21.0011	44.73787	34.70132	inactive
NCGC00015257-06	1.1	-5.72535	21.94738	3773.003	2659.927	active	4	NA	1.584489	15.26234	0	inactive
NCGC00015444-04	-2.2	-5.77535	-23.4778	52.40567	62.21548	active	4	-7.87535	-1.96699	-4.52346	14.47113	inactive
NCGC00015609-05	2.1	-5.12535	-19.0529	1905.483	2472.09	active	4	-6.27535	-8.18485	-17.4676	9.164262	inactive
NCGC00015772-13	-1.2	-5.32535	-26.7918	28.09679	40.92087	active	4	NA	-6.78986	-21.988	0	inactive
NCGC00015790-02	1.2	-8.92535	17.61649	200.2869	56.96254	active	4	-5.12535	-17.6678	26.74787	29.70138	inactive
NCGC00016889-05	-2.2	-4.97535	-6.22601	131.5719	39.78707	active	4	-4.87535	-17.0542	10.91798	25.46508	inactive
NCGC00017245-12	-2.1	-4.87535	-72.5427	46.85414	99.32277	active	4	NA	0.288724	-0.30395	0	inactive
NCGC00091455-08	-2.2	-4.92535	-34.6259	75.43558	56.82117	active	4	-4.67535	-21.0613	32.88834	36.77352	inactive
NCGC00091920-03	-2.2	-5.88222	-8.03916	-109.213	55.59202	active	4	NA	-10.3601	-34.9567	0	inactive
NCGC00093889-13	-2.2	-5.33222	-35.3031	-54.8174	34.4819	active	4	-7.38222	-6.91172	4.564898	8.794065	inactive
NCGC00094717-05	-1.2	-8.17535	-2.64998	51.47928	32.11689	active	4	-9.17535	-4.556	26.34432	13.89691	inactive
NCGC00095003-06	2.1	-4.67535	1921.154	973.1571	2330.473	active	4	NA	15.43843	37.28789	0	inactive
NCGC00160217-03	1.2	-7.53222	24.2976	36.19465	34.40787	active	4	-6.03222	6.115959	31.14199	14.80022	inactive
NCGC00160428-02	-2.1	-4.87535	-103.473	144.9229	152.1478	active	4	-6.12535	1.303467	69.84788	21	inactive
NCGC00161602-05	-2.2	-5.07535	-31.0696	122.9121	66.97042	active	4	-5.12535	-3.72536	37.27123	12.97044	inactive
NCGC00161641-04	-2.2	-5.02535	-37.4494	41.19476	71.29565	active	4	-4.97535	-18.9679	10.83564	24.76145	inactive
NCGC00165736-02	-2.2	-5.07535	-41.4981	2.891438	55.79774	active	4	-6.97535	-5.70773	10.45102	18.72608	inactive
NCGC00165814-04	-2.2	-5.38222	-43.0308	-26.3855	55.51221	active	4	-4.73222	-1.52224	41.80994	13.32669	inactive
NCGC00168971-02	1.2	-7.09211	15.35852	4.203743	45.00687	active	4	-8.79211	-1.3082	13.03424	25.84709	inactive
NCGC00169427-03	-2.2	-5.61017	-22.3813	28.34132	42.0826	active	5	-8.16017	-68.2864	-371.582	40.62929	inactive
NCGC00169595-03	-2.2	-5.04211	-38.697	-55.6431	37.92768	active	4	NA	-21.181	-82.3871	0	inactive
NCGC00169833-02	1.2	-8.39211	37.60413	122.2588	37.71827	active	4	-8.79211	13.91604	40.63455	31.18773	inactive
NCGC00177995-04	-1.2	-5.37535	-30.2989	104.0385	64.88016	active	4	-4.92535	-15.2105	21.37174	26.25261	inactive
NCGC00180409-03	-2.2	-5.46017	-43.0344	-42.0059	60.85197	active	4	-5.21017	-15.1414	37.81336	31.16974	inactive
NCGC00182047-02	-1.2	-5.72535	-18.5298	67.7125	59.52176	active	4	-5.27535	-11.272	-7.03618	12.02646	inactive
NCGC00185994-02	-1.2	-5.27535	-53.6604	-97.3885	51.90856	active	4	-5.12535	-35.4703	-94.887	19.54888	inactive
NCGC00186000-02	1.2	-9.11017	5.349262	13.86662	41.41144	active	4	-7.46017	4.188574	44.07953	13.68532	inactive
NCGC00188866-01	-1.2	-5.52535	-47.6187	23.39914	80.57216	active	4	-4.97535	-27.7817	23.95189	42.80485	inactive
NCGC00229704-01	-2.1	-4.87535	-62.9324	129.0382	103.1499	active	4	-4.92535	-16.0651	9.826415	26.77817	inactive
NCGC00242497-02	1.2	-9.12535	10.2525	91.01729	59.47327	active	4	-8.92535	9.530909	39.17524	19.49315	inactive
NCGC00247735-02	-2.2	-5.02535	-51.8621	26.11035	75.53426	active	4	-4.82535	-26.2643	6.045899	40.01714	inactive
NCGC00249390-05	-2.2	-4.88222	-87.6461	-135.693	99.67031	active	4	-4.73222	-19.0967	0.893214	24.41601	inactive
NCGC00249392-01	2.1	-4.67535	1958.059	1021.166	2375.146	active	4	-5.02535	-13.4441	11.45667	18.25556	inactive
NCGC00250400-09	-1.2	-6.33222	-71.8747	-131.821	85.12469	active	5	-6.68222	-125.494	-484.179	37.46663	inactive
NCGC00263125-01	-1.2	-5.22535	-10.8065	91.89676	36.93042	active	4	-4.87535	-25.7806	21.13917	34.66631	inactive
NCGC00263192-02	-2.1	-4.97535	-98.854	-6.60954	113.902	active	4	-5.67535	-4.53842	29.32499	19.8807	inactive
NCGC00263204-10	-2.2	-5.18222	-69.8733	-83.3885	72.29183	active	5	-4.48222	-126.565	-514.076	50.73029	inactive
NCGC00263223-01	-1.2	-6.32535	-30.563	27.51286	50.80972	active	4	-6.27535	-24.92	3.485745	38.0906	inactive
NCGC00344508-01	-2.1	-4.97535	-80.5177	-24.8708	106.783	active	4	-8.07535	-22.2539	5.058482	18.70474	inactive
NCGC00345822-02	-2.2	-5.23222	-44.3004	-24.1679	53.4797	active	4	-4.68222	-12.5987	17.40514	22.11841	inactive
NCGC00345833-06	-2.1	-5.38222	-90.0382	-111.625	111.5642	active	4	-4.98222	-20.4142	43.20175	35.14312	inactive
NCGC00345845-02	-2.1	-5.53222	-102.151	-116.683	106.4829	active	5	-5.53222	-123.12	-515.92	17.85252	inactive
NCGC00346458-01	-2.2	-4.97535	-35.5348	112.8693	79.87768	active	4	-8.77535	-7.75603	42.87571	22.14544	inactive
NCGC00346535-01	-2.2	-4.92535	-19.392	177.0868	63.99977	active	4	-4.67535	-18.0337	26.78321	31.14044	inactive
NCGC00346548-07	-2.1	-5.28222	-89.0241	-108.852	87.34732	active	4	-4.68222	-5.98081	3.916506	9.176977	inactive
NCGC00346551-01	-2.1	-4.92535	-55.2817	130.6614	93.2049	active	4	-5.77535	4.748251	86.27478	15.5	inactive
NCGC00346568-05	-2.2	-5.03222	-57.6836	6.759136	74.90216	active	4	-5.18222	-15.8482	24.93751	29.01784	inactive
NCGC00346569-01	-1.2	-5.17535	-17.6178	104.0468	46.88437	active	4	NA	-6.3523	-12.3469	0	inactive
NCGC00346663-03	-2.2	-5.24211	-67.8758	-17.143	79.00222	active	4	-5.24211	-9.46109	45.82409	24.8533	inactive
NCGC00346670-01	-2.2	-4.97535	-46.3174	35.39675	72.76836	active	4	-6.62535	-5.06738	11.29192	14.0471	inactive
NCGC00346689-01	-2.2	-5.07535	-57.7212	35.37739	75.40785	active	4	-5.02535	-26.1197	34.41724	38.2141	inactive
NCGC00346697-05	-2.1	-6.33222	-44.0557	-210.966	107.4932	active	4	NA	-8.53563	-31.5621	0	inactive
NCGC00346939-01	2.1	-4.67535	1548.915	782.2832	1880.503	active	4	-5.02535	-11.2154	31.37544	28.95846	inactive
NCGC00346944-01	-2.2	-4.97535	-40.4881	45.42515	76.56433	active	4	-4.92535	-14.251	54.62141	32.10115	inactive
NCGC00347906-01	-1.2	-5.42535	-1.9455	97.28224	31.59198	active	4	-4.92535	-19.3476	-19.2862	24.21707	inactive
NCGC00347946-02	-2.2	-5.23222	-44.7685	-25.9968	70.32915	active	4	-7.68222	7.149196	18.36571	8.169033	inactive
NCGC00348107-03	-2.2	-4.93222	-49.6119	-9.14085	74.97675	active	4	-4.98222	-15.7558	17.82359	23.90691	inactive
NCGC00351477-09	-2.1	-5.53222	-119.351	-148.126	136.0148	active	5	-7.28222	-118.88	-468.255	32.00944	inactive
NCGC00370800-01	-2.2	-5.38222	-55.3257	-72.0194	74.37101	active	4	NA	3.687107	55.72451	0	inactive
NCGC00370922-01	1.2	-7.48222	-13.7008	38.53921	31.53394	active	4	-5.98222	-1.02993	15.9746	13.31121	inactive
NCGC00378542-02	2.2	-5.98222	-9.75929	52.96335	33.32298	active	4	-7.43222	1.46962	5.812116	5.715825	inactive
NCGC00378593-04	-1.2	-5.27643	-21.679	85.56927	56.25754	active	4	-4.92643	-24.4165	46.41924	42.05509	inactive
NCGC00378596-07	-2.2	-5.28222	-70.9183	-70.7492	78.53647	active	4	-8.63222	-7.19575	9.313875	22.1349	inactive
NCGC00378763-01	-1.2	-5.63222	-43.3534	-59.8851	42.87483	active	4	NA	10.95145	39.22214	0	inactive
NCGC00378797-01	-2.2	-5.58222	-40.4381	-55.5055	59.84112	active	4	-6.93222	-9.08798	-5.24101	7.40558	inactive
NCGC00378959-01	-2.2	-4.93222	-66.3151	-65.7912	67.96786	active	4	-4.98222	-28.7825	-20.8275	28.039	inactive
NCGC00379057-01	-1.1	-5.83222	-113.016	-216.086	107.0969	active	5	-5.28222	-113.35	-522.522	2.993603	inactive
NCGC00380455-01	-1.2	-7.85469	1.83772	37.85268	36.21607	active	4	NA	1.122948	-6.38858	0	inactive

NCGC00380481-01	-1.2	-5.74345	-44.3387	-77.1049	40.26842	active	4	-8.39345	9.715236	-9.12279	13.94499	inactive
NCGC00380599-01	-2.2	-5.24345	-56.6188	-16.1888	85.72853	active	4	-5.29345	-8.45485	7.157178	17.64582	inactive
NCGC00380619-01	2.2	-6.34345	-4.42501	33.25454	38.91937	active	4	-5.19345	2.605325	-18.7957	8.534653	inactive
NCGC00380711-01	-1.2	-6.56017	-34.915	-78.0039	31.11329	active	4	-5.66017	-8.61203	-2.31853	11.83444	inactive
NCGC00380820-01	-2.2	-5.44211	-52.2799	-50.3515	60.52547	active	4	NA	4.639163	21.90109	0	inactive
NCGC00380840-01	-2.1	-4.98222	-74.5349	-15.6759	94.10749	active	5	-4.63222	-102.718	-321.249	52.92449	inactive
NCGC00380879-01	-2.2	-5.34345	-36.5126	9.219247	53.618	active	5	-9.39345	-91.5869	-376.432	32.16749	inactive
NCGC00380910-01	-2.2	-5.38222	-65.6177	-65.7116	67.86759	active	4	-7.83222	-2.99201	3.128115	10.76099	inactive
NCGC00380957-01	2.2	-6.09345	-16.455	66.58467	49.86258	active	4	-6.59345	-7.13149	-24.8512	6.513668	inactive
NCGC00381002-01	-2.2	-5.69345	-31.0846	1.149901	43.23059	active	4	-5.29345	-16.8505	24.92976	37.72059	inactive
NCGC00381056-01	-1.2	-6.44345	-34.0823	-39.5826	40.72289	active	4	-5.34345	-20.3355	2.607736	28.90265	inactive
NCGC00381144-01	-2.2	-5.13222	-11.1338	80.06196	36.3605	active	4	-6.53222	-6.35567	20.98696	17.35206	inactive
NCGC00381186-01	1.2	-7.54345	-11.1848	-86.9984	55.98175	active	5	-6.84345	-10.9823	-209.337	88.50446	inactive
NCGC00381246-01	-2.2	-5.59211	-31.5316	-7.91679	46.23094	active	4	-4.89211	-15.4224	34.349	30.00693	inactive
NCGC00381326-01	-1.2	-5.99211	-16.3607	24.64555	38.69774	active	4	-5.34211	-7.52042	18.61499	15.52451	inactive
NCGC00381337-01	1.2	-8.45535	5.89739	3.640358	38.59565	active	4	NA	0.836654	5.528117	0	inactive
NCGC00384655-01	-2.2	-5.46017	-37.3166	-52.0094	44.27998	active	4	-5.91017	1.902428	-1.70451	9.85472	inactive
NCGC00384807-01	-1.2	-5.69211	-14.5916	31.03662	31.03307	active	4	-4.89211	-8.56015	5.968191	13.27218	inactive
NCGC00384829-01	-1.2	-6.25535	-1.04323	91.98716	31.92313	active	4	-8.05535	15.45493	41.28143	15.70066	inactive
NCGC00384849-01	-1.2	-8.19345	-4.74966	32.46377	45.71592	active	4	-8.64345	19.19492	67.23887	20.5	inactive
NCGC00385020-01	-1.2	-6.53222	-25.2941	-5.17206	36.2161	active	4	-5.33222	0.899409	5.493136	20.2917	inactive
NCGC00385050-01	-2.2	-5.14345	-44.8433	-63.7576	56.00258	active	4	NA	7.951366	13.84782	0	inactive
NCGC00385063-01	-2.2	-6.05535	-62.2918	-117.837	67.7487	active	4	-5.45535	-16.3921	7.713867	27.67056	inactive
NCGC00385071-01	-2.2	-5.79211	-19.558	-10.2704	38.46964	active	4	-8.44211	-2.45779	17.33846	15.41971	inactive
NCGC00385076-01	-1.2	-7.09345	-7.8475	79.58471	43.71247	active	4	-7.19345	3.081624	-3.96199	5.23672	inactive
NCGC00385276-01	-1.2	-8.24211	0.428101	-76.9025	38.71812	active	4	NA	20.32036	38.38004	0	inactive
NCGC00385294-01	-1.2	-5.89345	-47.5692	-73.6223	52.8942	active	4	-7.39345	3.748922	-17.6927	12.29562	inactive
NCGC00385304-01	-2.2	-5.63222	7.080961	-97.8223	79.98891	active	4	-4.68222	14.36318	11.30545	16.19195	inactive
NCGC00385422-01	-2.2	-5.74211	-45.2639	-40.4194	78.26152	active	4	-8.79211	-2.08021	22.69381	13.90989	inactive
NCGC00385606-01	-1.2	-5.78222	-39.9319	-52.0056	41.78792	active	4	NA	7.286523	26.15106	0	inactive
NCGC00385663-01	1.2	-6.16017	31.47441	69.15859	31.41549	active	4	NA	8.215062	61.88995	0	inactive
NCGC00385679-01	1.2	-7.29345	10.42231	115.3719	41.35749	active	4	NA	5.366919	28.94978	0	inactive
NCGC00385813-01	1.2	-6.89345	1.813679	-90.2688	38.25261	active	4	-5.34345	17.74959	42.41602	20	inactive
NCGC00386070-01	-1.2	-7.59345	-34.9782	-73.4682	57.39514	active	4	-8.34345	5.332254	53.65681	9	inactive
NCGC00386087-01	-2.2	-5.66017	-61.7701	-73.4524	66.92883	active	4	-8.26017	-8.60026	4.610163	8.234524	inactive
NCGC00386379-01	-2.2	-6.34345	-28.2962	-25.2302	48.50396	active	4	-4.99345	-9.09401	27.95689	21.41282	inactive
NCGC00386554-01	1.2	-7.93222	3.235756	-3.69181	30.68123	active	4	-6.03222	-5.46395	-22.6071	36.12608	inactive
NCGC00386615-02	1.2	-8.18222	-2.39032	77.46743	52.90162	active	4	-6.13222	-2.78061	14.00405	14.10424	inactive
NCGC00386661-01	1.2	-8.58222	-8.40647	48.80524	40.80098	active	4	-4.88222	-8.75243	-1.02409	14.50291	inactive
NCGC00386738-02	-2.2	-5.28222	-43.2425	-63.1516	44.53097	active	4	-5.73222	2.932629	13.35447	20.45416	inactive
NCGC00386905-01	-2.2	-5.03222	-68.0113	-52.0398	73.09727	active	4	NA	-24.6931	-74.2283	0	inactive
NCGC00387103-01	1.2	-7.48222	6.302043	-41.9571	42.00204	active	4	-5.38222	4.868057	20.63352	23.51555	inactive
NCGC00387146-01	-2.1	-5.08222	-69.9501	21.22002	95.04636	active	4	-4.73222	-18.6469	28.35159	31.37628	inactive
NCGC00387147-01	2.2	-6.08222	19.51346	103.0721	46.82268	active	4	-5.68222	-3.15472	21.14616	14.12036	inactive
NCGC00387770-01	-2.1	-4.88222	-101.219	-55.1698	126.0814	active	4	-4.98222	-10.2102	57.89331	26.75226	inactive
NCGC00387848-03	-2.2	-5.18222	-57.4896	-61.2658	61.81908	active	4	-6.13222	-25.7664	-54.8335	21.11477	inactive
NCGC00389194-01	-1.1	-6.98222	-71.9671	-130.891	97.65712	active	5	-5.43222	-110.626	-428.028	30.4094	inactive
NCGC00389274-02	-2.1	-5.23222	-84.276	-32.2981	120.4589	active	5	-4.93222	-122.928	-370.726	50.55074	inactive
NCGC00389744-01	-2.2	-5.33222	-65.301	-70.2947	65.37698	active	4	-4.98222	-25.7534	-4.54375	30.90404	inactive
NCGC00390451-01	1.2	-8.48222	25.30018	73.02793	50.03253	active	4	-5.08222	-7.14595	-198.617	45.68612	inactive
NCGC00487056-01	-2.1	-4.93222	-79.1449	0.336407	107.6529	active	4	-5.08222	-19.8906	21.59587	31.86877	inactive
NCGC00159455-04	-1.2	-7.86412	-48.4759	-99.2855	65.33714	active	-1.2	-5.96412	-33.4207	-32.9322	41.05571	active
NCGC00167503-02	-1.1	-6.27535	-93.319	-68.9109	131.9306	active	-1.1	-5.52535	-96.5558	-106.595	131.4248	active
NCGC00246968-02	-1.1	-6.57535	-91.6542	-139.933	118.9878	active	-1.1	-5.87535	-97.2406	-143.621	111.3356	active
NCGC00263104-01	-1.1	-6.57535	-87.9915	-154.102	103.2923	active	-2.1	-5.52535	-101.285	-170.383	138.2509	active
NCGC00263154-01	-1.2	-5.66412	-51.1545	1.697017	68.42283	active	-2.2	-4.71412	-68.9424	-46.4226	84.7166	active
NCGC00344990-01	-1.1	-5.97535	-104.155	-37.639	127.2346	active	-2.1	-5.07535	-98.5247	-66.4881	141.7594	active
NCGC00345784-01	-1.1	-5.82535	-83.6484	-81.8049	104.3508	active	-2.1	-5.02535	-93.1216	-121.327	114.2559	active
NCGC00346589-02	-1.1	-6.78222	-92.3594	-207.954	105.0051	active	-1.1	-6.03222	-131.236	-218.946	137.7651	active
NCGC00346664-01	-1.1	-6.07535	-94.2306	-102.778	106.9607	active	-1.1	-5.27535	-75.8175	-93.4688	81.09825	active
NCGC00346681-01	-1.1	-10.3254	-104.512	-490.565	100.1312	active	-1.2	-8.77535	-101.76	-467.472	56.34084	active
NCGC00346896-02	-1.1	-6.38222	-118.764	-174.697	99.285	active	-2.1	-5.38222	-119.886	-149.937	159.6988	active
NCGC00346940-02	-1.1	-6.38222	-116.403	-249.169	132.4355	active	-2.1	-5.68222	-100.933	-138.106	112.7779	active
NCGC00386172-02	-1.2	-7.08222	-64.3135	-108.596	58.22765	active	-2.2	-5.03222	-63.698	-27.6141	96.44859	active
NCGC00387827-02	-1.1	-6.13222	-86.0593	-76.2741	124.1843	active	-2.1	-5.43222	-106.349	-106.254	111.5786	active
NCGC00390549-01	-1.1	-6.99345	-105.817	-236.931	113.8546	active	-1.1	-6.29345	-119.105	-199.989	124.9906	active
NCGC00485950-01	-1.1	-6.08222	-113.292	-190.306	126.033	active	-2.1	-5.28222	-100.066	-99.1718	119.5041	active

CCLASS2 denotes curve class 2 as described in the text. LAC50 is the logAC50 value. TAUC is the total area under the curve. EFF is efficacy. Klass denotes whether the compound was active or inactive against the line based on the curve class. Compounds of interest include: NCGC00159455-04 (gefitinib), NCGC00167503-02 (aclarubicin), NCGC00246968-02

(olmesartan), NCGC00263104-01 (foretinib), NCGC00263154-01 (AZD-6482), NCGC00344990-01 (not annotated), NCGC00345784-01 (PF-3758309), NCGC00346589-02 (cinchonidine), NCGC00346664-01 (paeoniflorin), NCGC00346681-01 (NVP-BGT226), NCGC00346896-02 (MCOPPB trihydrochloride), NCGC00346940-02 (CGP60474), NCGC00386172-02 (clindamycin), NCGC00387827 (dinaciclib), NCGC00390549-01 (NMS-P715), and NCGC00485950-01 (cobimetinib).

APPENDIX B: REAGENTS & EQUIPMENT USED

Ab150113, goat polyclonal anti-mouse AF488 (Abcam)

Ab150079, goat polyclonal anti-rabbit AF647 (Abcam)

Accuprime buffer II (Thermo Fisher Scientific)

Accuprime *Taq* DNA polymerase (Thermo Fisher Scientific)

Albumax II (Gibco)

Anti-GFP antibody ab290 rabbit polyclonal (Abcam)

Anti-GFP antibody CST#2956 rabbit monoclonal (Cell Signal)

Anti-GFP antibody OSE00003G rabbit polyclonal (Thermo Fisher Scientific)

Ampicillin (Sigma)

APAD (Sigma)

AvrII (NEB)

BamHI (NEB)

BL21 *E. coli* cells (Invitrogen)

Blasticidin (Gibco)

Bmt1 (NEB)

BtgZI (NEB)

$CaCl_2$ (Sigma)

Chloroquine diphosphate (Sigma)

CloneAmp Hifi PCR master mix (Clontech)

DHA (WWARN)

Diaphorase (Sigma)

DreamTaq Green Master Mix (2X) (Thermo Fisher Scientific)

DSM1 (MRA)

EcoRI (NEB)

EDTA (Sigma)

EGTA (Sigma)

Gentamicin (KD Medical)

GFP-trap_M (Chromotek)

Glucose (Sigma)

Glutaraldehyde (2.5%) in sodium cacodylate buffer (Electron Microscopy Sciences)

Glutaraldehyde 25% aqueous solution (Electron Microscopy Sciences)

Glutathione (reduced) (Sigma)

HEPES (Sigma)

HEPES solution (Sigma)

Hypoxanthine (Sigma)

Hypoxanthine solution (EMD Millipore)

In-Fusion HD Cloning Kit (Clontech)

K-TMBP (Echelon Biosciences)

L-Glutamine (Sigma)

LB Agar, powder (Lennox L agar) (Thermo Fisher Scientific)

LB Broth, powder (Lennox) (Sigma)

LR White acrylic resin (Electron Microscopy Sciences)

Mefloquine hydrochloride (Sigma)

Milk (Blotting-grade Blocker non-fat dry milk, Bio-Rad)

MitoTracker Deep Red (Thermo Fisher Scientific)

$MgCl_2$ (Sigma)

Monarch DNA gel extraction kit (NEB)

NaCl solutions (Baxter)

$(Na)HCO_3$ (Sigma)

NBT (Thermo Fisher Scientific)

NcoI (NEB)

NotI (NEB)

NucleoBond PC EF plasmid DNA purification (Macherey-Nagel)

NucleoSpin Gel and PCR Clean-up kit (Macherey-Nagel)

NuPAGE LDS Sample Buffer (4X) (Thermo Fisher Scientific)

NuPAGE Novex 4-12% Bis-Tris Protein Gel (1mm, 10 well) (Thermo Fisher Scientific)

NuPAGE Sample Reducing Agent (10X) (Thermo Fisher Scientific)

One Shot TOP-10 chemically competent *E. coli* cells (Thermo Fisher Scientific)

Paq5000 mix 2x PCR Master Mix (Agilent Technologies)

PBS (Thermo Fisher Scientific)

PciI (NEB)

PD-10 desalting column (GE Healthcare).

Percoll (GE Healthcare)

Phenol red (Sigma)

Pierce 16% paraformaldehyde, methanol-free (Thermo Fisher Scientific)

Pierce ECL Western Blotting Substrate solution (Thermo Fisher Scientific)

PIP Strip (Echelon Biosciences)

QIAGEN Plasmid Maxi kit (Qiagen)

QIAprep Spin Miniprep Kit (Qiagen)

QIAquick Gel Extraction kit (Qiagen)

Quinine sulfate (Sigma)

RPMI 1640 (KD Medical)

RPMI 1640 Vitamins (100x) (Sigma)

RPMI 1640 Amino Acid Solution without L-Glutathione (50x) (Sigma)

Saponin (Sigma)

SapphireAmp Fast PCR Master Mix (Clontech)

SOC outgrowth medium (NEB)

Sorbitol (Sigma)

Stellar competent *E. Coli* cells (Clontech)

SYBR green I (Invitrogen)

T4 DNA ligase (NEB)

Triton X-100 (ThermoFisher Scientific)

WR99210 (Jacobus Pharmaceuticals)

XhoI (NEB)

XmnI (NEB)

β-10 competent *E. coli* (NEB)

Equipment

Accuri flow cytometer (BD Biosciences)

Avani J-E centrifuge JS-13.1 (Beckman Coulter)

Centrifuge 5427R FA-45-30-11 (Eppendorf)

Centrifuge 5415D F45-24-11 (Eppendorf)

Centrifuge 5810 A-4-81 (Eppendorf)

DU800 UV/vis spectrophotometer (Beckman)

EnVision plate reader (Perkin Elmer)

FLUOstar OPTIMA instrument (BMG Labtech)

Gene Pulser Xcell (Bio-Rad)

H-7500 transmission electron microscope (Hitachi High Technologies)

Kodak X-OMAT 2000A processor (Kodak)

Leica SP5 inverted confocal microscope (Leica Microsystems)

Multidrop Combi Reagent Dispenser (Thermo Fisher Scientific)

Pierce G2 Fast Blotter (Thermo Fisher Scientific)

XR100 CCD camera (Sony)